Characterisation of coastal fjords and buried glacial valleys at the sub-Antarctic Auckland Islands using high-frequency seismic data

Edward J. Perkins

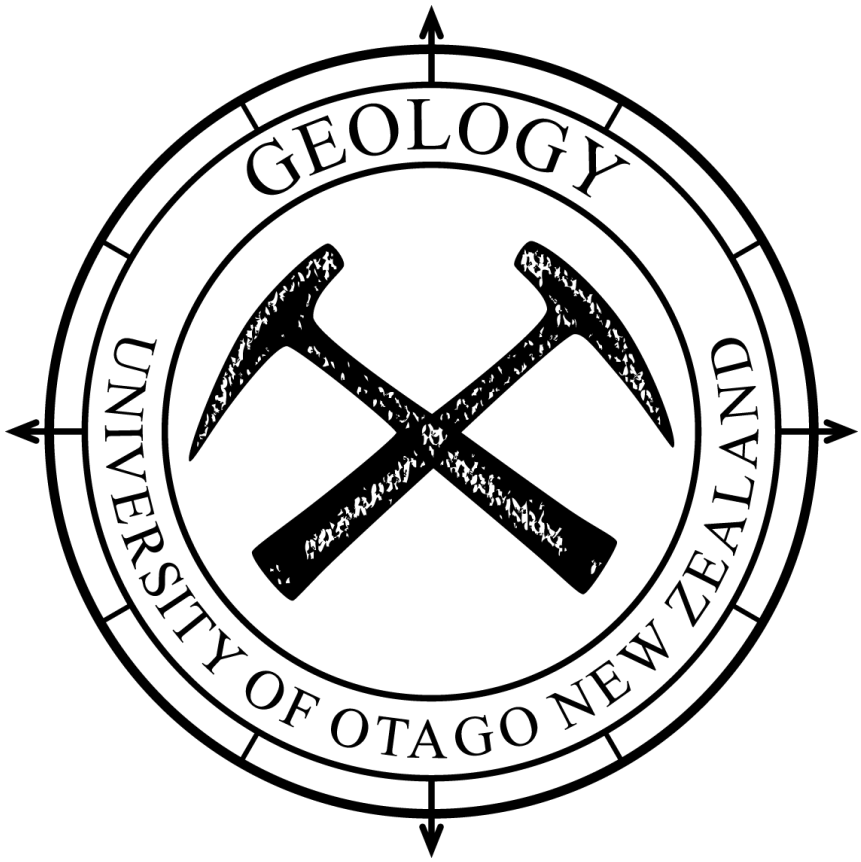

A thesis submitted for the degree of
Master of Science (Geophysics)
University of Otago, Dunedin,
New Zealand.

"There are days when these islands are enveloped in an unsurpassed bleakness and days of bright blue clarity when they are the most invigorating and wild places on earth."

- Excerpt from World Heritage Area Nomination, 1997.

High-resolution seismic surveying by the University of Otago has shown that the leeward side of the sub-Antarctic Auckland Islands (51° 44'S, 166° 06'E) is dominated by Quaternary glacial landforms that extend offshore. These offshore glacial landforms, as a part of the wider glacial history at the Auckland Islands are still poorly resolved. However, over 1200 km of high-frequency seismic data from previously unsurveyed fjords, harbours and specific shelf localities are presented here with a corresponding multibeam bathymetric survey. Using a suite of high-resolution geophysical and geologic surveying techniques, this project constrains the infill stratigraphy and topographic morphology of drowned, glacially incised valleys and coastal fjords. Specifically, this thesis will (***i***) *examine glacial extent and sedimentary regimes in fjords and drowned valleys to further understand the local glaciation and sedimentation history, (**ii**) identify potential submarine lacustrine deposits as future coring targets for high-resolution climate proxies, (**iii**) use paleo sea levels to constrain paleo shorelines during the last glacial maximum, (**iv**) characterise the eroded eastern shelf platform during the last glacial maximum and the corresponding sea level lowstand.*

First-order observations and interpretations from the data show sedimentary deposits and widespread buried topography consistent with coastal glaciation. Analysis of the processed seismic data through the evaluation of seismic velocities in combination with new seafloor bathymetry data, provide high resolution inputs into specific geologic modelling packages. This refines spatial constraints on sedimentary lithologies, valley morphologies and valley formation. These reconstructions of offshore topography and stratigraphy during glacio-eustatic lowstands help to identify localities where lacustrine deposits may occur separately from marine influences. Lacustrine deposits are to be targeted for coring with relation to high-resolution Southern Hemisphere paleo-climate proxies as a wider research objective. These methods and approaches advance understanding of glacial extent, climate parameters and the emergent Auckland Island landmass during the last glacial maximum at mid-high southern latitudes where geologic archives are sparse.

Six years ago as a St Bede's College graduate beginning at the University of Otago, I would never in a million years believe that I am moments away from completing a Masters using geophysical techniques in one of the most isolated and unique locations at the edge of the world. Albeit, two years ago this project innocently began as a characterisation project, but turned out to be a long skirmish with computers, acoustic waves and a rivalry with Microsoft Word to last a lifetime. This thesis is the account and only remaining archive of this process. It cannot express the long days spent in the lab, enduring Southern Ocean storms below deck, praying for good results, the ensuing downward spiral of bad results, and the crowning moments of utter triumph with results synthesis to realistic scientific interpretations.

This 'process' would not be possible without the continued support and encouragement from many people.

I would like to thank Associate Professor Andrew Gorman for the opportunity to undertake a unique and exciting project that I am passionate about. Equally, the rare opportunity to go on an expedition to the sub-Antarctic on the R/V *Polaris II* would not have happened without Chris Moy. I am forever grateful for taking me on as part of your research expedition.

During the initial first few days in the Auckland Islands trying to plan a seismic survey with zero experience, the mentoring and advice from Bob Dagg cannot be overstated and he deserves a special thanks. The Polaris II crew – Bill Dickson, Steve Little, Steve King, Warren Wilson and Evan Kenton is owed thanks for safe passage across the Southern Ocean, as well as Sir Richard 'Hannibal' Hayes for the memorable, cross island helicopter services.

The academic staff at the University of Otago's Geology Department must be mentioned as a key part of this process, especially James Scott, Daphne Lee, Christian Ohneiser, Christina Riesselman, Hamish Bowen and Luke Easterbrook who was always willing to help and answer questions.

A credit to the fellow students over the years. A special mention to Taliesen Partridge for your advice and tutoring in those rough early years, in which I would not be in this position if it wasn't for your help and friendship. Thanks in no particular order: Andrew McRae, Andy Holt, Douglas Fraser, Sebastian, Patrick Lepine, Ben Ross, Fraser Shand, Rebecca Parker,

Mathew Vanner, Ian Geary, Elliot Bowie, Briar Taylor-Silva, Andrew Mason, Ben Pickles, Jim Dickie James Fleming, James Parks, George Stick, Talal Kaldada, Marcus Richards, Dianne Nyhof, Glenda Payne, Dylan Baker, Patrick Fletcher, Tim Lutter Christine McLachlan, Harris Anderson, Greer Gilmer, Diglet, Anna Nesbit, Dom Melchers, Mike Duncan, Brusier (B^2), and Zaneta Koppen-Pavolvich. Everyone involved, especially in the past two post-graduate years, have been thoroughly enjoyable, memorable and defining.

Academic education aside, the time spent in Dunedin has been equally as defining. The people that I have met and the lifelong friends acquired has been a genuine highlight. Special mention to the early years Aquinas College team with special mention to Sam Spermerins, Tama Solomon, Todd Elder, Michael Jensen, Micheal Mahima, Joshua '0.8' Paff, Angus 'Gus' Wilson, Sam McKenzie, Daniel 'X' Boyle, Ross 'Horse' Dickinson, Zac Nevison, Gavin McLeod, Huw Laver, Kelsi Horne, Nina Williams, Meghan Seamark, Lisa Caldwell, Sophia Faure, Marlene Adams, Steve Downey, Bonnie Humphrey, Olivia Sutton, Anna Taylor, Terina Stockwell, Hattie 'ironlungs' MacDonald, Lidushan Chandrakumar, Ben Duckworth, Simon Lack, Tom Cuming, Dan Fouhy, Caleb 'Gravy' Grove, Thomas 'T-Coops' Cooper, Jordan 'Gary' Kingan, Tom 'Fat Tom' Gourlay Tim 'Ice Cream' O'Connor, Taylor Wright, Mimi Simpson, Stephanie Polson, Georgia Robertson, Rebecca Crump, Maddie Ollivier, Ben 'the tackle' Vincent, Maddy Partridge, Zahara King, Chloe Wilson, Stephanie Moody, Josh 'the battery' Reid, Charlotte 'the female battery' Manning, Kelly Stewart, Mindy Ishikawa, Lovey Taimani, Amy (and Arlo) Whittington, Willy Koreman, Kirby Teviotdale Mana Wright, Kwaye Raumati, Jordan Arnold, William Ward, Jono Ruru, Alexander Germley, Rhys Coleman, Marcus Gobald, Sala Ioane, Brogan Kerrison, Josh Perry, Alex Ryder, Hunter Stewart, Kadin Boyle, Corey Sutton, Gianna Leoni, Shaun Tahau, David Reedy, the entire extended South PAC raiders family, Alison Douglas, Jessica Chen, Kip Wastrom, Becca Rawlings, Jessica Miller, Mitch Caywood, Ben Krechevsky, Kiril Davidovski, Emilie Josefine-Reese, Logan Beasley, Rhys Williams, Tom Pelly to name a few and many many many more (space is a factor).

The ongoing support of my family cannot go unmentioned. Mother Rachel, father Wayne, stepmother Betty, Walter, Pop and Gran, Adrienne and Les and brothers Sammy and Max; this above all, would not have been a possibility without you all.

It's finally done. Next stop: Central America.

iv Table of Figures •

Chapter 1 • Introduction:

Chapter 2 • Climate & Glacial History:

Chapter 3 • Regional Geology:

Chapter 4 • Literature Review:

Chapter 5 • Methods:

Chapter 6 • Results:

Chapter 7 • Discussion:

Chapter 8 • Conclusion:

Appendix:

Chapter 1 •

Introduction

1 Introduction •

1.1 Motivation •

The current understanding of Quaternary glacial onset, extent and connected climatic parameters at the New Zealand sub-Antarctic islands and the wider Southern Ocean is poorly constrained. Yet, climatic changes through the Late Cenozoic are of significant importance, as paleoclimate reconstructions can be used as analogues for future global climate systems and ice sheet projections (Lamy et al. 2010; Hodgson et al. 2014). Sub-Antarctic islands in the vast expanse of the Southern Ocean are distinguished by their sparse and isolated nature. These islands are governed by intense oceanic climates which are tightly coupled with the prevailing Southern Hemisphere westerly wind belt (SHWW) (McGlone et al. 2000). Due to this tightly coupled relationship with the Southern Hemisphere climate, sub-Antarctic islands are among the first to respond to regional warming and climate fluctuations (Gordon et al. 2008; Cook et al. 2010). The location of the Auckland Islands (51° 44'S, 166° 06'E) offers an ideal reference point for constraining paleo-climates, ice extent during the last glacial maximum (LGM) and boundary conditions for physical parameters at mid-high southern latitudes during the Quaternary where geological archives are sparse.

An extensive review by Hodgson et al. (2014) endeavoured to constrain the extent and timing of the LGM at numerous sub-Antarctic localities using terrestrial and submarine evidence. The review aimed to provide Antarctic maritime and sub-Antarctic locality inputs to the Scientific Committee for Antarctic Research (SCAR) program for Antarctic ice sheet reconstructions in 5000 year time portions since the end of the LGM (19 ka). The review, however, revealed a lack of constraints on sub-Antarctic glaciation, underlining a need for future work. Specifically, Hodgson et al. (2014) highlighted the demand for onshore and offshore past glaciation constraints using geophysical and sedimentological investigations to image and date submarine glacial features.

The *Department of Conversion* (New Zealand) released in 2005, the 'New Zealand Sub-Antarctic Islands Research Strategy' which outlines key future research themes for the island group. These research themes were identified for the purpose of

advancing multi-disciplinary research at the islands for effective management of this internationally significant group. The report characterises the sub-Antarctic islands as internationally important due to their unique mid-high latitude location in the Pacific Sector of the Southern Ocean combined with their relatively natural condition. This unique locality originates from their longstanding isolation from major landmasses, coupled oceanic climate, topography and relationship to marine topography. Due to this, the New Zealand sub-Antarctic islands have established unique ecosystems with a high degree of endemism (West 2005). The identified research themes focus on current knowledge gaps. This thesis is applicable to numerous themes directly and also to some beyond the scope of this research. Directly applicable themes within the strategy include answering questions over the glacial history of the islands with respect to ice cap coverage and the likely effects on the island area during fluctuations in past sea level, with a specific reference to geophysical approaches. Outcomes of this research will advance multi-disciplinary research of highly endemic ecosystems established on these islands and impart further paleo-climate and atmospheric research at these latitudes.

Three separate expeditions to the sub-Antarctic Auckland Islands aboard the *R/V Polaris* II were undertaken by the *University of Otago* in early 2014, 2015 and 2016. Multidisciplinary geologic data were collected, including over 1200 km of seismic transects. These transects were gathered to image properties of the sub-surface in fjord and shelf localities. This data set contributes to a limited but growing number of offshore seismic investigations of this nature in the sub-Antarctic and Southern Ocean. Correlating multi-beam bathymetric data were collected by *IXSURVEY* as tendered for *Land Information New Zealand* (LINZ). These data sets are available to complement the seismic data through identifying and correlating topographical features on the seafloor. Constraining the infill stratigraphy within fjords and previously imaged offshore buried valley systems furthers the understanding of what processes have occurred, under what climatic conditions and to what extent at these latitudes throughout the Quaternary. These questions are critical for understanding Late Cenozoic Southern Hemisphere paleo-climates, modern day climatic fluctuations and Quaternary glacial cycles (Bergstrom et al. 1999; McGlone et al. 2000; McGlone, 2002; Hodgson et al. 2014).

1.2 Study Area • Auckland Islands, Southern Ocean

The windswept Auckland Islands (51° 44'S, 166° 06'E) are located about 465 km south of New Zealand (*Figure 1a & 1b*) and are regionally situated on the western margin of the Campbell Plateau. The group is the largest of the New Zealand sub-Antarctic Islands (which also include the Antipodes Islands, Campbell Island, Bounty Islands and The Snares - 47-52°S). These southern latitudes of the *Roaring Forties* and *Furious Fifties* are defined by prevailing westerly winds, highly variable weather and notorious storms. The topography of the island chain bares heavy scares of erosion.

The positioning of the Auckland Islands within the Southern Hemisphere westerly wind belt provides an ideal location to investigate paleoclimates and Quaternary glacial history. This is due to the sensitive, coupled nature of geologic archives at these latitudes to Southern Ocean climate fluctuations. Interpreting the glacial history of the Auckland Islands is a critical step for resolving sub-Antarctic and wider Southern Ocean climate dynamics on glacial/interglacial timescales.

Figure 1.1a • (**Left**) Location of the Auckland Islands (50° 44'S 166° 06'E), south of New Zealand.

Figure 1.1b • (**Right**) Auckland Islands localities, including islands, fjords, inlets, harbours and noted topographic highs.

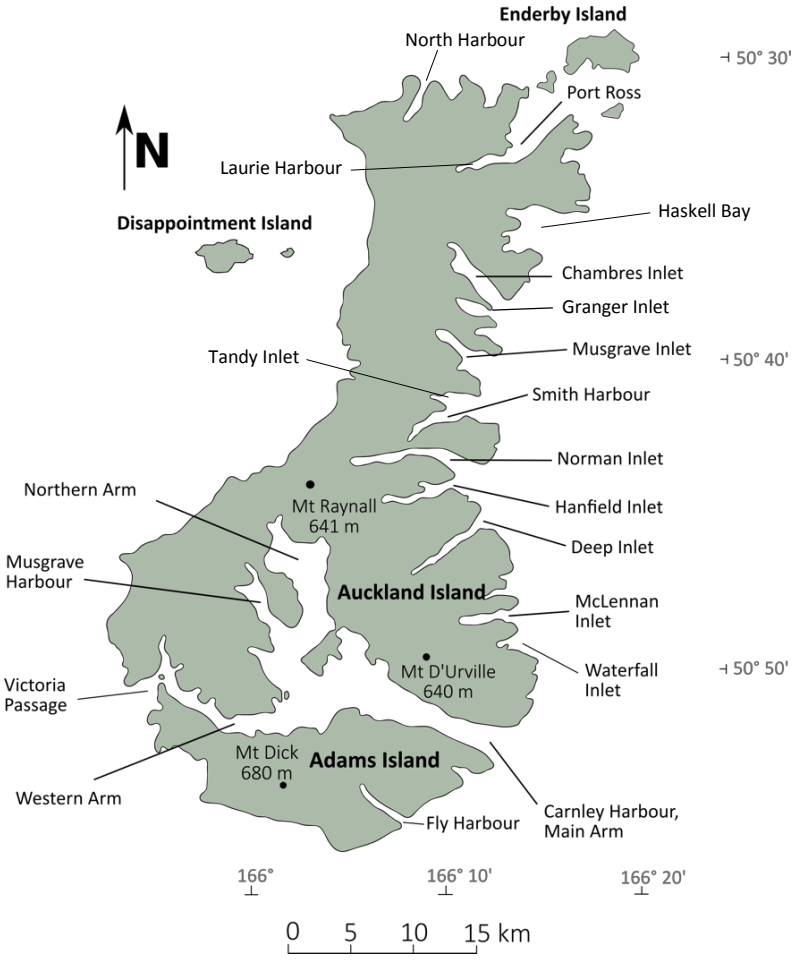

1.2.1 Physiography •

The Auckland Islands landmass consists of two remnant shield volcanoes (Gamble & Adams, 1985) that have been substantially excavated through marine, fluvial and glacial erosion. The entire western flank, similar to numerous other sub-Antarctic localities has been subjected to persistent westerly winds and heavy seas. This results in extensive ongoing erosion that forms continuous high cliffs along the windward, western coast. In contrast, the leeward side of the islands preserves numerous terrestrial glacial features that were first observed and described by Speight and Finlayson (1909). Imposing, deeply cut U-shaped valleys, fjords and inlets that trend west to east dominate the eastern margins, indicative of the extensive Quaternary glaciation history at the Auckland Islands (*Figures 1.2, 1.3 & 1.4*). These features are incised onto Cenozoic shield volcanoes that hosted extensive ice fields on Carnley Harbour in the south and Disappointment Island to the north (*Figure 1.2*) (Quilty 2007; Hodgson et al. 2014). As shown by valley distribution patterns, ice flowed down in a radial arrangement from ice fields that advanced through the valleys and fjords observed today which progress offshore. Hanging valleys, moraine-dammed lakes (Hinemoa - *Figure 1.4* & Tutanekia) and high altitude cirques are also prevalent features at the Auckland Islands.

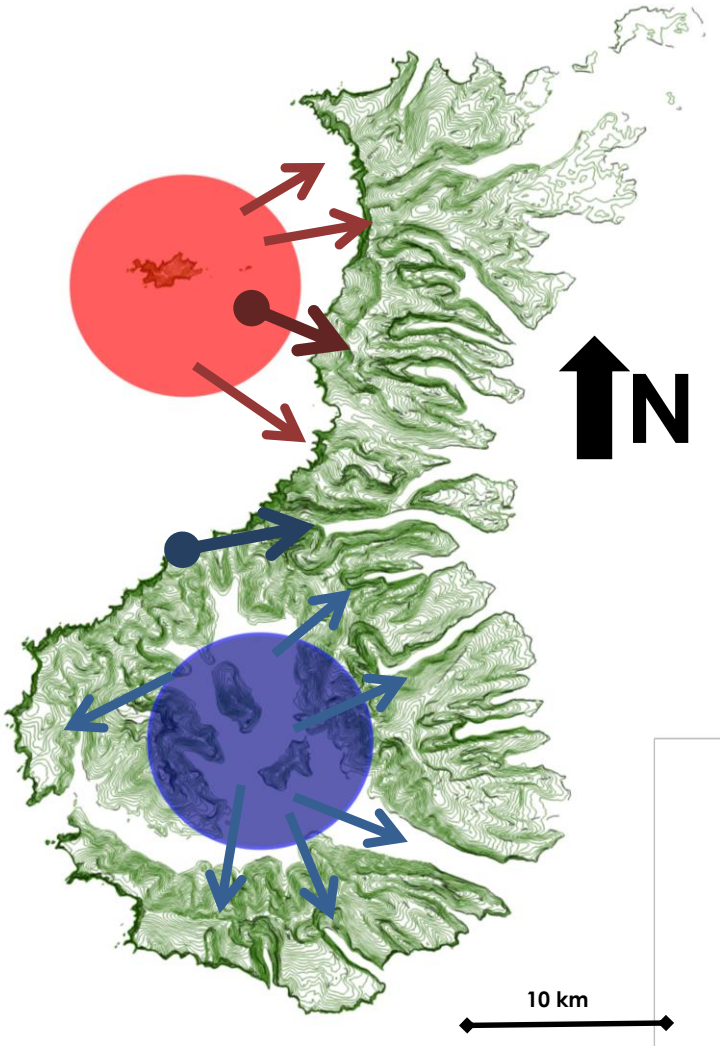

Figure 1.2 • Arrows representing the approximate radial arrangement of glacial flow direction around the former ice domes situated on the centers of the Ross (**red**) & Carnley (**blue**) volcanoes (Derived from Hodgson et al. 2014). Topographic contours (20 m).

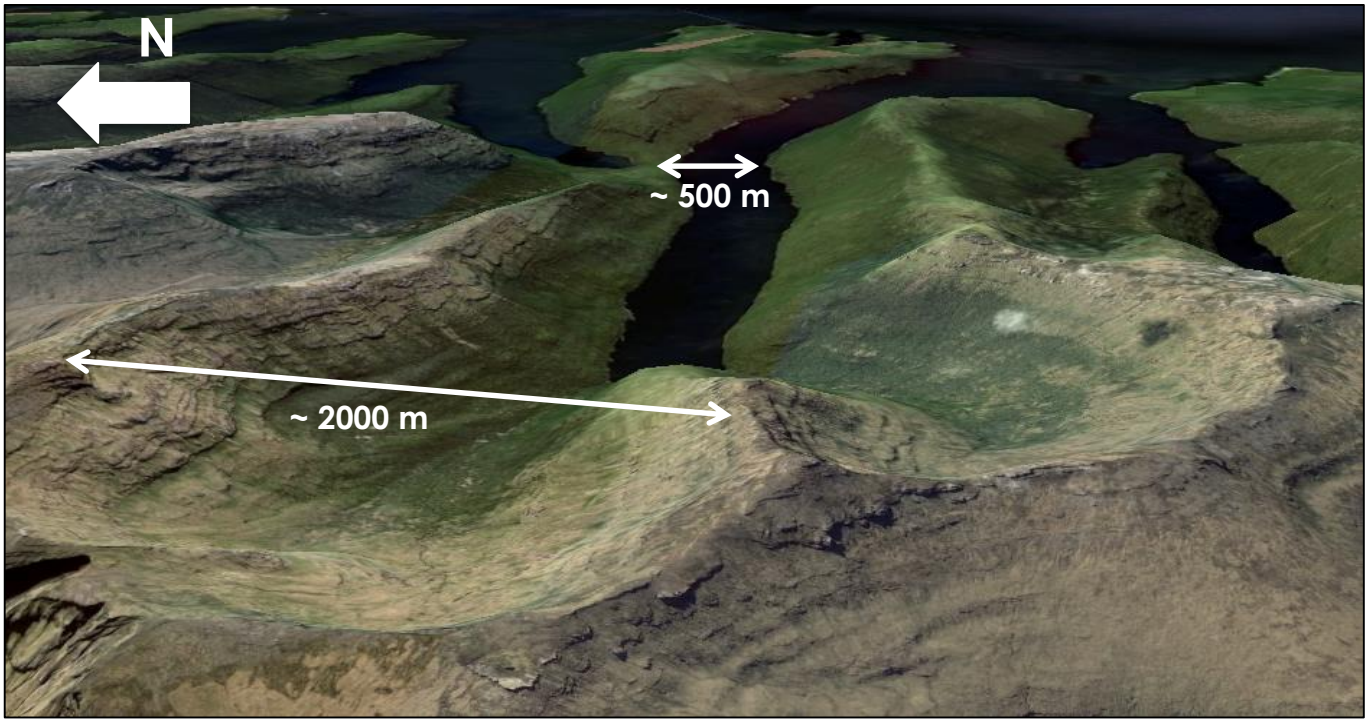

Figure 1.3 • Looking east over two cirque basins that converge at the head of Norman Inlet. Extensive coastal fjords on the eastern coast of the Auckland Islands are present. (Glacier flow direction and locality on *Figure 1.2* – **blue bulb arrow**) (Image from Google Earth).

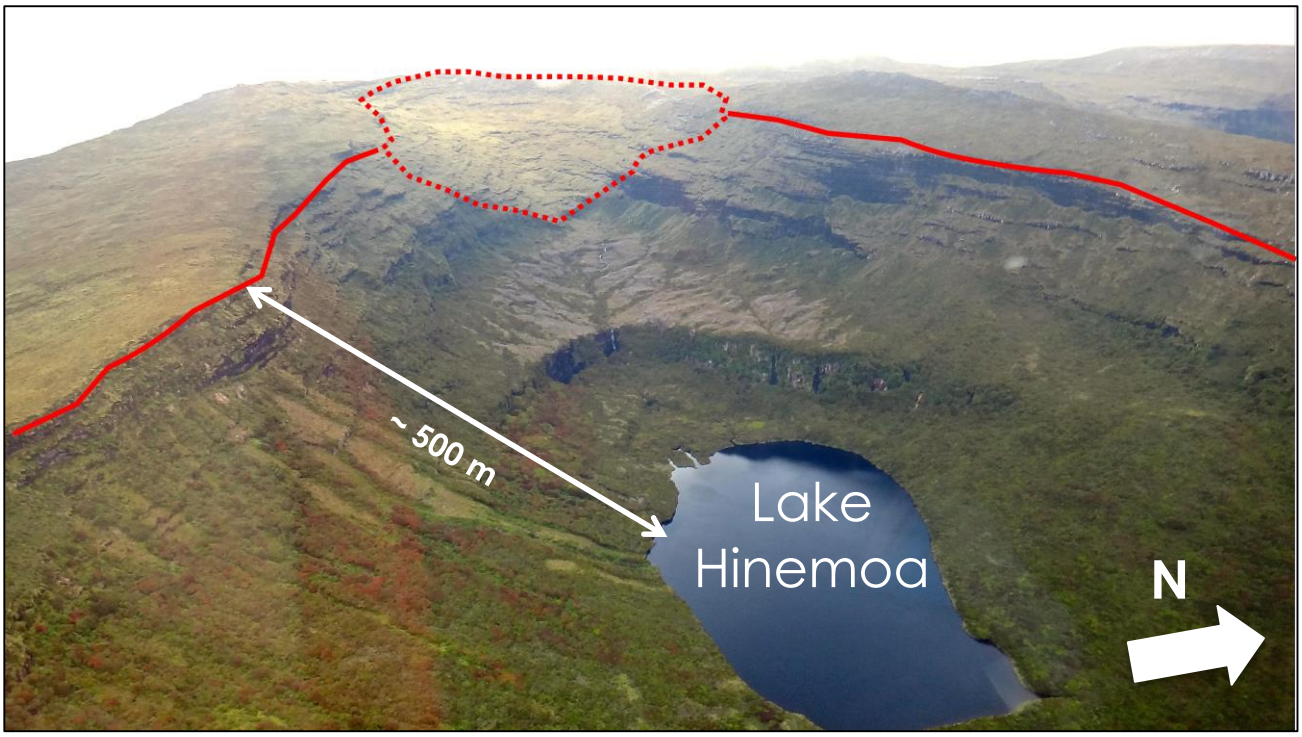

Figure 1.4 • Looking west over Lake Hinemoa - a moraine-dammed lake in the footprint of an extensive glacial valley at the head of Musgrave Inlet. Solid red lines showing the wide extent of the glacial valley and the dashed lines exhibiting the higher altitude cirque basin. Glacier flow direction is shown on Figure 1.2 (**Red bulb arrow**) (Photo credit – Briar Taylor-Silva).

1.3 Previous Data • 14PL001

Inaugural data sets were collected at the Auckland Islands during an early 2014 cruise (14PL001 – *Figure 1.5*) aboard the R/V *Polaris II*. This was a precursor expedition to the 2015 (15PL001) and 2016 (16PL119) cruises. Similar to 14PL001, multidisciplinary geologic data were gathered off and onshore in 2015 and 2016. Up to 400 km of high-frequency seismic data were collected in tandem with chirp sub-bottom profiling of several eastern fjords and shelf localities of the island group during 14PL001. Seismic data collected within fjord and inlet localities along the eastern margins revealed variable seafloor and sub-surface topography, indicative of a range of dynamic processes. Offshore, eastern shelf transects at varying distances from the coast uncovered an intricate incised valley system, extending at least 15 kilometres from the modern day shoreline (e.g. *Figure 1.6*). The valleys are in-filled with sediments that vary spatially and stratigraphically. Profiles collected within multiple inlets (e.g. *Figure 1.7*), relate to the onshore glacial evidence of steep 'U' shaped valleys, moraine-dammed lakes and high-altitude cirques. Reconnaissance piston, gravity and lake cores were also collected from specific eastern fjords and terrestrial lakes. Expanding on the success of 14PL001; 15PL001 and 16PL119 data were collected to complement and expand on these previously collected data sets.

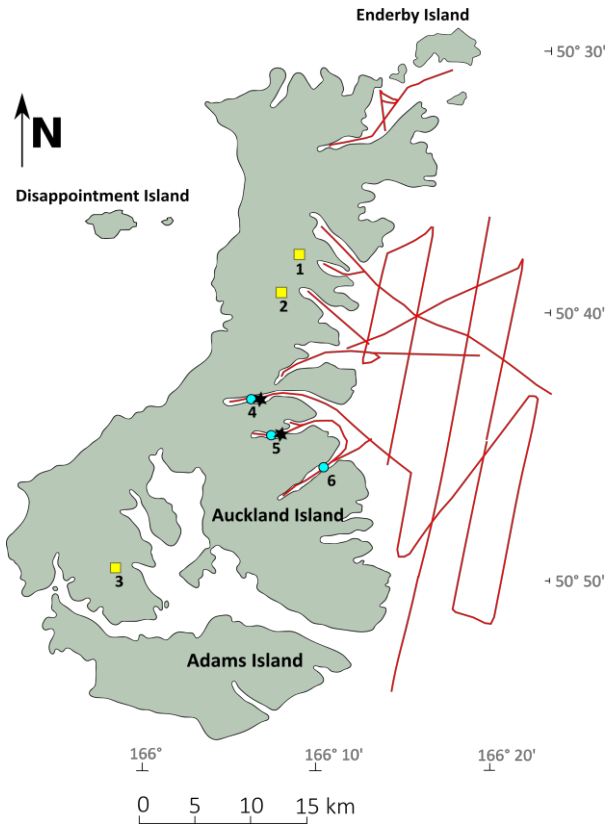

Figure 1.5 • Multi-disciplinary geologic data gathered from the 2014 Auckland Islands expedition (14PL001).

- Seismic survey transects and chirp data taken from eastern fjord and shelf localities (**red Lines).**
- Fjord piston/gravity core localities of varying length (**blue circles).**
    - Six cores were taken in Hanfield Inlet (**5**), one core in Norman inlet (**4**) and one in Deep Inlet (**6**).
    - Box cores (black stars) were also taken at Norman (**4**) & Hanfield (**5**) localities.
- Localities of terrestrial lake cores at Lake Speight (**3**), Lake Hinemoa (**2**) & Lake Tutanekai (**1**) (**yellow squares**).
- 38 grab samples were taken from Port Ross, Chambres, Granger, Norman and Hanfield Inlets. Four CTD measurements were also taken from Norman and Hanfield inlets as well as a shelf locality. These are not represented in this diagram.

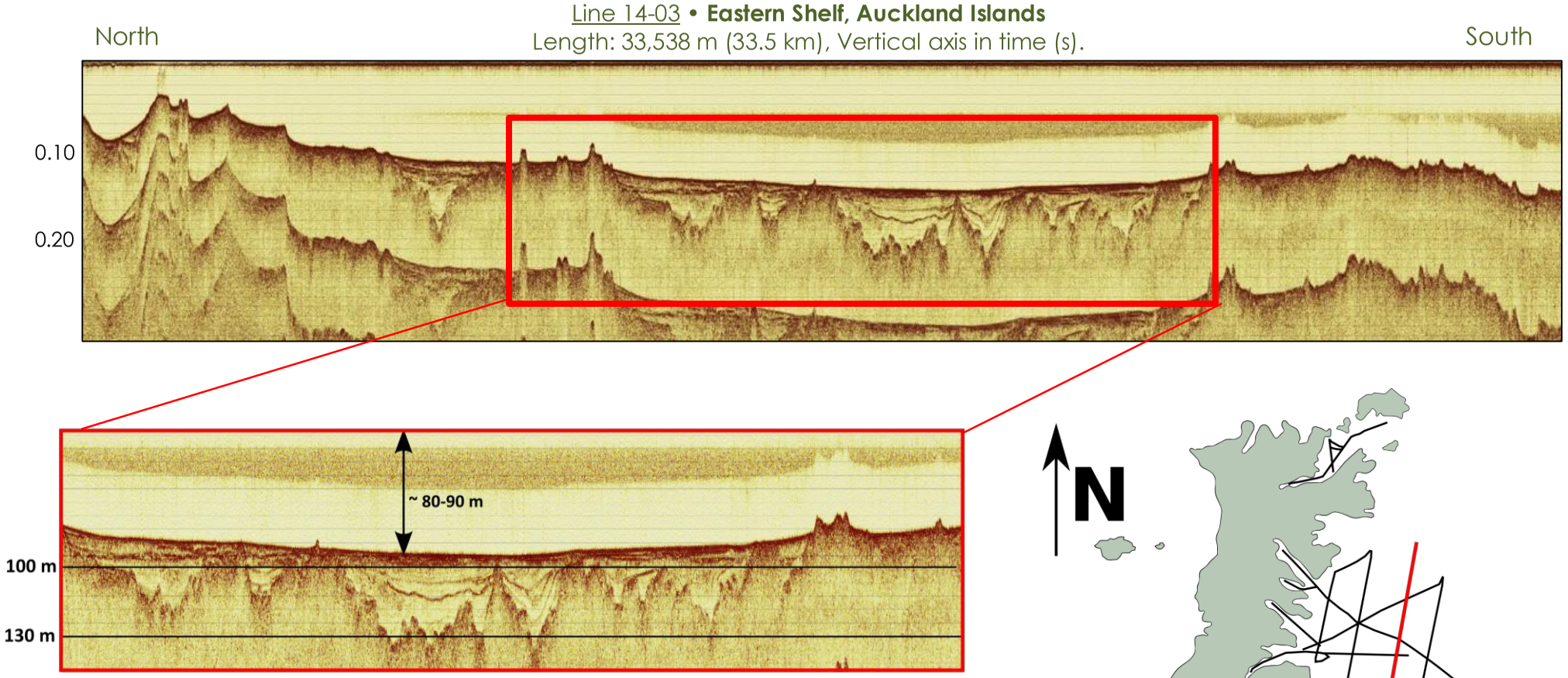

Figure 1.6 • Line 14-03 and an enlarged section displaying an extensive buried valley system on the eastern coast of the Auckland Islands. Numerous, laterally continuous sedimentary horizons are observed within the valleys. 15PL001 and 16PL119 seismic survey designs aimed to further target this offshore valley system for additional analysis, advancing on the inaugural data set gathered in 14PL001.

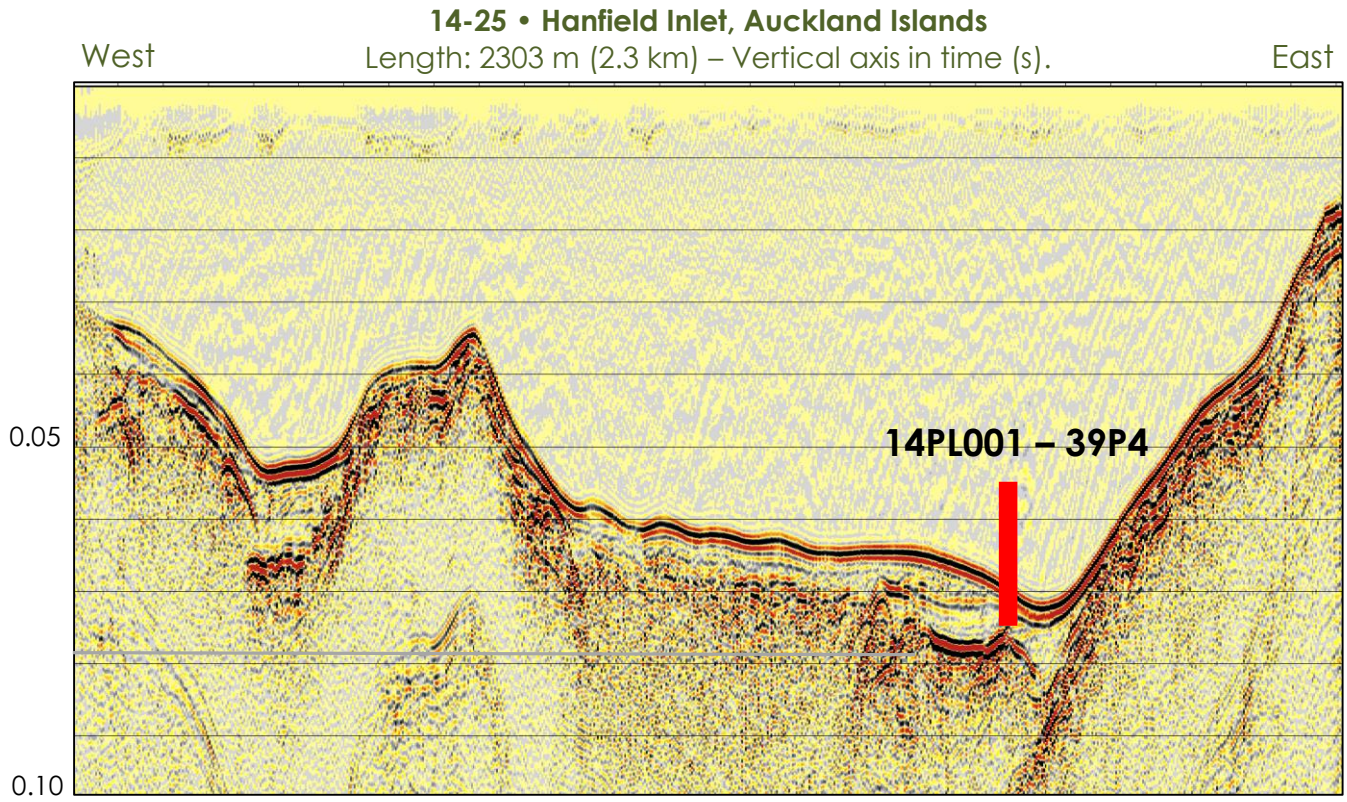

Figure 1.7 • Line 14-25 in Hanfield Inlet on the eastern side of Auckland Island. This transect exhibits a glaciated profile with a shallow entrance sill and a sedimentary package within the overdeepened fjord basin. This sedimentary package was cored by a 6 m piston core (14PL001 – 39P4) and crossed a terrestrial/marine transition dated at 8 ka (Einvik-Heitmann, 2014).

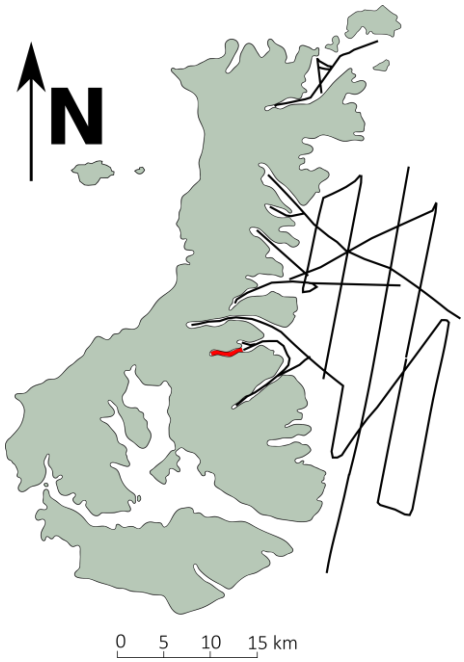

Figure 1.8 exhibits the complete Auckland Islands topographic and bathymetric data that existed prior to 14PL001. The topography of the islands was assessed using through *Shuttle Radar Topography Mission* (SRTM) elevation models; however accuracy of the model was determined by the survey resolution. *Land Information New Zealand* (LINZ) nautical charts were compiled using sparse depth soundings from out-dated, low resolution hydrographic surveys. Some fjords and inlets (e.g. McLennan Inlet, Deep Inlet and Fly Harbour) have little and in some cases no depth soundings. Bathymetry offshore, previous to 14PL001, showed a gentle progression on the eastern shelf towards the shelf break in comparison to the highly varied, incised topography of the exposed Auckland Islands landmass.

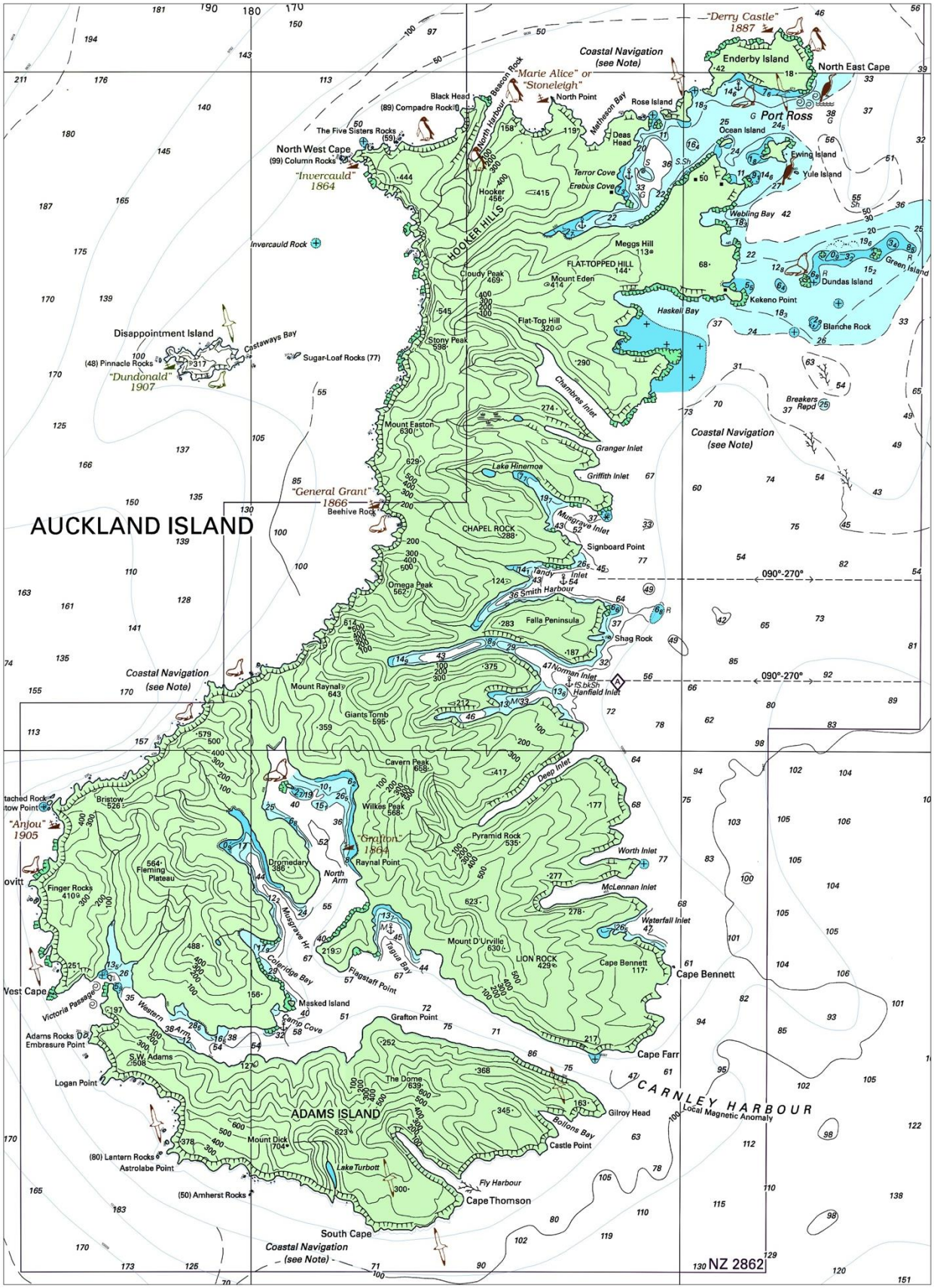

Figure 1.8 • Topographic and bathymetric data at the Auckland Islands before the 14PL001 cruise. Sparse bathymetry depths are presented offshore, with some fjords and inlets showing little or no depth soundings. The eastern shelf setting from the soundings show a gentle progression towards the east. (From Land Information New Zealand – LINZ).

1.4 Aims •

There are currently no high-resolution submarine constraints on the Quaternary glaciation at the Auckland Islands. Terrestrial glaciation features at the Auckland Islands have been long known. They were first described by Speight (1909), with later preliminary de-glaciation radiocarbon dates by McGlone et al. (2000) & McGlone (2002). However, offshore constraints of past glaciations, associated geomorphology, assessments of exposed lowstand landmasses and interpretation of glacial/postglacial sequences, require greater emphasis to advance our understanding of the Auckland Islands and the wider sub-Antarctic glaciation history. Seismic data combined with high-resolution bathymetric imaging are ideal methods to examine Quaternary glaciation features, extents and associated sedimentary deposits on the seafloor and subsurface. The wider outcomes of this research project can contribute to specific Antarctic Ice Sheet models. This can strengthen the understanding of sensitive sub-Antarctic and maritime Antarctic ice masses during the last glacial period and throughout the Quaternary. These inputs will contribute towards answering questions about relative climate pacing, terrestrial habitats during glacial periods and de-glaciation rates throughout the late Pleistocene/early Holocene at these latitudes.

Main Objectives: Using a combination of seismic data, bathymetric mapping and 3D modelling, this research has four main objectives:

(i) *examine glacial extent and sedimentary regimes in fjords and drowned valleys to further understand the local glaciation and sedimentation history.*

(ii) *identify potential submarine lacustrine deposits as future coring targets for high-resolution climate proxies.*

(iii) *use paleo sea levels to constrain paleo shorelines during the last glacial maximum.*

(iv) *characterise the eroded eastern shelf platform during the last glacial maximum and sea level lowstand.*

1.5 Approach •

Advancing on the collected data sets, the work undertaken at the Auckland Islands will assess glacial ice progression during the last glacial period, associated sedimentary deposits and processes, as well as assessing the emergent landmass. This research acts as a case study that can be compared to other sub-Antarctic localities in the Southern Hemisphere during glacial periods. The findings will provide glaciation constraints, sedimentary regimes and exposed lowstand landmasses for the understudied Auckland Islands (and sub-Antarctic region in general), achieved through geophysical methods.

Seismic surveying is an effective means for imaging sub-surface topography and sedimentary deposits otherwise not observed. These methods can be used to describe the distribution and morphology of buried bedrock surfaces with associated stratigraphic infill. Over 1200 km of processed and interpreted multichannel seismic data make it possible to identify sedimentary facies, buried bedrock surfaces, and allow for seismic velocity control. This control constrains the physical properties of sediment within the fjord basins and incised valleys to provide insights into formation and sedimentation mechanisms. This has implications for characterising paleo ice extent. Reconstructions of coastal fjords, offshore exposed topography and infill stratigraphy during sea-level low stands can identify localities where lacustrine/glacial-lacustrine deposits may occur, separate from marine influences. Lacustrine deposits act as dynamic response systems that capture fine terrestrial sediments which archive environmental, climatic and tectonic forcings into a continuous, high-resolution record of local and regional changes (Gierlowski-Kordesch and Belts, 2006).

Multibeam bathymetric data at sub-Antarctic localities have been effectively used to evaluate ice extent and associated processes using geomorphological evidence (e.g. Graham et al. 2008; Hodgson et al. 2014). Multibeam data are now a standard method for characterising localities that were recently glaciated as the technique provides high-resolution maps over large areas of the seafloor. This allows for the characterisation of previous glacial flow extents based on glacial geomorphology and textural seabed attributes to infer particular glacial processes. Recently acquired multibeam bathymetric data at the Auckland

Islands will be used to complement seismic survey data using specific modelling software. This will help identify seafloor morphological expressions and glacial features, as well as seafloor sediments within fjord systems and on the eastern shelf. This will allow for a re-evaluation (with improved imagery at greater detail) of the Auckland Islands paleo-shorelines during glacioeustatic low stands, identification of seafloor sedimentary variability in relation to ice extent and an assessment of available terrestrial habitats during these periods of lower global sea levels.

1.6 Thesis Outline •

This thesis commences with chapters on the climate and known glacial history (2) of the Auckland Islands with respect to the wider Southern Ocean. This understanding is vital for understanding changes in surface processes on the Auckland Islands and the surrounding shelf during the Quaternary. Subsequently, the regional geology (3) of the study area is discussed as the framework for these processes and is a historical link to research at the Auckland Islands. A brief literature review (4) is presented using research of similar geophysical approaches at glaciated margins as an analogue for this research. The seismic and bathymetric methods used (5) within this research are explained to give context and reasoning to the chosen acquisition methods and how they will contribute to the research. The imaged fjords and incised offshore valleys are subsequently described (6) and presented with seismic facies allocation in combination with bathymetry data of individual surveyed localities. These findings are interpreted using previous research as analogues for the described results at the Auckland islands (7). These interpretations are used to answer the main objectives of the research described in section *1.4*.

Chapter 2 •

Climate & Glacial History

2.1 Modern Climate •

The Auckland Islands lie within the transition from the relatively warmer waters of the Subtropical Convergence in the north to the cooler waters of the Antarctic Convergence in the south (*Figure 2.1*). This zone between oceanic fronts creates large mid-latitude depressions that form every five to six days (Streten 1988). This results in incessant westerly wind flows, heavy seas and moderate to high precipitation with over 300 expected rain days per annum (*Table 2.2*) (DeLisle 1965). Although never officially measured at the Auckland Islands, sunshine hours (from Campbell Island) and total solar radiation are low due to the persistent cloud cover that characterises the New Zealand sub-Antarctic Islands (*Figure 2.4*).

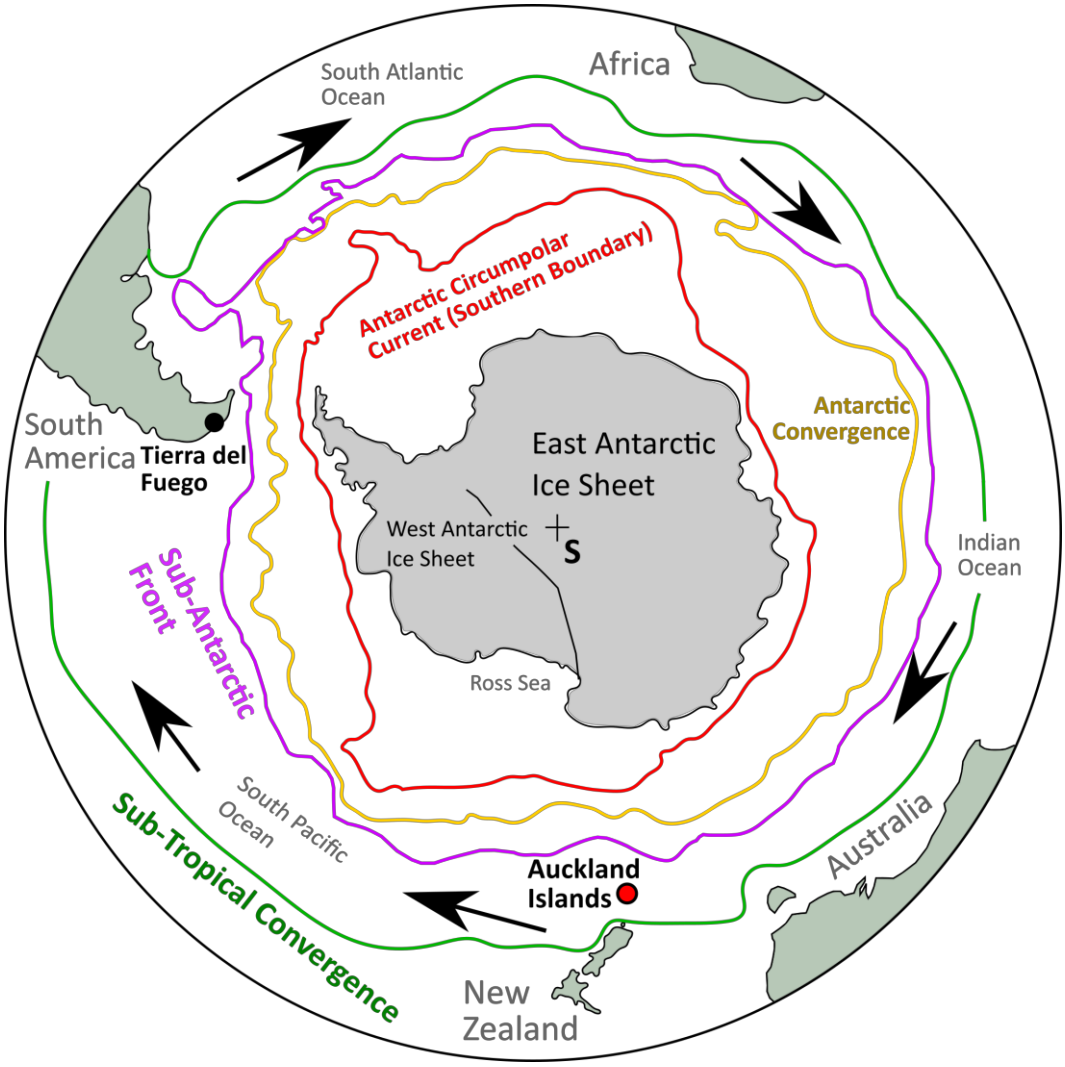

Figure 2.1 • Map of the extreme southern latitudes in the Southern Hemisphere. Locality of the Auckland Islands is shown relative to the Sub-Tropical Convergence (**green**), sub-Antarctic Front (**purple**), Antarctic Convergence/Polar Front (**yellow/orange**) & the Antarctic Circumpolar Current (**red**). Westerly wind circulation direction is indicated by the black arrows. (Derived from Hodgson et al. 2014).

January (Summer) Average Temp. (°C)	June (Winter) Average Temp. (°C)	Average Sea Surface Temp. (°C)	Average Wind Speed (km/h)	Average Precipitation (mm/year)	Average Sunshine Hours (hours/years)
11.2	5.4	7.5 - 8.1	~41 - ~61	1500-2100	664

Table 2.1 • Available climate data for the Auckland Islands. Average wind speed not available, data from Macquarie & Campbell Islands (De Lisle, 1965). Average sunshine hours from Campbell Island (New Zealand Meteorological Service 1973). Other values from McGlone et al. (2000).

2.1.1 Southern Hemisphere Westerly Winds •

The Southern Hemisphere westerly wind belt (SHWW) (35°S – 60°S) is a prominent driver of global ocean circulation and is tightly coupled with mid- to high-latitude climate dynamics (DeLisle 1965; McGlone et al. 2000; Varma et al. 2012). Deep water up-welling in the Southern Ocean, driven by the westerlies, exerts a critical influence on global ocean circulation and global climate through the subsequent release or draw-down of CO_2 (Toggweiler & Samuels, 1995; Rahmstorf & England 1997). Due to the unique location of the Auckland Islands within the circumpolar westerly belt in the Southern Ocean, the relatively small landmass is subjected to an extreme oceanic climate year round. The climate exhibits narrow temperature changes between austral summer and winter, which is mediated by the strong persistent westerly winds. The position and intensity of the wind belt varies over

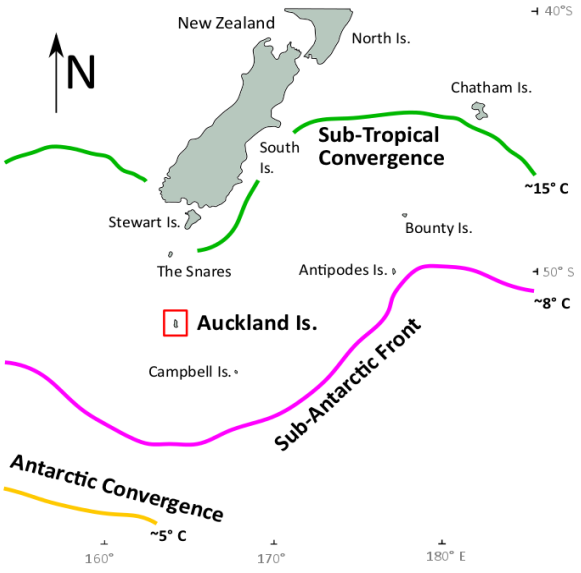

Figure 2.3 • (**Left**) Position of Auckland Islands between the Sub-Tropical Convergence to the north and the Sub-Antarctic Front to the South (Nelson et al. 1993), **Figure 2.4** • (**right**) a typical day in the Auckland Islands looking west down Norman Inlet, with strong westerly winds, cloudy skies and intermittent precipitation.

different timescales (Varma et al. 2012). Seasonally, during the austral winter, the wind belt extends northward with decreasing wind intensities at the core, while during summer the belt contracts and the core wind intensifies. These variations are a function of changing sea-surface temperatures between austral seasons (Lamy et al, 2010). Multi-centennial shifts are observed over larger timescales, correlating with stronger/weaker winds and increased/decreased precipitation respectively (Markgraf et al. 1992; Lamy et al. 2001; 2010). These larger changes over glacial and inter-glacial timescales are influenced through orbital cycles and subsequent changes of incoming solar radiation (Milankovitch 1941).

2.2 Paleoclimate - Quaternary & the Last Glacial Maximum •

The Quaternary period (2.588 Ma – present) (*Figure 2.5*) in the Southern Hemisphere is characterised by orbital variations with respect to incoming solar radiation to Earth. These variations resulted in a succession of glacial advances and retreats over varying timescales. Successions of orbital variations are termed 'Milankovitch cycles' and can occur on 41 (obliquity) and 100 (eccentricity) thousand year cycles (Milankovitch 1941; Bennett 1990). Today, glaciers and ice sheets are estimated to encompass 28.55 x 10^6 km^3, correlating to about 10% of the Earth's surface (Marshall 2005). However during the last glacial maximum (LGM) between 26.5 – 19 ka (Clark et al. 2009), the total ice volume at its peak was estimated by Denton & Hughes (1981)

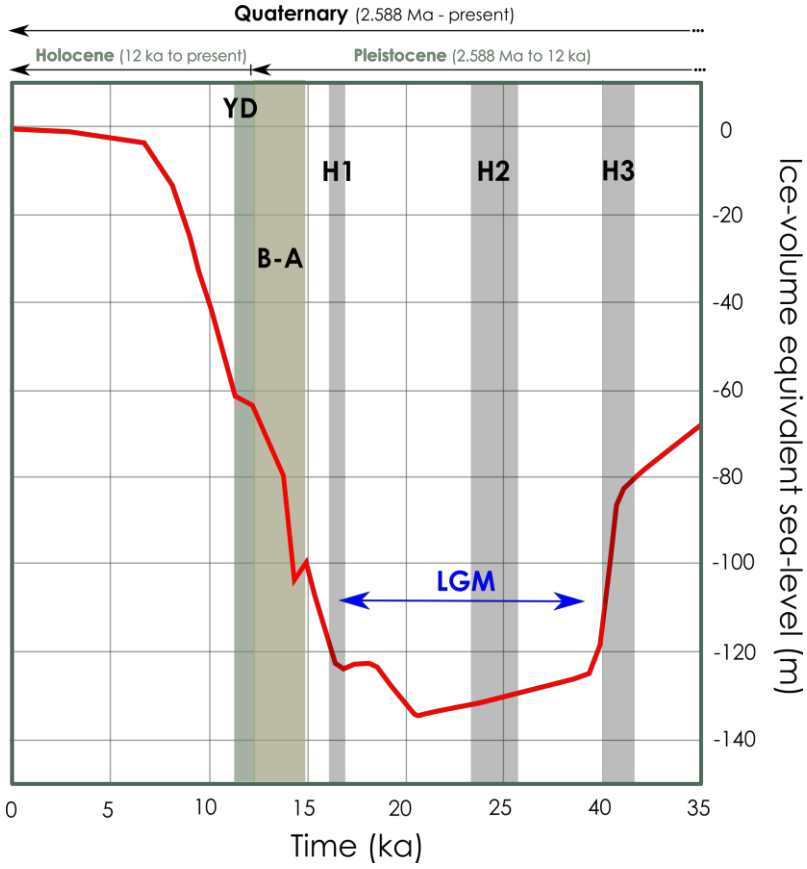

Figure 2.5 • Simplified equivalent sea level (metres) over the past 35,000 y. Also shown is the major climatic events during this period. Last glacial maximum (LGM), Heinrich events H1 to H3 (massive ice sheet carving events into the global ocean), Bølling-Allerød warm period (B-A) and the Younger Dryas cold period (Y-D). (Adapted from Lambeck et al. 2014)

to be on the order of 2.5 times larger than present day ice cover. The glacioeustatic lowering of sea level preceding the LGM is estimated to have reached around 120 m below current-day sea level as inferred from oxygen-isotope records, raised marine terraces, and reefs (Fairbanks and Matthews, 1978; Shackleton 1987; Pinter and Gardner, 1989).

Previous research at the Auckland Islands (e.g. Fleming et al. 1976; McGlone 2002 and Quilty 2007) affirmed a presence of extensive LGM glaciers that were dominant over the Auckland Island landmass with radial drainage patterns centred around former Oligocene/Miocene shield volcanoes (*Figure 1.2*) (Quilty, 2007; Hodgson et al. 2014). However, the presence of modern endemic biota rules out complete glaciation cover during the LGM (Hodgson et al. 2014). First outlined by Speight and Finalyson (1909), the impressive abundance of glacial features discussed in section *1.2.1* is evident of extensive past glacial activity during the Late Cenozoic, although the islands are not currently glaciated. Glacial ice extent, de-glaciation timing and the emergent landmass at the Auckland Islands during the LGM and Late Cenozoic is currently poorly constrained. While the estimated combined volume of sub-Antarctic and maritime LGM glacial ice is relatively insignificant in proportion to global ice mass, sub-Antarctic and maritime ice masses are amongst the quickest to respond to rapid regional warming (Gordan et al. 2008; Cook et al. 2010). These ice masses provide a sensitive indicator of the link between the Southern Hemisphere climate and ice sheet stability (Hodgson et al, 2014).

The oldest Auckland Islands radiocarbon date is placed at ~18.5 ka, originating from glacial sediments that contain fine organics that were subsequently overlain by peat blankets on the lower slopes of the Hooker Hills (McGlone 2002) (e.g. *Figure 2.6*). This area was interpreted to be previously overrun by the Laurie Harbour/Port Ross paleo-glacier and provides an apparent minimum deglaciation age for the area following the assumed maximum ice extent of the LGM at the Auckland Islands, peaking between 26.5 – 19 ka (McGlone 2002). This 7,500 year interval correlates with the peak sea-level low stand (*Figure 2.5*) (Clark et al. 2009). De-glaciation timing at the Auckland Islands correlates with glacial

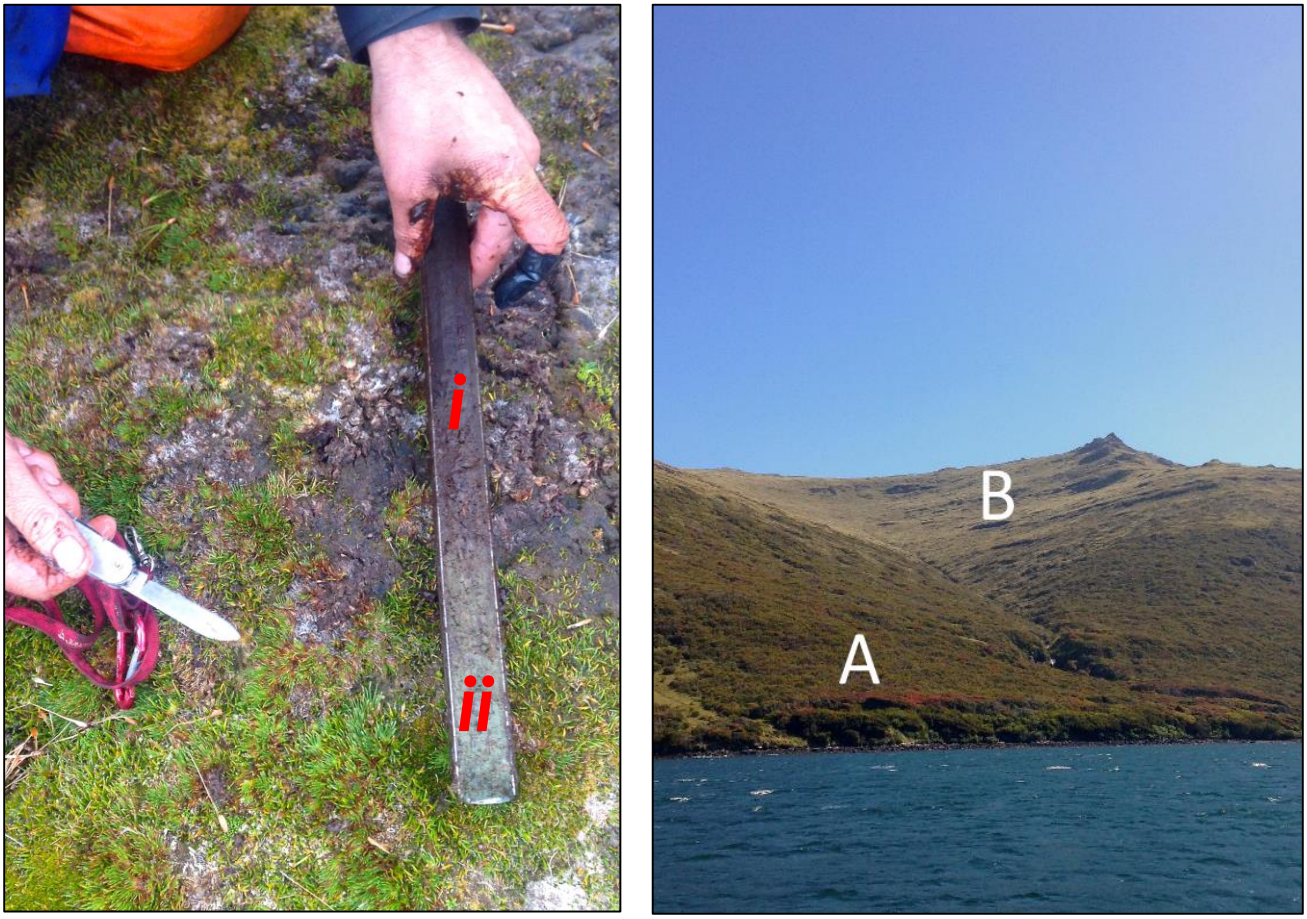

Figure 2.6 • (**Left**) Peat core sampling from the Auckland Islands, 2015. Lighter sediments at the base (**ii**) are glacial sediments, overlain by brown fibrous peat (**i**). The transition represents the end of the LGM at the Auckland Islands, **Figure 2.7** • (**right**) vegetation types on Adams Island. Woody, low-land forest (**A**), Highland shrub tundra (**B**).

retreat on mainland New Zealand (Suggate 1990). During the latest Pleistocene, the onset of an increasingly warmer climate coincided with the termination of the LGM (McGlone et al. 2000; McGlone 2002). Marine sediment cores collected from the Campbell Plateau and Campbell Rise shows a rise in sea surface temperatures (SSTs) from 18 - 11 ka, where sustained warming developed towards a rapid increase throughout the Holocene (Fenner et al. 1992; Weaver et al. 1998; Nelson et al. 2000; McGlone 2002). Sea surface temperatures in the Southern Hemisphere during the LGM were several degrees lower than today with the sub-Antarctic Front extending at least 5° north towards the Auckland Islands (Nelson et al. 1993; Nelson et al. 2000). Sea ice extending from expanded Antarctic ice sheets was known to be in close proximity to the island group (Fraser et al. 2009).

Substantial vegetation was not pronounced on the Auckland Islands until the Mid Holocene (McGlone et al. 2000; McGlone, 2002). Mountain tundra assemblages were dominant during the Late Pleistocene and Early Holocene, due to the intense oceanic setting, extensive cloud cover and relatively warmer temperatures that supported soil saturation. This made for unfavourable conditions for large woody vegetation to become established (McGlone et al. 2000; McGlone 2002). This early Holocene period in the mid-high southern latitudes is defined by warming SSTs between 11 and 5 ka and is termed the 'Holocene Thermal Maximum' (Morley & Dworetzky 1993; Renssen et al. 2012). By the Mid to Late Holocene, tall forest vegetation began to develop due to an increasingly sunny climate and clearer skies that were associated with increasing south-easterly airflow. Compared to the Early Holocene Thermal Maximum, cooler and windier conditions in the Mid Holocene prevailed, further promoting the establishment of tall forest growth in pockets of sheltered lowland sites (McGlone et al. 2000). Vegetation and climate coupling at the Auckland Islands (~51° S) is matched by other Southern Hemisphere records, for example with *Nothofagus* forests becoming established during the Holocene in Tierra del Fuego, South America (~53-56° S) (Heusser 1989; 1990) (*Figure 2.1*). Markgraf et al. (1992) argue that the common factor of these localities with respect to a delayed development of tall woody forests is due to relatively warmer climates and weakened westerlies during the Early Holocene. These conditions led to stable, humid and cloudy conditions which in an intense oceanic setting hinders evapotranspiration and leads to saturated soils with decreased forest growth (McGlone et al. 2000). Since the mid-Holocene, the establishment of lowland woody forests and highland tundra/scrub (*Figure 2.7*) has fluctuated through decline and recovery due to a strong coupling with changing climatic patterns which affect airflow, humidity, SST and precipitation (McGlone 2002). Furthermore, constraining an emergent land mass during glacial periods, especially at the LGM, has biological implications for terrestrial biota of the Auckland Islands during sea level lowstands (Hodgson et al. 2014).

Chapter 3 •

Regional Geology

3.1 Campbell Plateau •

The New Zealand Sub-Antarctic Islands group (The Snares, Antipodes, Auckland, Bounty and Campbell Islands) lie atop of an expansive extension of thinned continental crust to the south of New Zealand - the Campbell Plateau (Adams 1962; Denison & Coombs 1977; Beggs et al. 1990; Quilty 2007). Identified basement rock at various island localities in combination with petroleum exploration well data provide two classes of rock characterising the plateau basement. Dated silicic plutonic rocks (Denison & Coombs 1977; Adams 1983; Richie & Turnbull 1985; Gamble & Adams 1985; Beggs et al. 1990; Scott et al. 2015) that intrude into older Paleozoic metasedimentary rocks (Beggs 1978; Cook 1981) reflect a phase of intrusion and cooling of plutonic bodies during through the onset of the Rangitata Orogeny in mid-Cretaceous times (Aronson 1968; Adams 1983). These plutonic intrusions and low-grade quartzose metasedimentary rocks that form the Campbell Plateau basement have noted correlative localities in southern New Zealand, Australia and Antarctica (*Figure 3.1*). Exposures of plutonic granitoid bodies at NZ sub-Antarctic island localities (e.g. Auckland, Campbell and The Snares) are interpreted as younger, southern continuations of the South Island

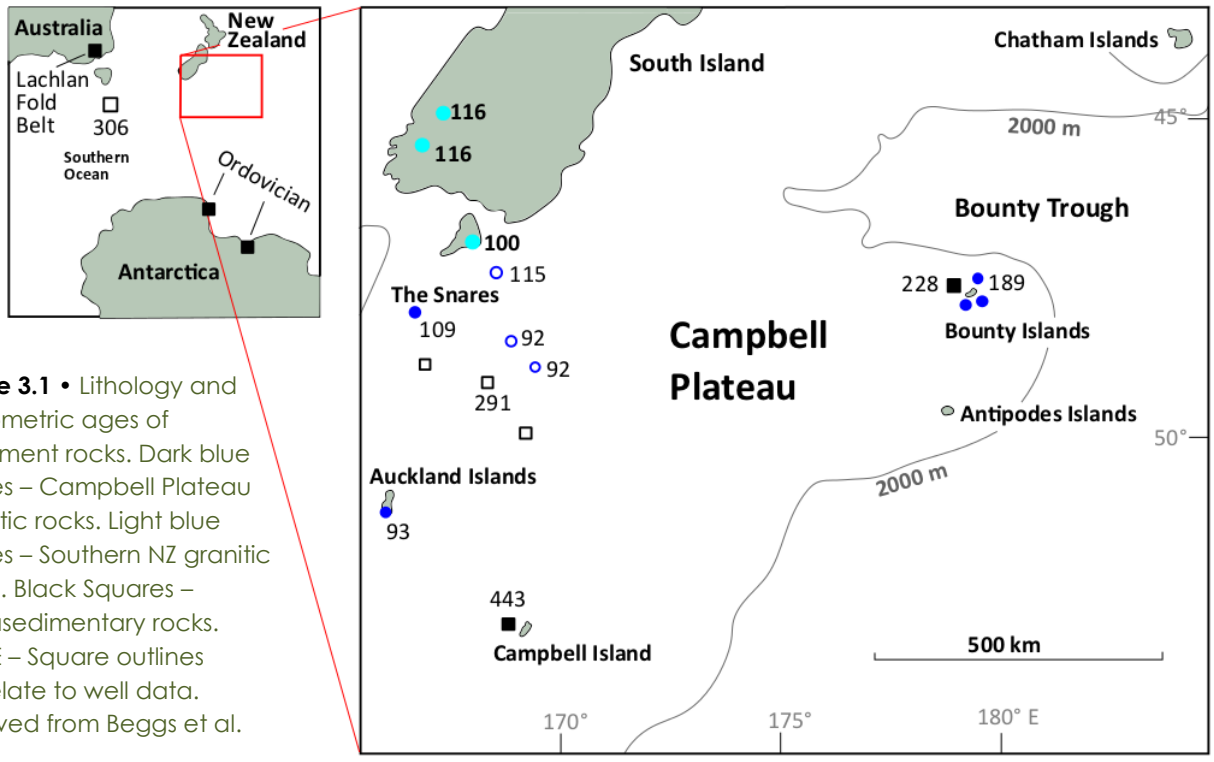

Figure 3.1 • Lithology and radiometric ages of basement rocks. Dark blue circles – Campbell Plateau granitic rocks. Light blue circles – Southern NZ granitic rocks. Black Squares – Metasedimentary rocks. NOTE – Square outlines correlate to well data. (Derived from Beggs et al. 1990)

north-south trending Mesozoic granite belt (Dennis & Coombs 1977; Adams 1983). Paleozoic metasedimentary bodies are correlated with rocks on the West Coast of the South Island (Cooper 1974), Northern Victoria Land/Marie Byrd Land in Antarctica (Cullen 1975), the Lachlan Fold Belt in Southern Australia (Cooper & Grindley 1982) and the South Tasman Rise (Beggs 1978; Beggs et al. 1990). These large-scale rock distributions exhibit a Gondwana landmass distribution, indicative of substantial regional tectonic and volcanic regimes occurring throughout the Paleozoic and Mesozoic (Denison & Coombs 1977; Adams 1983; Beggs et al. 1990; Quilty 2007).

3.2 Auckland Islands Complex •

The modern Auckland Island landmass (~625 km^2) is composed almost entirely of late Cenozoic volcanic rocks, erupted from two volcanic centres of Carnley Harbour in the south and the Ross Volcano to the North; collectively termed the Auckland Island Complex (Wright 1966, 67, 68, 70, 71; Adams 1983; Gamble & Adams 1985; Ritchie & Turnbull 1985).

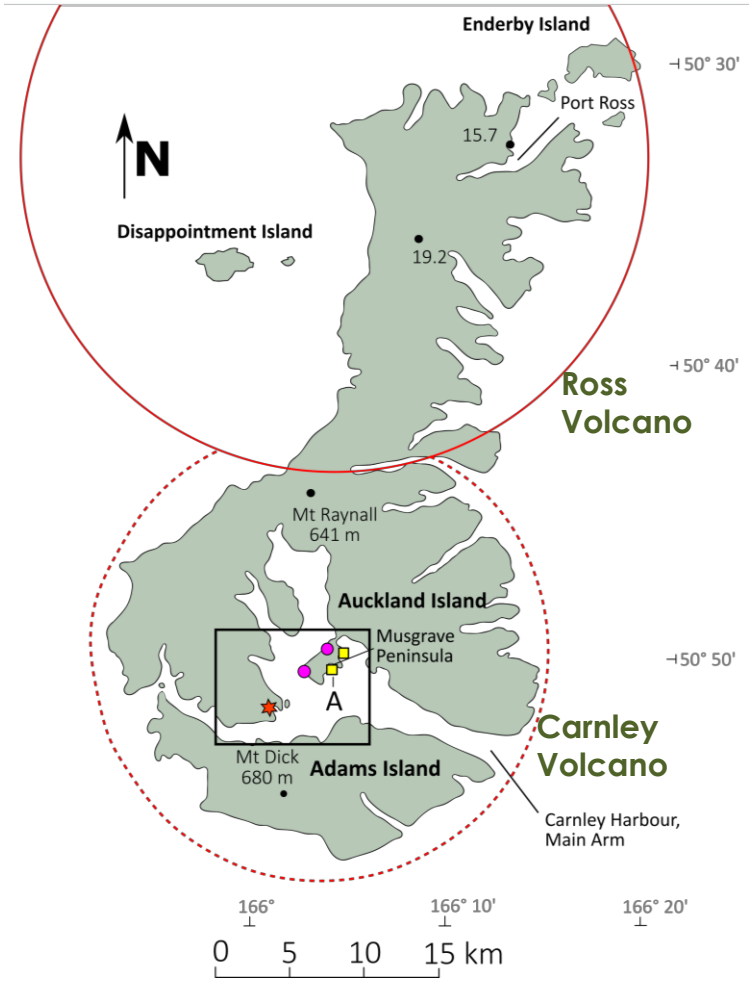

Figure 3.2 • Auckland Islands with extents of the Carnley Volcano to the south (dashed red line) and the Ross Volcano to the north (solid red line). – Derived from Gamble & Adams 1985. Red star – Camp Cove Conglomerate outcrop. Pink circle – Basement Granite outcrops. Yellow square – Musgrave Formation outcrops. Mentioned ages (ma) of Ross Volcano basalt flows.

3.2.1 Carnley Volcano •

The Carnley Volcano is a classic Cenozoic shield volcano centred in the southern region of the Auckland Islands (*Figure 3.2*). The volcano rests atop of continental basement, which in Carnley Harbour includes granite that was subsequently

overlain unconformably by a Cenozoic sedimentary sequence (*Figure 3*) (Gamble & Adams 1985; Ritchie & Turnbull 1985). The stratigraphic base of the sequence in Carnley Harbour is the Camp Cove Conglomerate (Speight & Finalayson 1909; Rickwood 1960; Cook 1981; Ritchie & Turnbull 1985). A clast supported matrix is observed, consisting of granitic material with small amounts of metasedimentary gneiss and schist, indicative of basement inputs into a fluvial or very shallow marine environment. The overlying Musgrave Formation (Ritchie & Turnbull 1985) includes variable Cenozoic sedimentary members and intercalated volcanics. Quartzofeldspathic sandstones, tuffs, grits and localised limestones with intensive dyke intrusions are reported, as well as extensive fossil fauna being present (*Figure 3.3*) (Richtie & Turnbull 1985). These Cenozoic sediments and pyroclastic rocks observed in Carnley Harbour represent a once peneplained erosional basement surface, deposited at a similar time as the then active Carnley Volcano. This signifies the establishment of a volcanic shield by the latest Oligocene (Gamble & Adams 1985; Ritchie & Turnbull 1985).

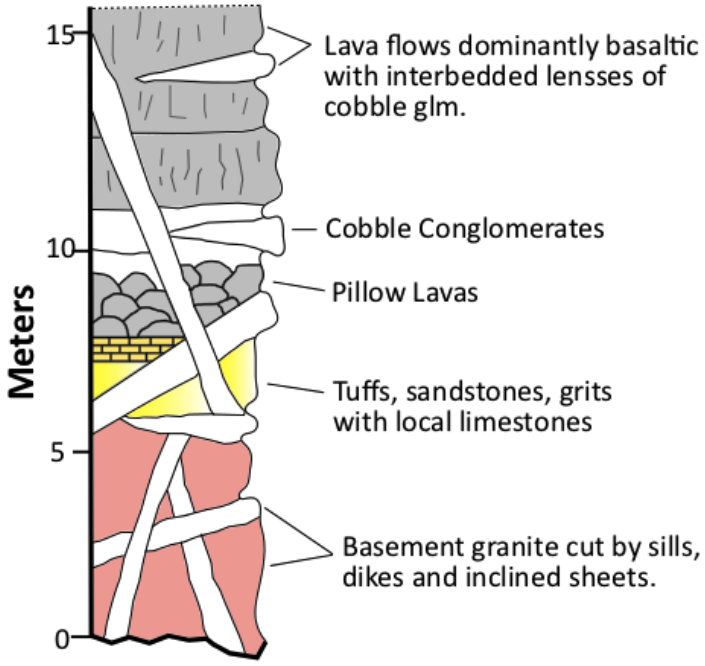

Figure 3.3 • Composite section of a volcanic and sedimentary sequence at Musgrave Peninsula (*Figure 3.2 - A*). Sequence shows dykes cross cutting granitic basement, sandstones, limestones and earlier basaltic flows. (Derived from Gamble & Adams 1985).

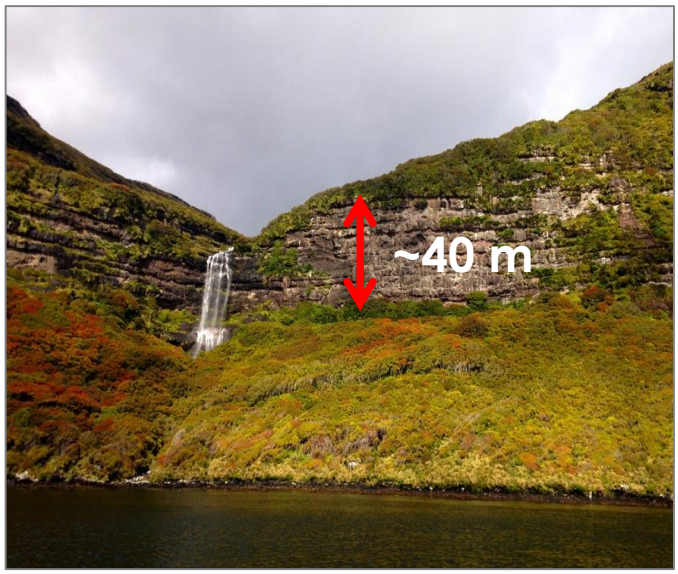

Figure 3.4 • Waterfall at McLennan Inlet with valley walls showing a sequence of laterally continuous layered basalt sheets from the Carnley Volcano.

Overlying the preceding sedimentary strata, preliminary shallow marine volcanism (pillow lavas) and sub-aerial volcanism centred on Musgrave Peninsula of the Carnley Volcano was dominant. Observed at this locality are intensive dyke swarms that intrude the basement granite, Cove Camp Conglomerate and Musgrave Formations (*Figure 3.3*). Each dyke varies in size from 1 cm to 12 m across, averaging ~1 m (Gamble & Adams 1985). Decreases in dyke intensity at other Carnley Harbour localities (McClure & Circular Head, Trinity Cove) suggests that Musgrave Peninsula in Carnley Harbour was likely the centre for dyke swarms (Gamble & Adams 1985). Among underlying localised trachytes and rhyolites, substantial outpourings of alkalinitic basalt were extensively erupted in sheet and sill like fashions, creating the characteristic layered basalts observed today at the Auckland Islands (Fleming 1959; Gamble & Adams 1985) (*Figure 3.4*). Ages for the Carnley Volcano vary between 19-37 ma (Hoernle et al. 2006).

3.2.2 Ross Volcano •

The younger Ross Volcano to the north (*Figure 3.2*) initially described by Wright, (1966, 67, 68, 70 & 71) shows many similarities stratigraphically, petrologically and chemically to the marginally older Carnley Volcano. The sequence shows rocks from the NW coast and the eastern shores of Port Ross forming a NE tilted basalt sequence with the main eruptive centre off the western coast in the vicinity of Disappointment Island (Adams 1983). The oldest dated flows from the Ross Volcano occur near Bivouac Hill and record a K-Ar age of 19.2 ma with down dip correlatives recording ages as young as 15.7 ma at Terror Cove (*Figure 3.2*) (Denison & Coombs 1977). This age difference of basalt flows is indicative of divisions between older and newer flows within the early- to mid-Miocene Ross Volcano (Adams 1983; Hoernle et al. 2006).

3.3 Cenozoic Shield Volcanism •

The approximate ages of Auckland Island volcanism are consistent with the pattern of Late Cenozoic alkali basaltic volcanism observed in southern New Zealand and the Campbell Plateau (Adams 1983, Hoernle et al. 2006). This pattern of major shield volcanoes of alkaline basalt association includes Banks Peninsula, the Dunedin Volcano, Auckland, Campbell and Chatham Islands which can be

explained through a diffuse intraplate volcanism regime (Hoernle et al. 2006). Removal/detachment of sections of the lithospheric keel beneath Zealandia resulted in asthenosphere upwelling and subsequent decompression melting at localized specific regions in southern New Zealand and on the Campbell Plateau (*Figure 3.5*) (Hoernle et al. 2006).

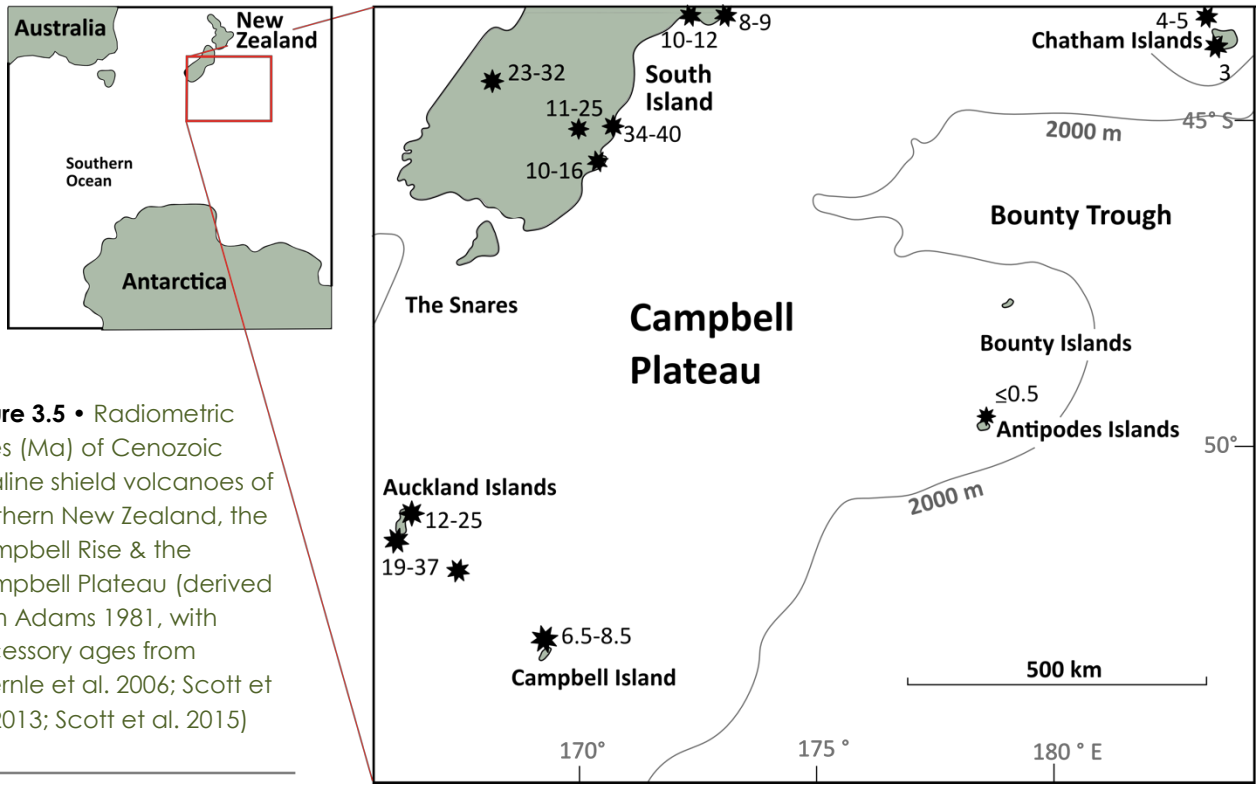

Figure 3.5 • Radiometric ages (Ma) of Cenozoic alkaline shield volcanoes of southern New Zealand, the Campbell Rise & the Campbell Plateau (derived from Adams 1981, with accessory ages from Hoernle et al. 2006; Scott et al. 2013; Scott et al. 2015)

Chapter 4 •

Literature Review

Advances and retreats of continental scale ice sheets in the Northern Hemisphere during Pliocene/Pleistocene times dramatically altered the topography of the Earth's surface (Ehlers et al. 1990). Extensive work has been undertaken to investigate such glacial effects in and around the margins of the North Sea, the north-west coast of the United Kingdom, Canada and the northern United States. These studies classify and describe glaciated landforms (e.g. fjords and buried incised valleys) that originated beneath continental scale ice sheets (Piper et al. 1983; Huuse & Lykke-Anderson 2000; Kluiving et al. 2003; Praeg 2003; Ahmad at el. 2009; Jansson & Näslund 2009; Hjelstuen et al. 2009; Jordan 2010; Stewart et al. 2013). Research undertaken at the Auckland Islands that focuses on fjords and offshore incised valleys can draw on the results of these Northern Hemisphere studies. The methods and approaches used by these authors can be applied as analogues for classification and interpretation of features observed at the Auckland Islands.

4.1 North Sea •

Buried tunnel valleys (elongated, deep, U-shaped incisions formed from subglacial meltwater occurring under continental ice sheets – Van der Vegt et al. 2012) in and around the margins of the North Sea have been extensively mapped and studied (e.g. Huuse & Lykke-Anderson 2000, Kluiving et al. 2003; Praeg 2003; Stewart et al. 2013). This is due to the large amounts of available 2-D and 3-D seismic survey data originally acquired for groundwater and petroleum exploration in deeper formations. Huuse et al. (2001) interpreted over 6400 km of offshore 2-D high-resolution multichannel seismic data in combination with 18,000 km of conventional seismic profiles. Regional maps were created (*Figure 4.1*) that portrayed the intricate patterns of buried tunnel valleys. The maps showcased the interior structure and correlating stratigraphy with accompanying well control in places (*Figure 4.2*). These buried tunnel valleys show some similarities to offshore incised valleys observed at the Auckland Islands. Morphologies observed in some

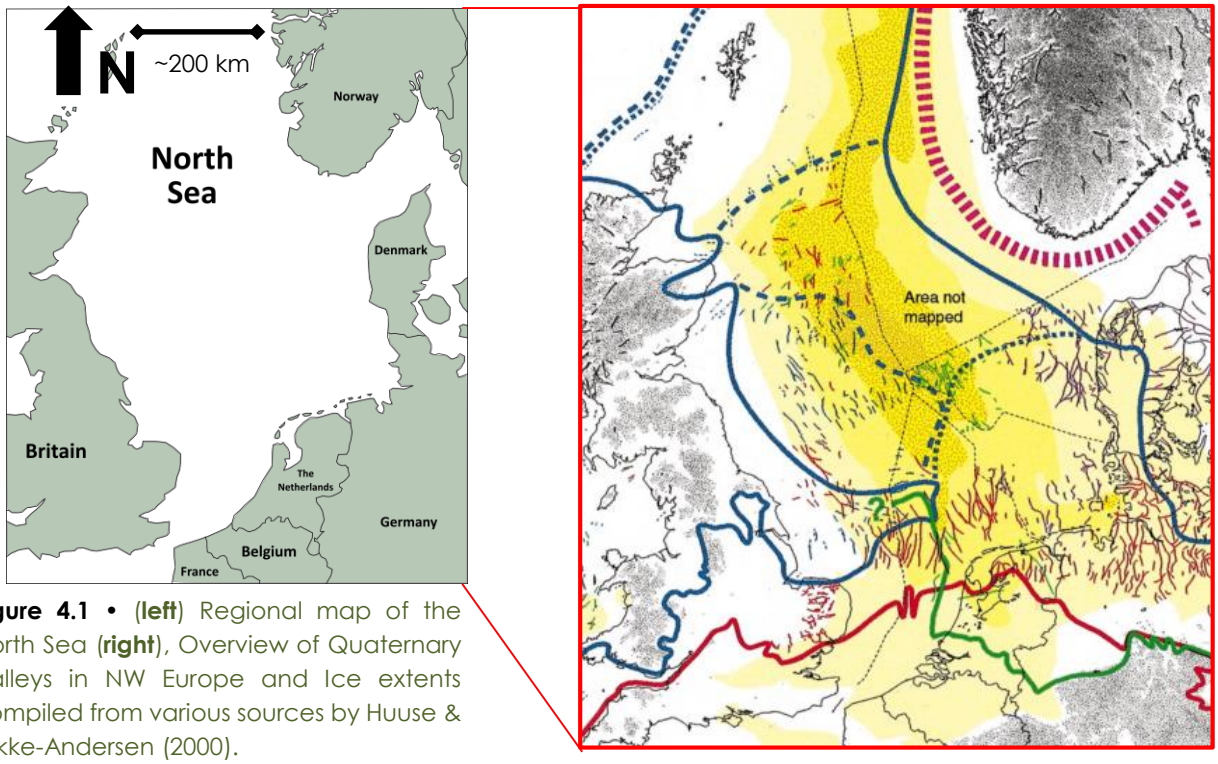

Figure 4.1 • (**left**) Regional map of the North Sea (**right**), Overview of Quaternary Valleys in NW Europe and Ice extents compiled from various sources by Huuse & Lykke-Andersen (2000).

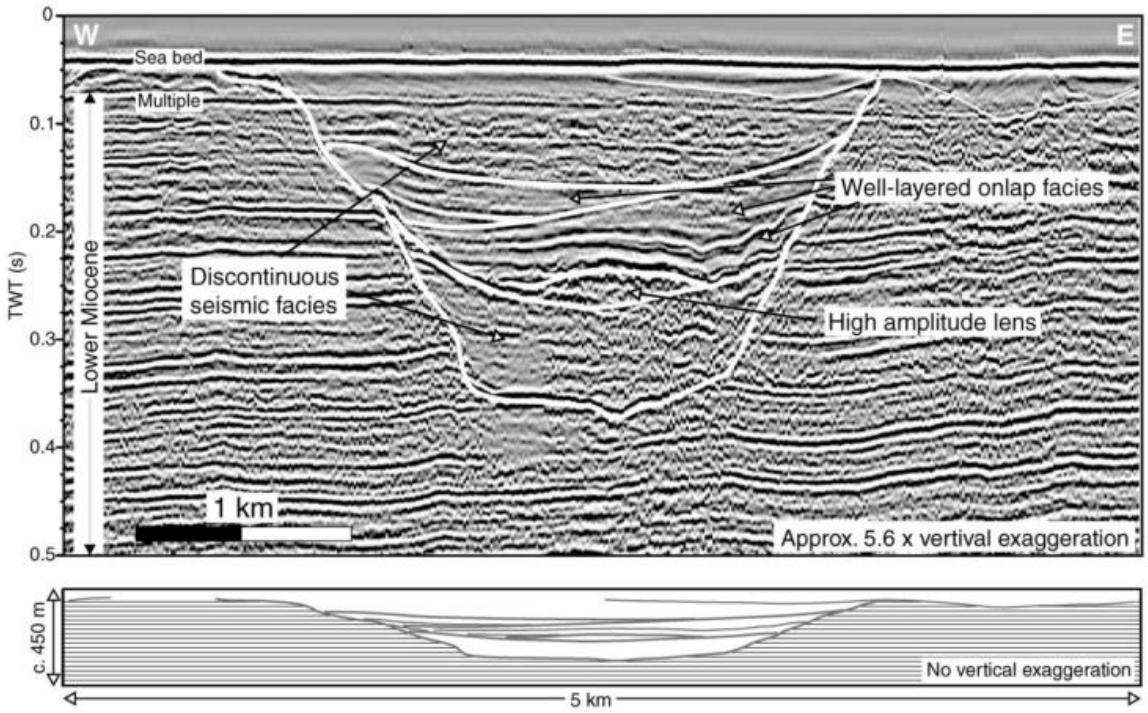

Figure 4.2 • Interpreted, high-resolution seismic profile from Huuse & Lykke-Anderson (2000) exhibiting a buried Quaternary valley situated in the North Sea.

of these features in the North Sea have comparable characteristics with some cases of similar in-fill stratigraphy. There are however some notable differences between the two settings. Valley shoulders in the North Sea examples generally are positioned 10-50 m below the seafloor, and can be hidden by seafloor multiples (Huuse & Lykke-Andersen 2000). Valley ridges at the Auckland Islands are generally

level with the modern seabed with some seafloor expression observed in places (i.e., not completely infilled). The infill stratigraphy observed within the North Sea examples varies from entirely chaotic packages to well-layered, on-lapping sequences. Typical sequences exhibit a chaotic/disrupted facies at the base, succeeded by a well-layered unit that progresses to a thin, seismically disrupted facies at the top (Huuse & Lykke-Anderson 2000). This sequence package is typical for North Sea buried valleys and is comparable to other northern European Quaternary deposits. These consist of glacio-fluvial sand and silt, ensued by glacio-lacustrine/marine silt and clay, capped by thin interglacial deposits (e.g. Ehlers et al., 1984; Ehlers and Linke, 1989). Formation mechanisms for buried valleys in the North Sea and other former lowland glaciated areas are debated; however there a many hypotheses in relation to valley formation: (1) steady-state sub-glacial drainage of meltwater and groundwater driven by hydrostatic pressure gradients, (2) catastrophic meltwater discharge, (3) glacial erosion, (4) erosion by rivers during glacioeustatic lowstands, (5) aggradation (stacking) of delta channels and (6) tidal scour (Huuse & Lykke-Anderson 2000). It is thought that origins of these valleys involve a combination of these mechanisms. A general consensus on the timing of valley formation converges on the last three major continental glaciations through the Pleistocene (Huuse & Lykke-Anderson 2000), however evidence of earlier glaciations has likely been over-printed by more modern advances.

It is also important to note the contrasting host-rock setting between the two localities. The North Sea tunnel valleys host rock is Mesozoic/Cenozoic soft rock sediments which is more easily eroded than the Mid-Cenozoic hard rock volcanics at the Auckland Islands. The classification of stratigraphy, morphology and formation processes used in various seismic studies in the North Sea will be used as analogues for research and classification at the Auckland Islands

4.2 Western Scotland •

Seismic surveys from Scotland's coastal lochs have numerous similarities to fjord data observed at the Auckland Islands. Howe et al. (2002) presented results from a high-resolution seismic and gravity coring survey undertaken within a deep sea loch on Scotland's western coast (*Figure 4.3*). The study focused on defining facies

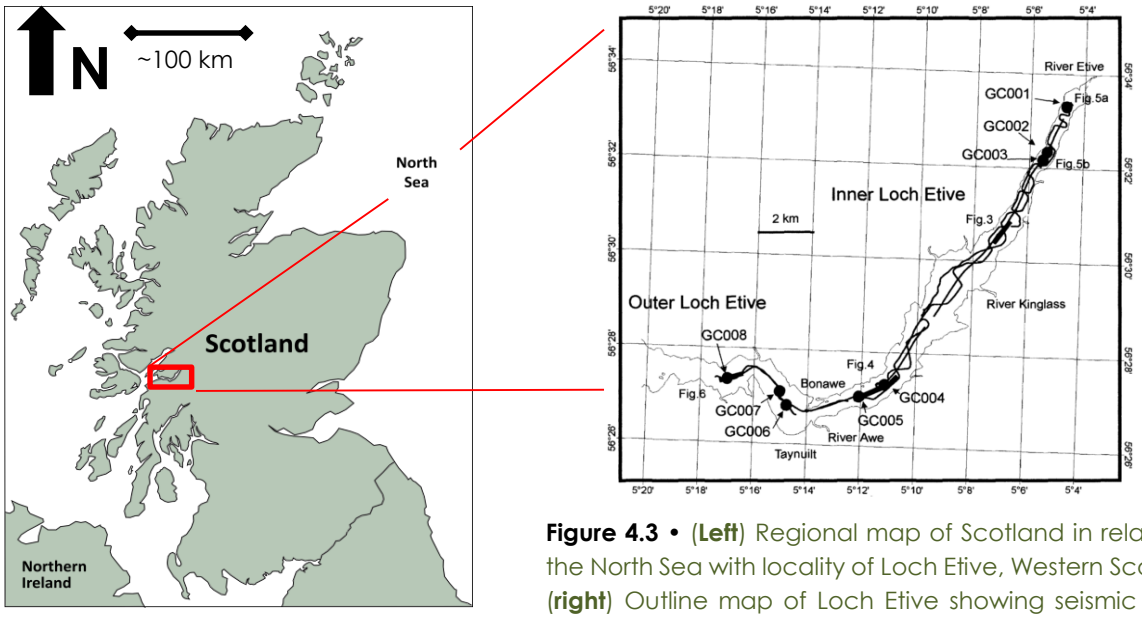

Figure 4.3 • (**Left**) Regional map of Scotland in relation to the North Sea with locality of Loch Etive, Western Scotland, (**right**) Outline map of Loch Etive showing seismic survey transects of the inner and outer basins within the loch.

within the sediments to examine high-resolution records of Holocene climate change and de-glaciation processes. The glacial loch exhibits an over-deepened profile, eroded by the flow of ice from Quaternary glaciation successions. During the Younger Dryas, ice extended the whole length of the loch (Howe et al. 2002)

An initial seismostratigraphy (i.e interpretation), constructed through seismic profiles, reveals two broad seismic facies that are partitioned by a well-defined reflector (*Figure 4.4*). An older, deeper sequence 'A', unconformably rests atop the eroded bedrock and is the most wide-spread facies within the loch. This facies displays well-laminated to transparent reflections with an intricate inner geometry. On-lapping and truncated reflections are also observed. The horizons within this facies display a draped appearance that resembles the form of the underlying bedrock. This type of sedimentary deposition within Loch Etive is extensively observed in fjords and offshore valleys at the Auckland Islands. Facies 'A' is succeeded by a younger, shallower sequence 'B'. This facies is highly reflective and smaller chaotic sub-facies are observed within the main body. 'A' and 'B' are separated by a well-defined reflector termed 'E1', which is observed through the length of the loch. The changing sedimentary stratigraphy with depth reflects different dominant sedimentary processes through late Pleistocene and early Holocene. Howe et al. (2002), established that the well-laminated/transparent

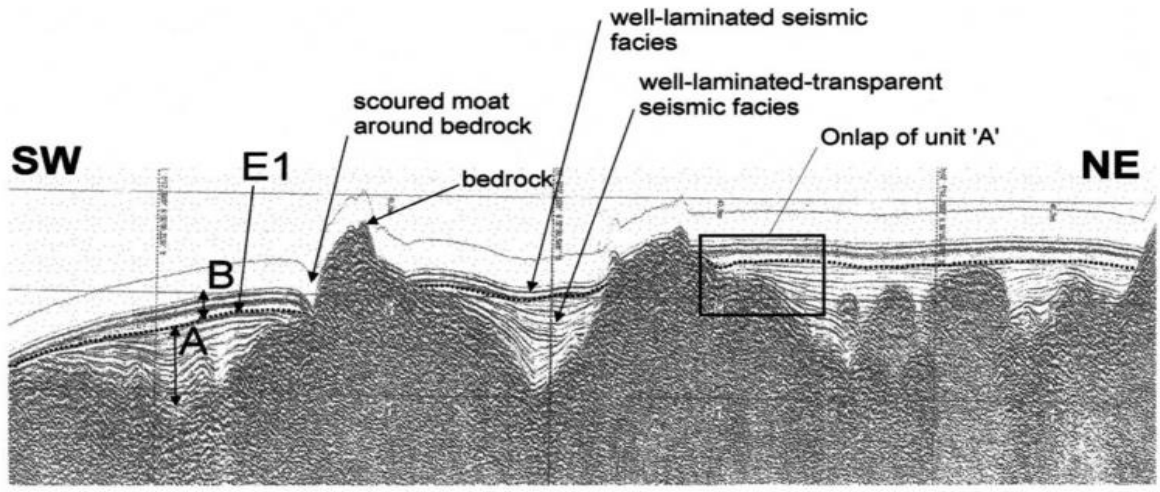

Figure 4.4 • Sub-surface seismic reflection profile from Loch Etive showing general geometry and stratigraphy. '**A**' – Well-laminated to transparent facies with on-lapping, '**B**' – well laminated facies. The '**E1**' reflector separates the two facies.

facies 'A' may have been deposited as a result of a 'variety of proximal glacio-marine processes'. This is indicated by on-lapping reflections interpreted to represent fine grain sediments that become trapped within a proximal glacial lacustrine system during de-glaciation. The overlying facies 'B' is interpreted to be an outcome of riverine inputs where deposition occurs from suspension and settling out once the energy of the system decreases. Various sub-facies that are observed as lens shaped pods are the result of direct river bed-load inputs that flow into the loch. The sedimentary stratigraphy observed through seismic data and gravity cores exhibit a de-glaciation succession since Loch Etive became ice free ~ 10 ka (Howe et al. 2002). Howe et al. (2002) describes this de-glaciation sequence at Loch Etive to be a simple two-stage process: (1) initially the glaciated loch was isolated from the sea and became a sink for glacio-lacustrine sedimentation during glacial retreat, (2) the modern sedimentation regime within the loch is dominated by river run-off and suspension deposition processes. The change within this two-stage process, separated by the reflector 'E1' may have been abruptly brought about by the transition to a fully open marine loch.

The seismic survey and gravity core study undertaken at Loch Etive, Western Scotland is a compatible analogue for Auckland Islands research. Similar features within the seismic data are observed and timing of sedimentary processes are known to occur on similar timescales during the late Pleistocene/early Holocene.

4.3 Maritime and sub-Antarctic Islands •

An extensive review undertaken by Hodgson et al. (2014), aimed to combine existing literature on maritime and sub-Antarctic island glaciation. The review summarised and classified Late Quaternary glaciation histories at numerous localities (30-70° S), with wider implications for Antarctic Ice Sheet reconstruction during this period. These localities are of significant importance due to island climates being closely coupled with the SHWW belt and the Southern Ocean climate. Due to this coupled relationship, sub-Antarctic and maritime Antarctic ice masses are the first to respond to regional warming and climate fluctuations (Gordon et al. 2008; Cook et al. 2010). This review found few high-quality

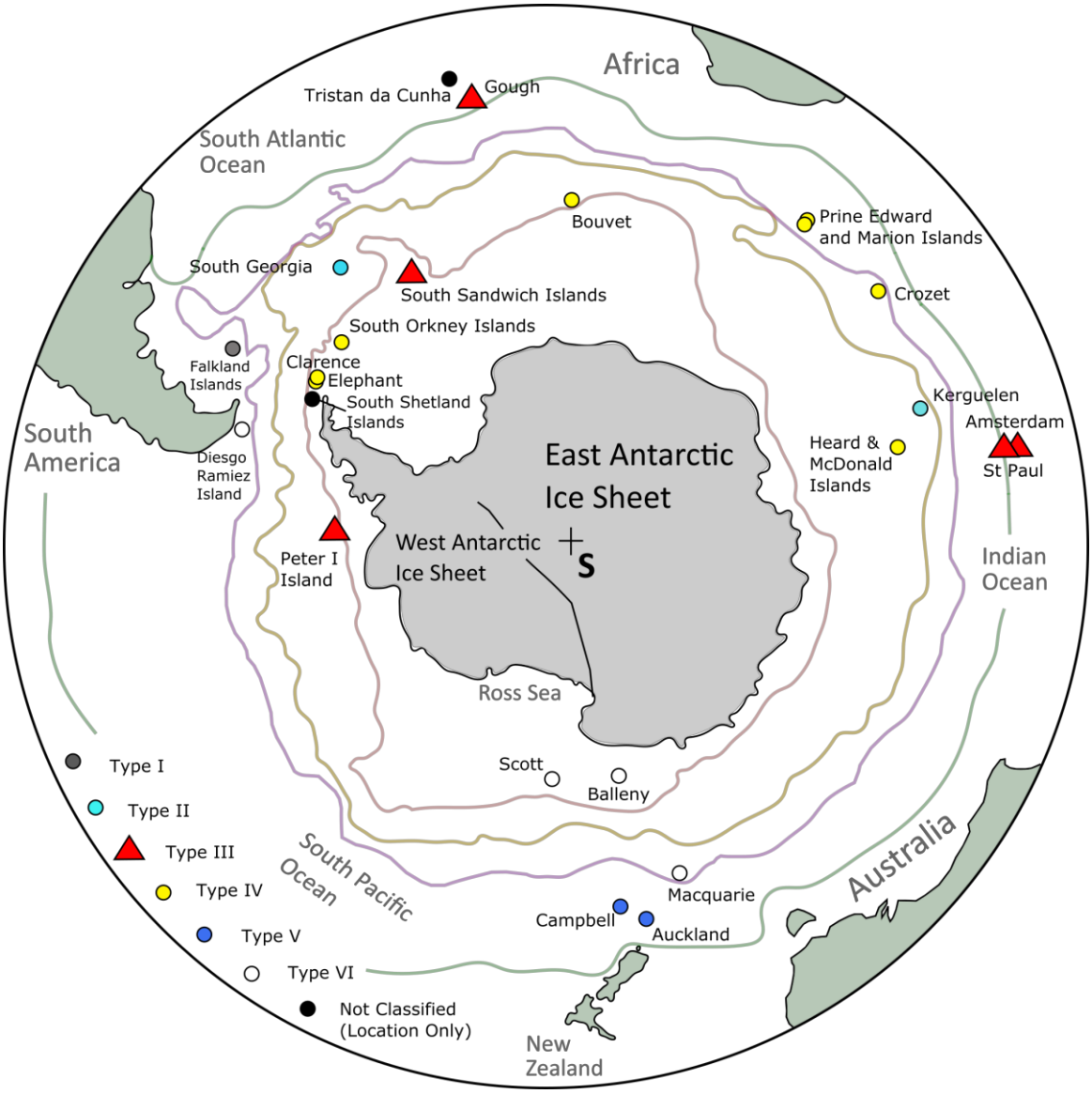

Figure 4.5 • Map of the extreme southern latitudes showing particular sub-Antarctic and maritime Antarctic Islands described and classified in an extensive glacial history review by Hodgson et al. (2014). Derived from Hodgson et al. 2014). Position of water mass boundaries are present (from the outside in), sub-Tropical Convergence (green), sub-Antarctic Front (purple), Antarctic Polar Front (yellow) and the Antarctic Circumpolar Current (red).

chronological constraints of glacier extent variability during Late Quaternary times in the sub-Antarctic and maritime Antarctic sector. In spite of this, Hodgson et al. (2014) proposed a classification scheme for sub-Antarctic and maritime Antarctic islands based on LGM ice extent, prior LGM glacial history as well as climate and topographic components that dictate glacial ice formation. This classification scheme is divided into the following categories: (*Figure 4.5*).

- Type I – Islands that accumulated little or no LGM ice.
- Type II – Islands with a limited LGM ice extent but evidence of extensive earlier continental shelf glaciations.
- Type III – Seamounts and volcanoes unlikely to have accumulated significant LGM ice cover.
- Type IV – Islands on shallow shelves with both terrestrial and submarine evidence of LGM (and/or earlier) ice expansion.
- Type V – Islands north of the Antarctic Polar Front with terrestrial evidence of LGM ice expansion.

The Auckland Islands are currently classified as Type V, due to the terrestrial geomorphological evidence of extensive prior glaciation and current understanding of LGM expansion. In-depth interpretation of acquired seismic and bathymetry data combined with subsequent outcomes of this research may enable the re-classification of the Auckland Islands under these classification guidelines for sub-Antarctic and maritime Antarctic islands.

Chapter 5 •

Methods

5 Methods •

5.1 Seismic Reflection & Bathymetric Surveying

An extensive series of high-frequency seismic reflection surveys has been undertaken in the Auckland Islands aboard the University of Otago's research vessel *Polaris II (Figure 5.1*). An inaugural survey in 2014 at the Auckland Islands (expedition 14PL001) identified and imaged an intricate system of buried incised valleys on the eastern shelf. Extensive surveying of northern, eastern and southern fjords was also undertaken. The surveyed fjords and offshore incised topography are characteristic of many high-latitude localities around the world (Farmer & Freeland 1983). However seismic data at these latitudes in the Southern Hemisphere, especially at maritime and sub-Antarctic localities is sparse. Seismic surveying was undertaken during expeditions 14PL001, 15PL001 and 16PL119 that spanned three seasons (2014-16) (*Figure 5.2*). The acquired data provides new insights into offshore subsurface features in correlation with previous information. This will allow for more detailed observations and interpretations of Quaternary glaciation, sedimentary processes and associated climate parameters at the Auckland Islands. These seismic reflection data will contribute to a growing, but limited number of these investigations at similar latitudes in the Southern Hemisphere.

Figure 5.1 • University of Otago's *R/V Polaris II* (21 m) starboard side in the Northern Arm of Carnley Harbour, Auckland Islands. The Polaris II accommodates up to 15 people, with a range to service the Chatham and sub-Antarctic Islands. Facilities are equipped to support an extensive range of geological and geophysical undertakings, as well as various marine biological and oceanographic activities.

This chapter provides details of the acquisition methods used during the 14PL001, 15PL001 and 16PL119 expeditions. Technical details and deployment of the seismic acquisition system, with its associated data sets are described and explained. A further holistic overview of seismic data processing within particular software packages is also described.

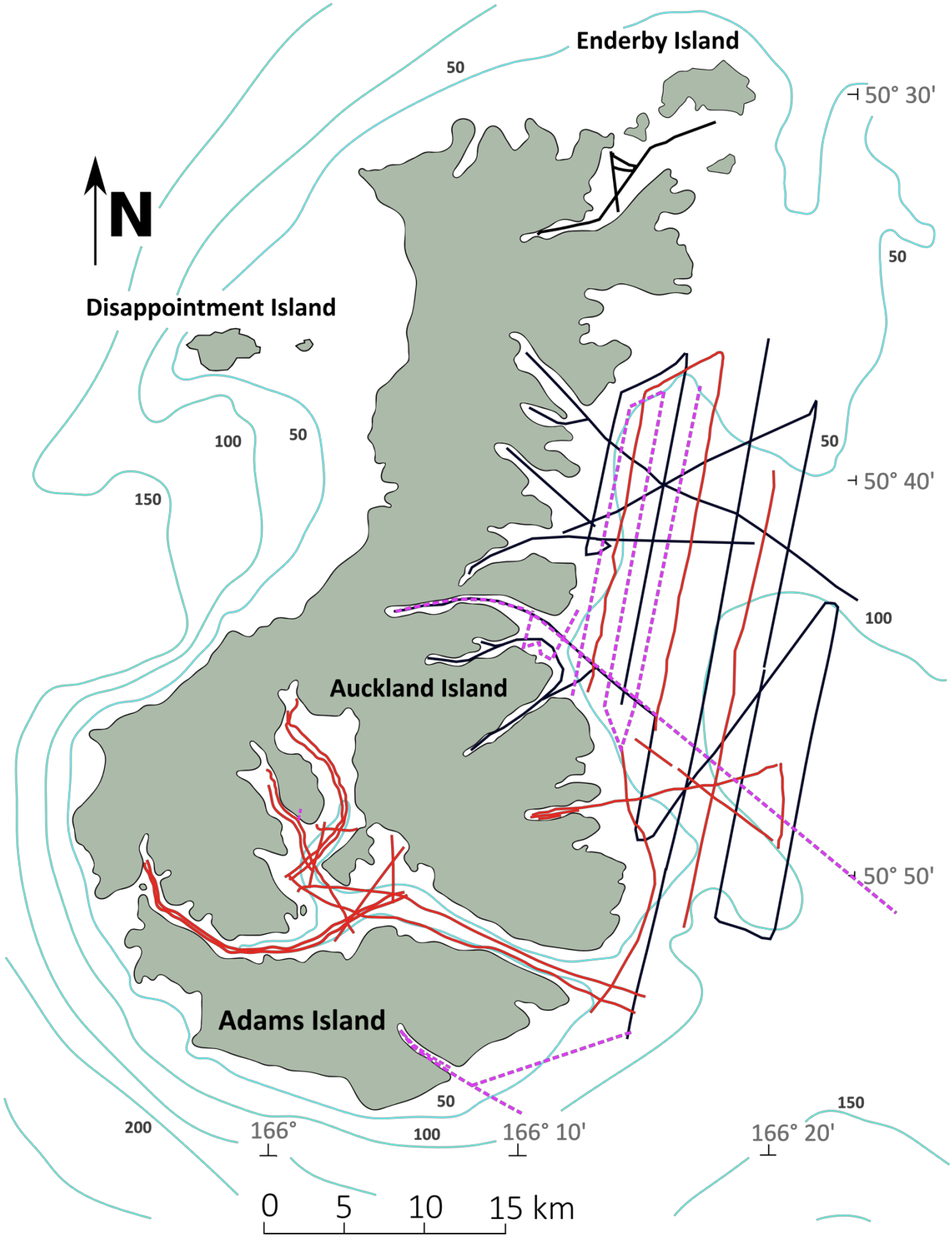

Figure 5.2 • Seismic survey transects of 14PL001 (**solid black**), 15PL001 (**solid red**) and 16PL119 (**dashed purple**) presented against bathymetry (m) at the Auckland Islands. 15 transects from 16PL119 and 24 transects (~308 km) from 15PL001 are included in the southern and eastern regions of the Auckland Islands in addition to previous 75 seismic lines to the north (> 400 km – 14PL001).

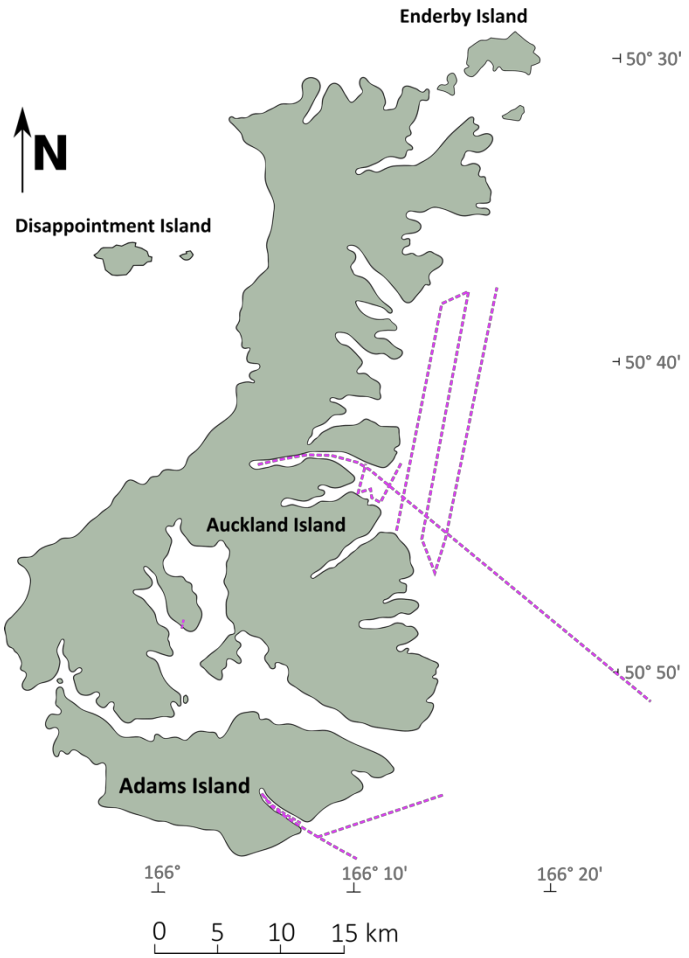

Figure 5.3a • 16PL119 survey transects.

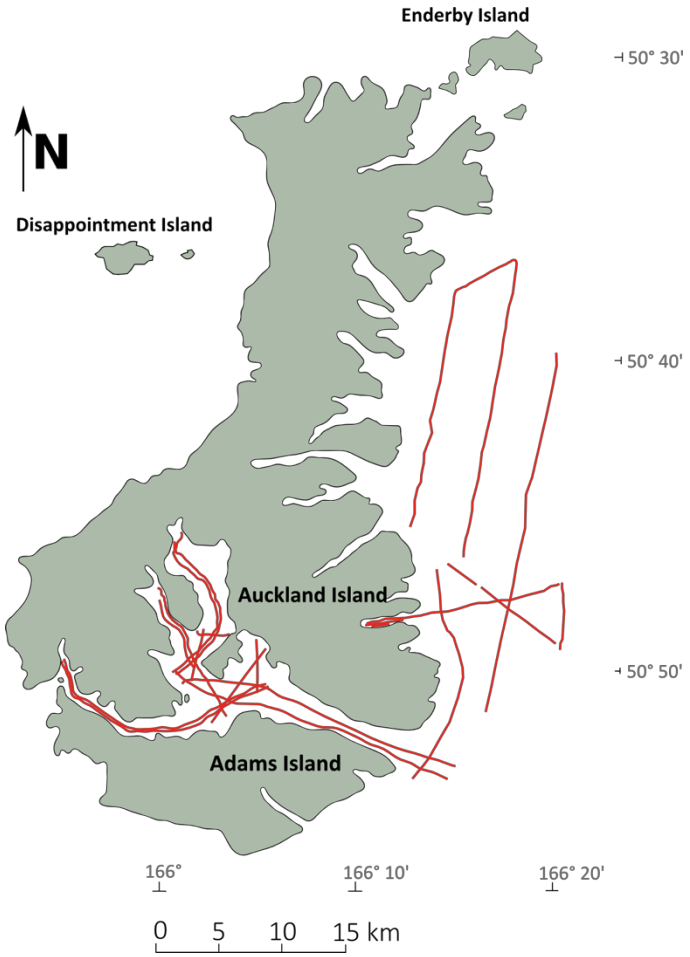

Figure 5.3b • 15PL001 survey transects.

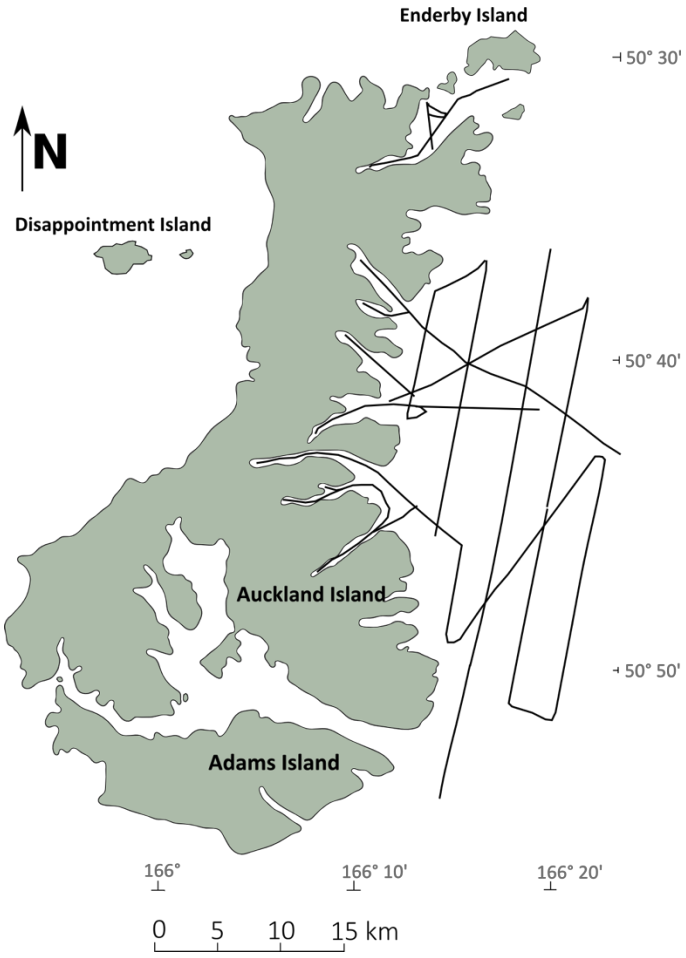

Figure 5.3c • 14PL001 survey transects

5.2 Survey Design •

The 16PL119 (*Figure 5.3a*) and 15PL001 (*Figure 5.*3b) surveys built on the previous data sets from 14PL001 (*Figure 5.3c*). This was achieved through targeting data gaps along the eastern and southern margins of the Auckland Islands. Seismic transects were collected on the eastern shelf, most coastal fjords and in the southern expanse of Carnley Harbour (*Figure 5.2)*. Offshore transects filled the spaces between 14PL001 transects *(Figure 5.3a, b)* in an effort to increase data density while also gaining as much additional data as possible. The offshore transects run mostly parallel to the eastern coastline in a consistent NNE-SSW orientation at varying, consistent distances from the coast. These parallel lines are spaced 1.5-2 km apart. Transects were also run perpendicular to the coast to tie parallel lines together. The transects within Carnley Harbour, McLennan Inlet and Fly Harbour had spacings of roughly 100 m in narrow inlets (e.g. Musgrave Harbour, Carnley Harbour) to 1 km in the larger expanses (Main Arm, Carnley Harbour). This close spacing within the southern inlets allows for better constraints on processes and variable sub-surface topographical features occurring within confined areas. All inlets and harbours were surveyed with more than one pass to ensure sufficient coverage for a holistic interpretation of observed features.

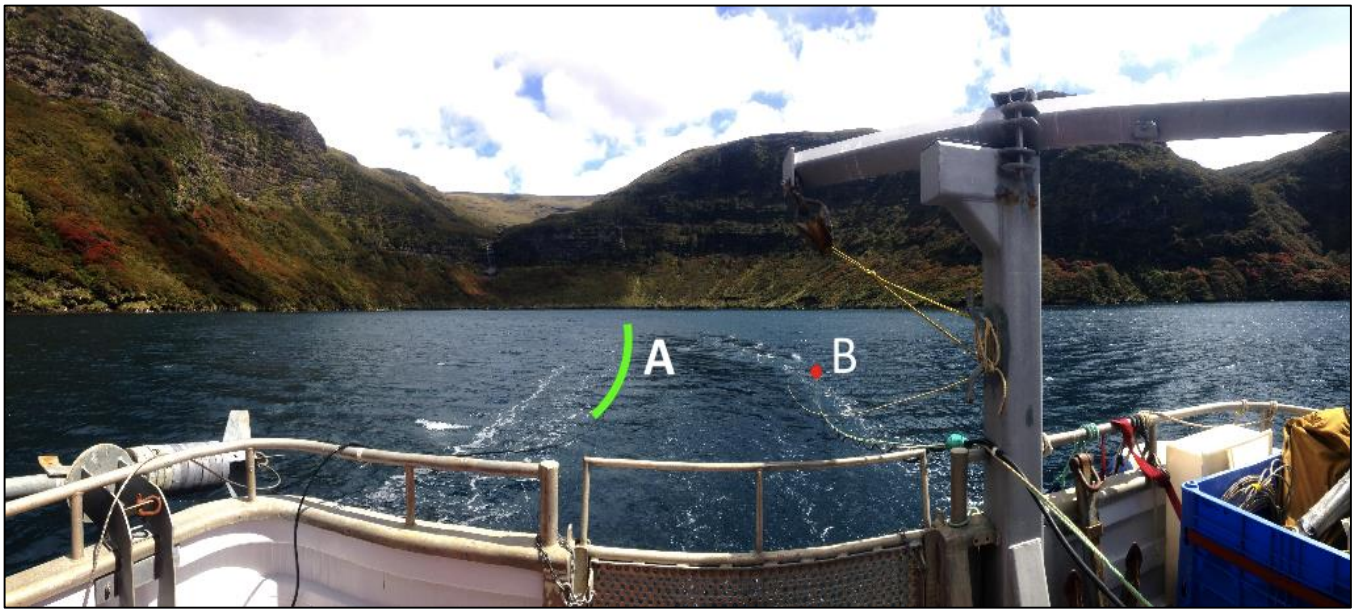

Figure 5.4 • Stern of the University of Otago research vessel *Polaris II* showing the acquisition of seismic reflection data from within McLennan Inlet looking west. (**A**) - 24 channel hydrophone receiver array extending for ~ 100 m behind the boat, (**B**) - seismic source (boomer) operating at a central frequency of 300 Hz.

5.3 Data Acquisition •

Historically the principles of seismology have been extensively used at a wide range of lengths and scales to estimate properties of the Earth's subsurface from reflected and refracted seismic waves (e.g. Mussett & Khan, 2000). The sub-discipline of seismology that makes use of seismic reflections to produce images of subsurface reflectivity is termed '*Reflection Seismology*' (Simpkin 2005). Boomer acoustic sources use high-frequency sound waves to produce high resolution sub-surface profiles, commonly in shallow water (0-200 m) (e.g. Gorman et al. 2010) (*Figure 5.4)*. The boomer source (*Ferranti 5210A – Figure 5.5a*) operates by generating consistent seismic acoustic wave signals known as 'shots' at a controlled rate (3.10 s for these surveys). These waves are projected through the water column and seafloor sub-surface. The velocity at which seismic waves travel is governed by the physical properties of the medium they travel through. The quantity of signal that is transmitted or reflected at boundaries in the Earth is governed by the 'acoustic impedance' of the materials on either side of the boundary.

Where the acoustic impedance, Z, is defined by the equation:

$$Z = V\rho$$

With V being the seismic wave velocity and ρ as the density of the rock.

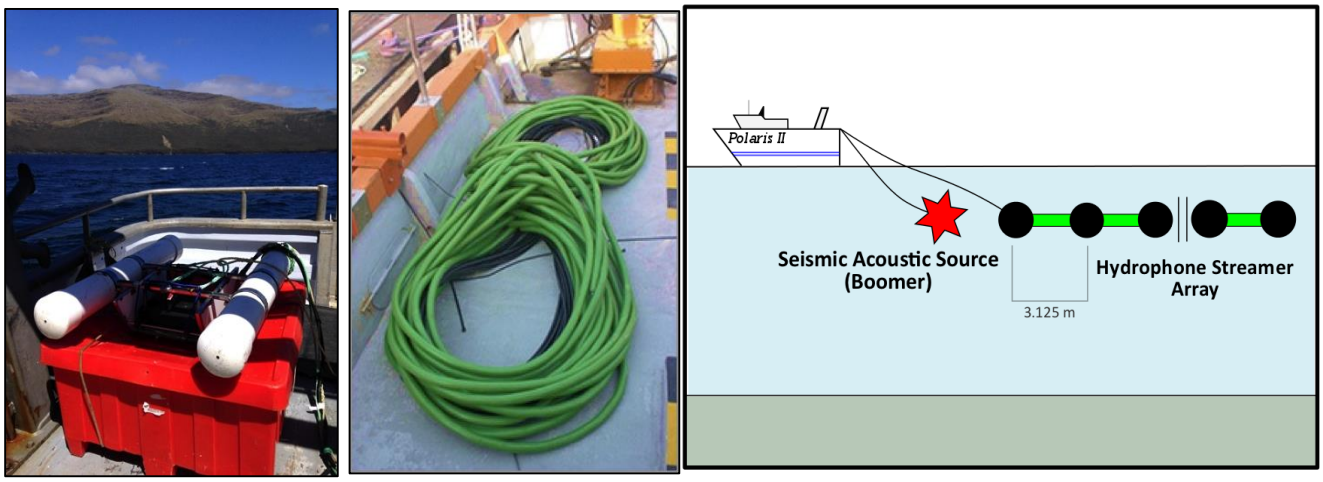

Figure 5.5a (Left) • *Ferranti* 5210A high resolution boomer, **Figure 5.5b** (middle) • 24 *Geometrics* 24 channel MicroEel streamer on deck, **Figure 5.5c** (right) • seismic acquisition schematic of boomer source and 24 channel hydrophone streamer array geometry (break in scale represented by two lines).

As the waves emitted from the source travel through the sub-surface, they encounter interfaces between various media with different acoustic impedances.

Some of the wave energy is reflected off the interface, which is refer to as 'reflector' (e.g. the seafloor, or a contact between two different lithologies). The reflected waves are subsequently received by a hydrophone streamer array (in the case of the *R/V Polaris II,* is a *Geometrics* 24 Channel MicroEel – *Figure 5.5b*) towed near the surface from the stern of the vessel travelling at 4 knots. For all three surveys, the streamer array consisted of 24 groups of pressure sensitive hydrophones (three hydrophones per group), with groups spaced 3.125 m apart (*Figure 5.5c*). The hydrophone receivers detect the incoming wave and transmits it as an analogue signal to an on-board seismograph that amplifies and digitises the signal. The seismograph is connected to a PC with appropriate software to gather and store the converted digital pulses as raw shot records (SEG-D format). The analogue-to-digital conversion, followed by the file creation, is a temporal constriction in the process, which means that the source can only fire every 3.1 s. The boomer source used in all three surveys created a signal with a central frequency of 300 Hz that provides metre-scale resolution while allowing up to ~300 m of penetration into the seafloor sub-surface. The frequency range emitted from the boomer source is a function of sub-surface penetration depths and data resolutions. These two parameters have an inverse relationship. Generally, lower frequencies (e.g. 150 Hz) allow for deeper penetration with a lower resolution, while higher frequencies (1200 Hz) provide higher resolution with reduced penetration.

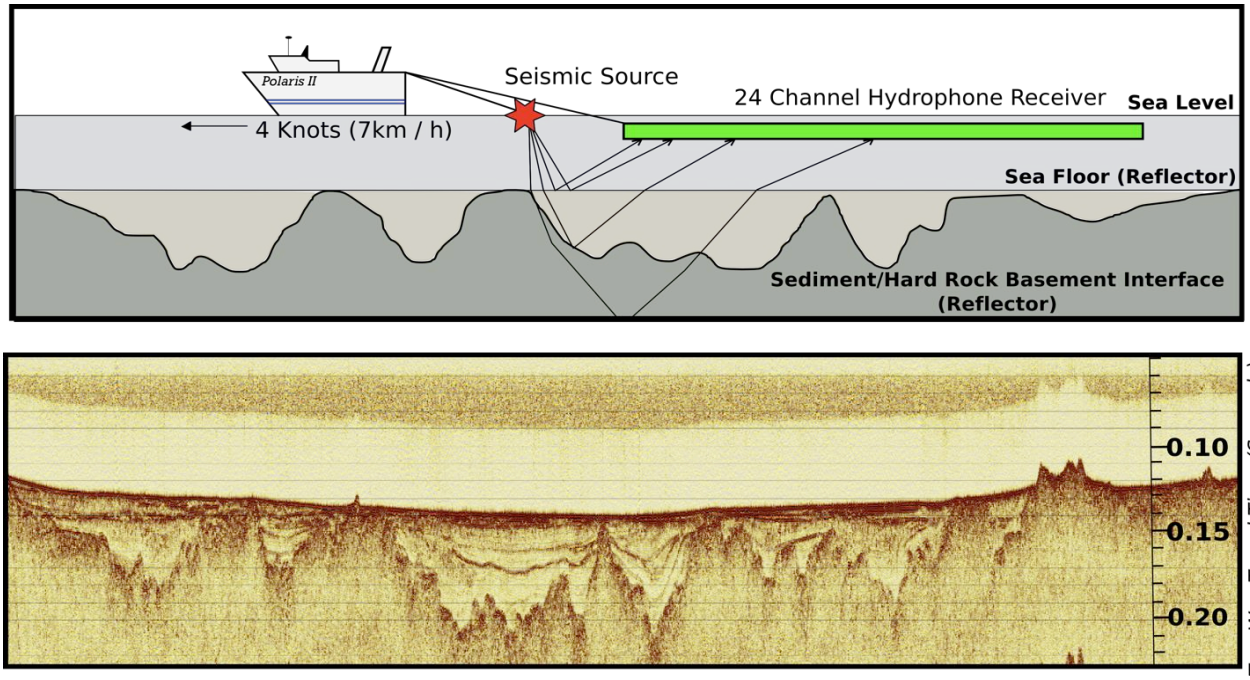

Figure 5.6a • (**top**) Seismic survey schematic displaying an operating towed seismic source and hydrophone receiver system, **Figure 5.6b** • **(bottom**) excerpt from line 14-03 (14PL001) exhibiting in-filled incised valleys in a pseudo-cross section of collected seismic data.

A complete series of collected and stored acoustic data of the surveyed sub-surface can be compiled together to form a pseudo-cross section, termed a seismic section (*Figure 5.6a, 5.6b*). Unlike the x-z axes used on classic geologic cross sections that are determined by distance/distance, seismic sections axis are measured in distance/travel time. This is the time taken from the acoustic source firing to the hydrophone receivers. Due to this difference, the Z-axis (or more appropriately, the t-axis) can become exaggerated, creating apparently misrepresented angles and depths of structures.

5.4 Data Processing • GLOBE *Claritas* seismic processing software

Monitoring of incoming data can be achieved during data collection by displaying single-channel gathers on a computer monitor on-board the vessel. This initial, low-resolution gather is key for making basic real-time observations, decisions regarding potential coring targets and real-time survey design adjustments. Further processing of the raw data is undertaken at a later date using all 24 available channels. The data here has been processed using the GLOBE *Claritas* Seismic Processing Software (Ravens, 2010). This provides higher-resolution data with more clearly distinguishes reflection boundaries and surfaces that are otherwise not observed due to a higher signal-to-noise (S/N) ratio.

5.4.1 Data Processing Flow •

1.Read in SEGD Files
2. Assgn Geometry
3.CDP Sorting
4. Gain Recovery + Filtering
5. Raw Stack
5a. Velocity Analysis
5b. Normal Moveout
6. Migration
7. Plotting

Figure 5.7 • Basic seismic processing flow used in the processing of surveys 14PL001, 15PL001 and 16PL119.

Processing of raw seismic data requires multiple steps, including data input, geometry application, filters and plotting. This method is referred to as a data processing flow or 'job flow'. Processing flows can be hugely variable and depend on the type of survey (e.g. 2D vs 3D). This flow uses common programs that fit with this survey type *(Figure 5.7)*. The following section explains the step-by-step seismic processing flow used in the GLOBE *Claritas* software with specific reference to selected modules, functions and processing parameters.

1 • Read in SEG-D Files

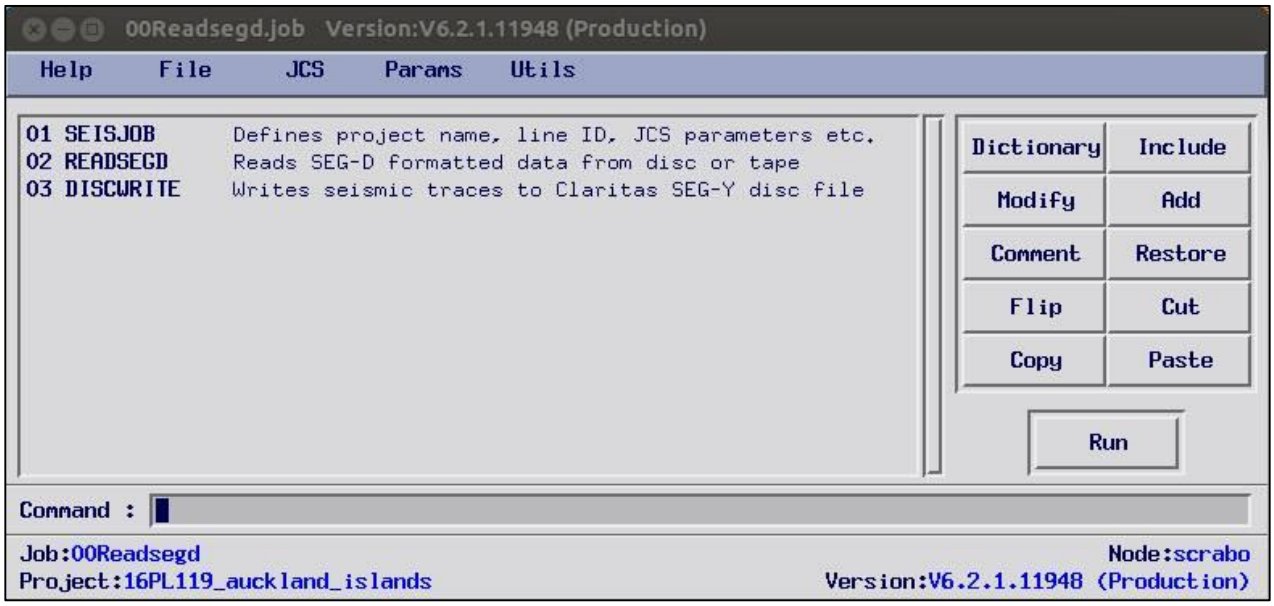

Figure 5.8a • *00 READSEGD* job *Claritas* module with job functions.

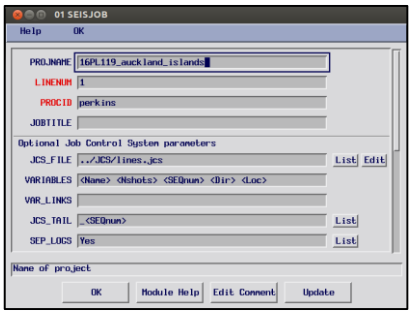

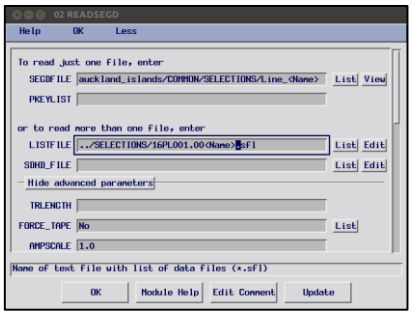

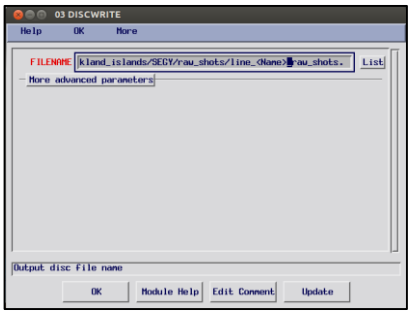

Figure 5.8b (Left) • *00/01 SEISJOB* that outlines the project name, Line ID and JCS parameters for the *00 READSEGD* job, **Figure 5.8c** (middle) • *00/02 READSEGD* reads in the raw SEG-D formatted data, via manual selection or a list text file, **Figure 5.8d** (right) • *00/03 DISCWRITE* writes seismic traces to *Claritas* SEG-Y file (.csgy).

5.4.1.1 Read in SEG-D Files •

All of the processing modules used in *Figure 5.7* contain the *01 SEISJOB* function that defines the over-all survey project name, the Line ID numbers and the Job Control (JCS) parameters (e.g. *Figure 5.8a, b*). Raw data acquired through the seismic acquisition process referenced in the previous sections are stored in binary SEG-D formatted seismic data files (with the .segd file name extension) (Barry et al. 1975). This initial job module reads these SEG-D files into *Claritas* from a disk or tape through the *00/02 READSEGD* function (*Figure 5.8c*). This function requires a .sfl text file that contains the stored file names and paths of the SEG-D files for a particular line. *00/03 DISCWRITE* writes out the SEG-D seismic traces into a single, merged SEG-Y format file (.csgy extension) (*Figure 5.8d*).

2 • Adding Geometry

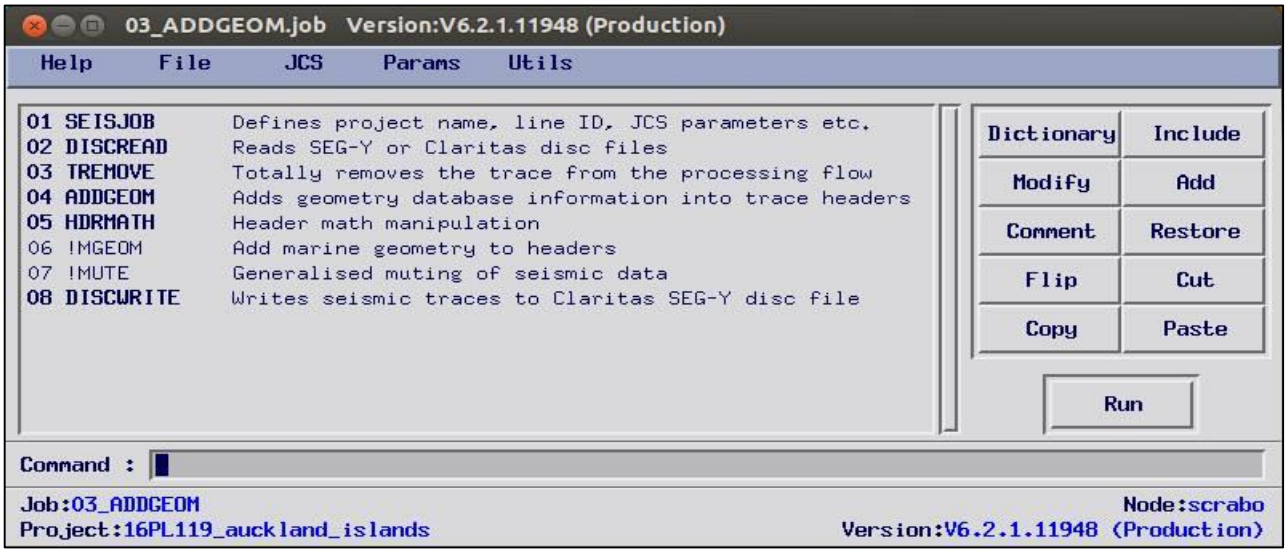

Figure 5.9a • 03 ADDGEOM module with job functions.

2a • Making .geom File for 03/04 ADDGEOM function

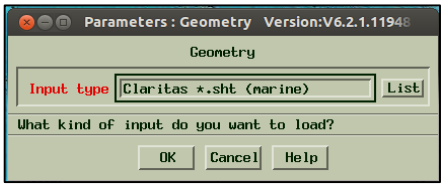

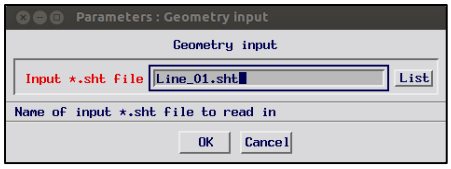

Figure 5.9b (Left) • Geometry input type – Shot File (.sht), **Figure 5.9c** (middle) • inputting of a shot file related to a particular survey transect, **Figure 5.9d** (right) • the conversion of the collected latitude and longitude coordinates to grid coordinates using a NZTM projection

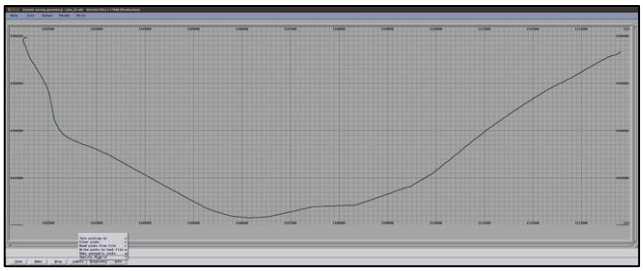

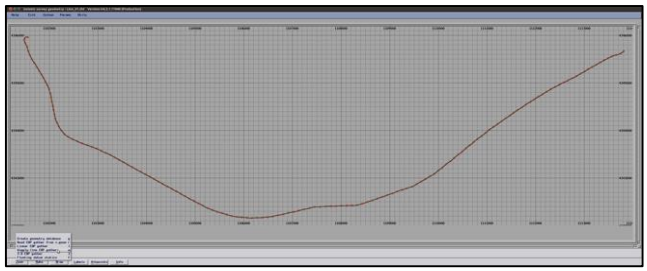

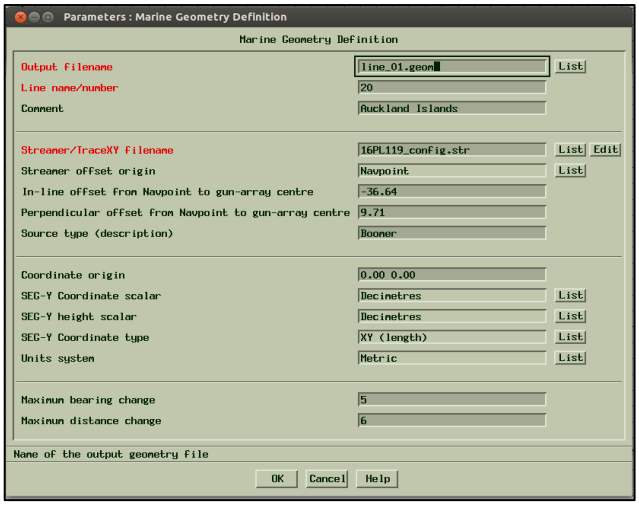

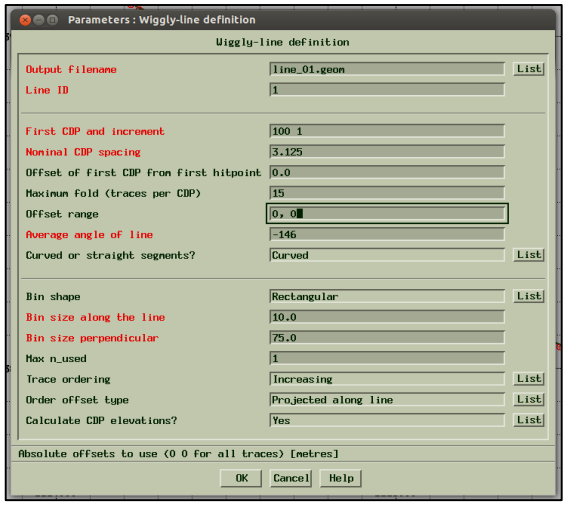

Figure 5.9e (Top left) • Seismic survey geometry for 14/01 with lat/long coordinates converted to NZTM grid coordinates, **Figure 5.9f** (bottom left) • marine geometry database with various survey parameters including the streamer geometry file comprising of further collection parameters, **Figure 5.9g** (top right) • automatically chosen hit points allocated along the line to assist the software in producing CDP gathers, **Figure 5.9h** (bottom right) • wiggly-line CDP gather database, output filenames, CDP spacing and other parameters – Geometry file (.geom) is output.

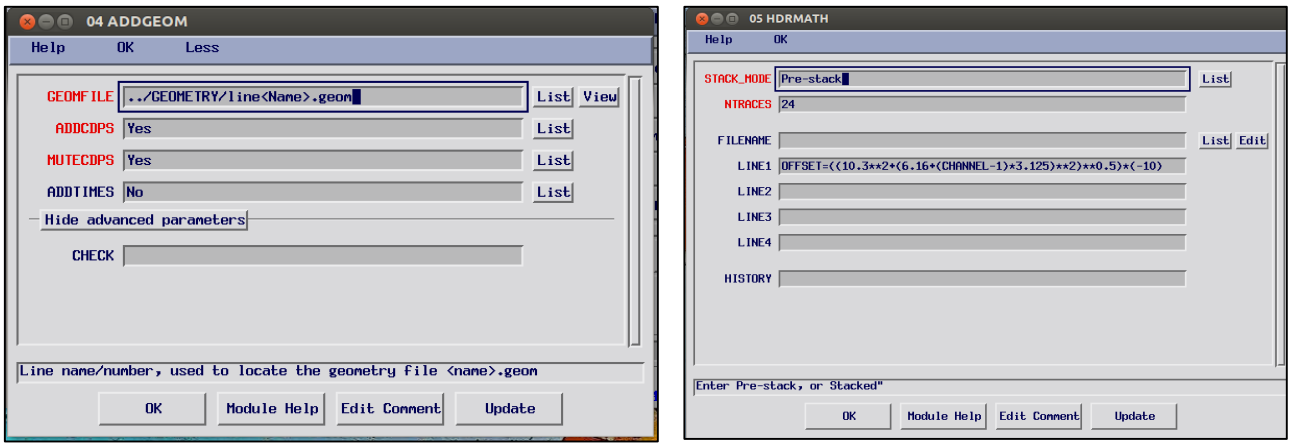

Figure 5.9i (Left) • *03/04 ADDGEOM* function adding the compiled 14/01 geometry file from *Figure 5.7e* and *5.7h* to an updated SEG-Y file (.csgy), **Figure 5.9j** • (right) *03/05 HDRMATH* - header math manipulation with offset equation,

5.4.1.2 Assign Geometry •

SEG-Y files require accompanying geometry files (.geom extension) for each line to place the raw seismic shots in the correct space. This process is undertaken using the *03 ADDGEOM* job module within *Claritas* (*Figure 5.9a-j*). A python script 'geometrics2sht.py' uses the merged SEG-Y file for a seismic line to produce a geometry file that is readable by the GLOBE *Claritas* Seismic Processing Software. The 03/*02 DISCREAD* function reads in the SEG-Y *Claritas* file (.csgy) created from the python script. A geometry file (.geom) is required for each seismic line (*Figure 5.9b-h*). To produce the .geom file, two accompanying text files are required: a coordinates to shot number file (.sht – *Figure 5.9b-d*) and a streamer geometry file (.str – *Figure 5.9f, 5.10)*.

Shown in *Figure 5.9e* and *5.9f*, the coordinates for a particular transect are combined with the streamer geometry as well as other survey parameters to create a geometry database. Hit points along the line are automatically picked to assist the software to reorganise the shots into 'wiggly line' CDP gathers (*Figure 5.9g-h*). This process creates a geometry file (.geom) that places the collected seismic data into real space. The .geom file is read into the *03/04 ADDGEOM* function (*Figure 5.9i*). The *03/05 HDRMATH* function (*Figure 5.9j*) manipulates the header math on the SEG-Y to adjust for streamer geometry discrepancies placing the seismic data into its proper geometrical space at higher-resolution scales. This process improves the signal to noise ratio creating a clearer seismic section. The

SEG-Y (.csgy) file is subsequently read out using the *03/08 DISCWRITE* function with the appropriate shots and geometry added in the correct space.

Polaris II Boomer, Streamer and GPS Geometry •

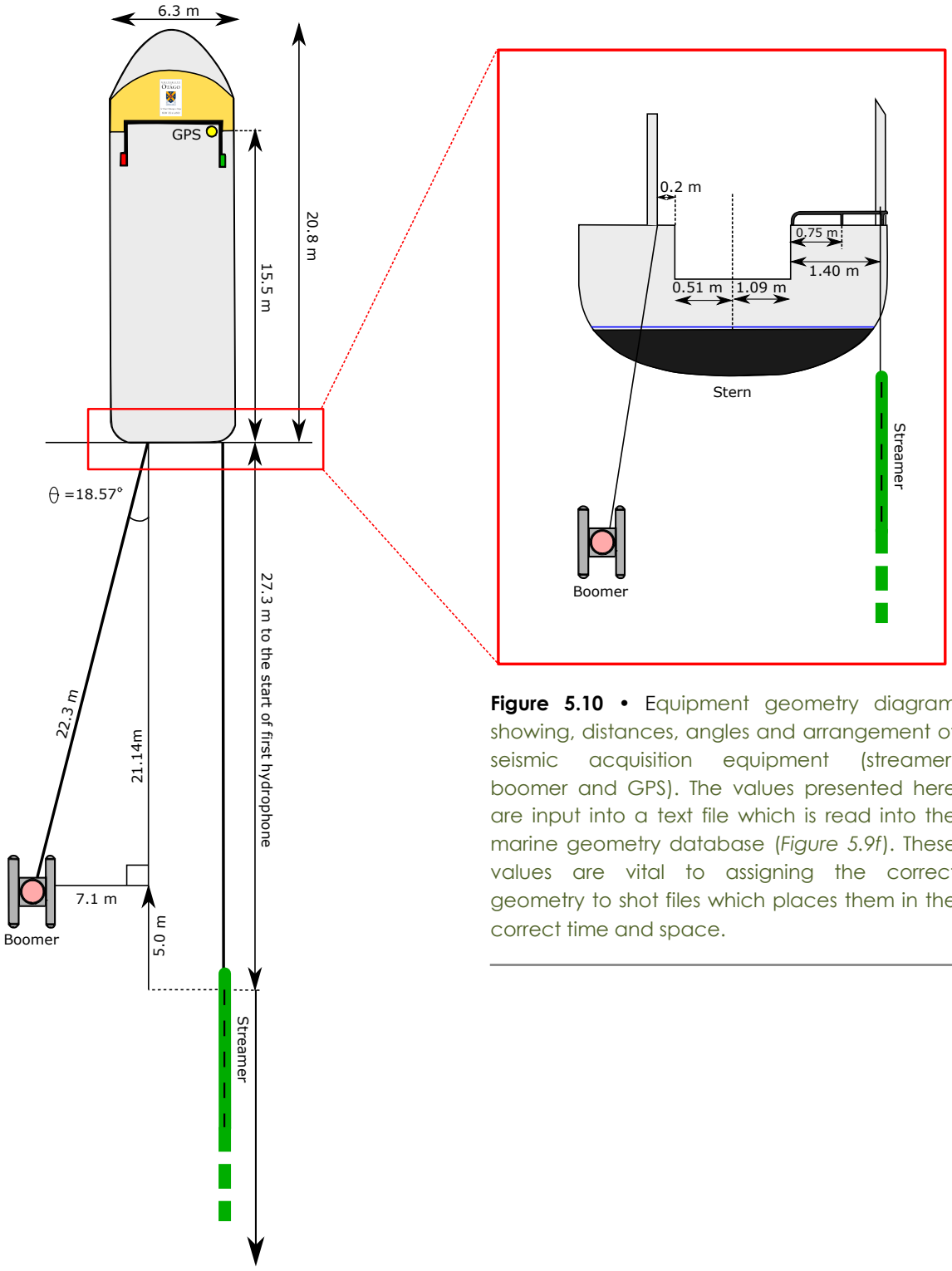

Figure 5.10 • Equipment geometry diagram showing, distances, angles and arrangement of seismic acquisition equipment (streamer, boomer and GPS). The values presented here are input into a text file which is read into the marine geometry database (*Figure 5.9f*). These values are vital to assigning the correct geometry to shot files which places them in the correct time and space.

3• CDP Sort

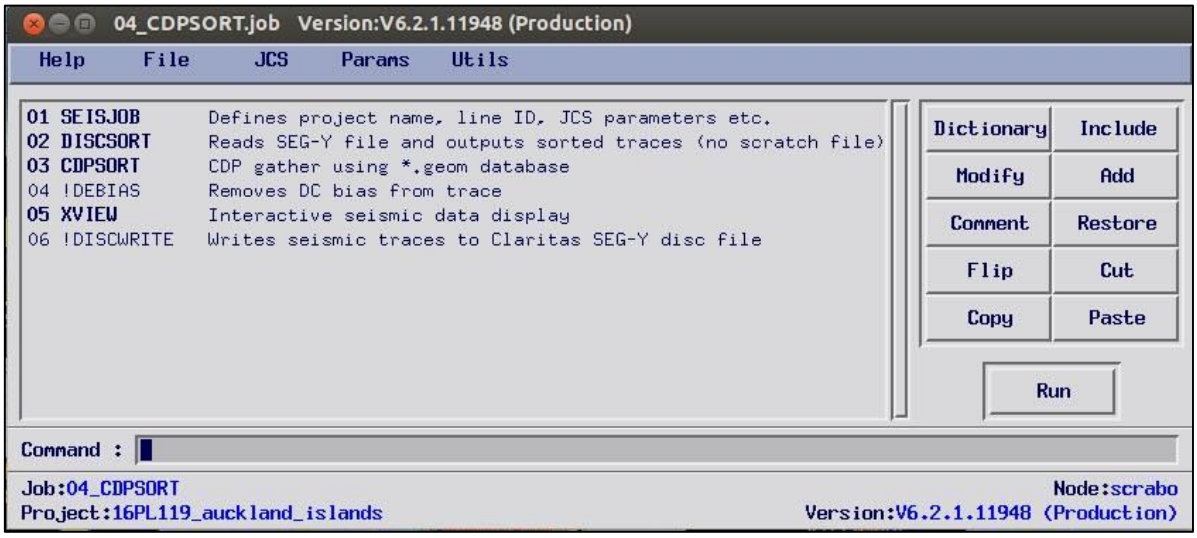

Figure 5.11a • *04 CDPSORT* module with jobs functions.

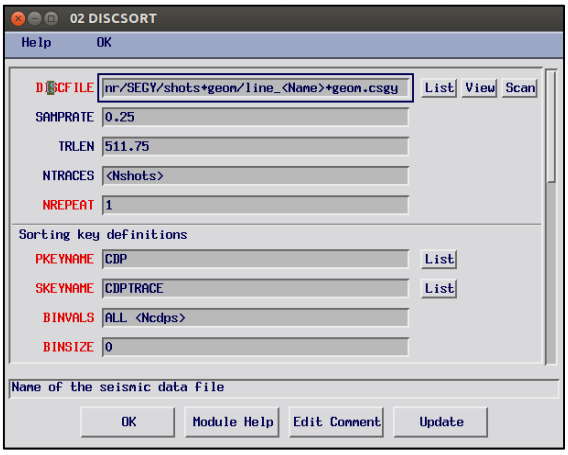

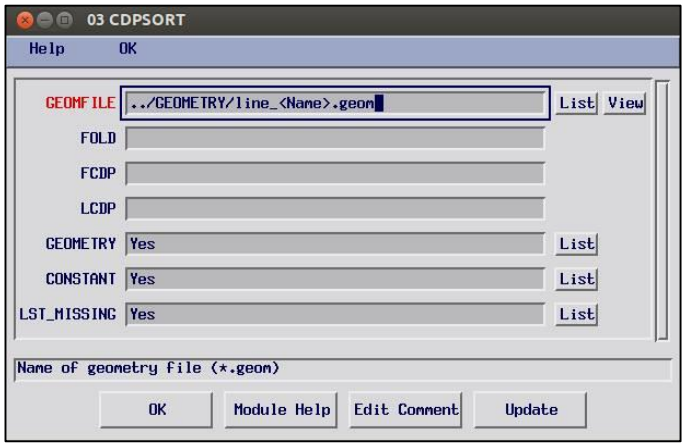

Figure 5.11b (Left) • *04/02 DISCSORT* function reading in the SEG-Y file (.csgy) with attached geometry data to output sorted traces, **Figure 5.11c** (right) • *04/03 CDPSORT* creates CDP gathers using the geometry file (.geom) database.

5.4.1.3 CDP Sort •

Seismic data acquisition is usually undertaken using a shot-receiver coordinate system. However, seismic reflection data processing requires midpoint-offset coordinates of grouped traces. This transformation of the coordinates is undertaken by sorting the data trace into Common Depth Point (CDP) gathers (Yilmax, 2001) (*Figure 5.11a*). Through the use of acquisition geometry information, each individual trace within a seismic transect is assigned to a midpoint halfway between its shot and receiver locations. Traces with the same midpoint location are grouped together, creating a CDP (or Common Mid-Point - CMP) gathers. The *04/02 DISCSORT* function (*Figure 5.11b*) reads in the .csgy file created from the previous job and combines it with the .geom file in *04/03 CDPSORT* (*Figure 5.11c*). The file is subsequently written out using *04/04 DISCWRITE* with sorted CDP gathers within the SEG-Y file associated with each seismic transect.

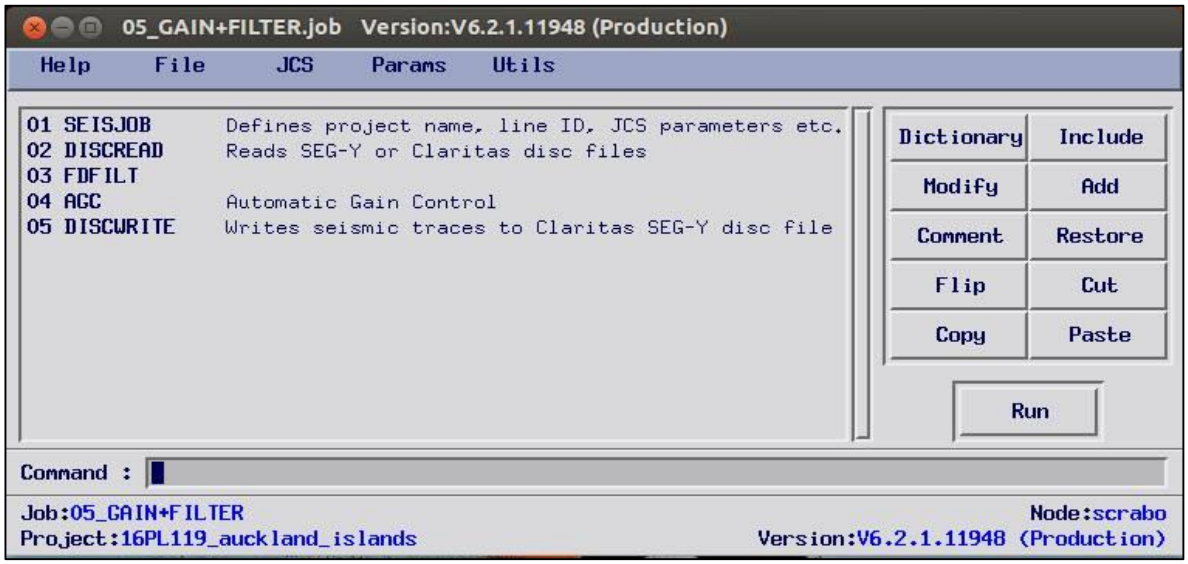

Figure 5.12a • *05 GAIN+FILTER* window with job functions.

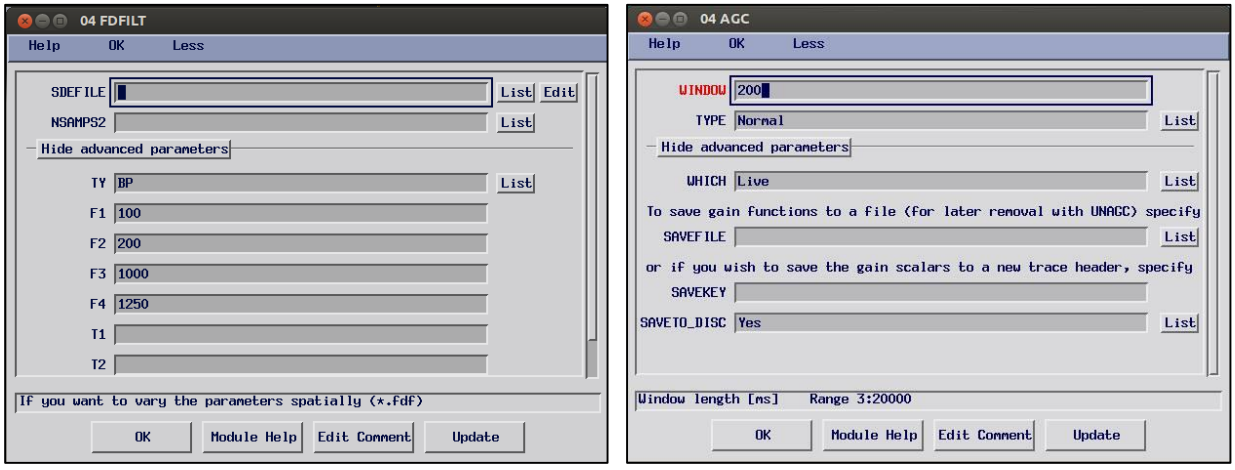

Figure 5.12b (Left) • *05/03 FDFILT - Frequency-domain time and spatially varying filter is a filter (zero-phase) applied to individual traces. The band-pass filter frequencies used are listed (F1-4),* **Figure 5.12c** (right) • 05/04 AGC - Automatic Gain Control (AGC) is a scaling process used for the uniform balancing of live traces.

5.4.1.4 Gain and Filter •

The collected seismic traces contain a mixture of both signal and noise. The desired seismic signal is a portrayal of a surveyed geologic feature in the subsurface, however seismic noise (unwanted seismic signal) creates distortions within the data which can be interpreted incorrectly. Collected seismic data can be filtered to improve the signal to noise ratio (S/N Ratio) and create more accurate data sets that reflect the true geology. In these data, frequency filtering was undertaken to improve the S/N ratio using the *05 GAIN+FILTER* module (*Figure 5.12a-c)*. A frequency filter can usually be applied when the frequency of signal and noise are different, thus the removal of the noise is a function of frequency. A trapezoidal band-pass frequency filter of 100-200-1000-1250 Hz was used to remove the majority of the noise within the *05/03 FDFILT* module (Figure 5.12b).

5 • Rawstack

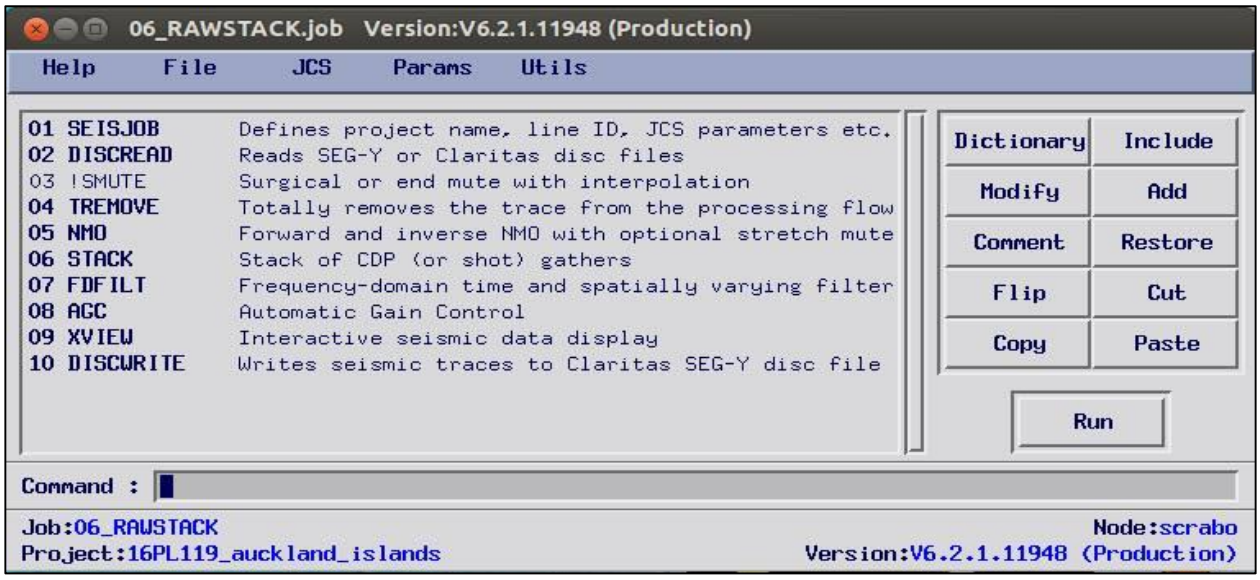

Figure 5.13a • *06 RAWSTACK* window with job functions.

5a • Creating 05 NMO File

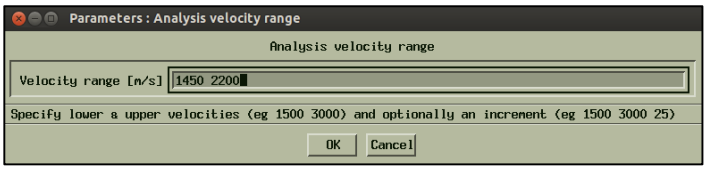

Figure 5.13b • Chosen velocity ranges for velocity picking.

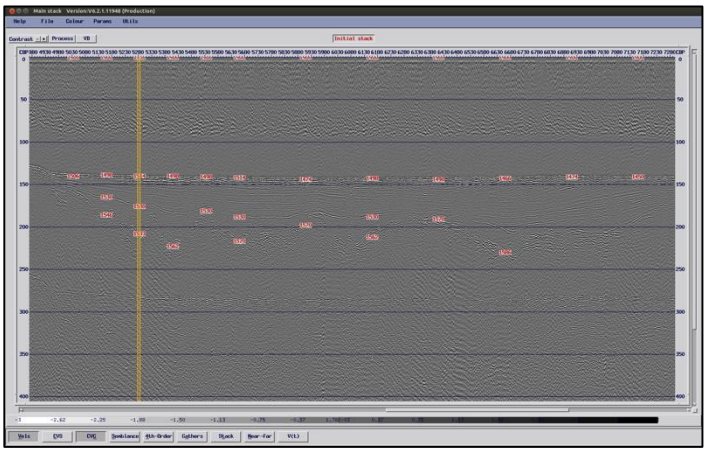

Figure 5.13c • Main stack with picked seismic velocities (red) and CVG location (yellow) shown in *Figure 5.13e* (right).

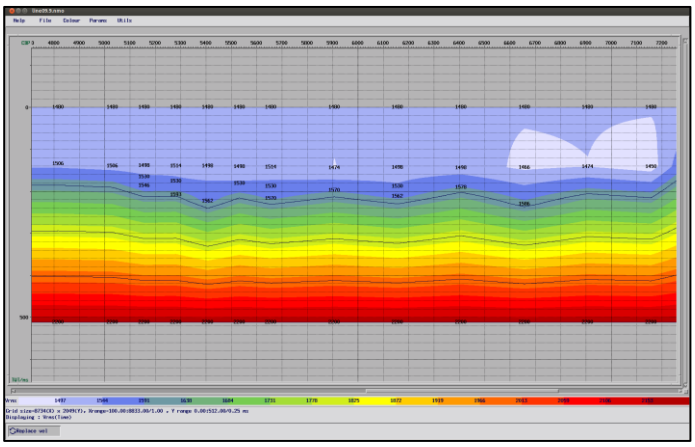

Figure 5.13d (Left) • Velocity Field created from picked velocities in the main stack window (*Figure 5.13c*), **Figure 5.13e** (right) • The CVG window that displays changeable velocities to stack the seismic signal of CDP gathers. The data is processed using FDFILT and AGC. This outputs a normal moveout file (.nmo file extension).

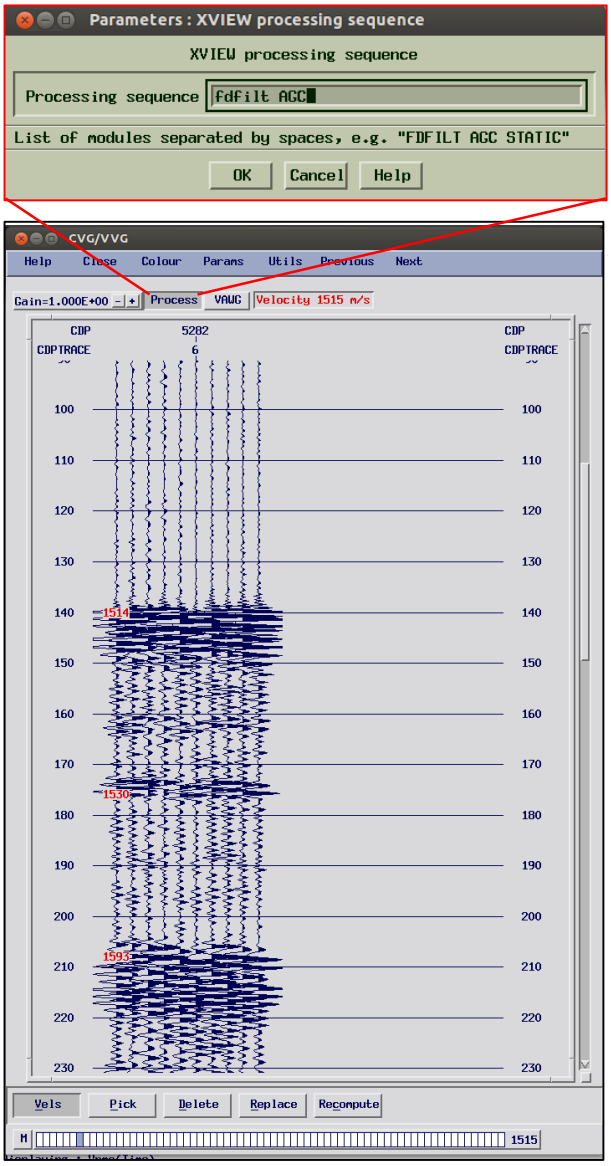

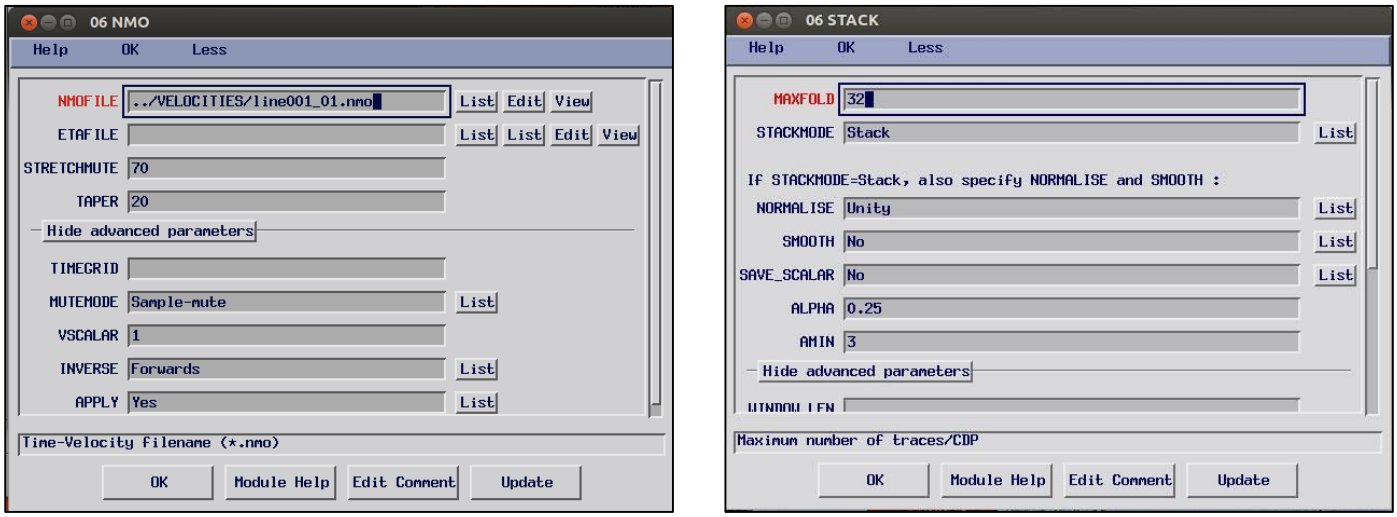

Figure 5.13f (Left) • *06/05 NMO* function inputting the created NMO file as part of the stacking process (*Figure 5.13b-e*), **Figure 5.13g** (right) • 06/06 STACK function tacking process where MAXFOLD is equal to the maximum number of traces per/CDP.

5.4.1.5 Rawstack, Velocity Analysis & Normal Moveout •

The rawstack and final stacking process (*Figure 5.13a-g)* of the data involves velocity modelling, where seismic wave velocities provide a link between time and depth (Yilmaz 2001). Velocity modelling of seismic data is a computing process that uses CDP gathers of adjacent data to align reflectors with a parallel velocity. Normal Moveout (NMO) within the data that is the difference between the travel time at a given offset and the two-way zero offset time (Yilmaz 2001) *(Figure 5.14)*. The NMO correction removes the trace time offset through an increase of time with offset which enables correct stacking of the data. This is undertaken in *Claritas* under the 'Velocities' tab and through the *Claritas* Velocity Analysis 'CVA' tool. The

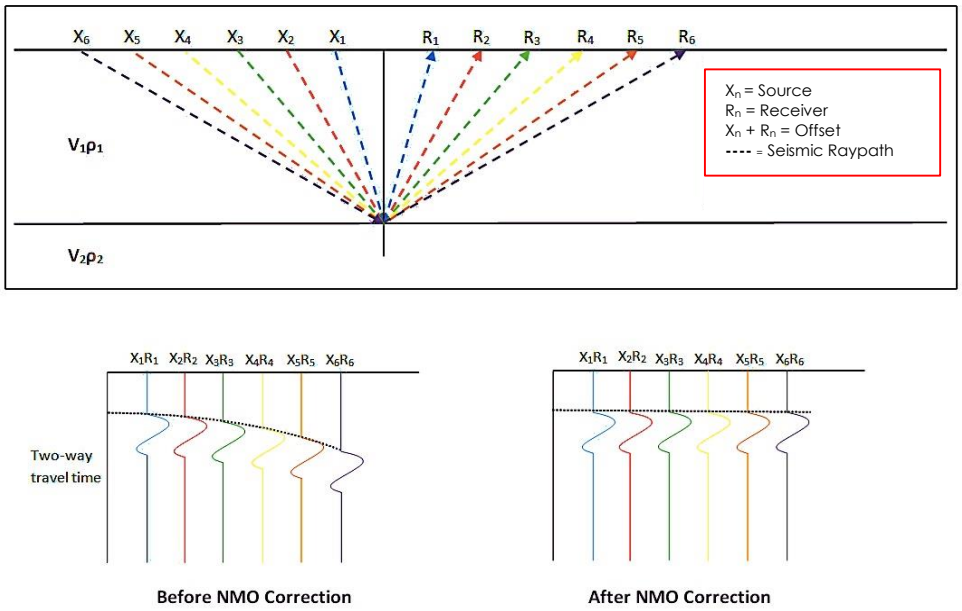

Figure 5.14 • Figure showing the normal moveout (NMO) of seismic traces and how the signal can be strengthened after the NMO correction.

SEG-Y file read out from the previous step is input, where an initial stack window and an initial velocity stack are defined and produced (*Figures 5.13b-d*). The CVG function within the initial stack window selects CDP gathers at chosen locations along the transect, with chosen velocity analysis ranges (*Figure 5.13e)*. FDFILT and Automatic Gain Control (ACG) processes are also applied (*Figure 5.13e - Top*). *Figure 5.13e* shows the corrected data process for NMO with picked velocities at certain flattened horizons within the CVG function. A repetition of picking velocities at consistent CDP increments along the length of the line creates a velocity model exhibiting increasing velocity with depth (*Figure 5.13d*). The NMO corrections within the data are achieved using this velocity model which places seismic energy correctly in time and space, thus making the data signal more effective. This process creates an NMO file (.nmo) that is input in the *06/05 NMO* function (*Figure 5.13f*). The main stacking process in *06/06 STACK* (*Figure 5.13g)* sums the stacked seismic traces from CDP gathers and outputs a single trace for each gather. The 'maxfold' is the maximum number of traces to sum into each output trace and is set at 32.

6 • Migration

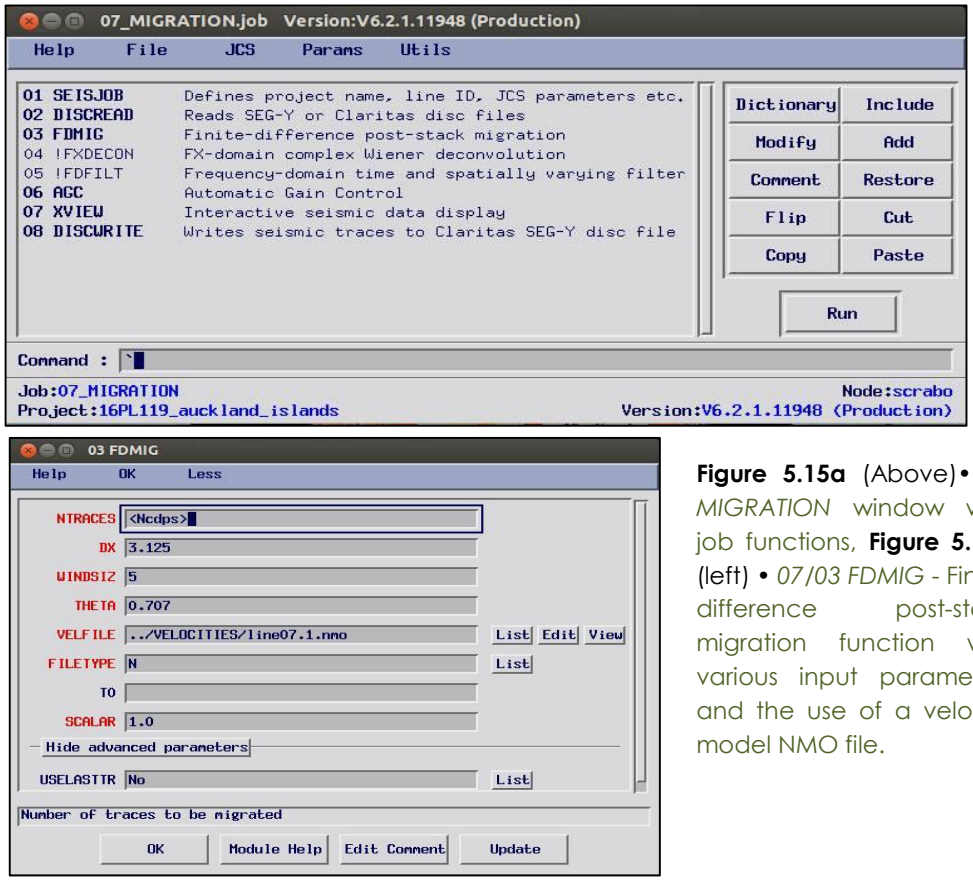

Figure 5.15a (Above)• *07 MIGRATION* window with job functions, **Figure 5.15b** (left) • *07/03 FDMIG* - Finite-difference post-stack migration function with various input parameters and the use of a velocity model NMO file.

5.4.1.6 Migration •

Migration is a processes of geometric re-positioning of seismic energy a correct, geologically consistent time and space (Yilmaz 2001). This is important due to dipping, curved or discontinuous geological boundaries that can lead to 'misplaced' energy in a seismic section. The process involves moving events from the offset location where they are recorded to the offset location corresponding to the surface position above where they occur and reducing the time accordingly. This helps to resolve more complicated areas of geology with higher resolution than non-migrated sections. Migration is a standard data processing technique for reflection-based geophysical methods (*Figure 5.15a-b*). The correction to account for misplaced reflections has been undertaken using the Finite Difference Time Migration (FDMIG) *07/03 FDMIG* function using the NMO File *(Figure 5.15b)*.

7 • Plotstack

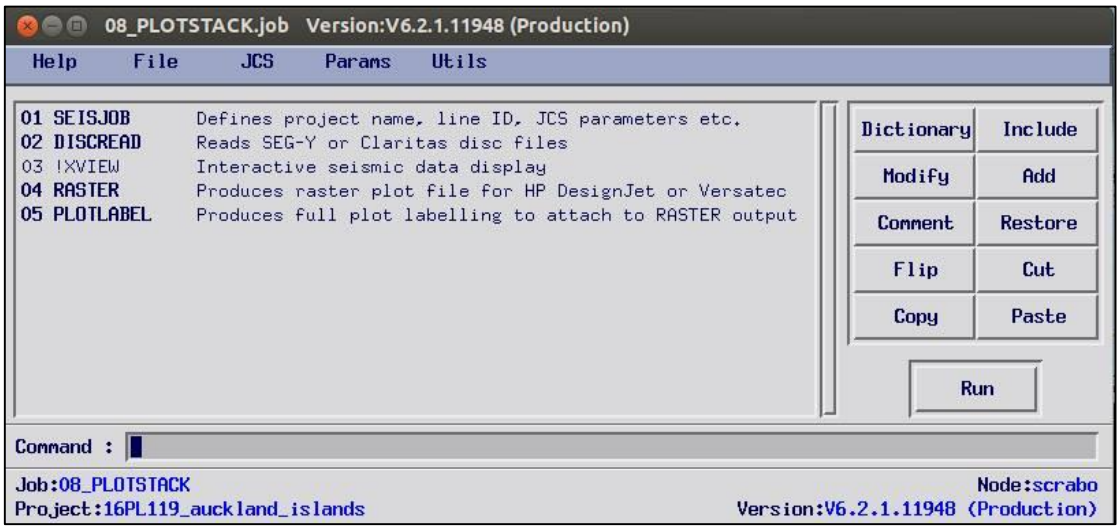

Figure 5.16a • *08 PLOTSTACK* window with job functions.

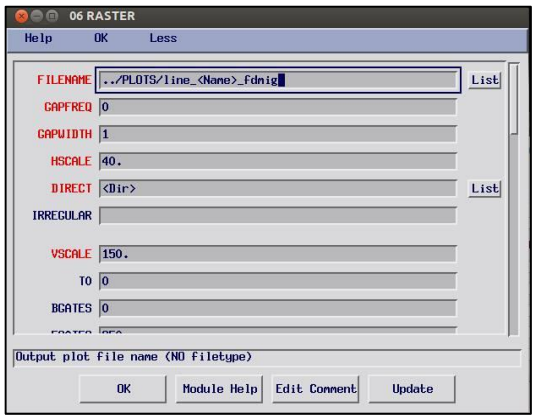

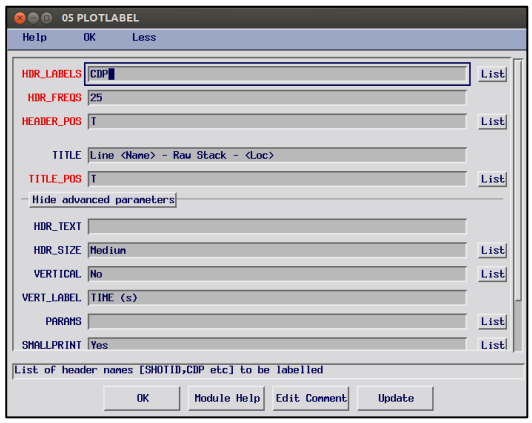

Figure 5.16b (Left) • *08/06 RASTER* - Inputted variables that can be changed such as color as well as horizontal and vertical scales, **Figure 5.16c** (right) • *08/05 PLOTLABEL* – Assigns labels and readout paths.

5.4.1.7 Plotting the stack •

The *08 PLOTSTACK* module is the last step of the seismic processing flow where the stacked processed data are plotted (*Figure 5.16a-c)*. Various parameters under the *08/04 RASTER* function (*Figure 5.16b*) such as horizontal and vertical scales can be changed. Changing colour settings within this function can be used to make various features within the data more prominent.

5.4.1.8 Job Control System (JCS) •

Due to the extensive number of associated shot and navigation files collected over three surveys (14PL001, 15PL001 and 16PL119), a Job Control System (JCS) is used to archive the shots and other associated parameters within their assigned seismic transect. The JCS makes projects with numerous transects and large quantities of meta-data more efficient through automation of various repetitive processes. This is achieved through assigning certain variables throughout the processing flow. The 01 SEISJOB function in each job (e.g. *Figure 5.8b*) outlines the JCS variables that relate to individual lines within a survey. *Figure 5.17a-b* shows the 16PL119 survey where variables entered within the flow are extracted from this table to streamline the process.

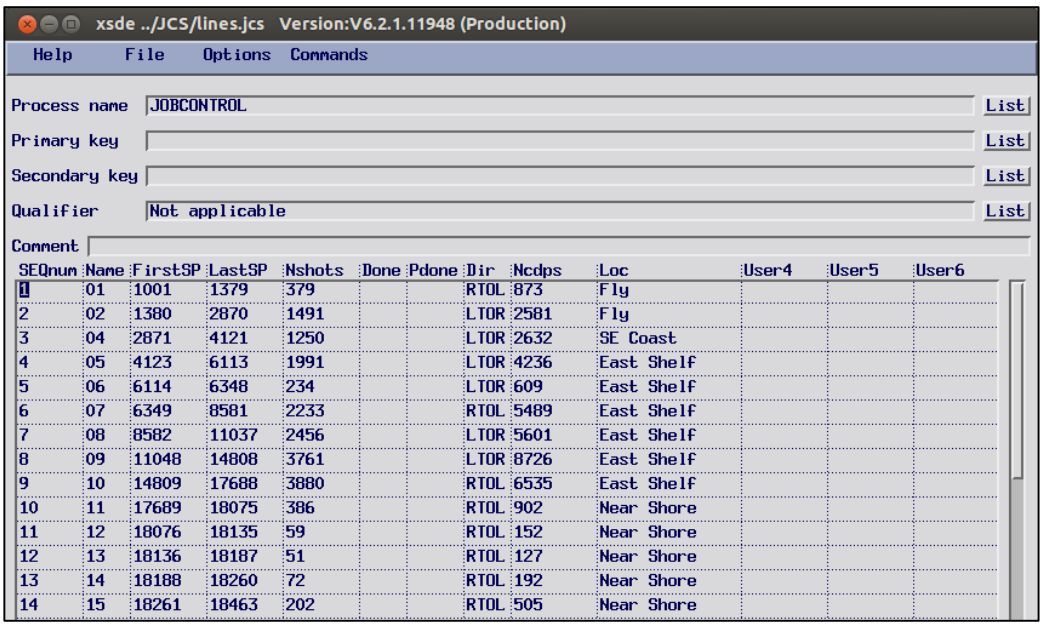

SEQnum	Name	FirstSP	LastSP	Nshots	Done	Pdone	Dir	Ncdps	Loc	User4	User5	User6
1	01	1001	1379	379			RTOL	873	Fly			
2	02	1380	2870	1491			LTOR	2581	Fly			
3	04	2871	4121	1250			LTOR	2632	SE Coast			
4	05	4123	6113	1991			LTOR	4236	East Shelf			
5	06	6114	6348	234			LTOR	609	East Shelf			
6	07	6349	8581	2233			RTOL	5489	East Shelf			
7	08	8582	11037	2456			LTOR	5601	East Shelf			
8	09	11048	14808	3761			LTOR	8726	East Shelf			
9	10	14809	17688	3880			RTOL	6535	East Shelf			
10	11	17689	18075	386			RTOL	902	Near Shore			
11	12	18076	18135	59			RTOL	152	Near Shore			
12	13	18136	18187	51			RTOL	127	Near Shore			
13	14	18188	18260	72			RTOL	192	Near Shore			
14	15	18261	18463	202			RTOL	505	Near Shore			

Figure 5.17a (Above) • Standard JCS input window within *01 SEISJOB* function within every job. Variables (e.g. <Name> <Loc>) are input and related back to the data within the JCS table, **Figure 5.17b** (below) • JCS table with variables from the survey 16PL119.

5.5 Multi-beam Bathymetric Data •

Multi-beam bathymetric data were collected at the Auckland Islands in early 2015 by the Australian survey company IXSURVEY on the *R/V Tranquil Image* (*Figures 5.18 and 5.19*) as tendered by *Land Information New Zealand* (LINZ).

The survey was undertaken using a *Kongsberg EM2040C* multibeam echo sounder (MBES) that operates at frequencies between 200 and 400 kHz. The sonar system operates by emitting hundreds of focused acoustic beams at particular frequencies in a fan shape or 'swath', typically 90-170° across that image the seafloor (Campbell 2015) (*Figure 5.20*). The travel times of the waves scattered off the seafloor are determined using a bottom detection algorithm. Using the velocity of sound through the entire water column, the depth and position of the returning signal is resolved from the receiver angle and the travel time. The compact array of narrow individual beams allows for high resolution and accuracy (Campbell 2015). The hydrographic survey was undertaken as a multiple use data set for the Department of Conservation (DOC), research purposes and coastal navigation safety along the northern,

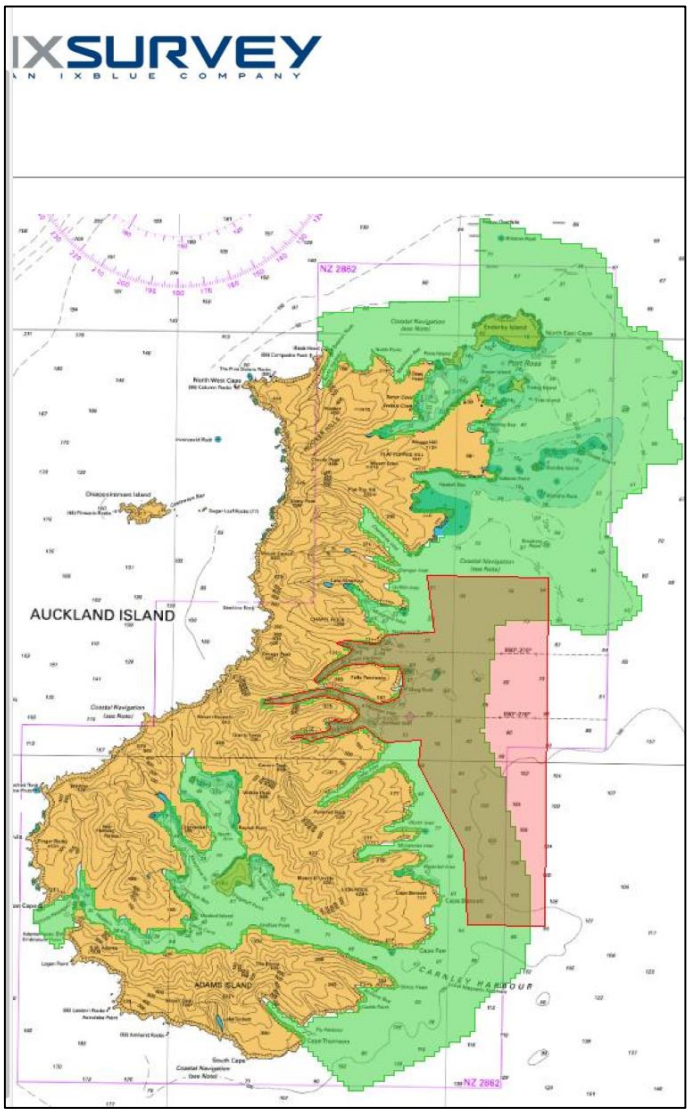

Figure 5.18 • IXSURVEY map of the bathymetric data collected in 2015 by the R/V *Tranquil Image* around the northern, eastern and southern regions of the Auckland Islands (**green**). A precursor survey was undertaken by the HMNZS *Monowai* in 1991 around the central Auckland Island regions (**red**).

Figure 5.19 • Multibeam survey boat *R/V Tranquil Image*, contracted by IXSURVEY to undertake an extensive multibeam survey at the Auckland Islands in early 2015.

eastern and southern coastlines of the Auckland Islands. The collected data sets are publically available.

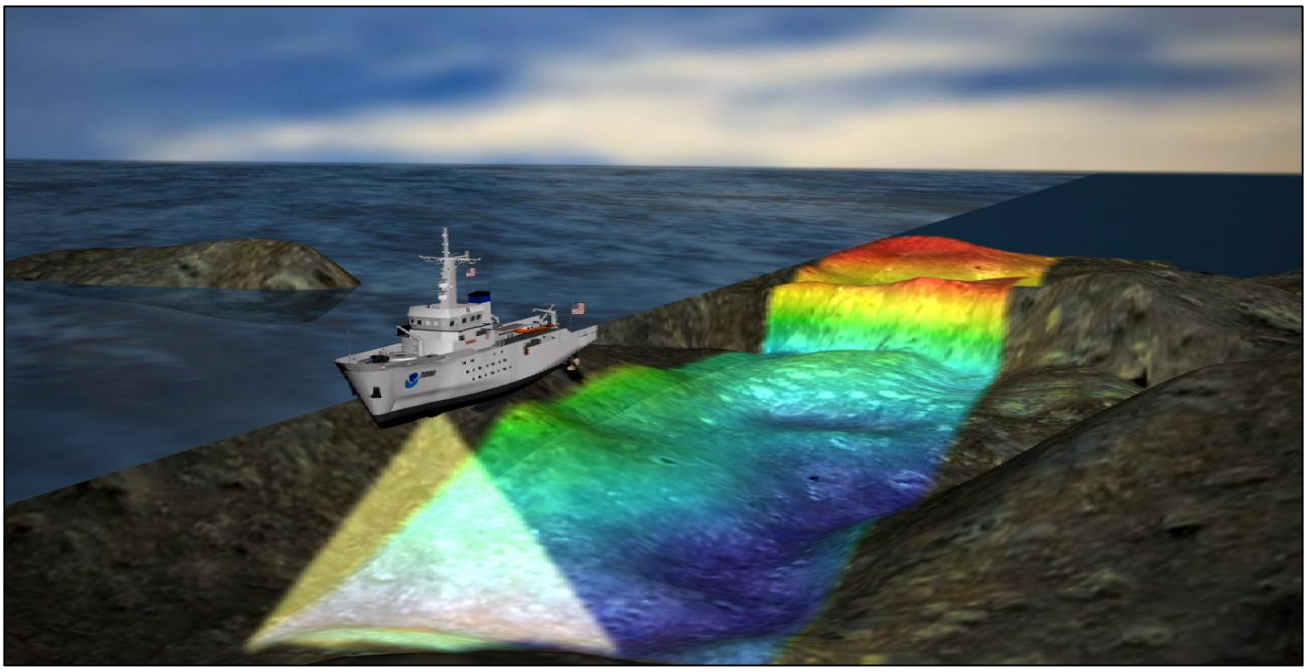

Figure 5.20 • Schematic of a multibeam echosounder survey imaging the seafloor. The system uses multiple focused acoustic beams in a swath formation emitted from a transducer placed on the ships hull. (Image from the United States National Oceanic and Atmospheric Administration – NOAA)

Bathymetry data have been used at other sub-Antarctic localities to define glacial extent and paleo shore lines (e.g. *Figure 5.21*). Geomorphic features are observed on the seafloor within high-resolution data to infer glacial feature morphologies and timing. The methods and applications used at these sub-Antarctic localities is to be undertaken using the Auckland Islands data to evaluate similar glacial features and associated processes (*Figure 5.22*).

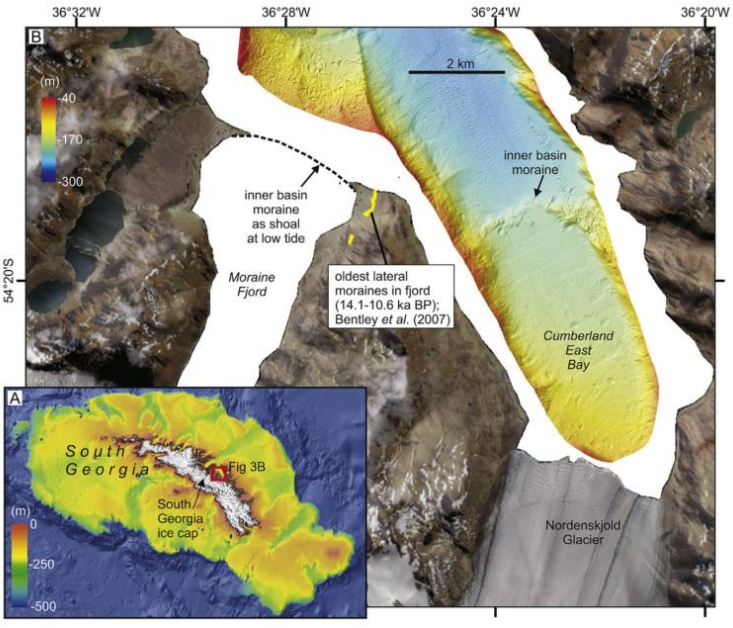

Figure 5.21 • Bathymetric data from South Georgia Island showing submerged fjord moraines and other glacial derived seafloor features (from Hodgson et al. 2014).

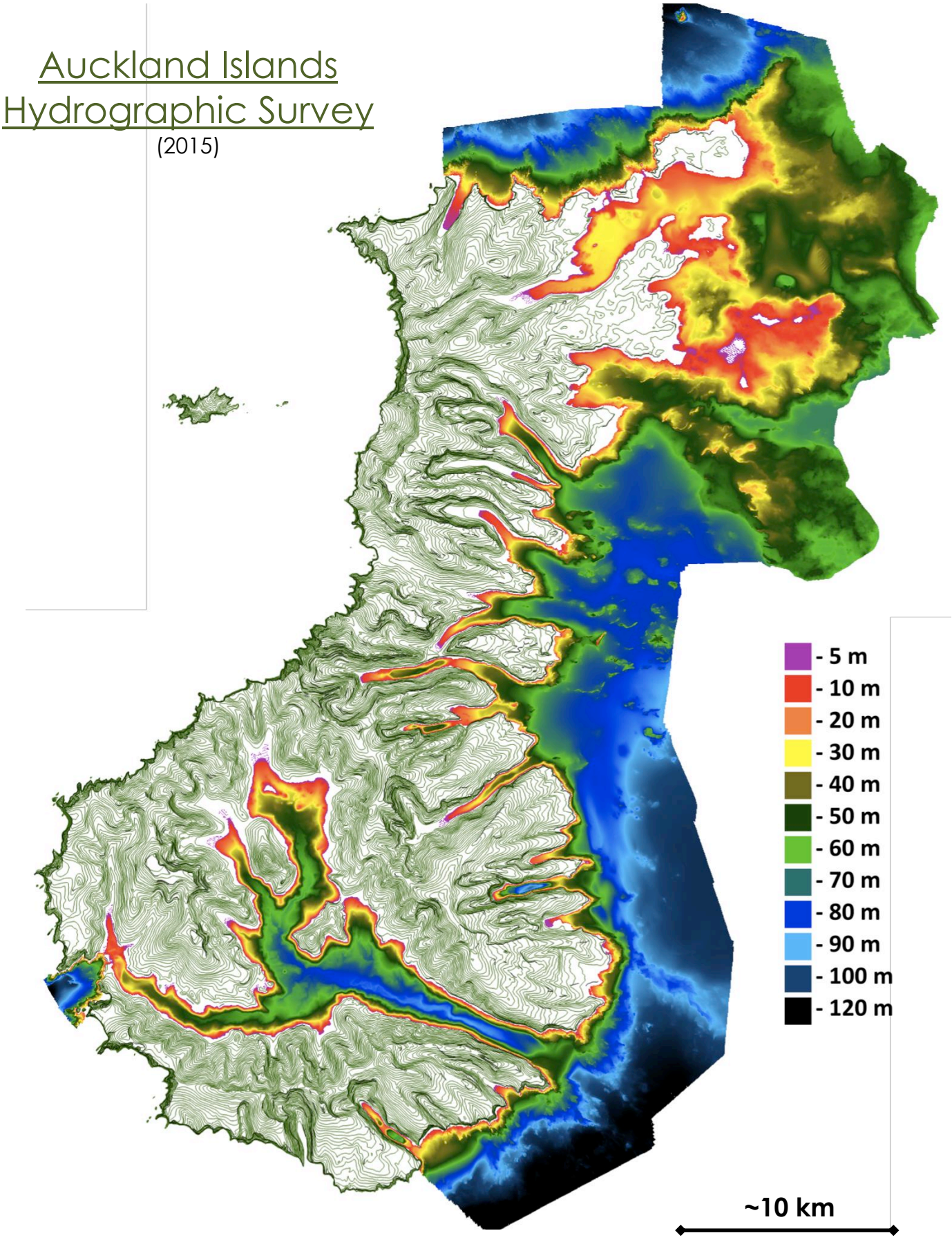

Figure 5.22 • Complete hydrographic survey of the northern, eastern and southern regions of the Auckland Islands collected in early 2015. (Land contours are on 20 m intervals)

5.6 Interpretation •

5.6.1 *IHS Kingdom* Seismic Interpretation Software •

Seismic survey transects from 14PL001, 15PL001 and 16PL119 have been collectively interpreted using the *IHS Kingdom* geophysical and geological interpretation software package. Processed SEG-Y files and bathymetric data were imported into the package. Within the seismic lines, and in surface bathymetry data where possible, sedimentary horizons, bedrock surfaces and channel morphologies were 'picked' to visualise features within the data. The *VuPAK* feature within *Kingdom* allows for three-dimensional analysis and interpretation of features observed within the respect data collectively. This enhances the capability to identify and correlate trends in the subsurface and on the seafloor.

5.6.2 *Leapfrog Geo* 3D Modelling Software •

Data were imported into *Leapfrog Geo* geologic modelling software package which is effective at integrating various data formats (e.g. seismic, bathymetric and onshore data). This allowed for the generation of mesh surfaces and contours for topographic modelling for holistic interpretation. This software was used for constraining paleo-shorelines and creating a 3D model of the offshore valley system to further understand and visualise changing valley morphology through time and space.

Chapter 6 •

Results

6.1 Seismic Data •

The following section describes the results and observations from seismic data acquired over three surveys at the Auckland Islands. Expanding on the inaugural 2014 survey - 14PL001, 15PL001 and 16PL119 aimed to fill data gaps in an effort to provide a holistic seismic data set on the eastern coast and shelf of the Auckland Islands (*Figure 6.1*). Seismic data within this section are presented in a processed format with accompanying bathymetry maps of the target area. This processed format improves the signal strength and improves the resolution of features within the data. The results shown here used data from all three surveys and were interpreted using 3D modelling software packages. This will provide interpretations to answer the questions of valley formation during glacial cycles and subsequent cyclic erosion and deposition through these periods. The following results with respect to seismic facies assignment are unique to each transect unless otherwise stated.

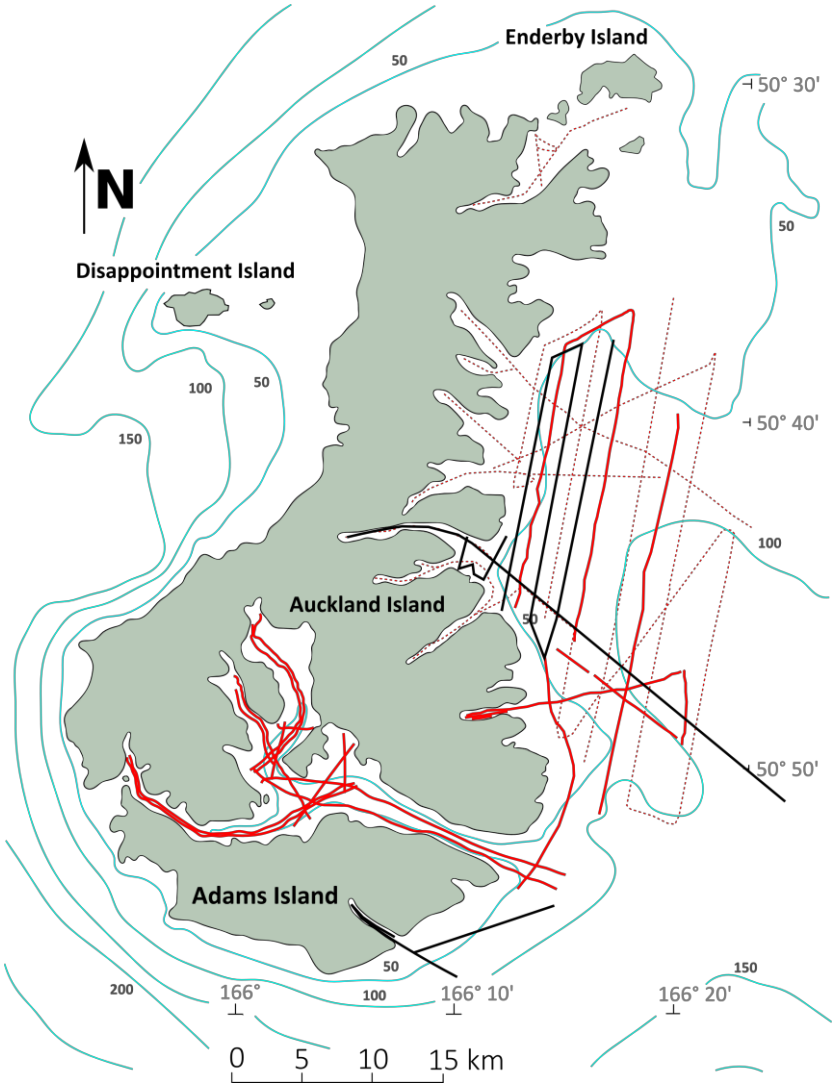

Figure 6.1 • Seismic survey transects of 14PL001 (**dotted Red**), 15PL001 (**solid red**) and 16PL119 (**solid black**) presented against bathymetry (m) at the Auckland Islands. 15 transects from 16PL119 and 24 transects (~308 km) from 15PL001 are included in the southern and eastern regions of the Auckland Islands in addition to previous 75 seismic lines to the north (> 400 km – 14PL001).

6.2 Fjords •

6.2.1 McLennan Inlet •

McLennan Inlet, a previously unsounded fjord on the eastern coast, was the subject of three seismic profiling transects. The Inlet is 4.4 km in length, stretching in a west-east orientation with a relatively consistent width of ~500 m. Contour elevations (20 m) around McLennan Inlet exhibit a steep sided profile with two hanging valleys at the head that progress seaward to a confluence in the main body of the fjord (*Figure* 6.2). One main bisecting transect and two further sub-transects were undertaken. Line 15-18 (*Figure* 6.3) exhibits a classic fjord profile with a shallow entrance sill seaward (~38 m), progressing into an extensive back basin that exceeds 100 m water depth at its deepest point. McLennan Inlet is the deepest coastal inlet at the Auckland Islands.

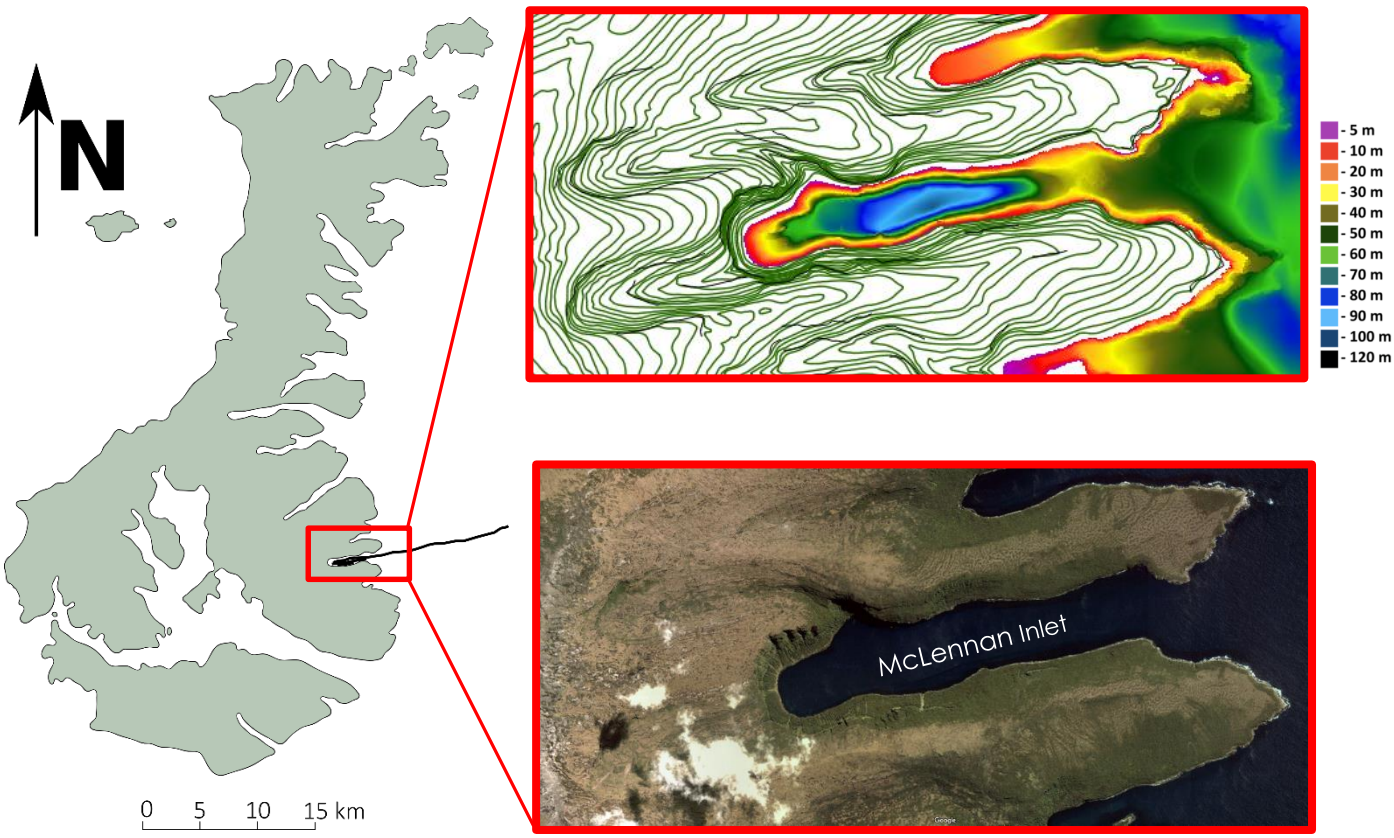

Figure 6.2 • Locality of McLennan Inlet on the eastern coast of Auckland Island with seismic lines (**left**), McLennan Inlet modelled by land contours (20 m) and seafloor bathymetry (**top**), satellite image of McLennan Inlet – Google Earth (**bottom**).

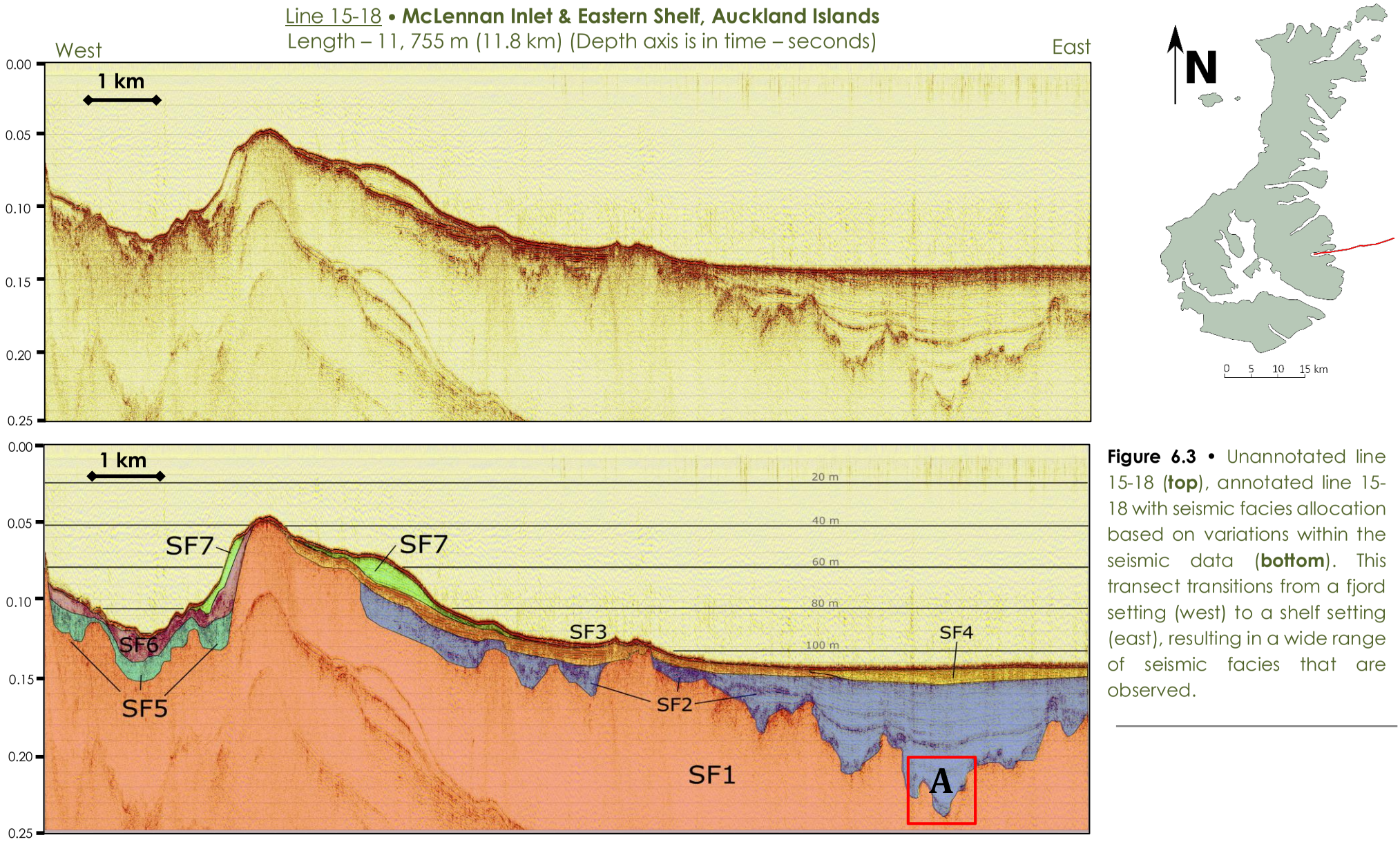

Figure 6.3 • Unannotated line 15-18 (**top**), annotated line 15-18 with seismic facies allocation based on variations within the seismic data (**bottom**). This transect transitions from a fjord setting (west) to a shelf setting (east), resulting in a wide range of seismic facies that are observed.

Line 15-18 originates at the head of McLennan Inlet and extends over 8 km west to the sea. The line exhibits seven seismic facies that vary spatially and can be separated into two environments; an enclosed fjord basin and a shelf sequence progressing seaward. Facies are segregated based on this variation in the seismic data and the location occurrence. The volcanic bedrock/basement of the Auckland Islands is observed as seismic facies 1 (SF1), which in this instance shows deep depressions within the body of the fjord with seafloor depths reaching 100 m. Seaward, the top of SF1 is observed down as deep as >180 m metres below modern sea-level within this transect (*Figure 6.3a*) (*Depths calculated assuming water velocities of 1500 m/s and sediment velocities of ~1630 m/s*). Unconformably overlying SF1, SF2 is a semi-transparent facies with laterally continuous, draped internal reflections. Some horizons are well-defined and are present over kilometre distances. This facies is interpreted to extend up the shelf landward. SF3 exhibits strong reflections that overly the semi-transparent SF2 and is more parallel in its internal structure. SF4 is similar to SF3; however appears to be incised into the underlying SF2 due to the presence of on-lapping truncations. SF5 within 15-18 (*Figure 6.3*) and 15-20 (*Figure 6.4*) is a variable unit within McLennan Inlet that sits unconformably over SF1. The basement/sediment interface is not apparent in these transects. Areas of SF5 are chaotic and unstructured in places; however some semi-continuous reflections are observed in the fjord basin. SF6 overlies SF5 within the basin and shows contrasting characteristics to the underlying facies. SF6 is defined by semi-transparent packages in places with weak, continuous internal reflections. These fjord sediments are observed in both transects presented here; however they are more

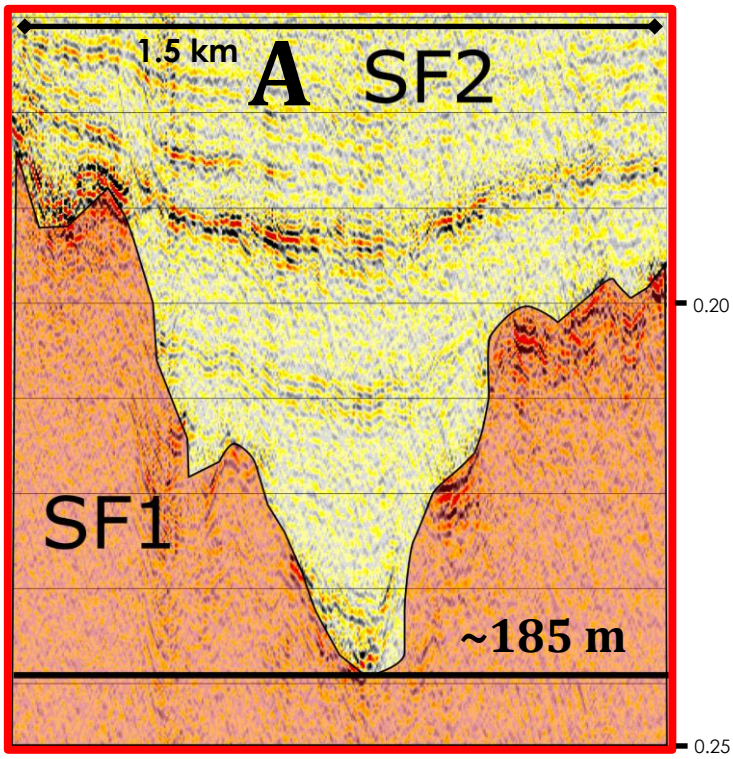

Figure 6.3a • Excerpt of 15-18 exhibiting the deepest point of the sediment/bedrock interface. (Depth axis is in time – seconds)

Line 15-20 • **McLennan Inlet, Auckland Islands**
Length – 2, 899 m (2.9 km) (Depth axis is in time – seconds)

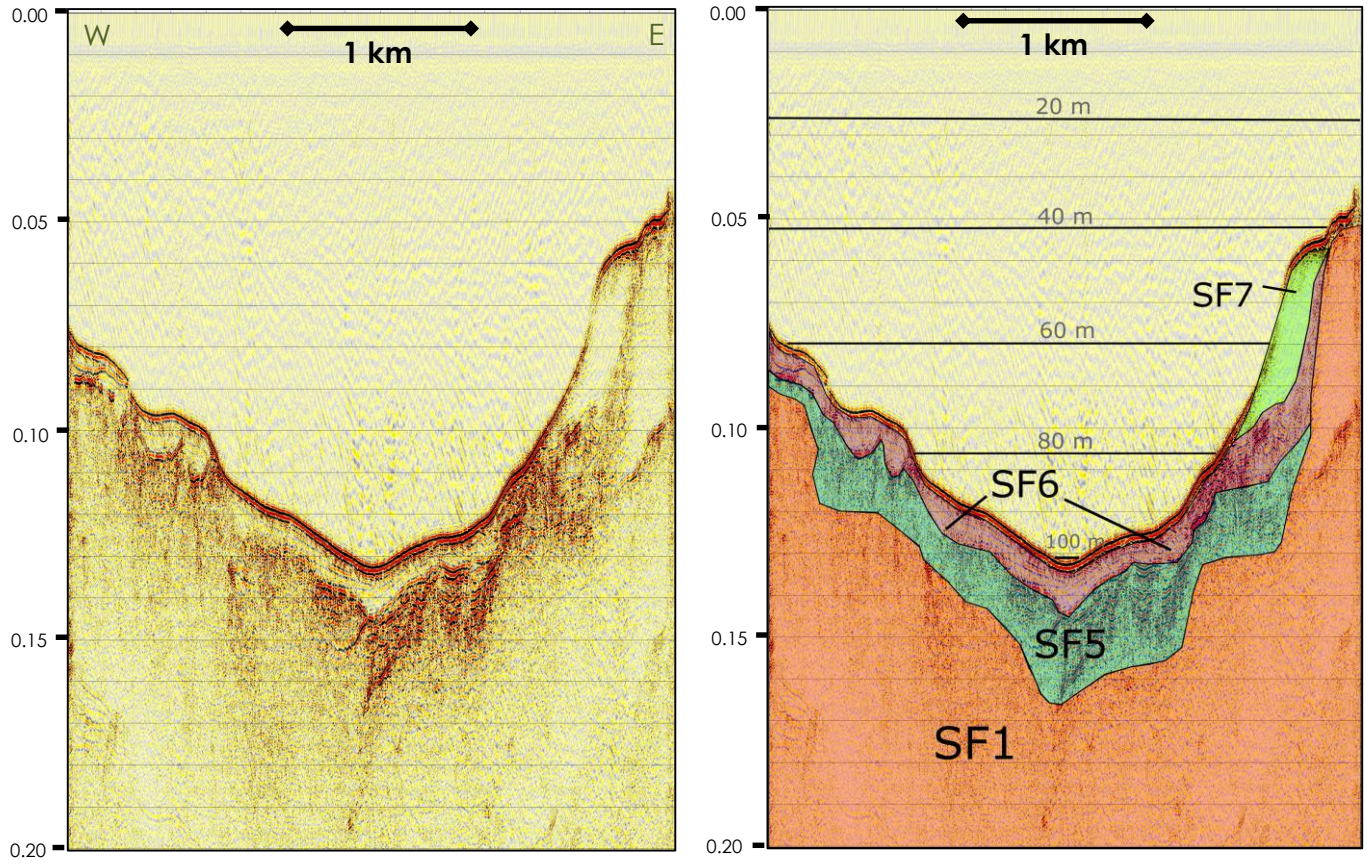

Figure 6.4 • Unannotated line 15-20 (**left**), annotated Line 15-20 with four seismic facies observed within the McLennan fjord basin (**right**) and correlates with facies from line 15/18 (*Figure 6.3*).

regular and well layered in 15-20 (*Figure 6.4*). SF7 is similar to SF6 and is present on the seaward face of the fjord basin progressing up, close to the entrance sill. SF7 is also present on the shelf that extends seaward. SF7 within the fjord basin and on the shelf have similar seismic characteristics and is assumed the same facies despite its differing localities.

6.2.2 Hanfield Inlet •

Hanfield Inlet is a fjord on the eastern coast of the Auckland Islands that has been the subject of extensive seismic surveying undertaken over three seasons (14PL001, 15PL001, 16PL119). The fjord, although being 4.4 km in length, is divided into three arms (North, Main, and South), but it still maintains a west-east orientation. Contour elevations (20 m) exhibit the steep sided nature within the inlet, increasing further landward with dramatic cliff faces and bluffs. Other valleys, and hanging valleys progress into the main body of the inlet observed on the southern side (*Figure* 6.5). Extensive surveying was undertaken within Hanfield Inlet during 2014 (14PL001) with eight lines sweeping through the inlet at regular a spacing. Line 14-25 in Hanfield Inlet reveals an over-deepened profile with sub-basins within the fjord (*Figure* 6.6). The main body of the fjord is enclosed seaward by a shallow entrance sill

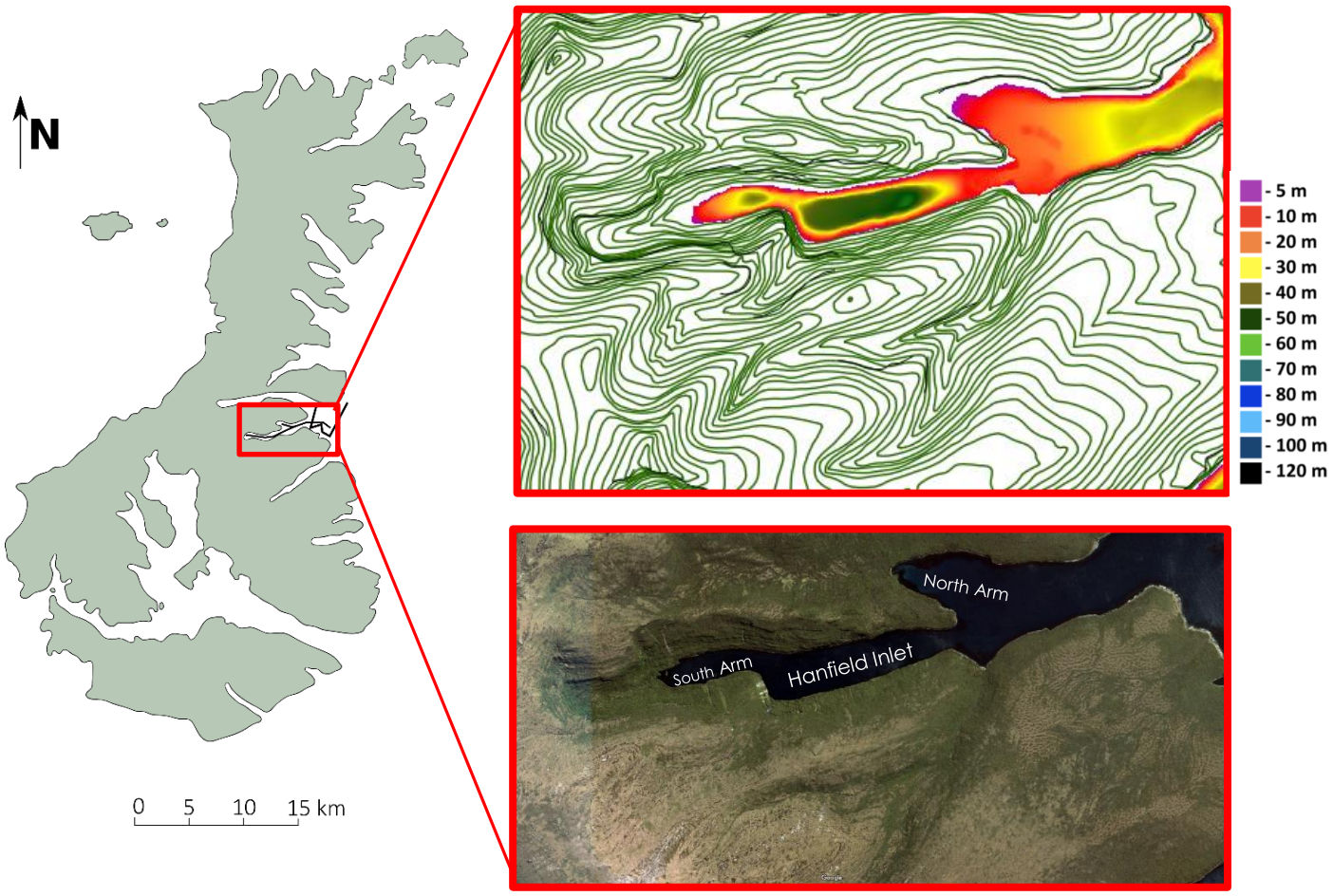

Figure 6.5 • Locality of Hanfield Inlet on the eastern coast of Auckland Island and accompanying seismic transects (**left**), Hanfield Inlet modeled by land contours (20 m) and seafloor bathymetry (**top**), satellite image of Hanfield Inlet – Google Earth (**bottom**).

Line 14-25 • **Hanfield Inlet, Auckland Islands**
Length – 2, 314 m (2.3 km) (Depth axis is in time – Seconds)

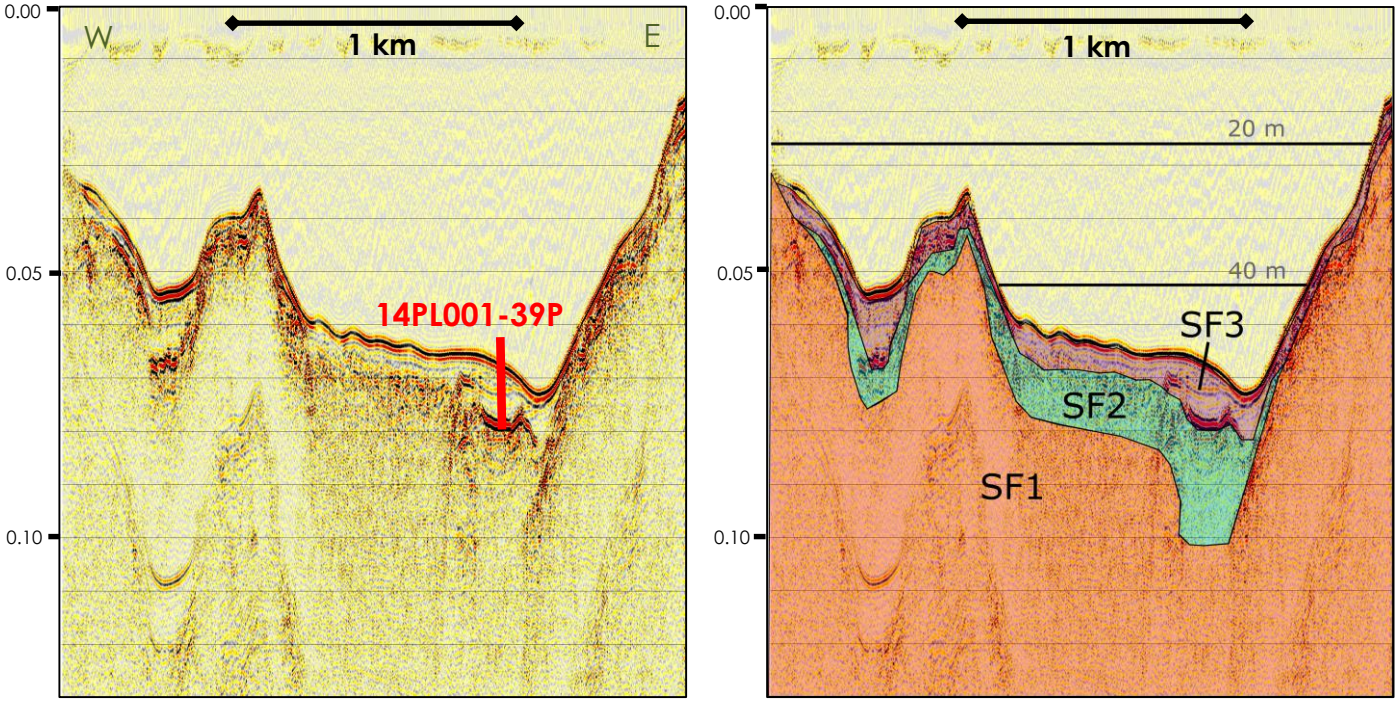

Figure 6.6 • Unannotated line 14-25 with coring locality and naming convention (**left**), annotated line 14-25 with three seismic facies present in Hanfield Inlet based on variations in the seismic data (**right**).

(~14 m deep) that progresses into the main outer basin reaching ~61 m at its deepest point. Landward, a smaller inner basin is bound by a deeper sill (~28 m) progressing to 40 m at the inner basins deepest point. Sediments observed within line 14-25 show two distinct seismic facies that range in thickness that overlie the volcanic bedrock/basement - SF1. Unconformably overlying SF1 is a chaotic facies with faint internal reflections observed in some places. The contact between the bedrock (SF1) and the overlying sediment (SF2) is unclear and is inferred. SF3 is present at the stratigraphic top and is observed as a semi-transparent facies with continuous internal reflections that weaken with depth. A highly reflective layer is observed on the boundary between SF2 and 3 towards the main sill, but is not laterally continuous and may be masked by the chaotic nature of SF2. The main basin was penetrated by a 6 m piston core barrel with 5.53 m of core being recovered (14PL001-39P). The core targeted the location of the thickest package within the basin, which crossed a terrestrial/marine transition dated at 8 ka (Einvik-Heitmann 2014; Brown 2015) (*Figure* 6.6).

6.2.3 Norman Inlet •

Norman Inlet, the longest inlet on Auckland Island, was the subject of 12 seismic survey transects during 14PL001 and 16PL119. Norman Inlet exhibits a more elongate glaciated profile than other fjord localities (~7.4 km in length). Contour elevations and the surrounding topography are symmetrical on either side of the fjord, with a gentler gradient than that observed at Hanfield Inlet. The head of the Inlet to the west has two large former cirque basins that progress to a confluence at the head of the inlet (*Figure 6.7*). An excerpt within line 16-09 from Norman Inlet shows an extensive fjord basin that approaches ~60 m depth (*Figure 6.8*). This basin is bounded by an entrance sill (~16 m deep) with minor sub-basins in places. Seven seismic facies are identified in the fjord basin and on the seaward shelf. The volcanic basement (SF1) varies in depth within the fjord. Topographic highs/outcrops of SF1 are present at the main entrance sill and a secondary, landward sill. The three seismic facies observed within the fjord section of line 16-09 exhibit a complex nature with many areas being masked by a chaotic seismic signal.

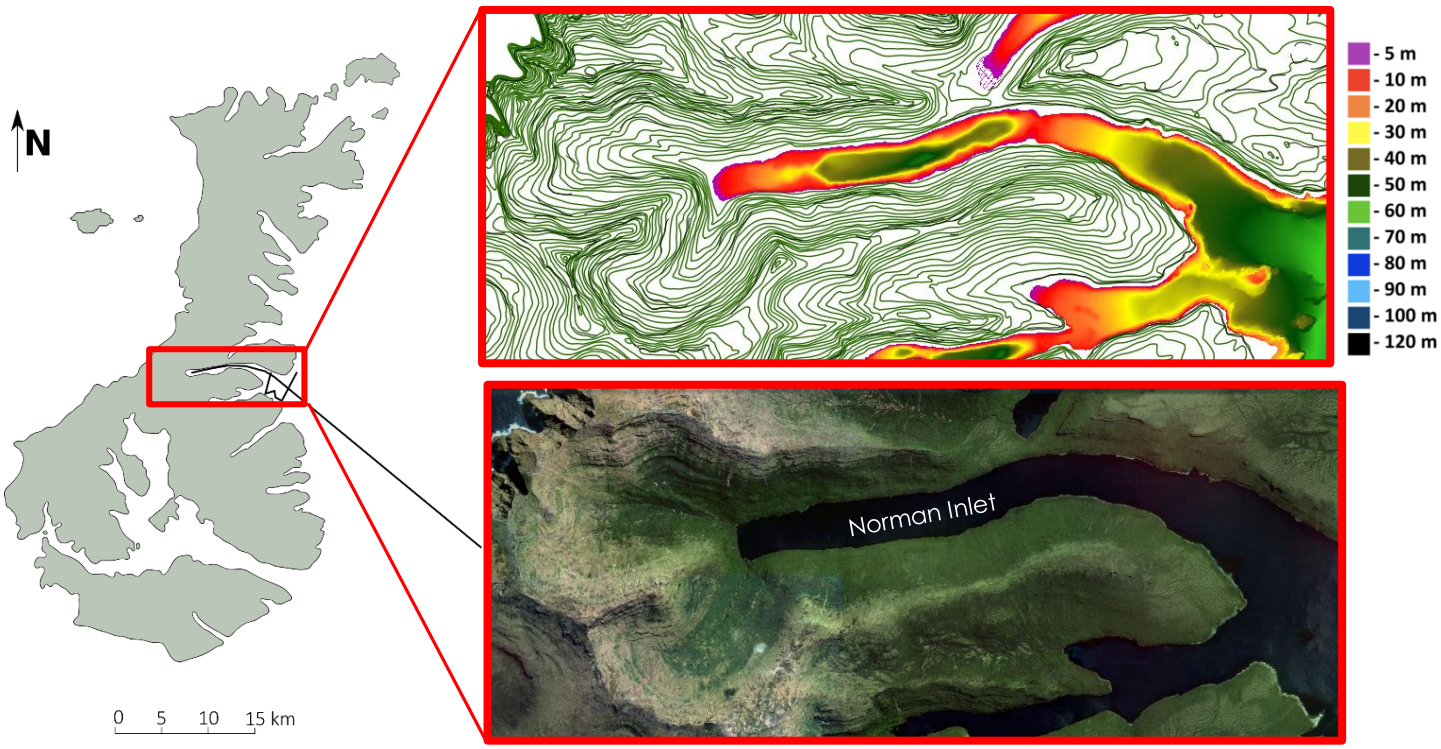

Figure 6.7 • Locality of Norman Inlet on the eastern coast of Auckland Island with seismic lines (**left**), Norman Inlet modeled by land contours (20 m) and seafloor bathymetry (**top**), satellite image of Norman Inlet – Google Earth (**bottom**).

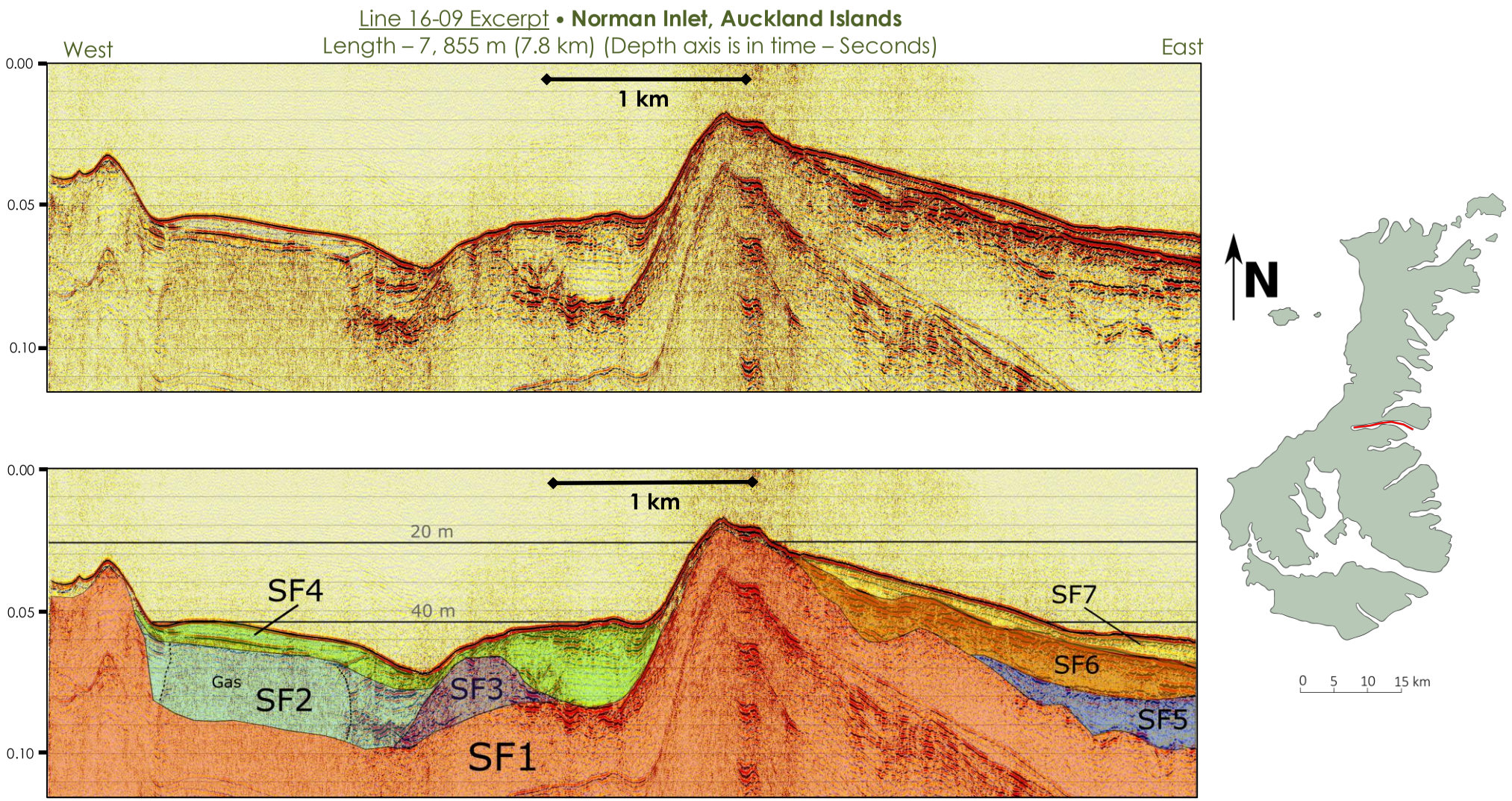

Figure 6.8 • Unannotated line 16-09 excerpt (**top**), annotated line16-09 (**bottom**) with seven seismic facies present within Norman Inlet and on the seaward shelf, based on variations within the seismic data and facies locality.

Much of SF2 that overlies SF1 has a chaotic structure with very weak internal reflections. Some stronger reflections are present within the facies and are juxtaposed to the chaotic section of SF2. SF3 is another facies that appears mostly chaotic with some weak internal reflections. Its mound-like structure contrasts the other facies in the basin (a similar feature is observed in Deep Inlet, but is not described in this thesis; however is presented in the appendix – A 1.4). SF4 is represented as a semi-transparent package with internal reflections; however is difficult to determine the lower and lateral bounds of the facies due to the irregular, masked underlying sequence. Although the basin stratigraphic sequence is complex, it does have similarities with other fjord basin systems. Norman Inlet exhibits a lower chaotic unit, overlain by a semi-transparent layered facies. This simplified stratigraphy is echoed at other fjord inlets (e.g. McLennan and Hanfield Inlets). Three seismic facies are observed on the outer section to the east that is still within the terrestrial bounds of the inlet. SF5 lies unconformably above the bedrock as a transparent facies with very weak, irregular internal reflections. SF5 is separated from SF6 by a strong, laterally continuous reflection. SF6 exhibits semi-continuous, strong reflections that is chaotic in places. SF7 is present at the stratigraphic top and is characterised by parallel, continuous reflections overlying the irregular SF6 surface.

6.2.4 Hanfield and Norman Inlet Confluence •

Four seismic transects were acquired at the confluence of Norman Inlet and Hanfield Inlet to contribute to the previous bisecting data. Transects perpendicular to the confluence have captured the inlets bedrock morphologies and sedimentary infill which vary between the inlets. At this locality, the topography opens up to an expansive embayment, which contrasts from the narrow, steep profiles of both inlets. Within the bathymetric data, a small ridge is observed which segregates the submarine limits of both inlets within the confluence (*Figure 6.9 – Top*). Line 16-11 has five seismic facies (*Figure 6.10)*. The volcanic bedrock, SF1, is observed outcropping at the seabed but within the Norman Inlet section is down at depths of <100m. Unconformably overlying SF1 is a semi-transparent unit with semi-continuous reflections and is chaotic in places. SF3 observed within the main section of the Norman Inlet paleo-valley exhibits irregular reflections with on-lapping truncations to the underlying SF2. SF4 is a similar facies to SF2; however is situated in two depressions correlating to the entrance of Hanfield Inlet. SF2 and SF4 are probably a correlating facies. SF5 is at the stratigraphic top of the package

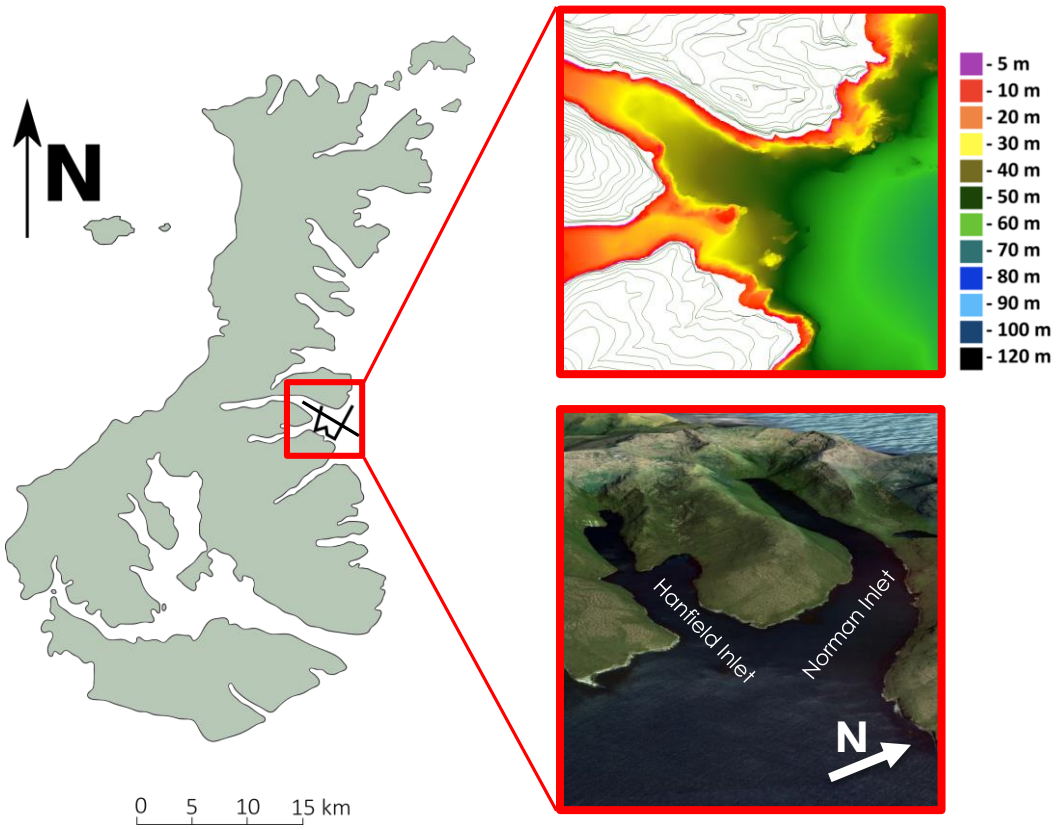

Figure 6.9 • Locality of the Hanfield and Norman Inlet confluence with seismic lines (**left**), surrounding topography modeled by land contours (20 m) and seafloor bathymetry (**top**), satellite image of Hanfield and Norman Inlet confluence – Google Earth (**bottom**).

Line 16-11 • **Norman & Hanfield Inlet Confluence, Auckland Islands**
Length – 2, 659 m (2.7 km) (Depth axis is in time – Seconds)

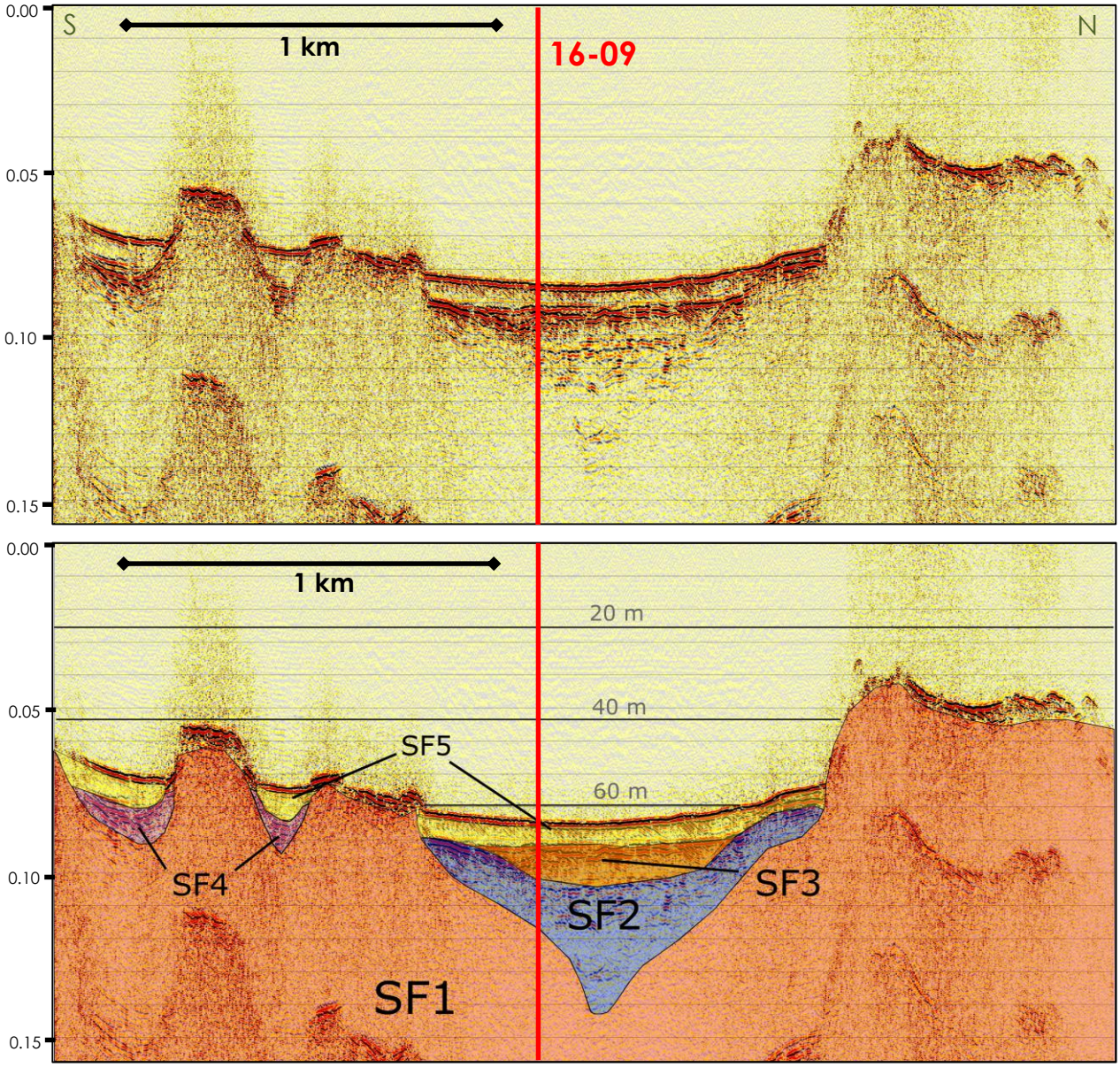

Figure 6.10 • Unannotated line 16-11 with tie line 16-09 locality (**top**, annotated line 16-11 with five seismic facies within the Hanfield and Norman Confluence with tie line 16-09 locality (**bottom**).

and is semi-transparent with weak parallel reflections. These facies have been observed in numerous other transects. Within the confluence of the two inlets, the valley originating from Norman Inlet is far more substantial and expansive in comparison to Hanfield Inlet. These facies correlate to an excerpt of line 16-09 that bisects the main length of Norman Inlet including line16-11. The facies within in line 16-09 are very similar to the facies presented in line 16-11; however line SF1

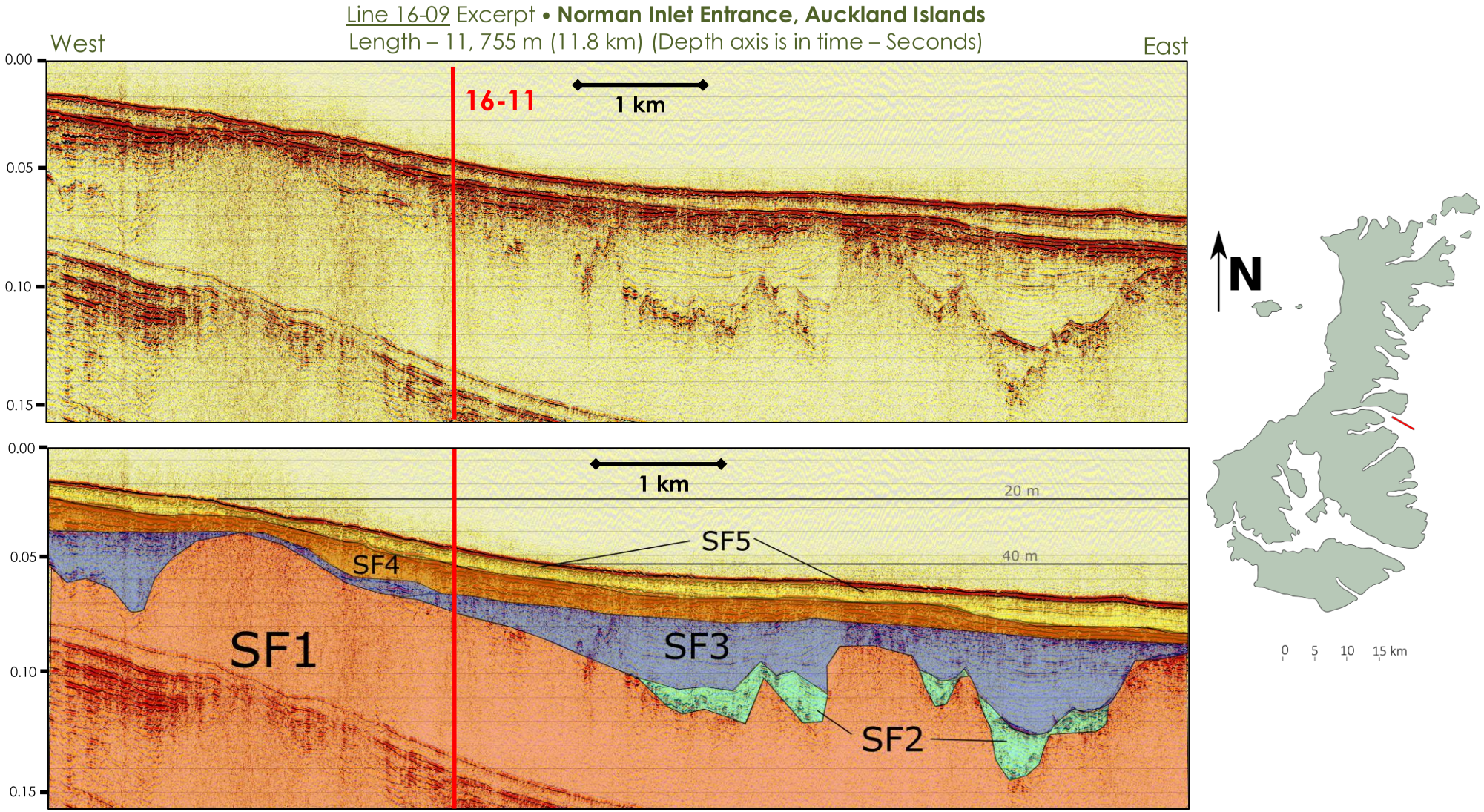

Figure 6.11 • Unannotated line 16-09 excerpt (**top**), annotated line 16-09 excerpt showing five seismic facies based on variations within the seismic data, (**bottom**) line 16-09 begins within the Norman-Hanfield Inlet embayment progressing east to the shallow shelf. Line 16-11 tie line locations is presented on both figures.

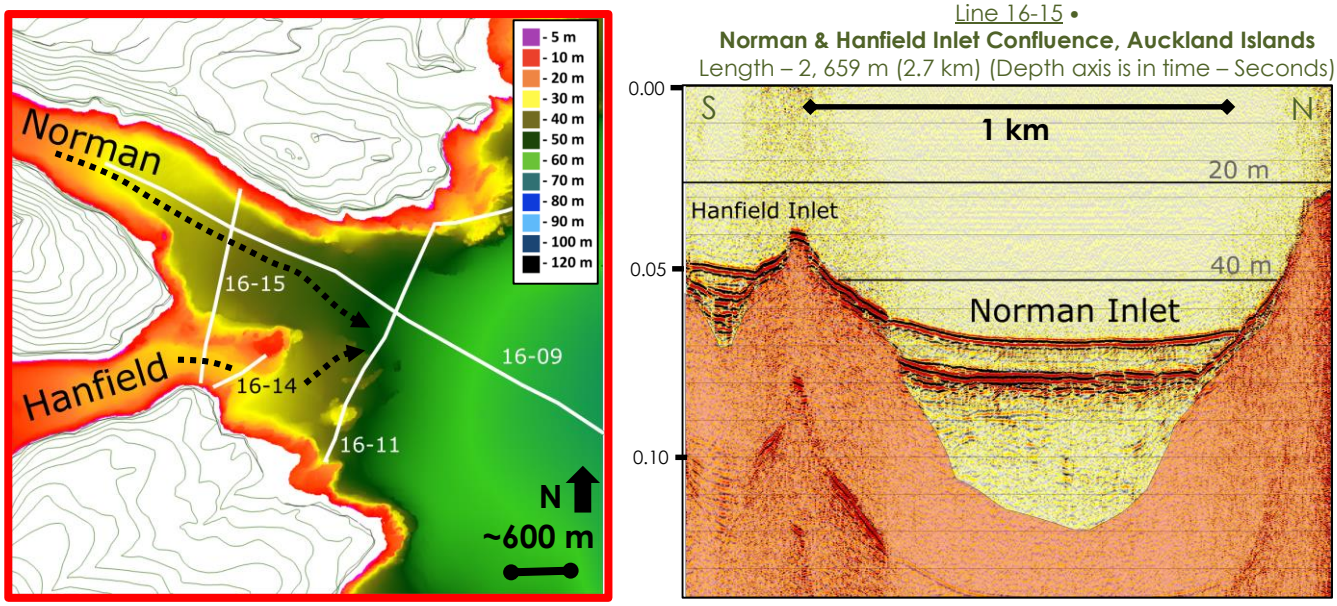

Figure 6.12 • (**left**) Bathymetry, seismic tracks and valley flow direction of Norman and Hanfield Inlets, annotated line 16/15 with valleys and correlating valley origins (**right**).

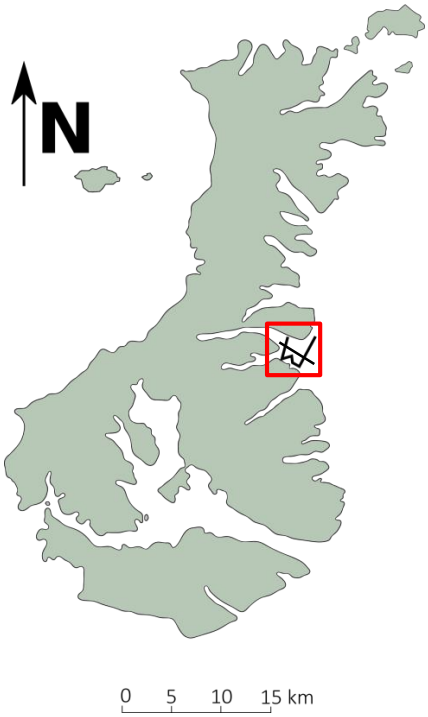

exhibits a more undulating, irregular nature, parallel with Norman Inlet. SF3 within line 16-09 is a basal unit observed seaward and overlays the bedrock (SF1) in a draped fashion. Figure 6.12 shows the bathymetry of Hanfield and Norman Inlets confluence against the seismic tracks. The main valley feature associated with Norman Inlet and the smaller sub-valleys of Hanfield Inlet are present within line 16-11 (*Figure 6.10*). Both of these valley features are observed ~1 km landward in line 16-15 (*Figure 6.12*).

6.2.5 Fly Harbour •

Fly Harbour is the southernmost fjord at the Auckland Islands and was investigated by two seismic transects bisecting the length of the fjord, extending to the shelf break. Prior to 16PL119, Fly Harbour had no previous soundings. The onshore characteristics of Fly Harbour resemble similar terrestrial glaciated inlets at the Auckland Islands with an elongate, steep sided profile that is orientated roughly west to east (*Figure 6.13*). Seismic profiles from Fly Harbour exhibit a classic fjord profile with a shallow entrance sill progressing into an over-deepened fjord basin (*Figure 6.14*). Another sill is also present within the harbour further landward leading to a second, shallower basin. The fjord transect 16-02 exhibits four seismic facies with a fifth facies observed on the shelf outside the fjord (*Figure 6.14*). The bedrock/basement (SF1) surface at Fly Harbour is exposed at seabed topographic

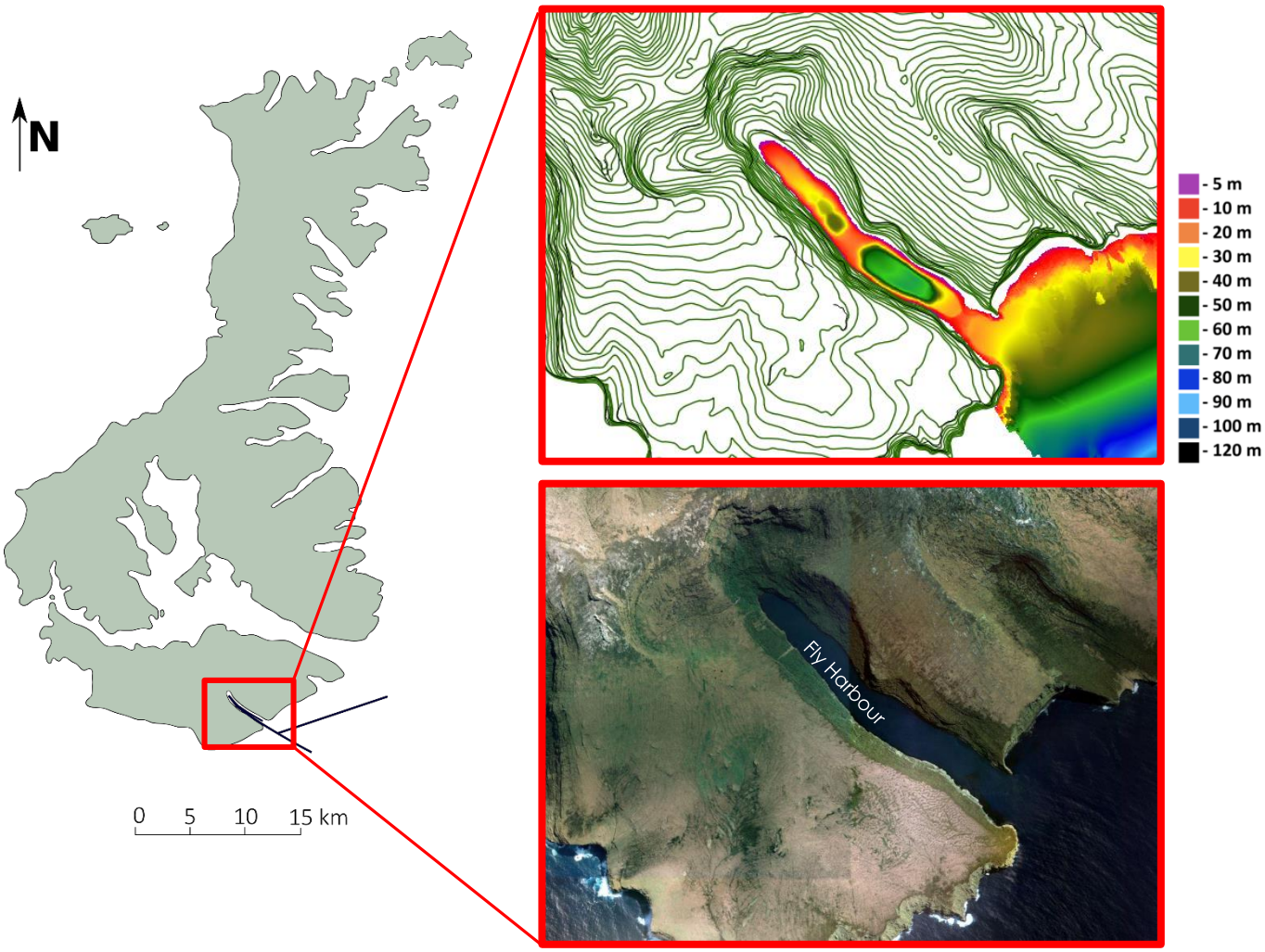

Figure 6.13 • Locality of Fly Harbour on the south-eastern coast of Adams Island with seismic lines (**left**), Fly Harbour modelled by land contours (20 m) and seafloor bathymetry (**top**), satellite image of Fly Harbour – Google Earth (**bottom**).

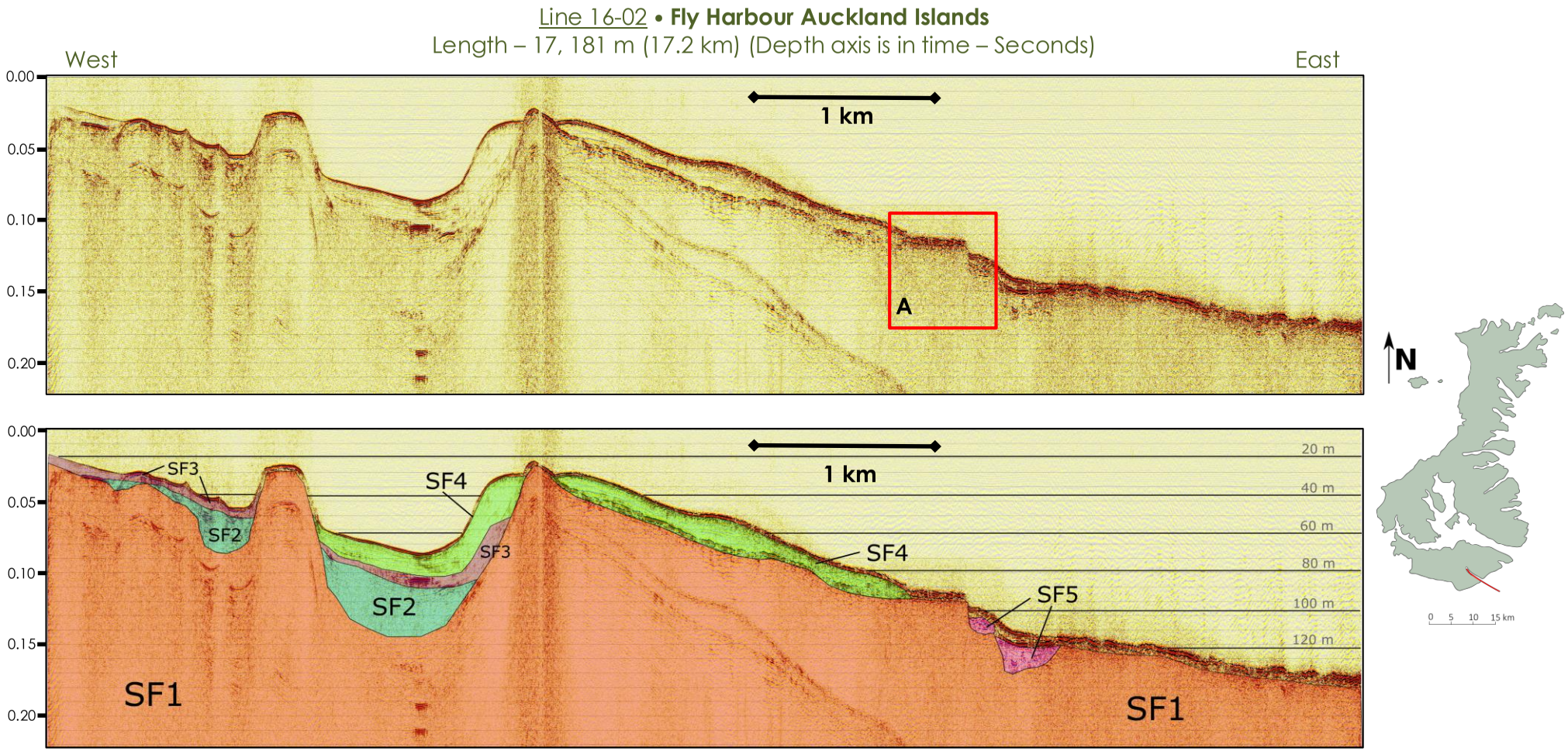

Figure 6.14 • Unannotated line 16-02 (**top**), annotated line 16-02 exhibiting five seismic facies based on variations within the seismic data (**bottom**). This transect progresses from a fjord system in the west to a shelf setting in the east.

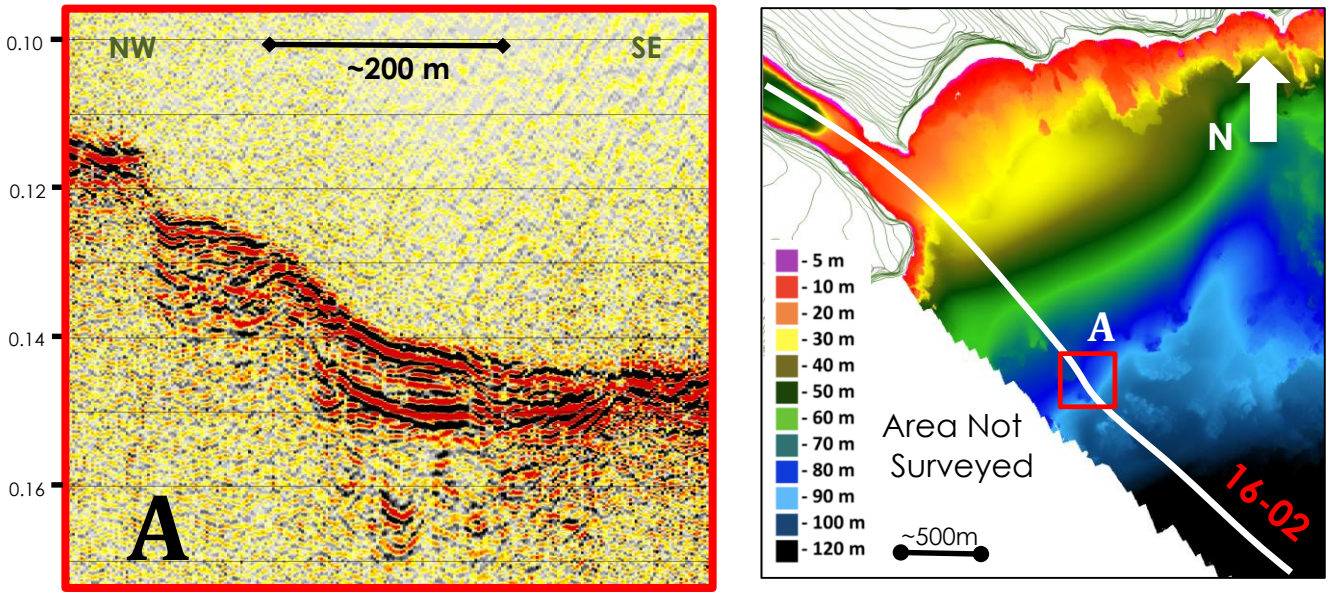

Figure 6.15 • Line 16-02 excerpt of a seafloor bedrock outcrop and a small sedimentary package, depth axis is in time (**left** - A) with accompanying bathymetry (**right**)

highs at the entrance and back basin sills, progressing down into the fjord where the sediment/bedrock surface is unclear. The bedrock surface on the shelf sits far closer to the surface with little sedimentary cover. SF2 sits unconformably over SF1 and is characterised by transparent, weak internal reflections. SF2 shows spatial variation between the main fjord basin and back basin in seismic characteristics; however the same facies are assumed. SF3 rests stratigraphically above SF2 and exhibits semi-transparent, semi-continuous reflections that are draped over the underlying topography. SF4 can be separated to a fjord section and a shelf section but they possibly constitute the same facies due to similar seismic characteristics. The facies is defined by semi-transparent, laterally continuous reflections that rise up the sill within the basin. The facies is present beyond the sill, seaward and progress down the shelf. These types of facies are prevalent at numerous other localities in the south-eastern corner at inlet entrances (e.g. Carnley Harbour, McLennan Inlet). SF5 observed on the shelf section of line 16-02 shows small packages of sediment overlying SF1 with an outcrop of bedrock between 100-120 m water depths. This is observed in the accompanying bathymetric data as a series rocky of outcrops (*Figure 6.15*), which is a common feature of the seafloor on the south-eastern coast in comparison to the extensive sedimentary basin to the north.

6.2.6 Smith Harbour •

Smith Harbour is a curved inlet on the eastern coast of Auckland Island. The harbour originates as a protected valley west of Fella Peninsula, with steep sided valley walls opening up to the eastern coast at a confluence with Tandy Inlet to the north (*Figure 6.16*). The harbour was the subject of seven transects at even spacings. Larger bisecting lines were undertaken from the head of Smith Harbour that progressed east onto the shelf. Perpendicular shelf lines correlate features that were observed within the Smith Harbour bisecting lines. Within the seismic and bathymetric data, Smith Harbour is in contrast to many previously described fjords and inlets. This is due to the lack of seafloor expression of a sill and over-deepened back basin when compared with other fjords (e.g. Fly Harbour, Hanfield Inlet). Line 14-08, which bisects Smith Harbour to the shelf margin, exhibits four seismic facies (*Figure 6.17*). SF2 rests unconformably atop of SF1 and has semi-transparent, semi continuous reflections that on-lap onto the bedrock. SF3 is a layer of strong, continuous reflections that are present throughout 14-08. SF4 is a transparent,

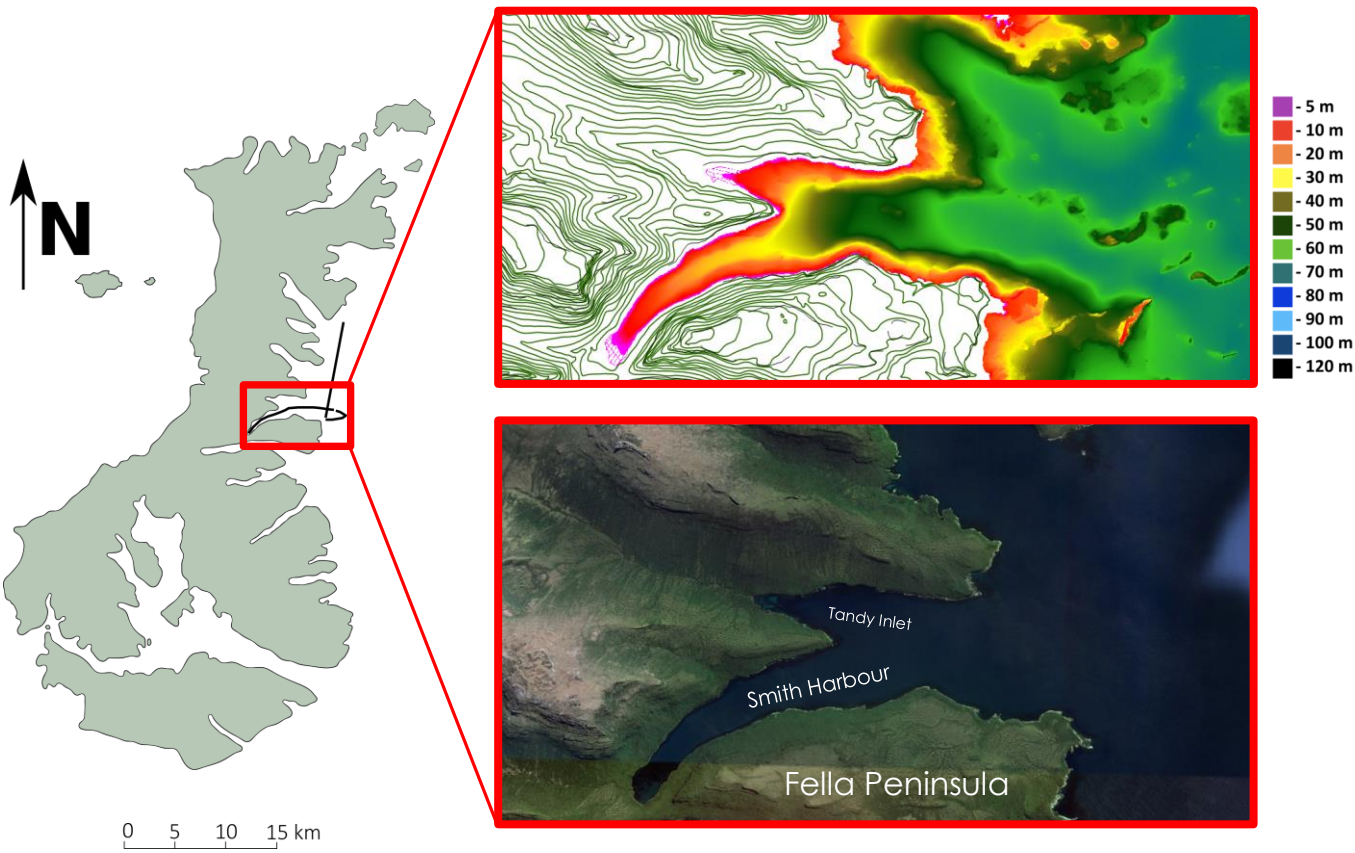

Figure 6.16 • Locality of Smith Harbour on the eastern coast of Auckland Island with seismic lines (**left**), Smith Harbour modeled by land contours (20 m) and seafloor bathymetry (**top**), satellite image of Smith Harbour – Google Earth (**bottom**).

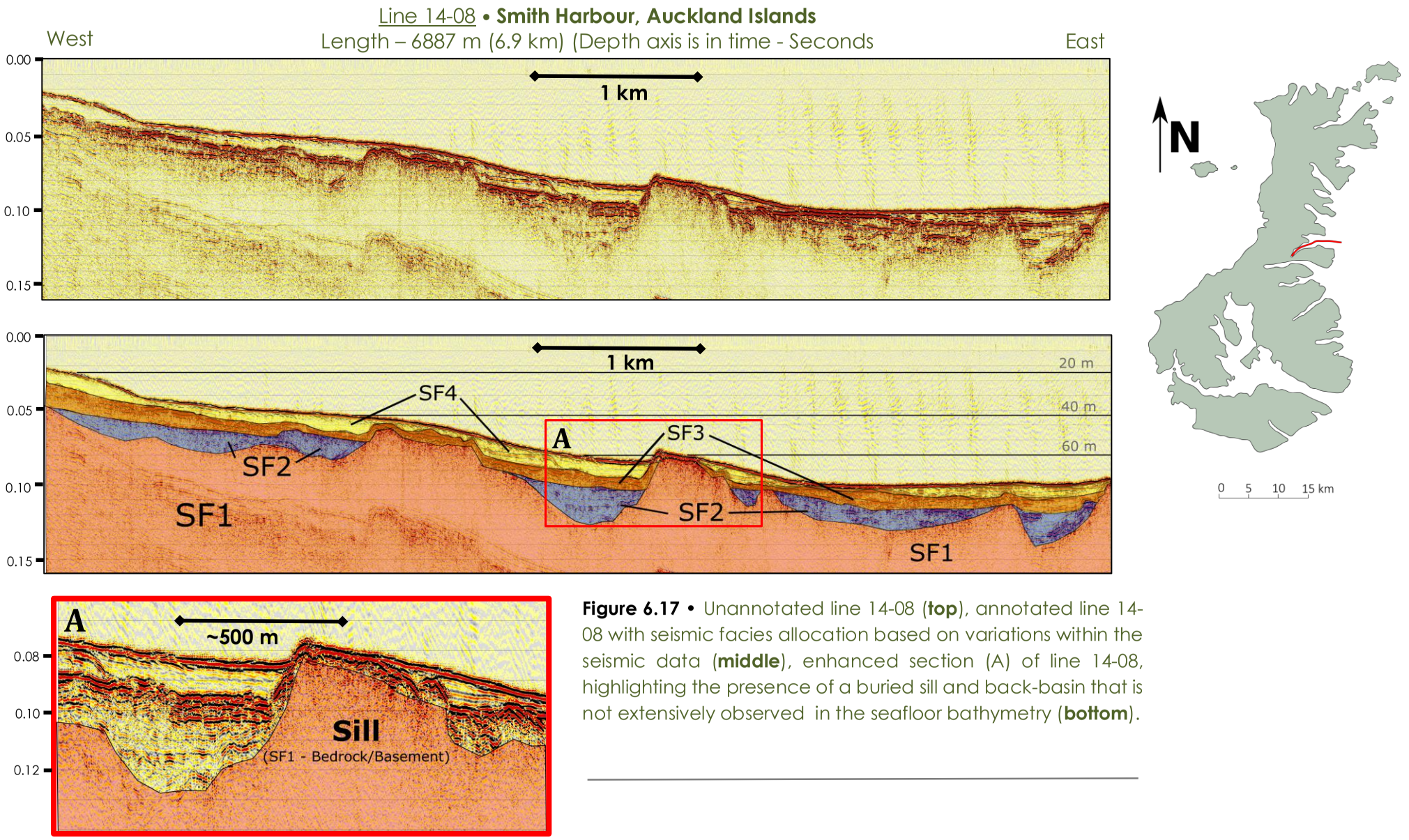

Figure 6.17 • Unannotated line 14-08 (**top**), annotated line 14-08 with seismic facies allocation based on variations within the seismic data (**middle**), enhanced section (A) of line 14-08, highlighting the presence of a buried sill and back-basin that is not extensively observed in the seafloor bathymetry (**bottom**).

laterally continuous package that is extensive throughout eastern coastline localities. Although Smith Harbour contrasts other fjord localities with the lack of a substantial entrance sill and over-deepened basin, bedrock (SF1) is observed and exposed on the seabed within the seismic data. A correlating back basin is also present within the data; however it has been extensively infilled with SF2, 3 and 4 (*Figure 6.17a*). Due to this extensive infill, the Smith Harbour basin and sill seabed expression have been masked within the bathymetry data.

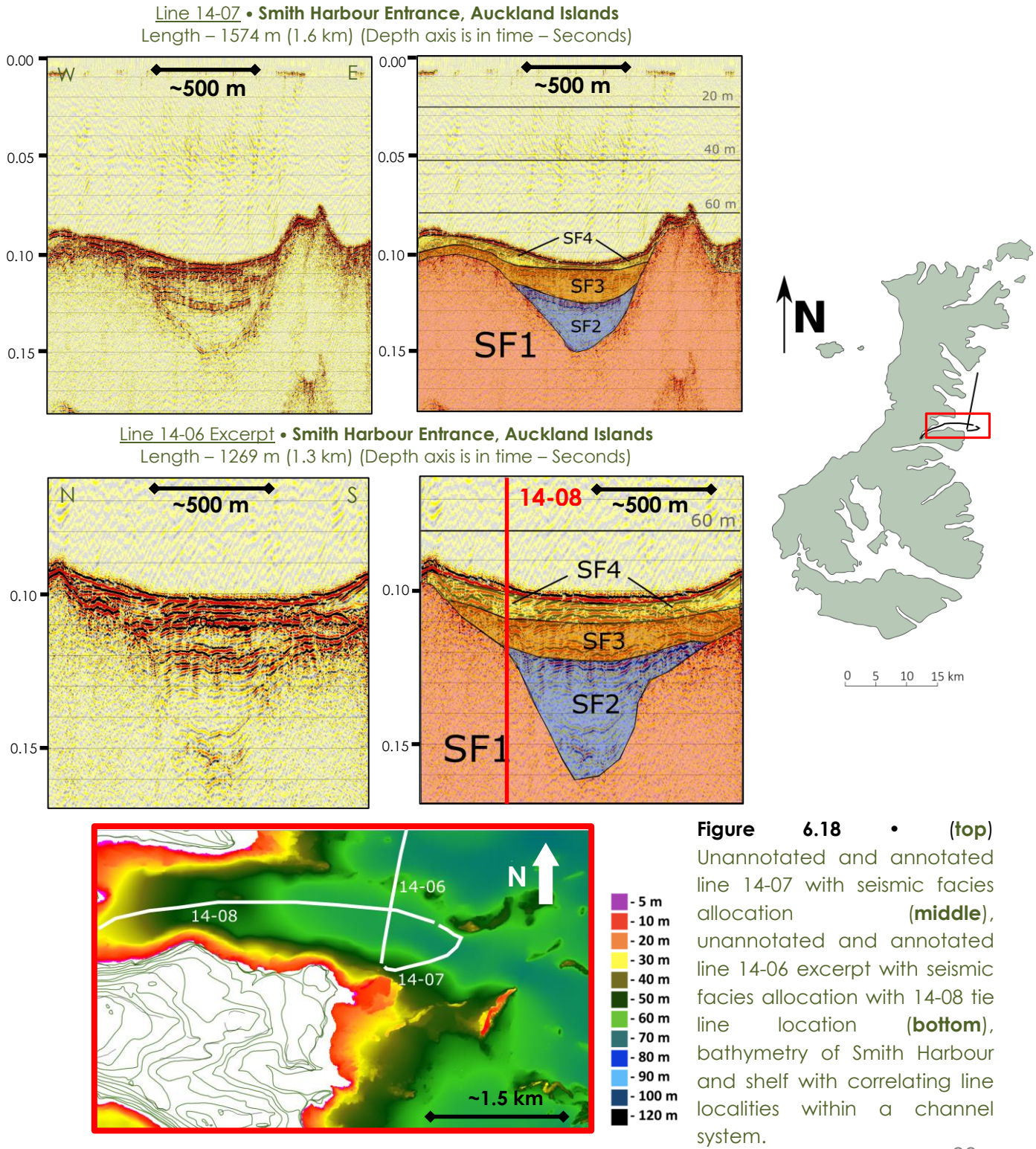

Figure 6.18 • (top) Unannotated and annotated line 14-07 with seismic facies allocation (**middle**), unannotated and annotated line 14-06 excerpt with seismic facies allocation with 14-08 tie line location (**bottom**), bathymetry of Smith Harbour and shelf with correlating line localities within a channel system.

Lines 14-07 and 14-06 correlate to an infilled valley feature originating from Smith Harbour and Tandy Inlet (*Figure 6.18*). Within line 14-07, the same seismic facies are present within the Smith Harbour bisecting line 14-08 that has infilled a valley feature. Line 14-06, extending N/S on the shelf, captures this valley feature at its southern extent while exhibiting the same seismic stratigraphic packages. The location of the valley in the seismic data relates to depth changes consistent with a sediment filled valley feature originating from Smith Harbour and Tandy Inlet in the west. To the north, within the bathymetry data, an exposed bedrock ridge is observed running parallel to the valley, partitioning the valley system from Musgrave Inlet.

6.2.7 Port Ross •

Port Ross to the north of the Auckland Islands was the subject of 11 seismic transects within the historic, shallow inlet. Port Ross in comparison to the majority of the other steep profile inlets, progresses from a deeply incised U-shaped valley to the west opening to a gentle rolling expanse eastward. The bathymetry contrast other previously mentioned inlets. This is due to the shallow, regular nature of the seabed with the maximum depths reaching ~30 m. Port Ross is the shallowest of the major inlets at the Auckland Islands. No expressed entrance sill or overdeepened basin are observed on the seafloor. Within the seismic data (*Figure 6.20*), a highly incised, buried bedrock (SF1) surface is present and is topographically bound to the west. This creates a sediment trap within the terrestrial confines of Port Ross. The bedrock/sediment interface is identified at depths of ~70 m in places. A basal unit (SF2) is present in some sections of the seismic data and is chaotic in nature. This facies may be present further east, however is masked by the multiple. SF3 is the main facies observed within Port Ross. This unit has a semi-transparent nature with

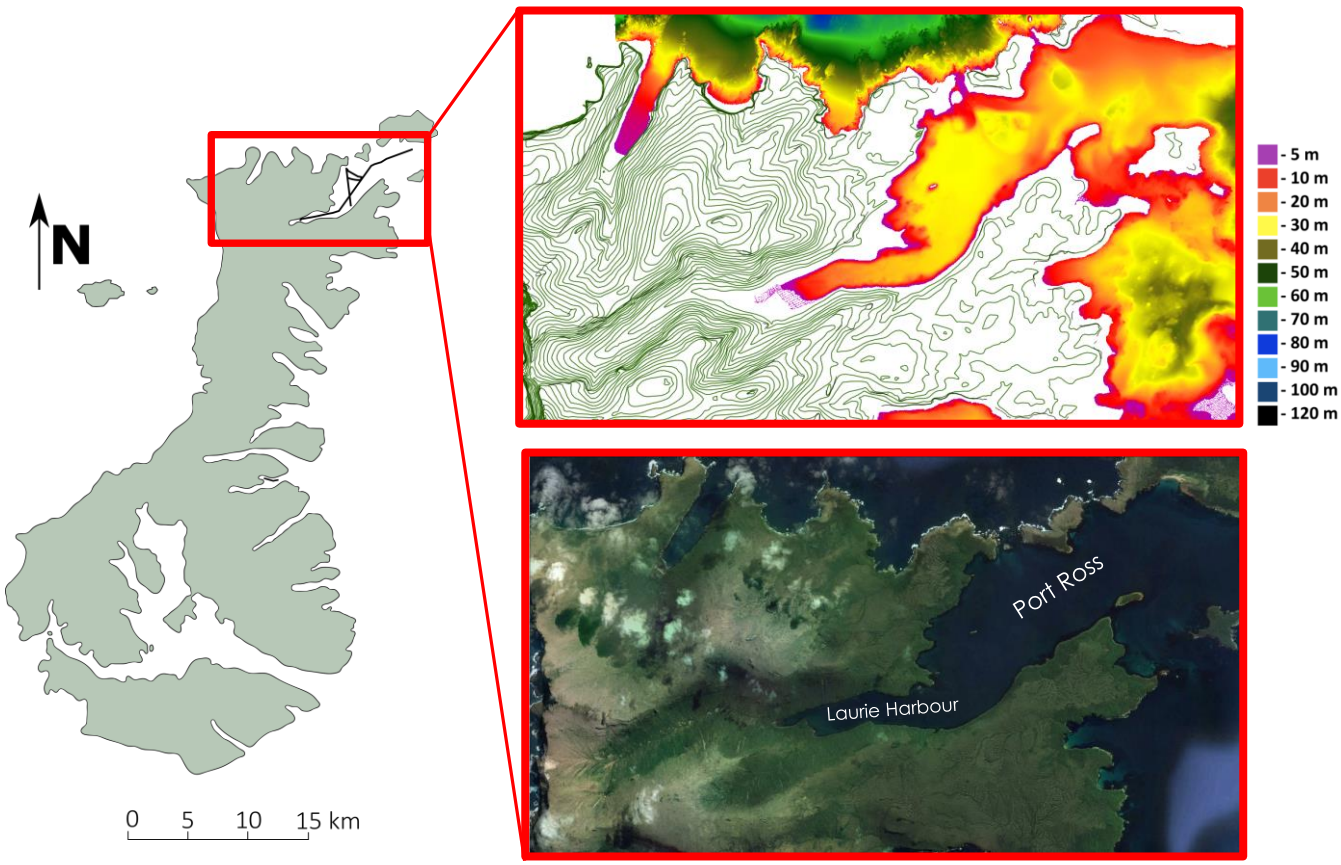

Figure 6.19 • Locality of Port Ross on the northern coast of Auckland Island with seismic lines (**left**), Port Ross modelled by land contours (20 m) and seafloor bathymetry (**top**), satellite image of Port Ross – Google Earth (**bottom**).

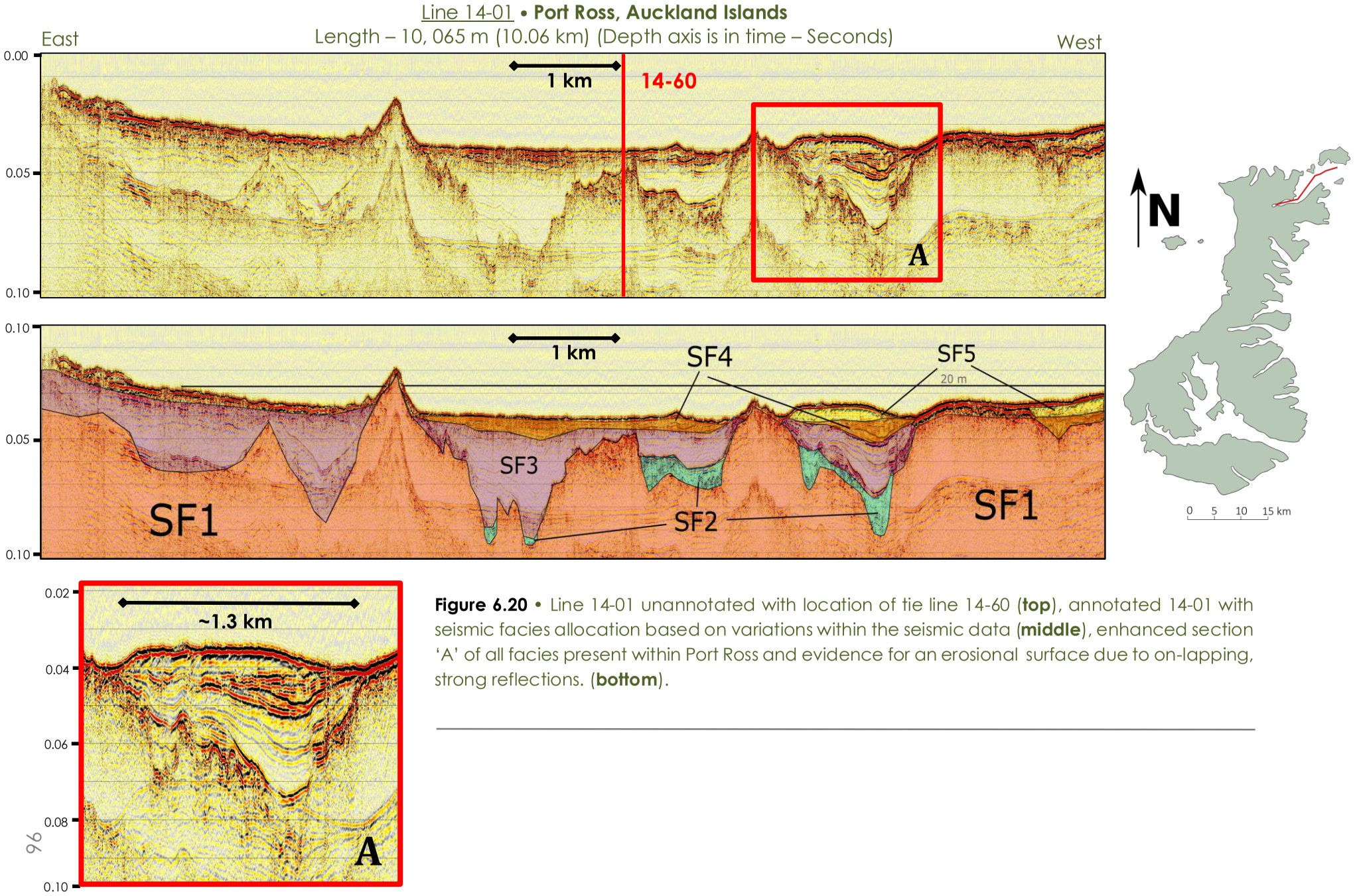

Figure 6.20 • Line 14-01 unannotated with location of tie line 14-60 (**top**), annotated 14-01 with seismic facies allocation based on variations within the seismic data (**middle**), enhanced section 'A' of all facies present within Port Ross and evidence for an erosional surface due to on-lapping, strong reflections. (**bottom**).

Line 14-60 • **Port Ross, Auckland Islands**
Length – 1, 340 m (1.3 km) (Depth is in time – Seconds)

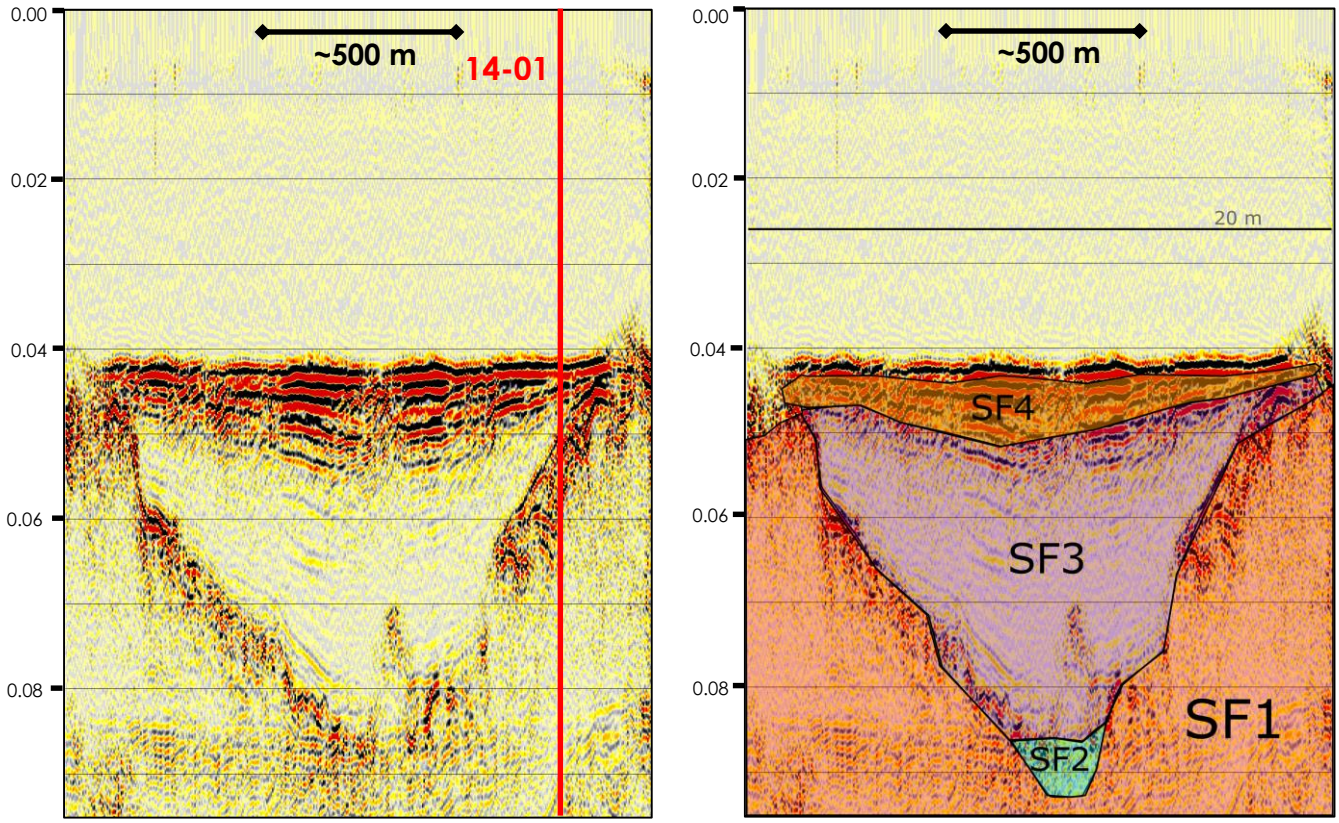

Figure 6.21 • Unannotated line 14-60 with location of tying transect 14-01 (**left**), annotated line 14-60 with seismic facies based on variations in the seismic data (**right**). The main Port Ross buried paleo-valley profile is observed perpendicular to the longitudinal valley profile observed in 14-01 (*Figure 6.20*).

draped internal reflections that are laterally continuous. SF4 overlies SF3 and is a reflective unit that likely has an erosional surface bound at the facies interface (*Figure 6.20a*). SF4 on-laps onto the underlying sediments. SF5 is a massive unit resting on SF4 with the locality correlating with a narrow passage between Enderby and Rose Islands to the north. The irregular bedrock nature within line 14-01 correlates to the seismic transect intersecting the main valley walls of the buried Port Ross paleo-valley. Tying line 14-60 exhibits the perpendicular profile of the main valley body (*Figure 6.21*) that exhibits the facies observed in line 14-01. The basin sedimentary infill, surrounding inlet topography and seabed expressions contrast other described localities and is unique to Port Ross.

6.2.8 Carnley Harbour •

11 seismic lines were collected within the previously un-surveyed expanse of Carnley Harbour. The topography surrounding the harbour has an open, expansive nature with a large catchment area (*Figure* 6.22). This is in contrast to the enclosed, steep sides of many of the eastern inlets (e.g. McLennan & Deep Inlet). Various features are observed within Carnley Harbour that vary from other fjord and inlet profiles. The seismic profiles and stratigraphy vary spatially through the differing arms within the harbour. Line 15-11 (*Figure* 6.23), traversing west to east through the main arm exhibits four main seismic facies. Unconformably overlying the bedrock (SF1) is a layered transparent facies with draped reflections that are continuous in

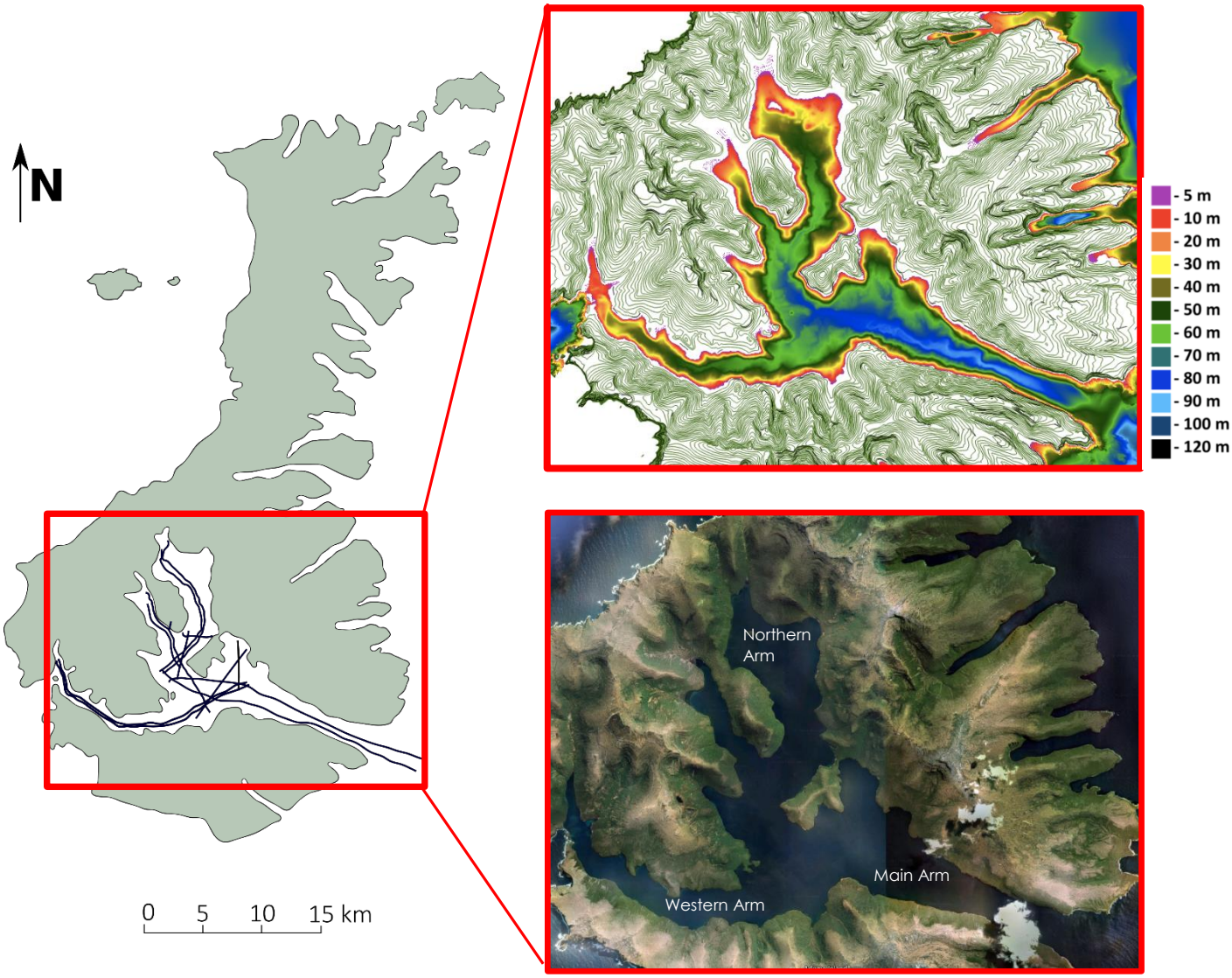

Figure 6.22 • Location of Carnley Harbour and seismic lines (**left**), Carnley Harbour topography (20 m) and bathymetry (**top**), satellite image of Carnley Harbour with arm localities (**bottom**) (Google Earth).

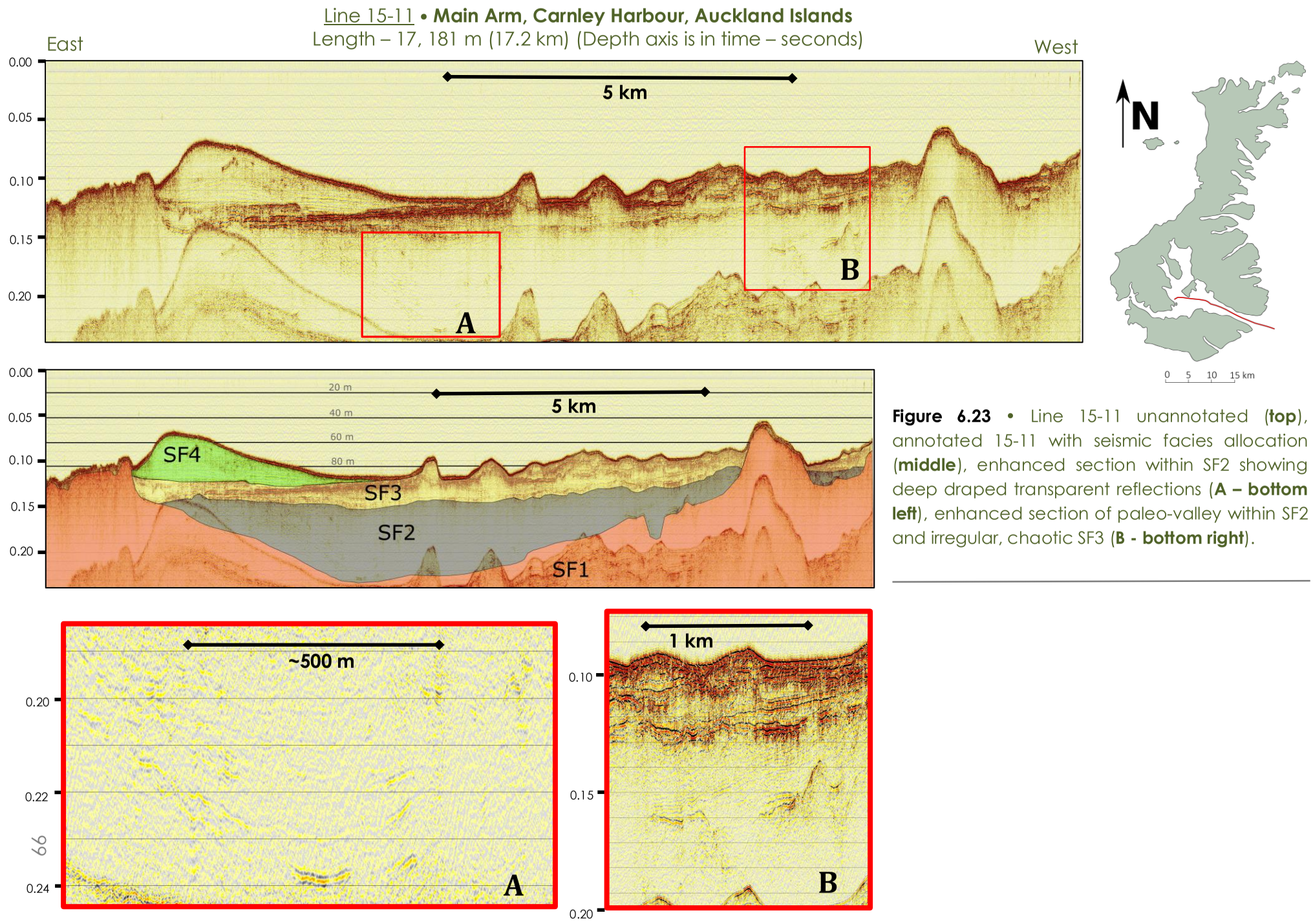

Figure 6.23 • Line 15-11 unannotated (**top**), annotated 15-11 with seismic facies allocation (**middle**), enhanced section within SF2 showing deep draped transparent reflections (**A – bottom left**), enhanced section of paleo-valley within SF2 and irregular, chaotic SF3 (**B - bottom right**).

places. These reflections are present to depths of at least 180 m below SL (*assuming sediment velocity ~1650 m/s*)and arriving before the multiple (*Figure 6.23a*). Within this facies is a paleo-valley feature with strong reflections on the valley shoulders with overlying transparent reflections draping down into a depression (*Figure 6.23b*). This feature is also observed within lines 15-03 and 15-02. Stratigraphically overlying SF2 is an irregular facies that exhibits semi-continuous, strong reflections that are chaotic/disrupted in places. This facies creates a non-uniform, undulating seafloor expression. SF3 has an apparent gentle dip to the east (seaward), parallel to the length of the Main Arm. Within line 15-11, the seafloor in the western extents has a highly variable nature with underlying, undulating internal reflections and many reflection truncations. This is also observed in correlating lines 15-02 (*Figure 6.25*) and 15/03 (*Figure 6.26*). This facies could be further sub-divided but the variable, disrupted nature of the reflections make this difficult. The undulating nature within the seismic data at the locality is reflected within the bathymetric data through channel systems observed converging in the Main Arm of Carnley Harbour, progressing east and increasing in depth (*Figure 6.24*). This facies is present through all Main and Western Arm Lines that are presented here. SF2 and 3 within the Western Arm (line 15-02) exhibit different characteristics to those of the Main Arm (*Figure 6.21*).

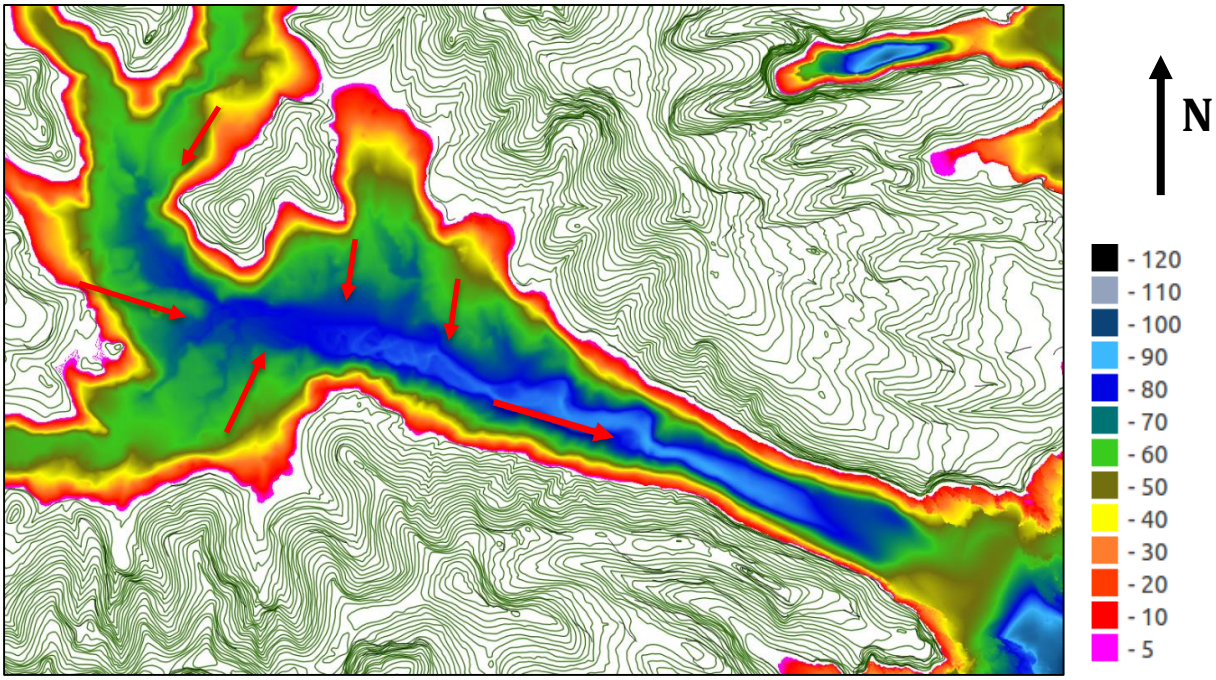

Figure 6.24 • Bathymetry of Carnley Harbour showing drainage incision patterns flowing into the Main Arm channel, deepening to the East. ***~3 km***

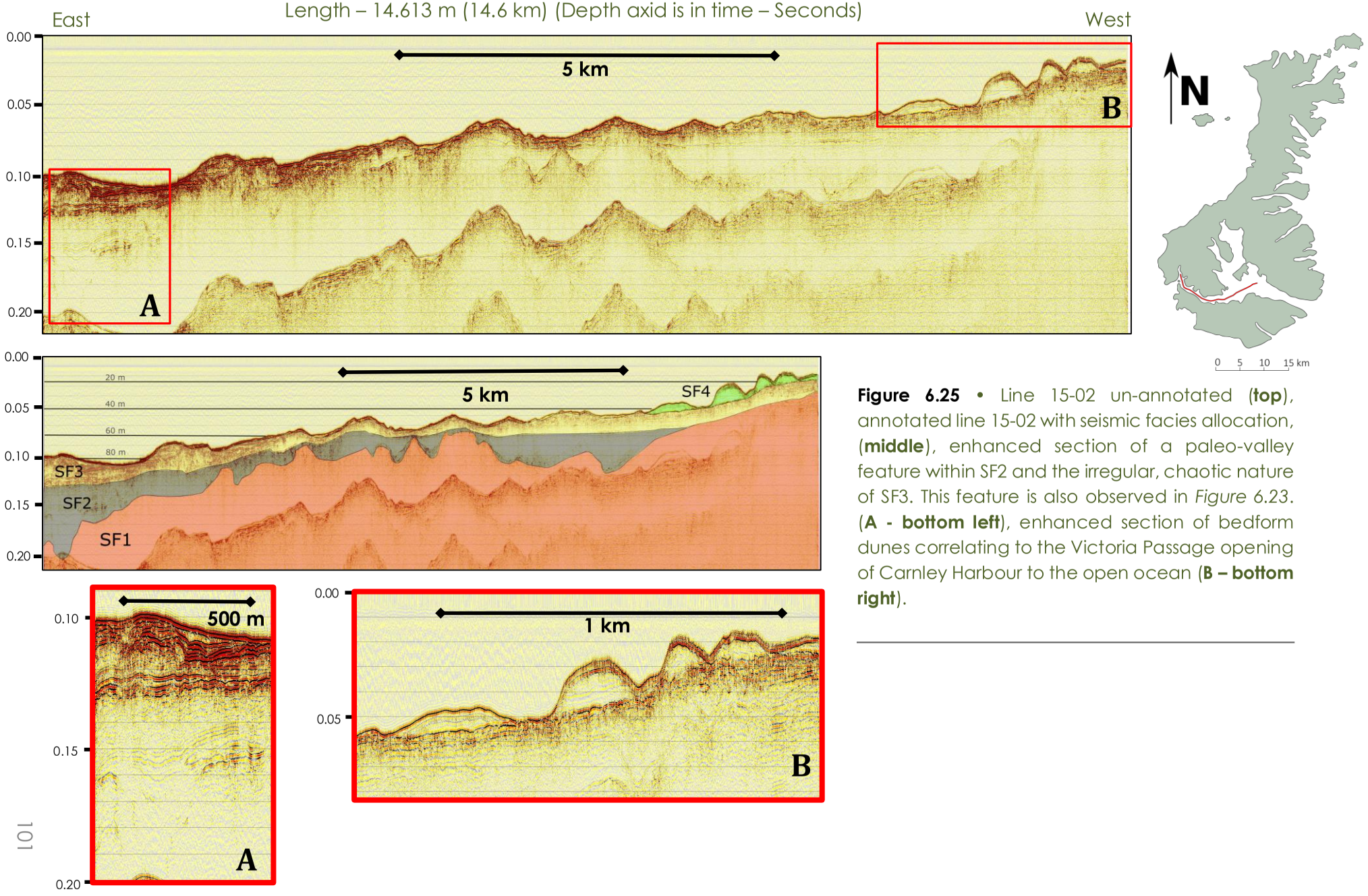

Figure 6.25 • Line 15-02 un-annotated (**top**), annotated line 15-02 with seismic facies allocation, (**middle**), enhanced section of a paleo-valley feature within SF2 and the irregular, chaotic nature of SF3. This feature is also observed in *Figure* 6.23. (**A - bottom left**), enhanced section of bedform dunes correlating to the Victoria Passage opening of Carnley Harbour to the open ocean (**B – bottom right**).

Line 15-03 • **Tagua Bay, Carnley Harbour, Auckland Islands**
Length – 3, 077 m (3.07 km) (Depth axis is in time – Seconds)

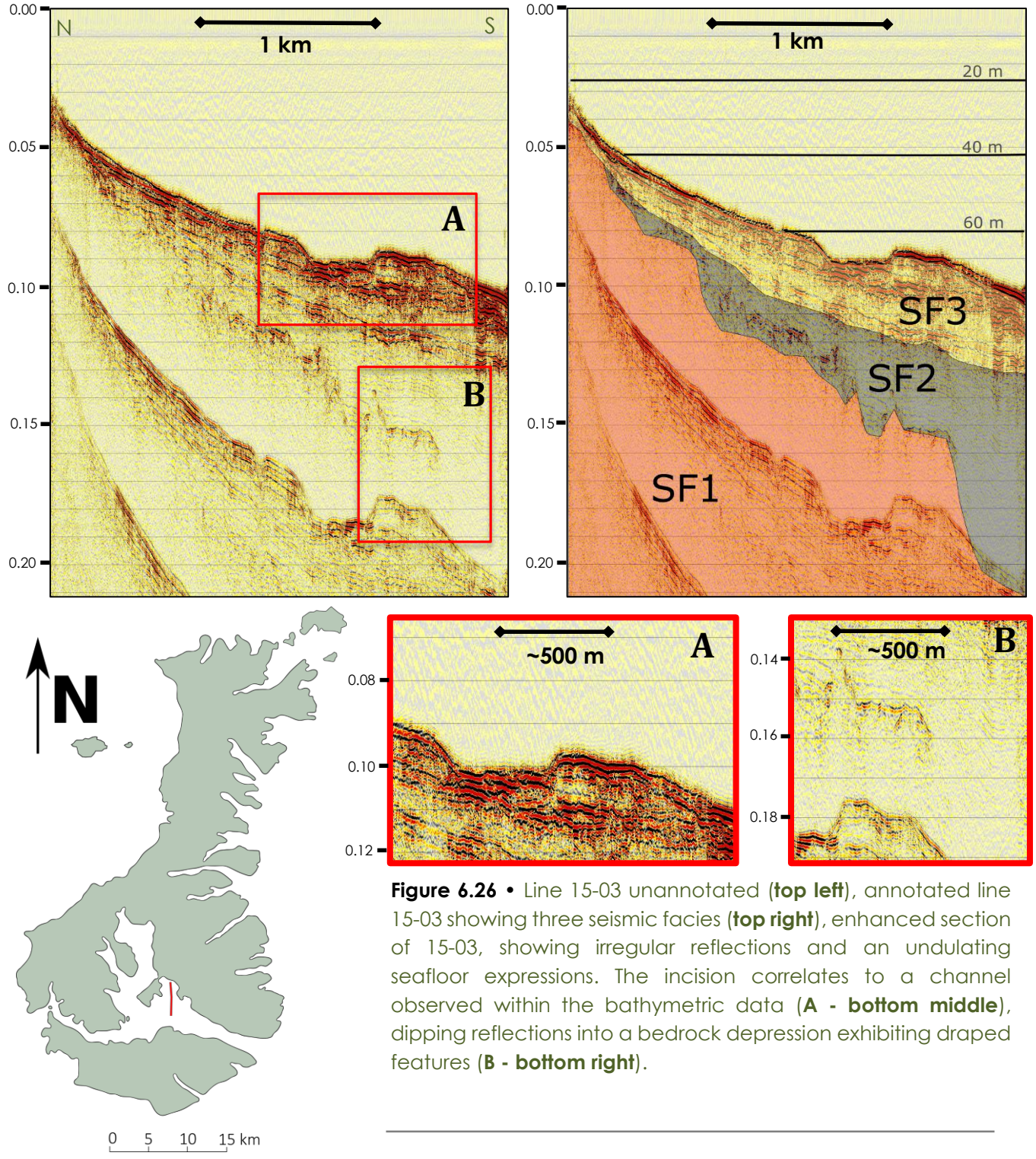

Figure 6.26 • Line 15-03 unannotated (**top left**), annotated line 15-03 showing three seismic facies (**top right**), enhanced section of 15-03, showing irregular reflections and an undulating seafloor expressions. The incision correlates to a channel observed within the bathymetric data (**A - bottom middle**), dipping reflections into a bedrock depression exhibiting draped features (**B - bottom right**).

The bedrock in the Western Arm is more apparent and is expressed closer to the surface, creating sub-basins where the seismic facies are definable. The facies packages vary in depth spatially in the Western Arm.

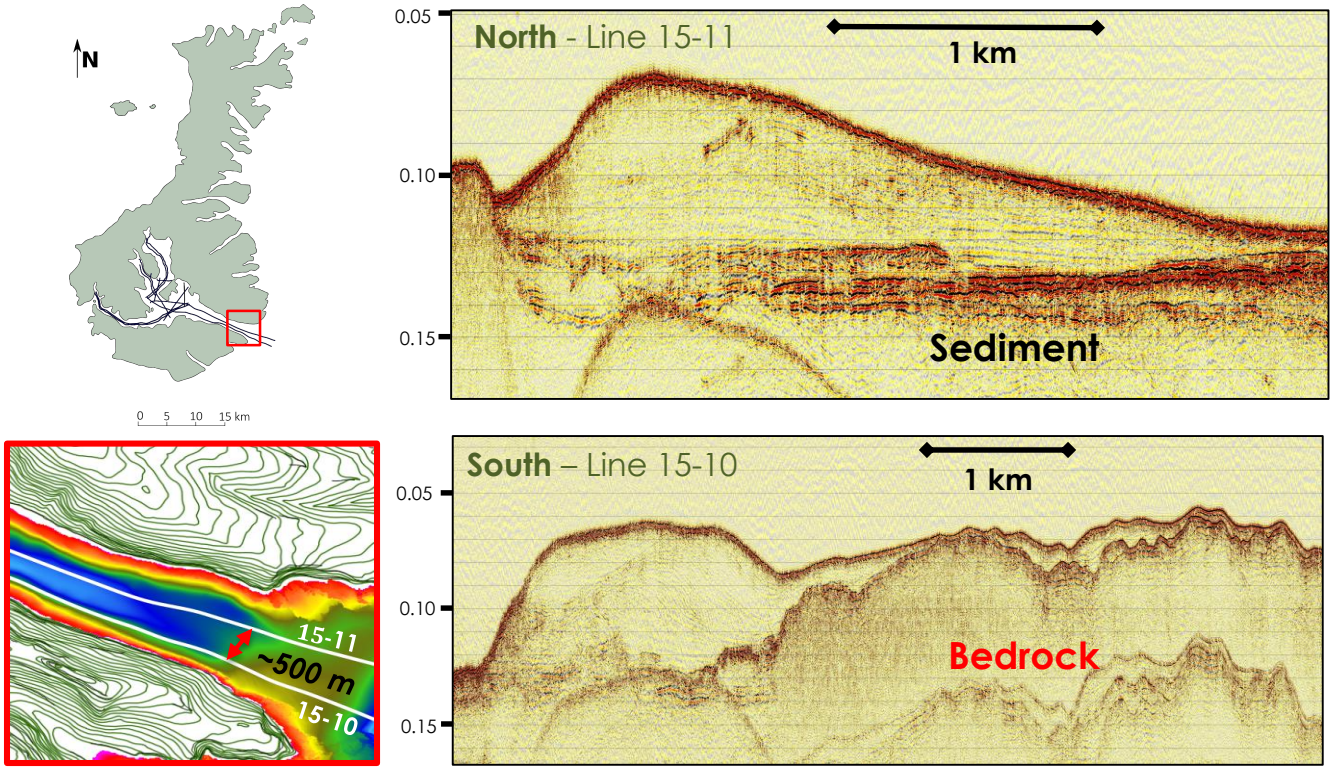

Figure 6.27 • Excerpts from line 15-11 and 15-10 with a spacing of ~500 m, exhibiting the presence of bedrock in line 15-10 (**bottom**) compared with a thick sediment package in line 15-11 (**top**). Indicative of a steep, deep bedrock surface in the Main Arm.

The sediment/bedrock (SF2/SF1) interface is difficult to constrain in some places and is inferred throughout transects, especially within the Main Arm. In a parallel transect to 15-11, 15-10 traverses closer to the southern shoreline of the main arm. Within this transect, bedrock is observed far closer to the surface with sedimentary packages not present as extensively within this transect (*Figure 6.27*). This suggests a steep sided nature of the bedrock within the main body of the Main Arm due to the close spacing of lines 15-10 and 15-11 (~500 m). This is also seen in line 15-03 (*Figure 6.26*) where perpendicular to the Main Arm, the bedrock dips steeply from the shore into the middle of the arm. This is indicative of a steep, deep bedrock surface. SF4 which overlies SF3 is observed in two localities at the two openings of Carnley Harbour (*Figure 6.27*). A large drift deposit with laterally continuous weak internal reflections is present at the head of the Main Arm with a steep eastern face, gently dipping to the east. At the end of the Western Arm, correlating to the Victoria Passage in the SW corner of the island, are accumulations of bedform deposits with internal reflections that are observed to be similar to those at the head of the Main Arm (*Figure 6.25b*). These features are observed within the bathymetric data.

6.2.9 Eastern Shelf Localities •

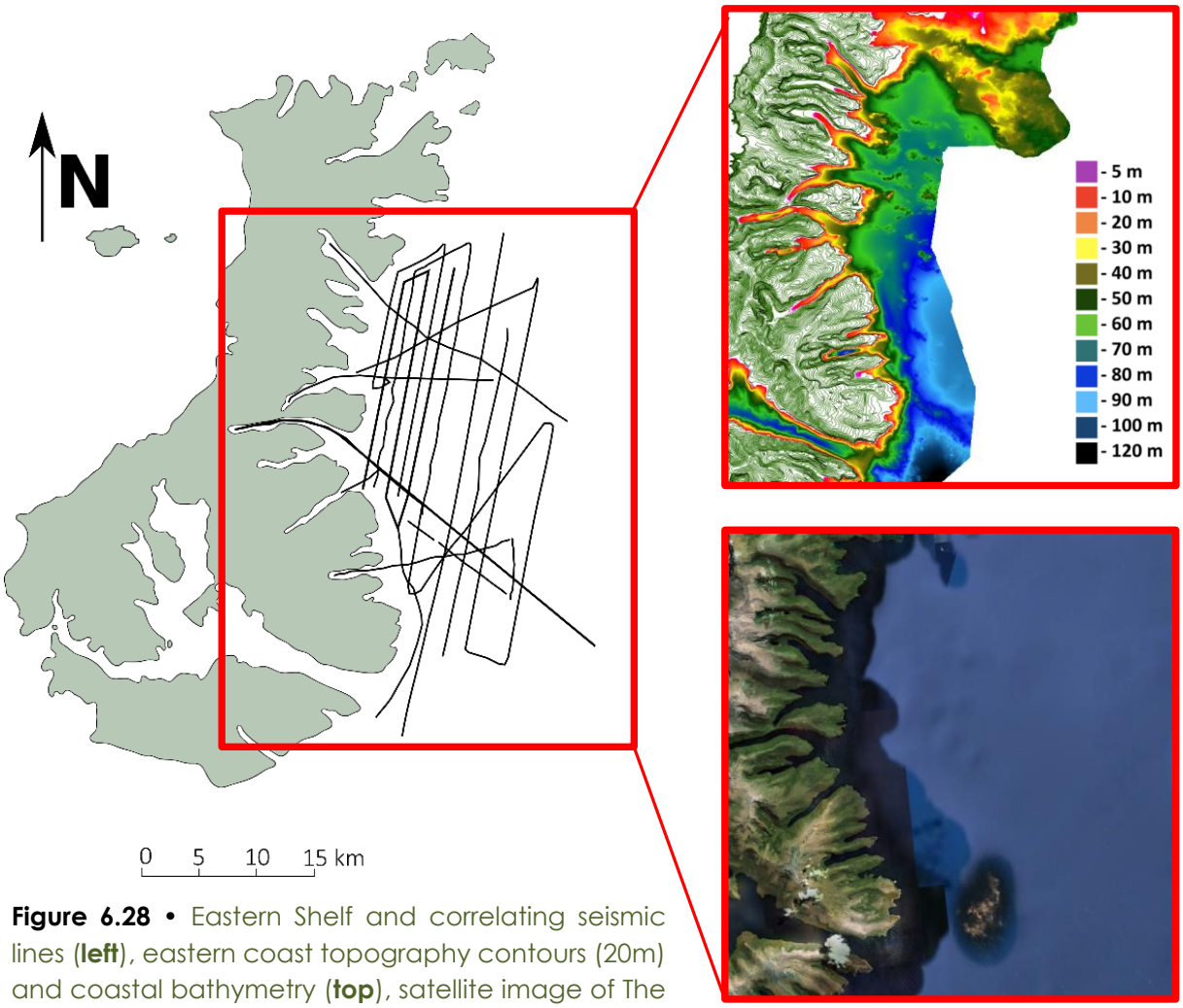

Figure 6.28 • Eastern Shelf and correlating seismic lines (**left**), eastern coast topography contours (20m) and coastal bathymetry (**top**), satellite image of The eastern coast and shelf (**bottom**) (Google Earth).

In the inaugural survey from 2014 (14PL001), dramatic topographic depressions and ridge systems were discovered in the seismic data on the eastern shelf of Auckland Island. Within these topographic depressions, extensive stratigraphic sequences were observed, leaving little or no sea-floor expression of the drowned valleys and ridgelines. At least 26 seismic transects were undertaken on the eastern shelf over three surveys. Lines collected from 15PL001 and 16PL119 were collected to expand the data density of the inaugural survey (14PL001). Transects were mostly collected in a similar parallel orientation at consistently variable distances from the modern coast. Perpendicular tie lines were also shot to provide a holistic perspective on the target area (*Figure 6.28*).

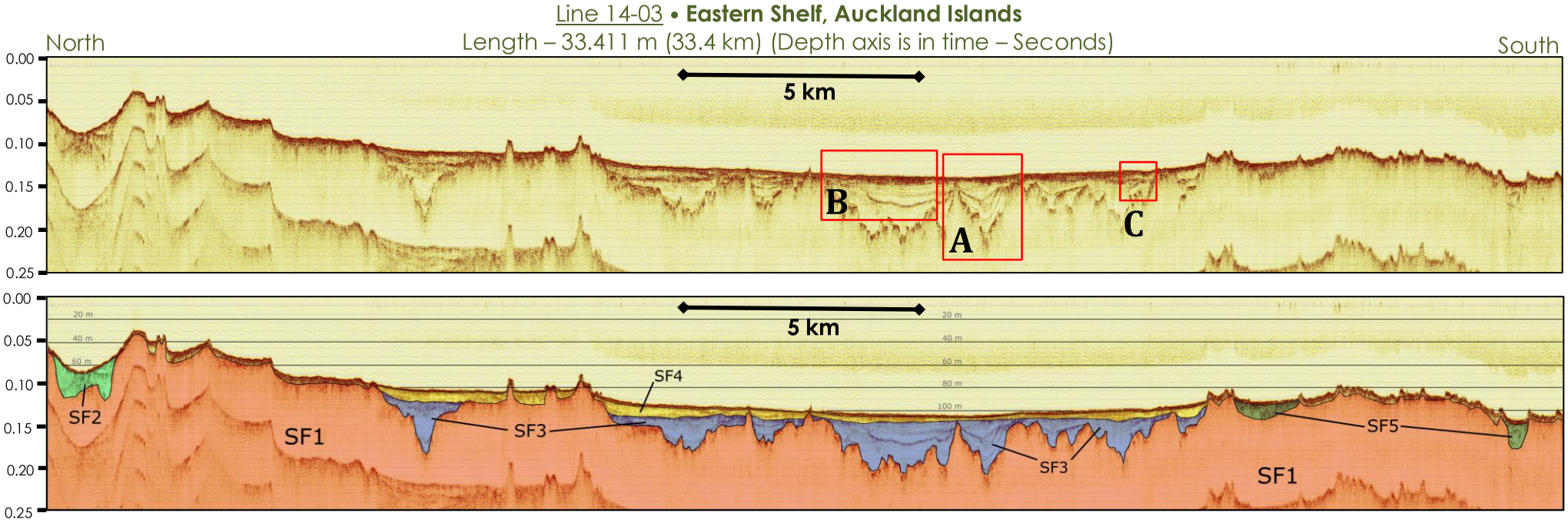

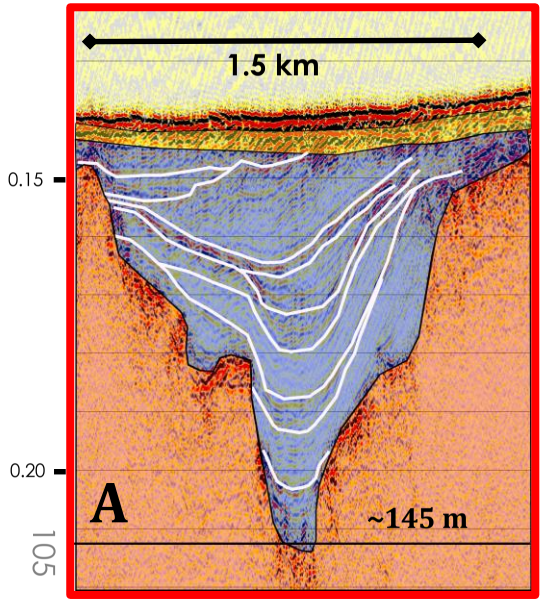

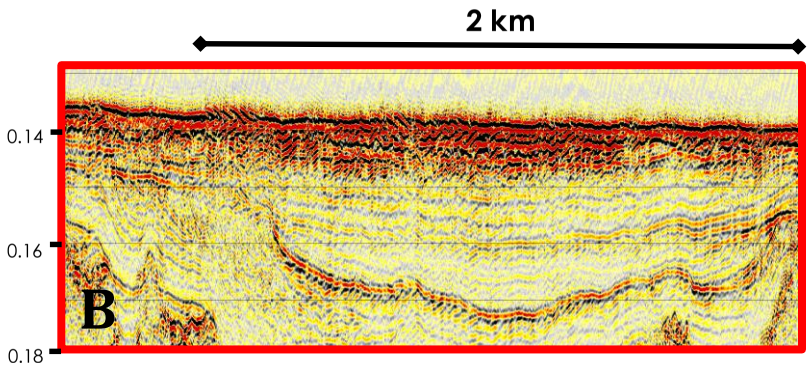

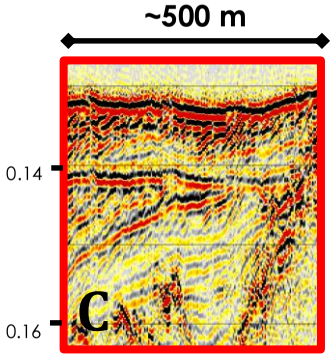

Figure 6.29 • Line 14-03 unannotated (**top**), annotated 14-03 with seismic facies allocation based on variations within the seismic data (**middle**), enhanced sections of 14-03 exhibiting various sedimentary features described in the text (**a, b & c – bottom**).

Line 14-03 is a long (33.4 km) N-S transect that exhibits many of the typical features observed on the eastern shelf. Within line 14-03, five seismic facies are present with most facies occurring over the entire eastern shelf (*Figure* 6.29). SF1 exhibits a highly irregular bedrock surface of regional highs expressed on the seabed with depressions observed down to at least 145 m below sea level within this transect (*Figure 6.29a*). Unconformably overlying SF1 is a thick sedimentary deposit, SF3, present throughout all seismic lines on the eastern shelf. The unit has a semi-transparent seismic character with numerous draped, laterally continuous internal reflections over kilometre scales. Strong, regionally continuous reflections are observed within SF3 that correlate with multiple other transects (e.g. line 15-18). Within SF3 are numerous internal truncations surfaces. Many reflections on-lap in a draped fashion atop the surrounding bedrock; however other horizons are observed that on-lap or down-lap onto underlying sedimentary units (*Figure 6.29a, b* & c). *Figure* 6.29a shows a valley like feature with a thick (~55 m) sequence, mostly correlating to SF3. Within this feature, draped reflections are observed as well as various horizon truncations that on-lap onto the bedrock and/or underlying sediments. *Figure 6.29b* and c highlight these truncations onto the underlying stratigraphy within the same seismic facies. Overlying SF3, SF4 exhibits a more laterally regular structure with strong continuous reflections, however is disrupted in places. This facies appears to be thicker at the northern and southern ends of the sediment basin within line 14-03. SF2 is a relatively small package observed within the line and is highly irregular to chaotic in its structure. It is positioned relatively higher stratigraphically than the other facies described and is situated topographically in a seafloor valley. This correlates to a valley feature originating off the coast of Haskell Bay (*Figure 6.30)*. However this is the only transect that crosses this area. SF5 is difficult to describe due to the chaotic and irregular nature within the data.

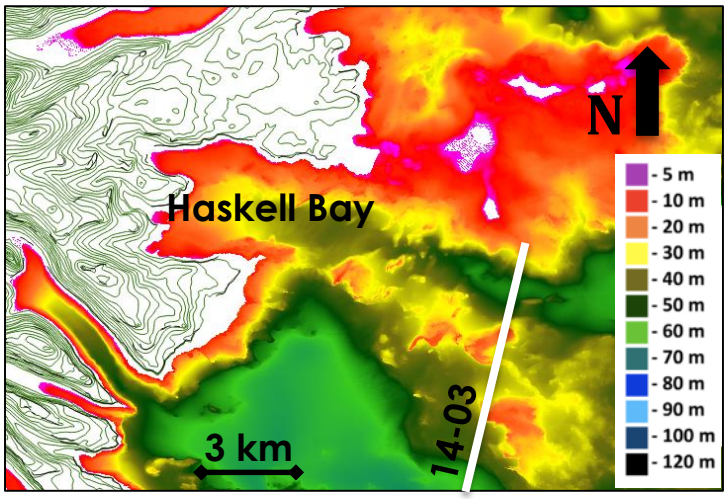

Figure 6.30 • Northern shelf bathymetry showing 14-03 crossing a channel like feature correlating with the seismic data.

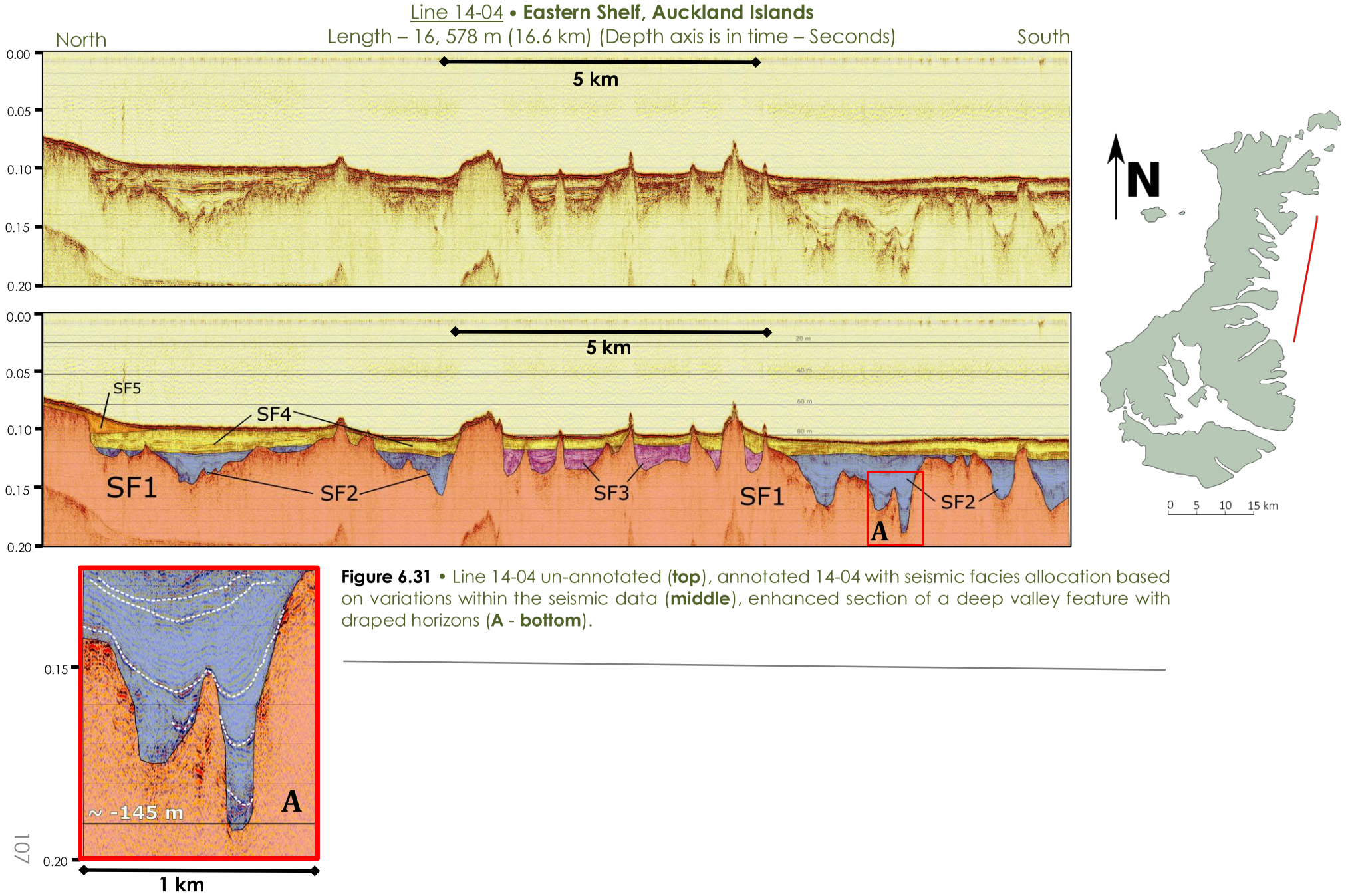

Figure 6.31 • Line 14-04 un-annotated (**top**), annotated 14-04 with seismic facies allocation based on variations within the seismic data (**middle**), enhanced section of a deep valley feature with draped horizons (**A** - **bottom**).

Line 14-04 is a parallel orientated transect to line 14-03, however it was surveyed ~3.7 km further landward. Due to this difference in proximity to the modern coastline, related features within these transects exhibit spatial variation. This transect captures the landward section of the shelf where seven major inlets flow. Five seismic facies are present within line 14-04 with most facies correlating to other facies seen in line 14-03. Similar to line 14-03, line 14-04 exhibits an irregular bedrock surface of topographic highs and depressions (SF1). Depressions observed, like those seen in line14-03, reach depths exceeding ~145 m below sea level (*Figure 6.31a*). However valley depressions are not as well developed nor extensive within line 14-04. Bedrock exposures that create seabed topographic highs are more prevalent within this transect (*Figure 6.32*). SF2, as in previous observations, sits unconformably over SF1 exhibiting transparent draped reflections transect wide. However within this facies at the base of topographic depressions is chaotic, unstructured basal unit that could be segregated further from SF2 and are not as apprent within transects further seaward. SF3 is situated stratigraphically higher than SF2 and bounded within small basins by topographic highs. SF4 mimics the facies observed within the previous seaward transect; however it is present in thicker, quantities that lie over SF2 with regular, laterally continuous internal reflections. SF5 has similar characteristics but appears to be prograding onto SF4 at the northern extent of the 14-04 transect (*Figure 6.31*).

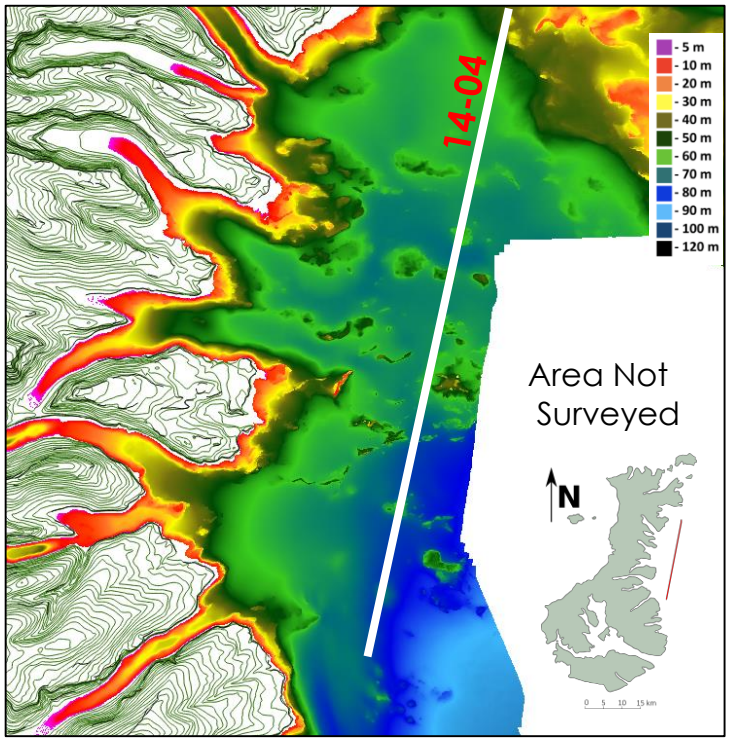

Figure 6.32 • Middle-eastern shelf bathymetry and line14-04 exhibiting seabed topographic highs and ridges.

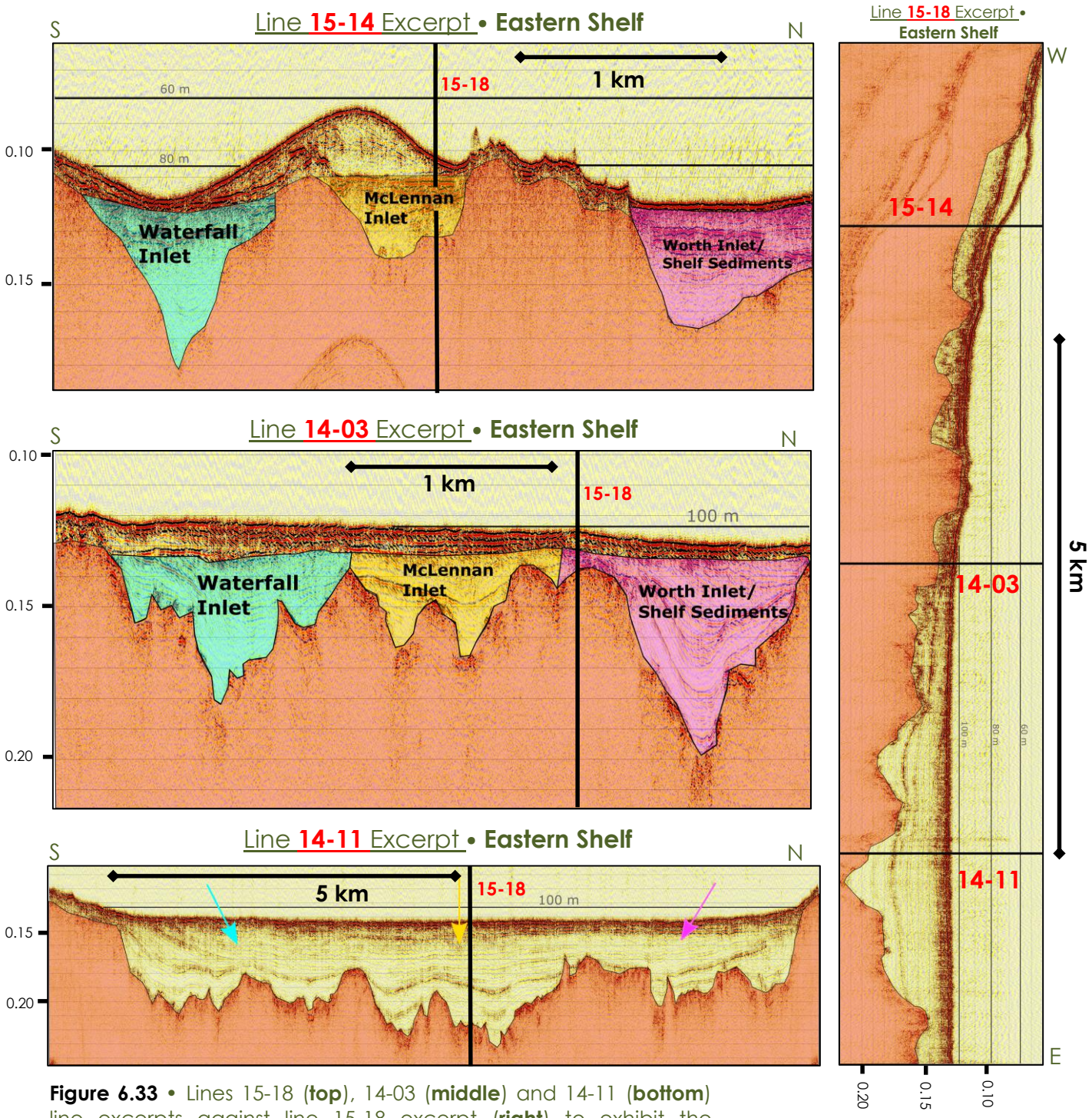

Figure 6.33 • Lines 15-18 (**top**), 14-03 (**middle**) and 14-11 (**bottom**) line excerpts against line 15-18 excerpt (**right**) to exhibit the changing nature of offshore valley depressions spatially.

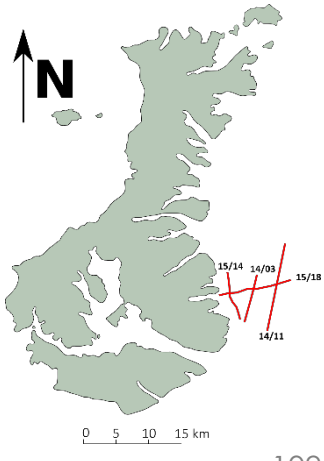

These spatial differences between seismic transects are highlighted in *Figure* 6.33. Varying morphologies of bedrock topographic ridges and depressions at varying distances from the modern coast are present here. Three transects (lines 15-14, 14-03, 14-11) were acquired perpendicular to

McLennan Inlet at varying, constant distances from the modern coastline. These transects are tied in through a bisecting transect (line 15-18), originating from McLennan Inlet (*Figure 6.33 - Right*). The most proximal line 15-14 captures three inlet valley continuations approximately 1 km from the modern coastline. Valleys are incised into the bedrock and have extensive stratigraphic sequences present. A large drift deposit is observed overlying the McLennan Inlet depression which is observed in line 15-18. Line 14-03, a further 2.2-2.7 km seaward, shows a further progression towards deeper, more irregular bedrock surfaces with well-defined internal reflections observed within the respective stratigraphic packes. The depression infill sequences are overlain by a regular, laterally continous package. Progression to line 14-11, ~6.3 km from McLennan Inlet, exhibits a far more expansive infill basin within multiple depressions and ridges that are characteristic of the seaward shelf setting at the Auckland Islands. These transects at varying distances from a modern fjord, shows progression of enclosed drowned valleys closer to the modern shore towards an extensive, collective sedimentary basin further seaward.

Chapter 7 •

Discussion

7 Discussion •

Seismic data collected from coastal fjords and eastern shelf localities at the sub-Antarctic Auckland Islands exhibit seafloor topography and sedimentation patterns that vary spatially. All coastal fjords and various shelf localities surveyed are consistent with prior coastal glaciation (Pickrill et al. 1992). Observed extensively over three surveys, fjord transects exhibit over-deepened valley profiles with shallow entrance sills present at most east coast Inlets (e.g. *Figures 6.3, 6.6 & 6.8*). These profiles are indicative of extensive glaciation in the past (Syvistski et al. 2012) that originated from former ice domes centred on Carnley Harbour to the south and Disappointment Island to the north (Quilty 2007). Incised buried valleys and ridges imaged on the eastern shelf (*Figure 6.1*) trend in an approximately west-east direction and are interpreted as offshore continuations of the numerous fjords and inlets that dominate the eastern margin. Stratigraphic infill of these incised valleys display evidence for cyclic transgression/regression regimes present within the seismic data. These regimes can be coupled with various glacial/interglacial periods throughout the Quaternary. These glacial and inter-glacial periods had a significant effect on the exposed Auckland Island landmass during these periods of sea level fluctuation. The following chapter interprets the described results from the previous section and is segregated by locality types. These interpretations at these locality types are then explained in relation to larger picture, with holistic interpretations of Quaternary processes at the Auckland Islands.

7.1 Fjords •

All fjords and inlets at the Auckland Islands are the products of the advance (and retreat) of glacial ice and glacioeustatic sea-level change during the Quaternary. This is supported within the respective data sets described in the previous results chapter. Seismic profiles from McLennan Inlet (*Figures 6.3, 6.4),* Hanfield Inlet (*Figure* 6.6), Norman Inlet (*Figure* 6.8) and Fly Harbour (*Figure 6.14*) all exhibit over-deepened, longitudinal fjord profiles with shallow entrance sills, indicative of an extensive glacial history (Syvitski et al, 2012). Further, bathymetry of each of these fjords exhibits over-deepened basins with steep sided valley walls progressing to an entrance sill consistent with coastal glaciation (*Figure 7.1*) (Pickrill et al. 1992).

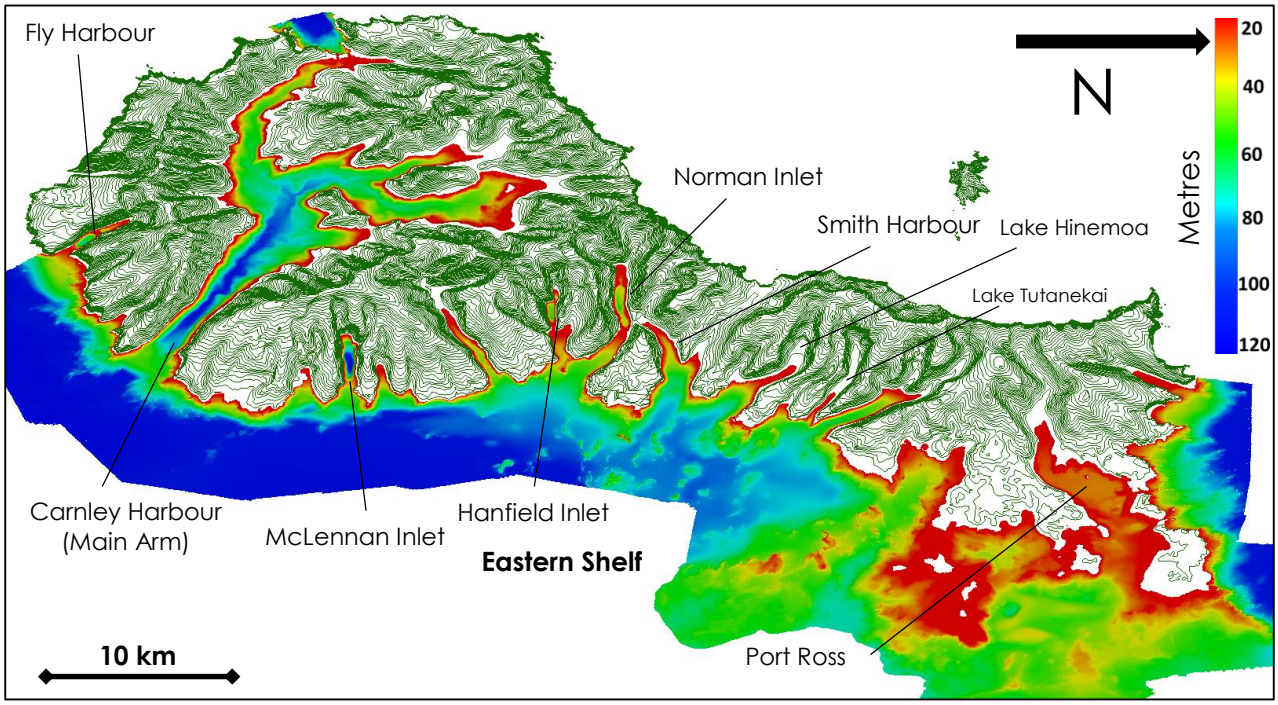

Figure 7.1 • Bathymetry and landmass contours (20 m) of the Auckland Islands with particular localities.

7.1.1 Hanfield Inlet •

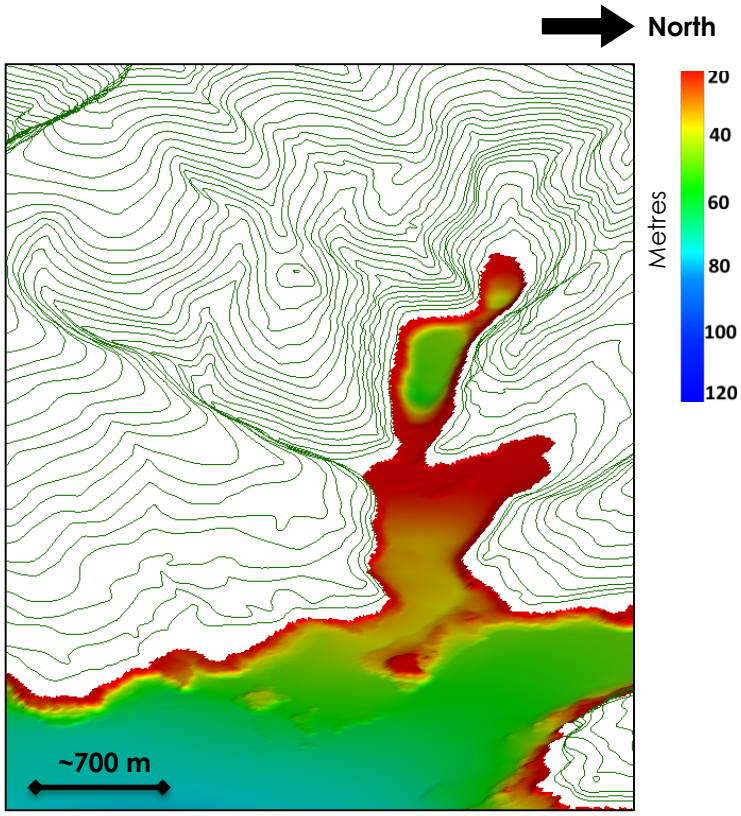

Figure 7.2 • Bathymetry and landmass contours (20 m) of Hanfield Inlet looking west. (Locality – *Fig. 7.1*)

Hanfield Inlet (*Figure 7.2*) seismic data display an over-deepened, multi-basin fjord system with a shallow entrance sill (*Figure* 6.6); indicative of extensive, and multiple phases of glaciation (Syvitski et al. 2012). Within the Main Basin, the sediment/bedrock interface is masked in most places by chaotic seismic noise. This is probably evidence for the presence of gas within highly organic rich sediments in the basin. This suggests a sediment starved environment within Hanfield Inlet. These are contrasted by overlying, well-structured sediments that have accumulated within the fjord basin with laterally continuous horizons. These sediments accumulate due to the enclosed fjord bedrock architecture

which include glaciolacustrine and/or lacustrine sediments. Based on the estimated ~120 m of glacioeustatic sea level rise since the LGM (Fairbanks & Matthews 1978; Shackleton 1987; Pinter & Gardner 1989), the Hanfield fjord basin during LGM de-glaciation at ~15 ka (McGlone 2002) would have supported an enclosed post-glacial lake. The lake would have been confined within the overdeepened footprint of previous Quaternary glaciers, free from marine influences. Modern analogues in the Auckland Islands for these lakes are present today at Lake Hinemoa & Tutanekai (*Figure 1.4*) at the heads of Musgrave and

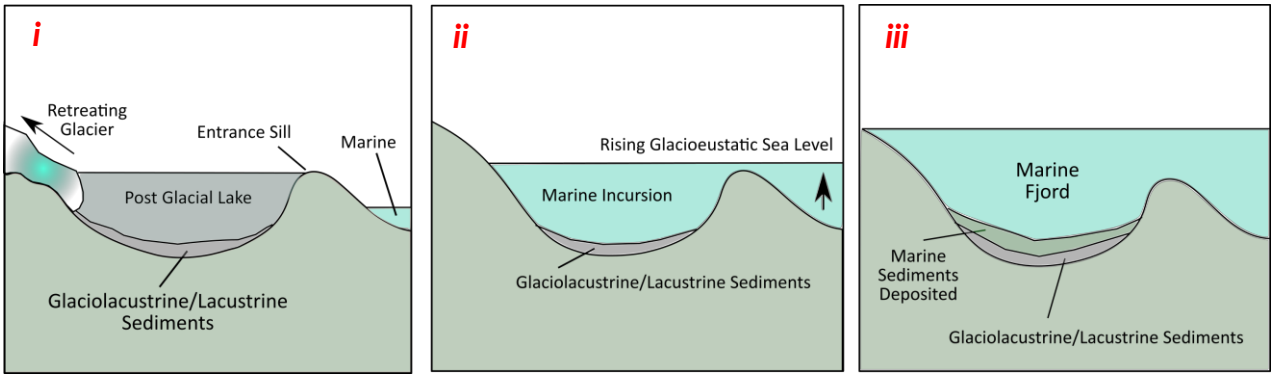

Figure 7.3 • Cartoon schematic showing the progression of a glaciated valley to a marine fjord. (***i***) Fjord basin with retreating glacier, supporting a post glacial lake with associated deposits, (***ii***) glacioeustatic sea level rise results in a marine incursion over-topping the enclosing sill, flooding the post-glacial lake with saline sea water, (***iii***) sea level continues to rise and marine sediments are deposited over the glaciolacustrine/lacustrine deposits.

Granger Inlets, respectively. These lakes trap incoming fine, clay size terrestrial sediments that archive the catchment area and processes within the lake. These lacustrine deposits are often preserved as varves that are deposited in yearly/seasonal cycles, recording high-resolution climate variability, glacial fluvial, and lacustrine processes (Sly 1978). Subsequent de-glaciation following the LGM resulted in rising glacioeustatic sea levels that eventually overtopped the entrance sill. This resulted in a marine incursion into the fjord basin, inundating the lacustrine/glaciolacustrine sediments (*Figure 7.3*). Work undertaken by Einvik-Heitmann (2014) on sedimentary core 14PL001 – 39P4 acquired in Hanfield Inlet (*Figure 1.7*), presented a terrestrial/marine transition present down-core. This transition was dated at ~ 8 ka, where a marine transgression breached the ~12m deep sill. This can be used as an initial, first order analogue for potential marine incursion into other inlets based on comparative sill threshold heights.

7.1.2 McLennan Inlet •

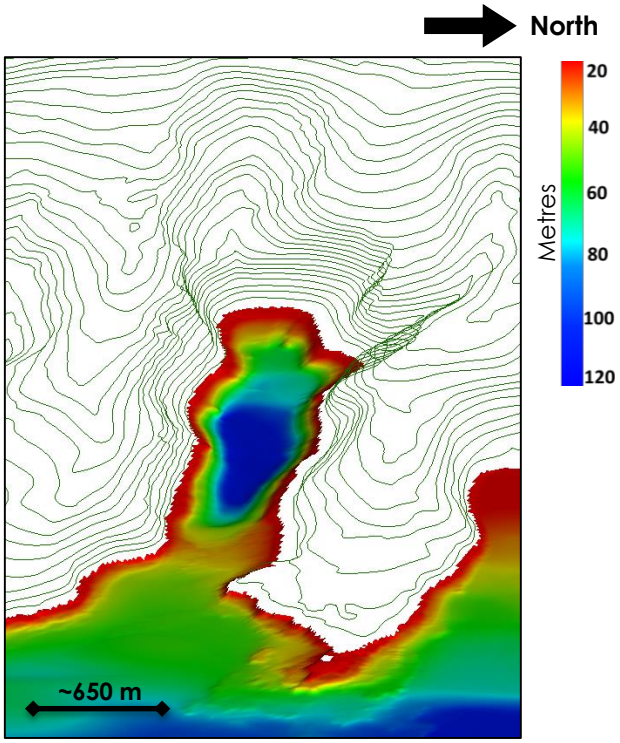

Figure 7.4 • Bathymetry and landmass contours (20 m) of McLennan Inlet looking west. (Locality – *Fig. 7.1*)

McLennan Inlet (*Figure 7.4*) on the eastern coast of the Auckland Islands exhibits an over-deepened fjord profile with a shallow entrance sill consistent with coastal glaciation (Syvitski et al. 2012). Within the single fjord basin, the deepest point has at least ~25 m of sediment that unconformably overlies the eroded bedrock (*Figure 6.3 and 6.4*). The sediment has comparable characteristics to Hanfield Inlet. Much of the bedrock/sediment interface is chaotic with little to no structure, again, indicative of organic rich sediments. These in turn are overlain by a well-layered sedimentary package with laterally continuous horizons throughout the fjord basin. This overlying package is likely related to an enclosed paleo-lake environment, succeeded by enclosed marine sediments similar to the respective core and seismic data at Hanfield Inlet. Using the marine incursion of Hanfield Inlet as an analogue, potential timing of marine incursion into McLennan Inlet can be calculated. McLennan Inlet marine incursion post-LGM, must have occurred earlier than ~8 ka, due to the difference in depth of the entrance sills at each locality. The entrance sill at McLennan Inlet is at ~48 m water depth compared to Hanfield Inlet's ~12 m depth. Due to this disparity, a marine incursion must have occurred far earlier than 8 ka at McLennan Inlet when glacioeustatic sea levels transgressed

7.1.3 Norman Inlet •

Norman Inlet contrasts the previously mentioned fjords due to its comparatively elongate profile, different fjord sub-surface sediments and the inlet confluence with Hanfield Inlet that coincides within an embayment south of Fella Peninsula (*Figure 7.5*). The fjord sediment stratigraphy is variable within the elongate basin. Similar to other fjords, some areas are interpreted to be masked by gas rich

sediments while in some areas the sediment/bedrock interface is tentatively present. Observed within the main fjord basin and described in the previous chapter, SF3 in line 16-09 (*Figure 6.8*) is unique to Norman Inlet. The mound like structure, with overlying sediments on-lapping onto it, is possibly a drumlin/moraine feature related to the advance of ice. The feature is not a bedrock sill as observed extensively on the eastern coast, as weak internal reflections are preserved within the facies. If this feature was created by the advancement of ice, it could be an indicator for ice advance during the last glacial period, falling within the confines of prior glacial advances. However more evidence is required to definitively draw conclusions regarding LGM ice extent and de-glaciation at this locality. Norman Inlet, like Hanfield Inlet, supported a paleo-lake within the confined fjord basin during the LGM. Norman Inlet (~16 m) and Hanfield Inlet (~12 m) share similar entrance sill depths which means the dated incursion (~8 ka) of Hanfield Inlet (Einvik-Heitmann 2014) can correspond to a slightly earlier marine incursion within Norman Inlet. It is difficult to constrain these sediments within the seismic data, due to the highly variable nature of the basin stratigraphy.

7.1.4 Norman Inlet and Hanfield Inlet Confluence •

As Norman Inlet and Hanfield Inlet progress seaward (east) (*Figure 7.5*), they arrive at a confluence which is observed within the data. The buried valley originating from Norman Inlet is far more substantial than the paleo-channels flowing from Hanfield Inlet (*Figure 6.10 & 6.12*). This area would have been a confluence for the Norman and Hanfield glaciers that advanced and retreated during Quaternary glacial and interglacial cycles. The confluence area also probably supported a paleo-lake and/or a sheltered fjord

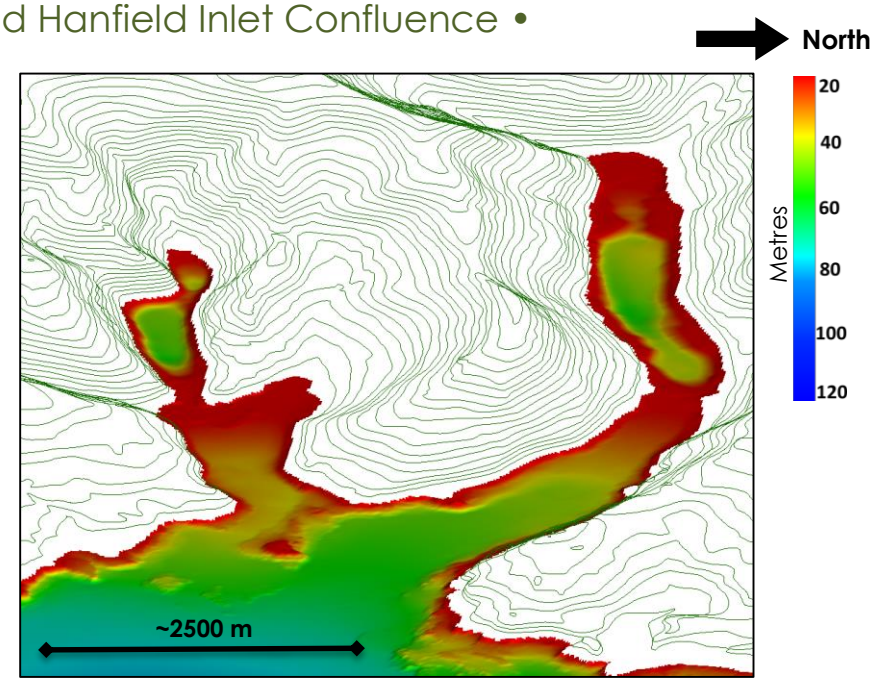

Figure 7.5 • Bathymetry and landmass contours (20 m) of Hanfield Inlet (**left**) and Norman Inlet (**right**) confluence embayment looking west. (Locality – *Fig. 7.1*)

environment, dictated by glacioeustatic sea level variation through time. Glacioeustatic lowstands supported fluvial river systems within the sediment laden confluence, which are observed within the seismic data. SF3 (*Figure 6.10*) occupies an erosional surface formed atop the underlying sediments with the buried valley. This surface is formed through fluvial erosion and re-working of eroded sediments. This was likely a braided river system flowing from enclosed lake systems within the respective fjord basins. Seaward of the main fjord basin in Norman Inlet (*Figure 6.8*), a series of sedimentary packages with evident erosional surfaces that unconformably overly a highly irregular bedrock surface. These packages are within the terrestrial bounds of Norman Inlet and are interpreted as sediments further related to the outflow of paleo-lakes that were subsequently drowned, exposed and re-worked during glacio-eustatic sea level fluctuations.

7.1.5 Fly Harbour •

Situated on the southern coast of the island group, Fly Harbour is a multi-basin fjord with two large, upstanding bedrock sills typical of glacial erosion (Syvitski et al. 2012) (*Figure 7.6*). The sediments within the main basin match the sediment facies observed at previously described inlets to the north. The presence of gas from organic rich sedimentary packages masks the bedrock/sediment interface. The overlying, well layered sediments are associated with paleo-lake and sheltered fjord settings. The seaward entrance sill is present at a depth of ~23 m, resulting in a marine incursion earlier than 8 ka as glacioeustatic sea level transgressed. Observed extensively on more southern fjords is the presence of modern seafloor sediments within sheltered

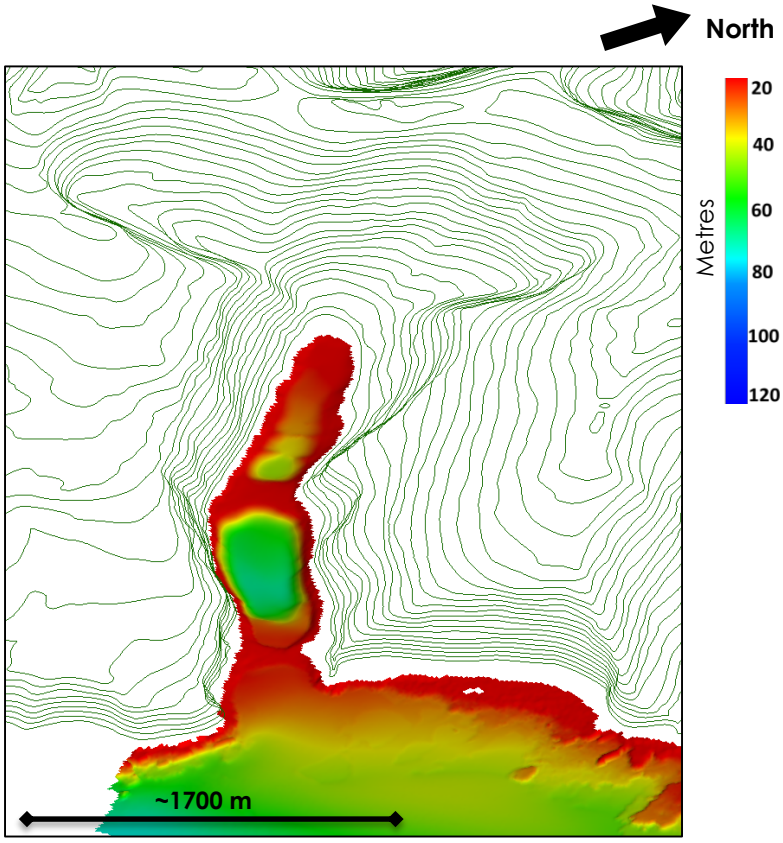

Figure 7.6 • Bathymetry and landmass contours (20 m) of Fly Harbour looking northwest. (Locality – *Fig. 7.1*)

inlet entrances (e.g. Carnley Harbour – Main Arm and Victoria Passage). These sediments progress down the shallow shelf towards the main shelf of Auckland Island. This is present at Fly Harbour. Extensive drift deposits present outside the fjord basin appear to over-top the entrance sill of Fly Harbour and deposit within the fjord basin. Evidence for this is through drift sediments outside the fjord rests at the same height as similar sediments observed within the fjord basin. These drift sediments are not present within the stratigraphically higher landward fjord basin. Fly Harbour also exhibits a thicker basin infill sequence in comparison to other localities; however it also has a smaller fjord catchment in a relatively sediment-depleted environment.

Within the transect originating in Fly Harbour (*Figure 6.14*), a basement outcrop with a corresponding sedimentary package rests between 100-120 m water depth. During the LGM glacio-eustatic lowstand, this locality would have been associated with a paleo-coastline due to the presence of eroded and exposed seafloor outcrops, potential paleo-beach sediments and correlating water depth to known LGM sea-level records (e.g. Kilian & Lamy 2012). This type of feature within the seismic and bathymetry data is only observed at this locality due to a rapidly deepening shelf to the south in comparison to the more progressive eastern shelf to the north.

7.1.6 Smith Harbour •

Smith Harbour is different from other aforementioned Auckland Islands fjords. The bathymetry of Smith Harbour does not express an entrance sill and over-deepened fjord basin (*Figure 7.7*), which is a characteristic feature of many inlets at the Auckland Islands (Syvitski et al, 2012). Terrestrial physiography suggests Smith Harbour was glaciated at some time during the Pleistocene due to an extensive landward fjord valley and cirque basin to the west as well as steep sided valley walls within the harbour confines (*Figure 6.16*). Similar to the Norman and Hanfield Inlet confluence, Smith Harbour and Tandy Inlet share a confluence embayment with a submerged ridgeline. Glaciers originating from respective valleys at the heads of Smith Harbour and Tandy Inlet would have converged within this embayment. Valley convergence is a common feature of glacial valleys observed

within the Auckland Islands topography and bathymetry. The lack of an entrance sill and over-deepened back basin is shown in the seismic data (*Figure 6.17*). Up-standing sills and basins within Smith Harbour are present; however they have a different architecture than that observed at other inlets. These basins and sills (e.g. *Figure 6.17a*) have been subject to comparative extensive sedimentation that has in-filled the basins up to the threshold depth of the sills. However, why this has occurred within this fjord and not in the previously described localities is yet to be determined. The cirque basins at the head of Smith Harbour and Tandy Inlet have been eroded away from the prevailing westerlies and incessant heavy seas. If glacial ice was present in fjords at the Auckland Islands during the LGM, this may have hindered development of glacial ice and subsequently received a different sedimentary regime compared to other inlets (Anderson et al. 2012).

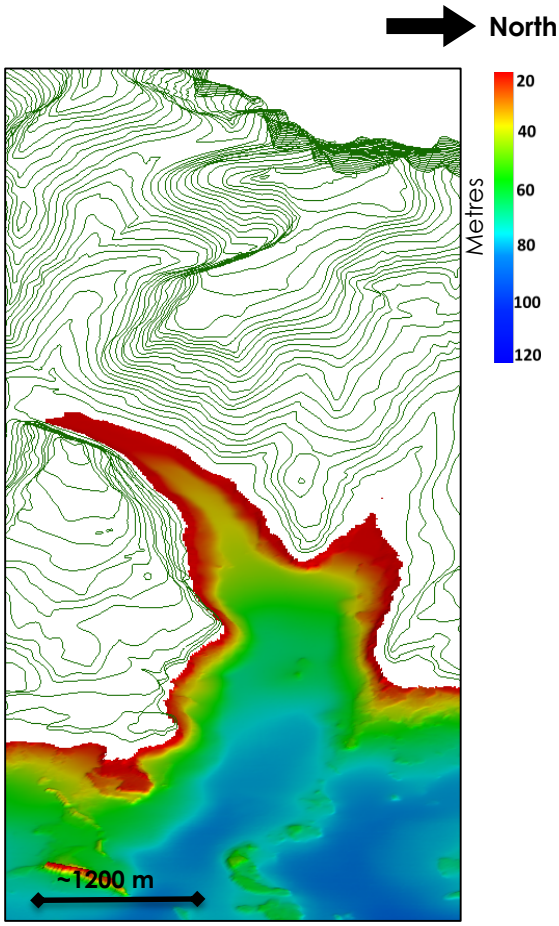

Figure 7.7 • Bathymetry and landmass contours (20 m) of Smith Harbour looking west. (Locality – *Fig. 7.1*)

7.1.7 Port Ross •

Port Ross, in the northern reaches of the Auckland Islands, varies from the traditional steep sided, deep inlets present at the Auckland Islands. Its relatively expansive, lowland nature progressing seaward (east) is the only region of the Auckland Islands that exhibits this topography (*Figure 7.8*). Subsequently the seismic transects and bathymetry data vary from more southern Inlets. The highly irregular, steep sided paleo valley walls within the seismic data and a terrestrial U-shaped valley present to the west (Laurie Harbour), point to prior glaciation during the Quaternary. Basal facies observed at some localities in the seismic data likely relate to the de-glaciation of the most recent ice advance stage within Port Ross from the Laurie Harbour paleo-glacier. Subsequently the semi-transparent, draped

facies corresponds to the establishment of a paleo-lake within the submerged topographic confines of Port Ross. This lacustrine sequence is vertically continuous without erosional surfaces. This represents a relatively complete, uninterrupted record of sedimentation within a quiet lacustrine depositional environment. Observed in *Figure 6.20*, an erosional surface with on-lapping sediments overlies this facies, which is indicative of subsequent fluvial erosional and deposition. This likely occurred at the LGM sea level lowstand with a corresponding paleo-river draining between the modern passage between Rose and Enderby Islands. Fleming et al. (1976), interpreted that during the LGM an extensive glacier flowed down from the highlands from the west into Port Ross, depositing till on Enderby Island, which possibly preserving two glacial advances during this period. ~41 m of sediment is present in the deepest areas of the Port Ross basin, reflecting paleo-lake infill since de-glaciation around ~15 ka (McGlone 2002). Fleming et al. 1976 propose two advances during this stage, in which the second advance progressed ice above the lake sediments. However, within the Port Ross seismic data, no evidence of an erosional ice advance within the lacustrine sediments is observed. The glacially derived sediments present on Enderby Island are therefore likely related to previous ice advances prior to the LGM. This interpretation is in agreement with other evidence of localised, smaller scale ice advances within Auckland Island fjords during the LGM.

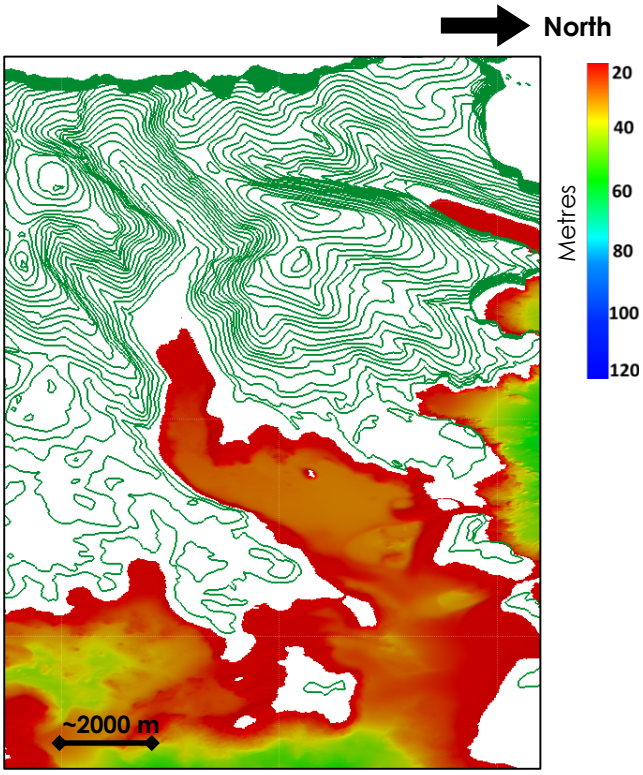

Figure 7.8 • Bathymetry and landmass contours (20 m) of Port Ross and Laurie Harbour looking west. (Locality – *Fig. 7.1*)

7.1.8 Silled Fjords vs. Un-Silled Fjords •

Modern fjords at the Auckland Islands as observed in the bathymetry data can be characterised by either the presence or absence of an entrance sill within the

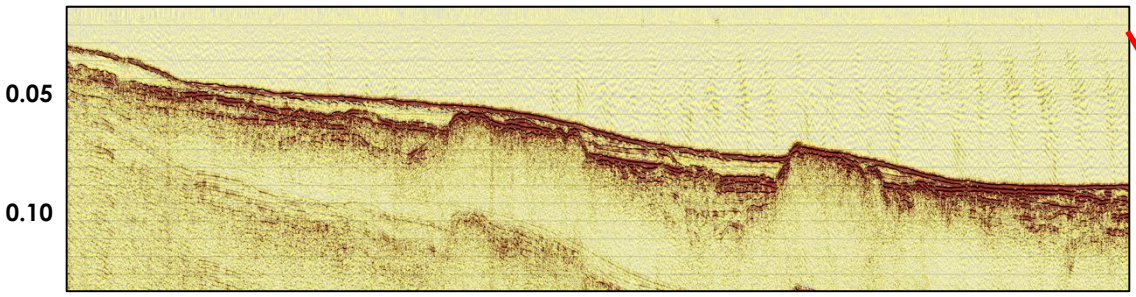

Figure 7.9 • Smith Harbour exhibiting a lack of an expressed entrance sill and over-deepened back basin. A different sedimentary regime and infill patterns are observed here in comparison to Fly Harbour (*Figure 7.10*).

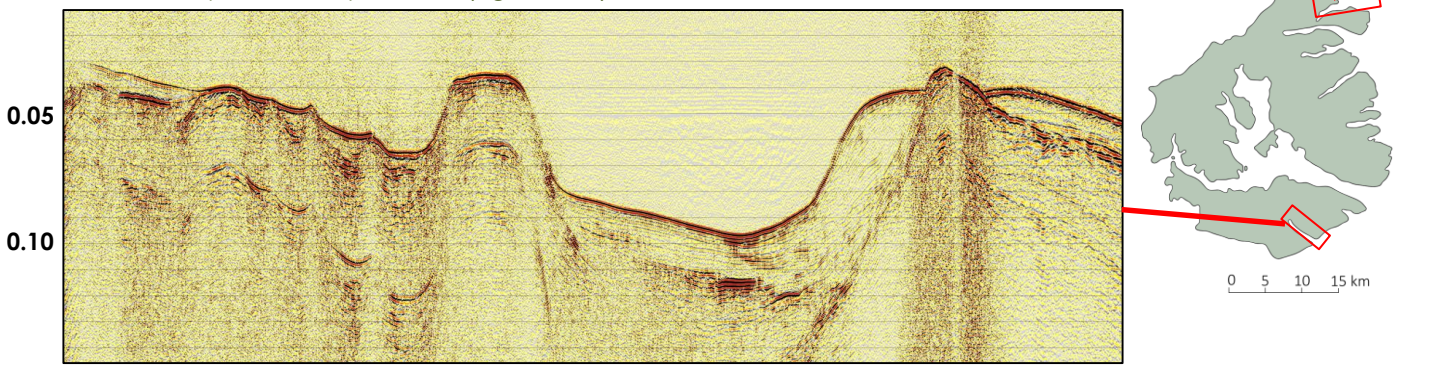

Figure 7.10 • Fly Harbour fjord basins with the presence of an entrance sill progressing to an over-deepened back basin. A second back basin and sill is also present. (Depth – seconds)

Fjord	# Sills	Depth of Sill (metres)	Over-Deepened Basin (y/n)	Length of Fjord (kilometres)
Hanfield Inlet	2	14 m	y	4.9 km
McLennan Inlet	1	38 m	y	4.4 km
Norman Inlet	2	16 m	y	7.7 km
Fly Harbour	2	23 m	y	3.77 km
Smith Harbour	0	Not observed	y (buried)	3.18 km
Port Ross	1	~24 m	y	12.57 km (Laurie Harbour to eastern Enderby Island)
Carnley Harbour	<1	~80 m	y	24.7 km (Victoria Passage to Main Arm entrance)
Deep Inlet	1	26 m	y	5.72 km
Chambres Inlet	0	Not observed	y (buried)	4.20 km
Musgrave Inlet	0	Not observed	n	4.14 km
Granger Inlet	0	Not observed	n	2.48 km
Tandy Inlet	0	Not observed	n	1.32 km
North Harbour	0	Not observed	Unknown	2.3 km

Table 7.10b • Table of Auckland Islands fjords with respect to number of sills, depth of sills (metres), the presence of over-deepened basins (yes/no) and the length of the fjord (kilometres). Grey boxes represent fjords not discussed in this thesis, but present in the Appendix. Red fjords correlate to the absence of seismic data. Grey text is where values are not conclusive and are estimated. All fjords have bathymetry data.

bounds of the fjord (*Figure 7.9, 7.10*). Northern fjords (Smith Harbour, Tandy Inlet, Musgrave Inlet, Granger Inlet and Chambres Inlet, Port Ross – *Figure 7.1*) are characterised by a general lack of an expressed entrance sill on the seafloor with extensive valley floor exposures present landward. This is accompanied by moraine dammed lakes at the heads of Musgrave and Granger Inlets. The moraine dammed lakes at the head of these Inlets are likely the remnants of last glacial period ice extent, preserved above modern sea level. These features, which are below present-day sea level in southern fjords, would have been transgressed as sea level rose. In comparison, more southern fjords (Fly, McLennan, Hanfield and Norman – *Figure 7.1*) are silled fjords with over-deepened back basins. The majority of the fjord basins in the south have been transgressed by sea level, leaving little valley floor present. Deep Inlet is an exception and is comparable to the northern fjords including the lack of an entrance sill with exposed valley floors at the head of the inlet (*Appendix A 1.4*). A remaining question is how the two types of fjords present at the Auckland Islands are differentiated through glacial ice flow dynamics. Within Smith Harbour (*Figure 6.17*), and other northern fjords not described in this thesis, there is the presence of sediment infilled back basins with larger entrance sills possibly present further offshore. However, this would be difficult to constrain further, due to the highly variable nature of incised valley systems (Schumm & Ethridge 1994). *Table 7.10b* defines individual charactersitics of Auckland Island fjords to respective lengths and the presence or absence of features.

7.2 Carnley Harbour •

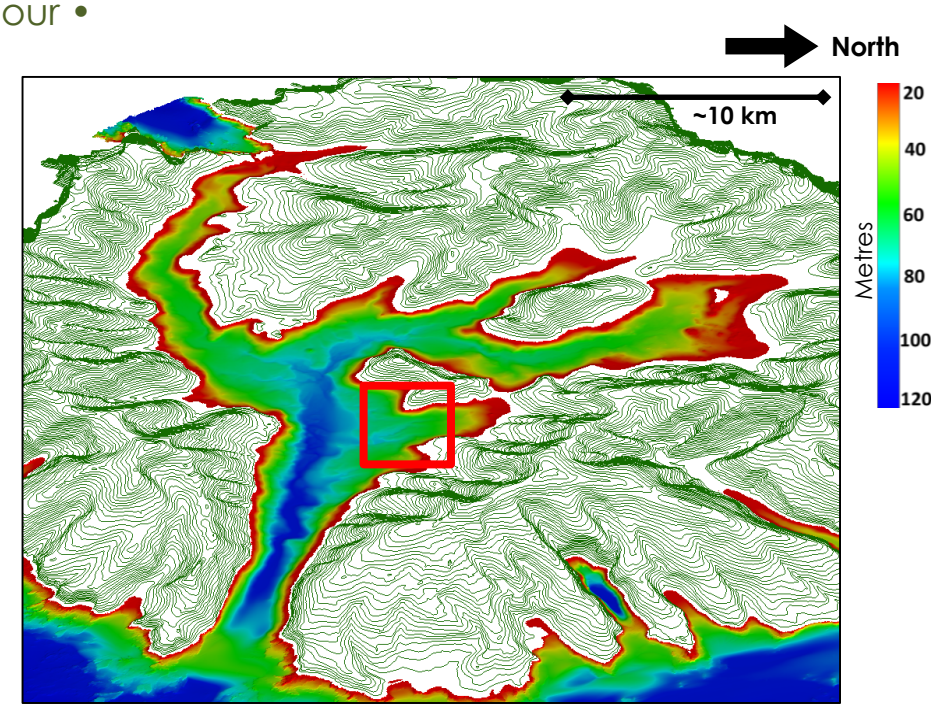

Figure 7.11 • Bathymetry and landmass contours (20 m) of Carnley Harbour looking to the west. (Main Arm – **bottom**, Western Arm – **left**, Northern Arm – **right**). (Locality – *Fig. 7.1*) (Red Box - Locality of *Figure 7.13*).

Seismic profiles collected from Carnley Harbour differ from those collected within other fjords and inlets at the Auckland Islands. The profiles, bathymetry and sub-aerial topography within Carnley Harbour portray a more open expanse, indicative of different erosional regimes through time. Collected transects depict a dynamic environment that has experienced recent, extensive fluvial processes due to the larger catchment area in comparison to other glacially dominated inlets (e.g. McLennan Inlet & Fly Harbour). The expanse of the modern Carnley Harbour is the remains of the Cenozoic aged Carnley Volcano, centred on Musgrave Peninsula (*Figure 3.2*) (Wright 1966, 67, 68, 70, 71; Adams 1983; Gamble & Adams 1985; Ritchie & Turnbull 1985). The volcano has since been dissected intermittently throughout the Quaternary by sub-Antarctic glaciation cycles, and particularly their glaciofluvial and fluvial processes.

7.2.1 Main Arm •

Within the Main Arm of Carnley Harbour, the relatively extreme depths of draped reflectors observed at least 180 m below modern sea level (*Figure 6.23a*) combined with bedrock architecture can be attributed to successive glacial and sub-glacial erosion during the Quaternary. During these glacial cycles ice fields centred on Carnley Harbour (south) and Disappointment Island (north) would have been widespread (Quilty 2007). Ice fields around Carnley Harbour have flowed in radial patterns around the shield volcano as observed by the modern physiography of glacial valleys (*Figure 1.2*), but also through internal, pre-glacial fluvial cut valleys

and depressions that have since been eroded away. These internal valley glaciers likely advanced to a paleo-confluence within the vicinity of modern day Musgrave Peninsula that flowed into the Main Arm and carved seaward (west). This correlates with the relatively deep seafloor and bedrock depths of the Main Arm (*Figure 6.23, 6.27, 7.11*). Due to the size of the Main Arm, including the catchment area and extreme basement depths compared to other modern inlets, the Carnley Harbour paleo-glacier would have been the most extensive glacier on the Auckland Islands. The basement/sediment interface is not present within the central body of the Main Arm (*Figure 6.23*), however a homogenous package (~100 m +) of semi-transparent, draped, laterally continuous sediment is interpreted to be a paleo-lacustrine/paleo-fjord deposits. This deep depression footprint and entrance sill left behind by various Quaternary glacial cycles would have been able to support a paleo-lake environment, creating a sediment sink. This paleo-lake would have periodically been subject to marine incursions creating an enclosed fjord system during interglacial cycles. Infill of the paleo-glacier footprint within a quiet environment has eventually filled the Main Arm basin to the height of the sill threshold. During periods of sea level regression during glacial periods, the absence of ice within Carnley Harbour on smaller amplitude cycles would have resulted in the development of fluvial environments. This likely was braided river systems flowing over the exposed lake sediments down the Main Arm. This is observed in the seismic data with semi-transparent facies being overlain unconformably by a semi-continuous, irregular sedimentary package with undulating seafloor expressions. The truncated nature of the horizons within this package is indicative

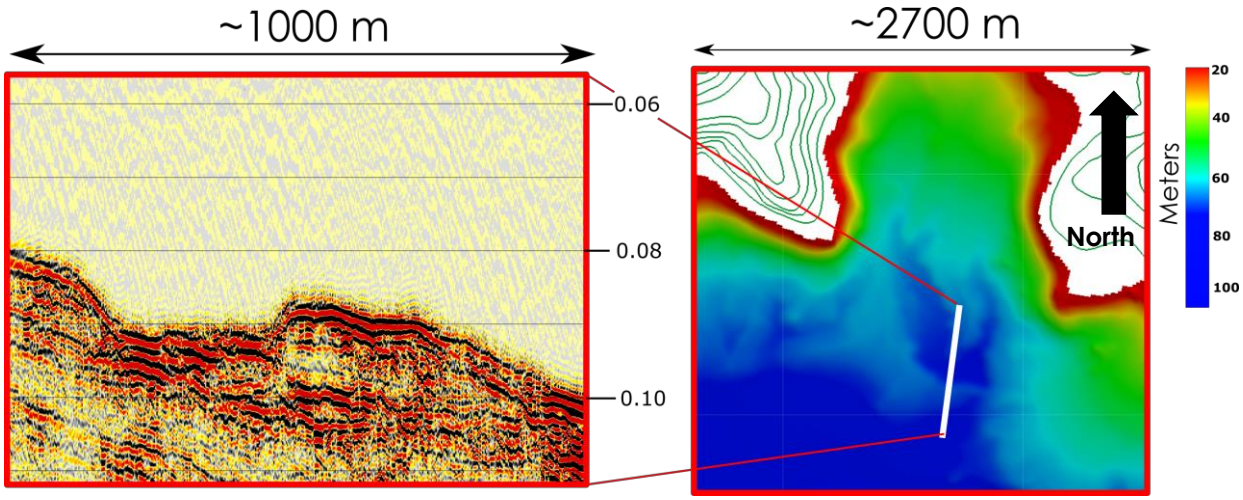

Figure 7.12 • River channel incised into fluvial sediments (**left**) with depth being in time (seconds), locality of the river channel against seafloor bathymetry (**right**). (Locality map in *Fig. 7.12*).

of dynamic river channels (Miall 1977, 1985 & 1996). These undulating seafloor expressions observed within the bathymetric data show drainage incision patterns of a paleo river (Carnley River), flowing into the Main Arm. The main channel incision meanders and deepens to the seaward (east). Locations of paleo-channel seafloor incisions in the bathymetry correlate with channel incisions within the seismic data (*Figure 6.22a, Figure 7.12*).

7.2.2 Western & Northern Arms •

The Western and Northern Arms of Carnley Harbour show similar seismic profiles that differ from that of the Main Arm. The bedrock in the Western Arm is observed closer to the surface, forming a series of sub-basins (*Figure 6.25*). These sediment-laden basins likely have been subject to glaciation at some time during the Quaternary, but probably have been subject to more fluvial erosion than the Main Arm during recent lowstands. This is because the Western and Northern Arm sits stratigraphically higher than Main Arm with respect to the underlying bedrock. The low-amplitude, semi-transparent facies that unconformably overlies the bedrock within the Western and Northern Arms mimics the main facies observed within the Main Arm. It is interpreted that these sub-basins may have had the potential to support a localised series of paleo-lakes that eventually in-filled to the basin threshold. Similar to the Main Arm, these in-filled basins have been succeeded by a facies with a semi-continuous, irregular nature of fluvial origin deposited during the LGM.

7.2.3 Modern Sediments •

Substantial sedimentary bedform deposits are present at the end of the Western Arm and the entrance to Carnley Harbour (*Figure 7.13*). These low amplitude, semi-transparent deposits with a continuously layered internal structure are interpreted as drift deposits. These are interpreted to be sourced from the dominant southwest wave direction. *Figure 6.25b* reveals these sedimentary bedform deposits as seen on line 15-02, and correlates with Victoria Passage. This passage is a narrow opening in the southwest corner of the Auckland Islands and is directly exposed to the dominant weather direction from the southwest. These sediments at Victoria Passage are interpreted to have been deposited by the intense current exchange

at this locality. Currents are enhanced through funnelling of southwest sea swells through a narrow restriction point (~300 m). Sediment is assumed to have originated from the heavily eroded southern and western margins that are directly exposed to the persistent westerly winds and erosive seas.

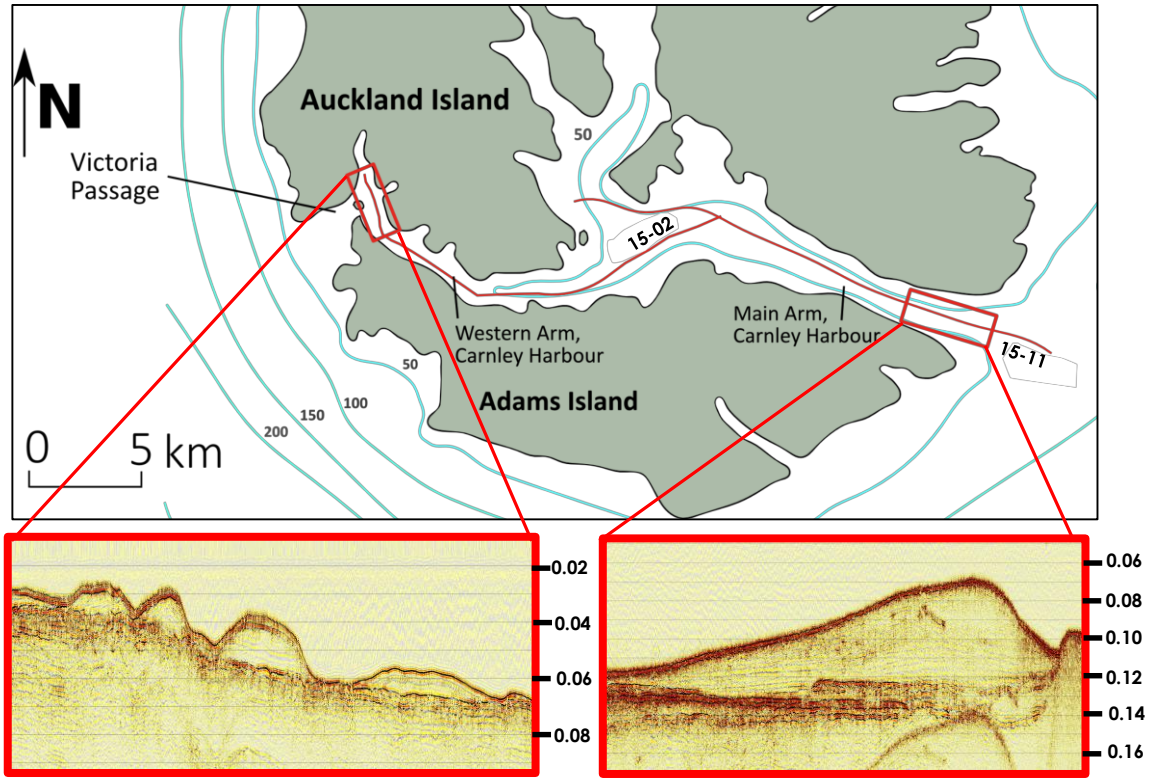

Figure 7.13 • Southwest corner of the Auckland Islands, exhibiting sedimentary bedform deposits within the seismic data and is related to current exchanges, originating from the dominant weather direction form the SW (**left**), entrance to Carnley Harbour portrays a large bedform deposit associated with refracting wave energy decreasing at the entrance (**right**). (Vertical axis is in time – Seconds).

A similar bedform deposit is also present at the entrance to Carnley Harbour (*Figure 6.23, 6.27 & 7.13*). This deposit exhibits very similar structures and characteristics within the seismic data to that observed at Victoria Passage. This Carnley Harbour deposit is interpreted to have formed from eddying currents that progress and refract around the southern extent of the Auckland Islands. As the currents progress around the landmass, they spill into the relatively sheltered entrance to Carnley Harbour. This results in a reduction of currents and subsequent deposition of sediments.

7.3 Eastern Shelf •

Described extensively in Chapter 6, numerous topographic depressions and ridgelines with extensive stages of sediment accumulation are present on the eastern shelf of the Auckland Islands (e.g. *Figure* 6.29). These features are distinguished as either paleo-valleys or incised valleys, a term that Thorne (1994) defines as encompassing a broad spectrum of topographic features formed by fluvial erosion. However, these drowned valleys are in close proximity to, or lie within, the bounds of formerly glaciated margins at the Auckland Islands. Incised valley systems have been extensively studied and provide complete evidence of lowstand to transgressive deposition in shelf/slope and shallow ramp depositional settings (Zaitlin et al. 1994).

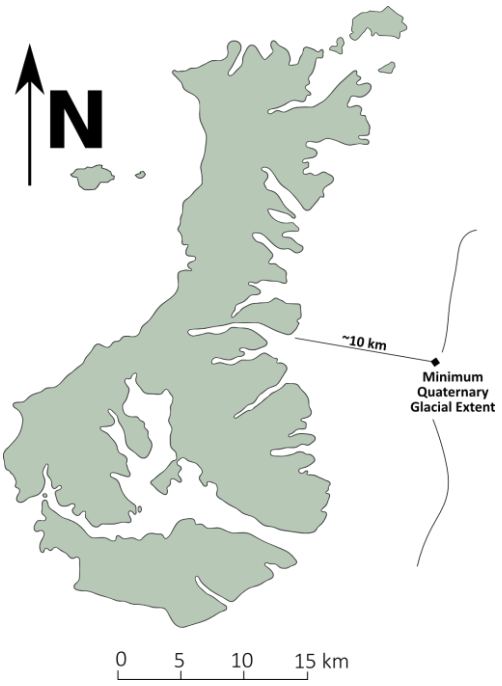

Figure 7.14 • Minimum Quaternary glacial extent as interpreted by buried valley morphology within the seismic data.

Interest in incised valley systems is related to their increasing significance to sequence stratigraphy principles, economic value and paleo-climate studies that provide ancient analogues to modern settings (Dalrymple 1994). Throughout the Quaternary, the Auckland Islands have been subjected to glacial and interglacial periods. These periods differ in intensity, primarily due to worldwide responses to orbital variability (Zachos et al. 2002). At the Auckland Islands, topographic highs, combined with the positioning in the middle to high southern latitudes during these glacial periods was crucial for the accumulation and retention of glacial ice (Hodgson et al. 2014).

Glacial features observed on the modern landmass must have originated during the Pleistocene within high amplitude glacial cycles; longer and more extensive than the LGM. This is due to the extreme depths of incised valleys that are observed

on the submerged eastern shelf, with some valleys extending to depths of ~185 m below modern sea level (e.g. *Figure 6.3a*). These depths can be explained through glacial carving; emanating from ice caps situated on Carnley Harbour and Disappointment Island (Qulity 2007). Glacial extents during these large cycles reached at least ~10 km to the east, perpendicular from the modern coast, as interpreted from buried valley morphologies (*Figure 7.14*). Contemporary terrestrial archives of these earlier glacial periods are not present due to the overprinting nature of glacial events. However, glacial till deposits are interpreted within the seismic data at the base of shelf stratigraphic sequences at various shelf localities. These initial extensive glacial valleys and channels would have been periodically eroded by glaciofluvial and fluvial forcing during de-glaciation phases. This is shown in the valley architecture on the eastern coast and is consistent with experimental studies undertaken by Shepard (1972). The study shows traverse profiles of fluvial incision into simulated bedrock that are comparable with profiles and features of the Auckland Islands shelf incisions (*Figure 7.15*).

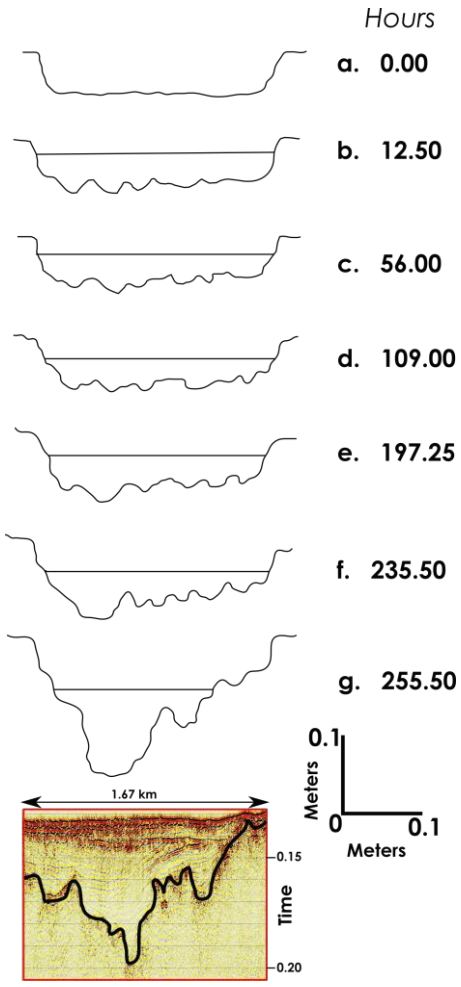

Figure 7.15 • Series of traverse profiles collecting during an experimental study of incision into simulated bedrock (from Shepard 1972) with a incised valley excerpt from line 14-03 on the Eastern Shelf showing similar morphological features.

Schumm and Ethridge (1994) further explain the evolution of an incised valley from initial channel incision progressing to widening by lateral migration and valley wall failure. This is followed by subsequent valley filling as a result of climate and/or sea level change. Glacial retreat at the Auckland Islands would have resulted in many of these incised valleys becoming glacial sluiceways that drained ice masses originating from the west. These valleys probably progressed to either enclosed paleo-lakes or fjords and subsequently to paleo-fjords, due to a transgressive regime.

These paleo-depositional environments correlate with the extensive draped, in-filled stratigraphy patterns observed overlying basal units and the eroded bedrock within the seismic data (Syvitski et al. 2012). However due to the complexity and irregularity of incised valley systems (Schumm 1994; Zaitlin 1994), it is difficult to accurately assign a lacustrine or quiet marginal marine/brackish setting for these sediments without well control. Draped sequences are punctuated stratigraphically by stronger, laterally continuous reflections that on-lap onto bedrock valley walls and/or underlying sediments as part of post-glaciation transgressive phases. These punctuations likely represent sub-aerial exposure events related to glacioeustatic sea level change over Quaternary glacial/interglacial periods. Within these periods of exposure, re-working of older deposited sediments on a paleo-exposed surface would occur through fluvial erosion and deposition. This occurred on the exposed shelf, likely in braided river systems.

Erosional reflections are present in varying strengths stratigraphically, but are observed continuously in different valleys laterally over kilometre scales. This likely represents multiple transgressive/regressive cycles at the Auckland Islands during the Quaternary (*Figure 7.16*). The erosional surfaces are succeeded by further draped reflections representing a further transgression of sea level, indicative of a cyclic sedimentary regime. The sedimentary response to changing periods of aggradation and erosion is known to produce abrupt lateral and vertical facies changes where younger units occupy channels eroded into older facies (Zaitlin 1994). This is observed in *Figure* 6.29*a* and 6.29b, with similar sediments on-lapping onto older, underlying sediments. There is no evidence within the incised valley stratigraphy of re-advancing glacial ice. This is due to the relatively heterogeneous nature of the package and the overprinting nature of prior Pleistocene glaciations within initial, glacially formed paleo-valleys. Well control at these localities would provide high-resolution assignment of lithofacies. This assignment would further resolve sea-level change and sedimentation regimes at the Auckland Islands on glacial/inter-glacial timescales. Dating of basal sediments would provide an age of potential last glaciation extents, subsequent de-glaciation timing as well as de-glaciation erosion/deposition processes.

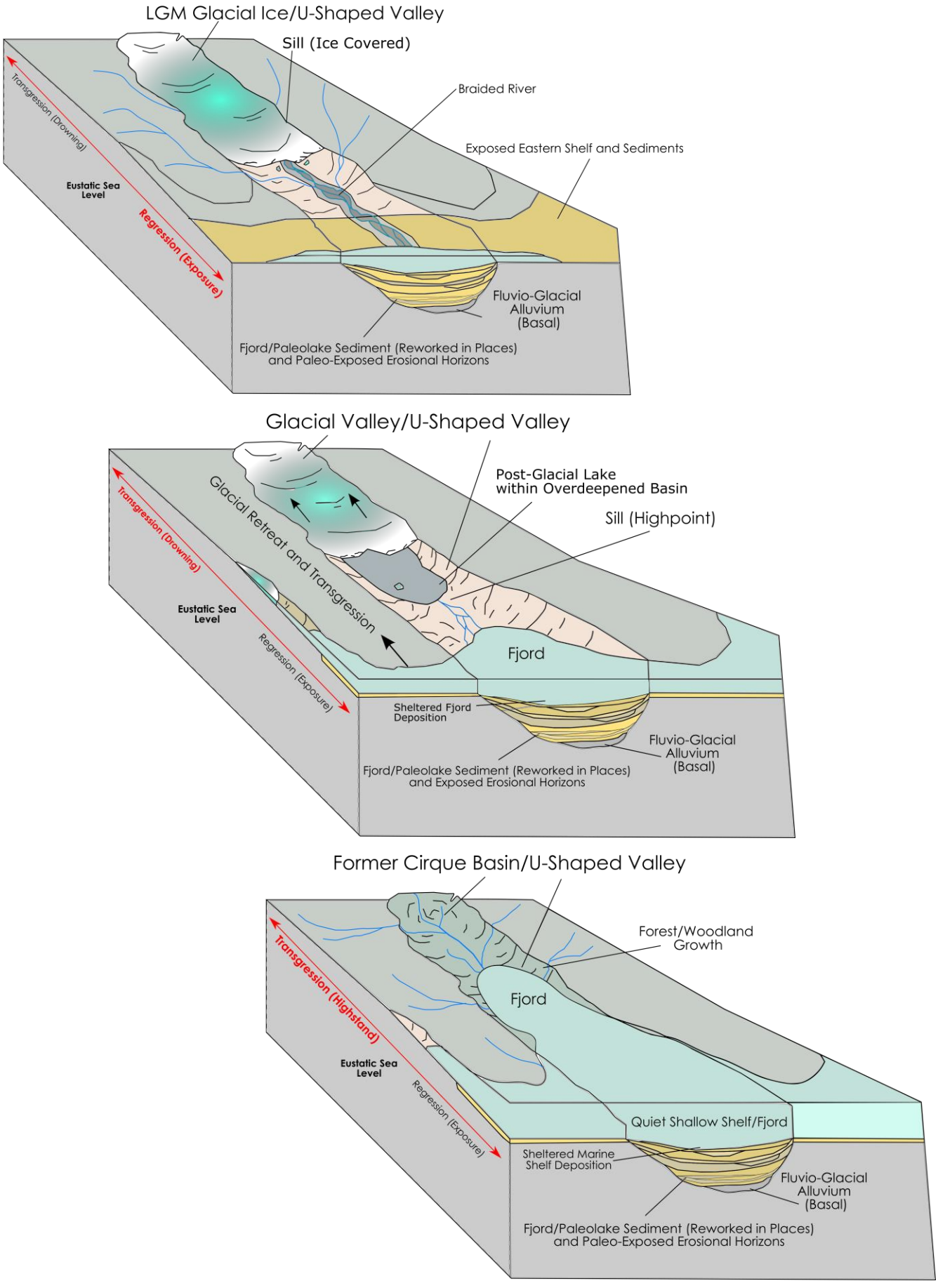

Figure 7.16 • Simplified cartoon schematic of eustatic sea level rise and fall over glacial/interglacial timescales and the effect on fjord and shelf settings.

7.3.1 Offshore Drainage Patterns •

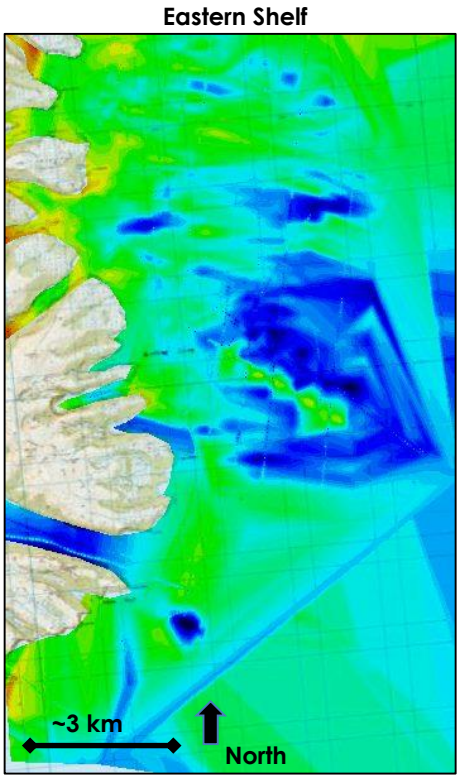

Figure 7.17 • 3D Model of basement topography of incised valleys on the eastern shelf. The topography shows a deepening to the south and southeast.

Eastern Shelf seismic data was input into a 3D modelling package, which can be used to interpret valley basement topography. This can provide regional clues to offshore shelf morphologies and drainage directions. The sediment/bedrock interface within the Eastern Shelf seismic transects were picked, interpolated and gridded into a 3D model, placing the varying depth interfaces in real space (*Figure 7.17*). The model exhibits a general deepening progression to the south/southeast within the bounds of the available seismic data. This correlates to the absence of valleys in northern reaches of the seismic data and contrasts with valleys on more distal transects present to the south. This south-south-east valley flow direction aligns with the Carnley Sea Valley to the south, which the majority of the incised valleys probably drain into. Although the eastern shelf has a high data density, focused on imaging these buried incised valleys, the highly irregular, anastomosing nature of the valleys is not able to be accurately modelled in 3D due to the insufficient spatial sampling of this data set.

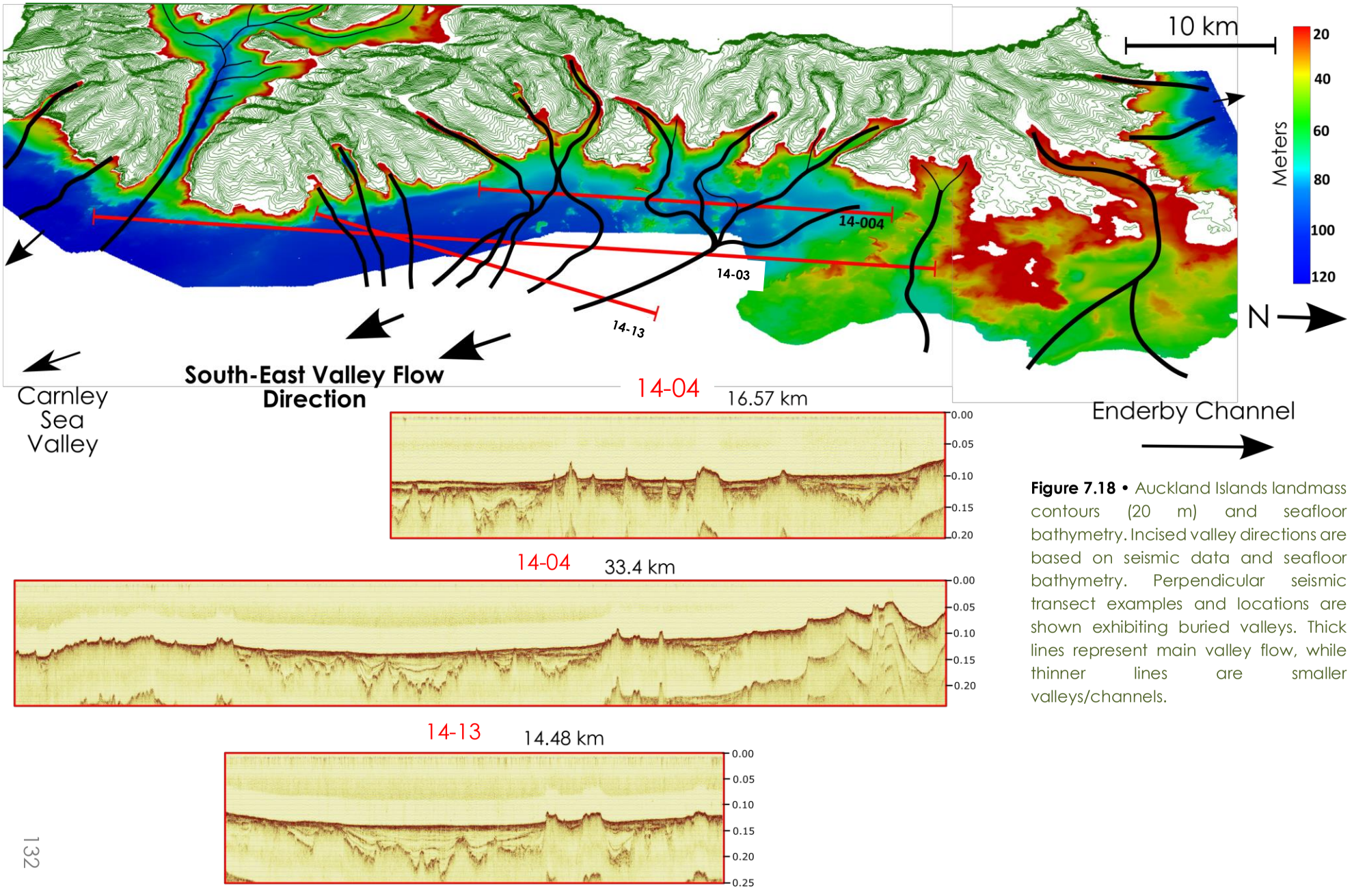

Figure 7.18 • Auckland Islands landmass contours (20 m) and seafloor bathymetry. Incised valley directions are based on seismic data and seafloor bathymetry. Perpendicular seismic transect examples and locations are shown exhibiting buried valleys. Thick lines represent main valley flow, while thinner lines are smaller valleys/channels.

7.4 LGM Ice Extent •

Seismic data and seafloor bathymetry collected from the eastern coast of the Auckland Islands show multiple cycles of glaciation and sedimentation events throughout the Quaternary. Multiple eastern fjords exhibit classic glaciated profiles with shallow entrance sills progressing into over-deepened back basins (Syvitski et al, 2012). These basins contain various stratigraphic packages that unconformably overlie the eroded bedrock. Offshore eastern shelf transects display an extensive, intricate incised valley system that originates from modern terrestrial glacial valleys and fjords. These offshore flooded valleys contrast the modern fjord systems with extensive, variable stratigraphic sequences that fill the valleys.

Early reconnaissance work undertaken at the Auckland Islands of terrestrial glacial features determined the Auckland Islands to have been extensively glaciated at the LGM with all coastal fjords being ice-filled (Wright 1967; Fleming et al 1976; Quilty 2007). However, glacial Ice at the LGM at the Auckland Islands was almost certainly confined to the foot-prints of previous glaciations and was far less extensive than the ice advances that formed the fjords. This presence of ice at the LGM is explained in part by the lack of sedimentation present within the fjord basins to what would be expected if there had been no fjord ice advance during this period. Some fjord basins (e.g. McLennan Inlet) reach 100 m water depth with only ~25 m of sediment overlying bedrock. If ice was not present during the LGM, more extensive sedimentary infill would be expected within these fjord basins.

Further terrestrial evidence for LGM ice advances is present within moraine dammed lakes at the heads of Musgrave and Granger Inlet (*Figure 7.19*). These lakes rest well within the footprint of the extensive U-shaped valleys flowing from topographic highs and continuing offshore. Dating of these lake sediments would provide ages of potential sediment accumulation after glacial retreat within these catchments. Further down these valleys within the main fjord body, no recent glaciation features are present within the seismic data. Recent sedimentary deposition created a smooth seafloor profile within the fjord, contrasting from other over-deepened inlets (e.g. McLennan Inlet, Fly Harbour).

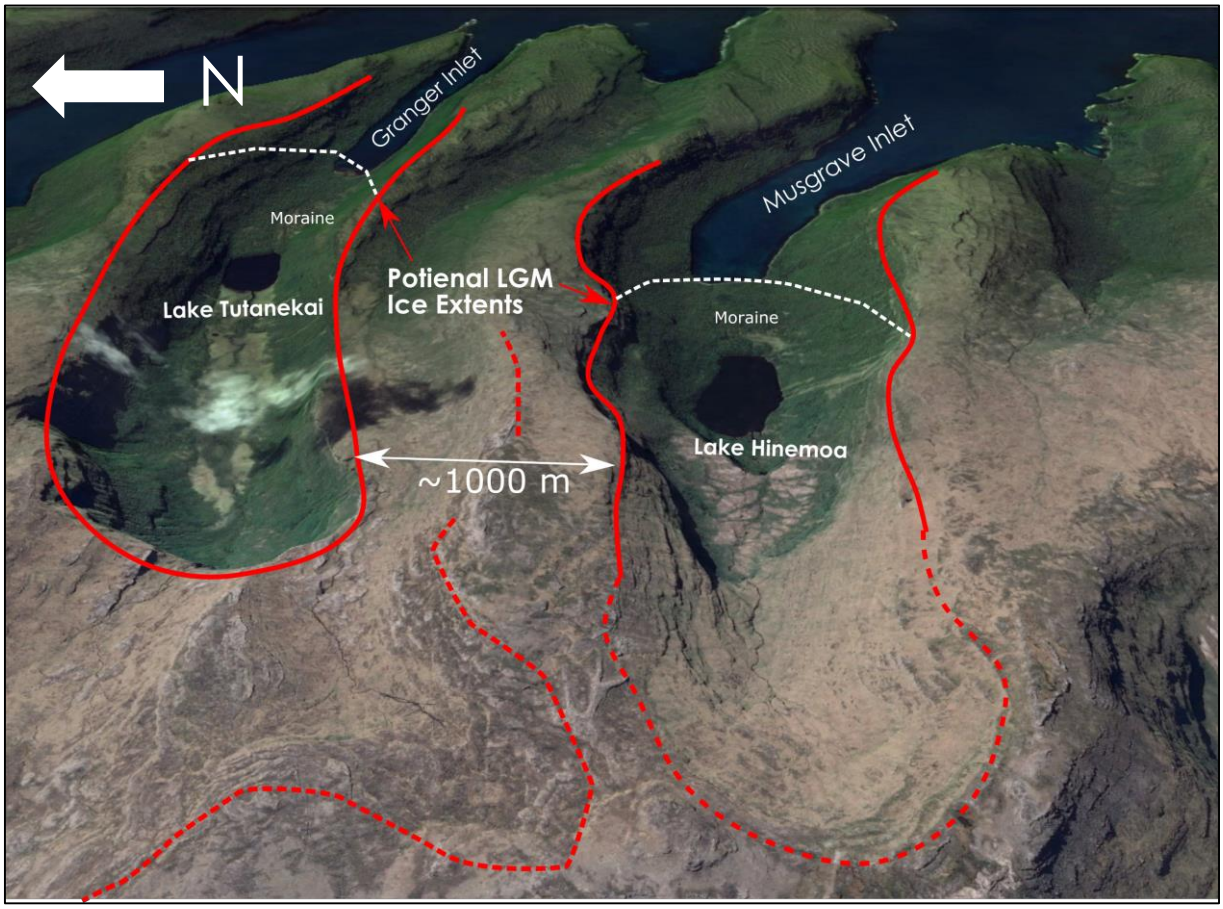

Figure 7.19 • Looking east down glacial valleys at the heads of Granger and Musgrave Inlets which exhibit moraine dammed lakes. Moraines are interpreted as a potential LGM ice extent. Solid lines are the valley confines and dashed lines are likely earlier Quaternary lateral ice extents due to the incision nature and more weathered surface appearance. (Image from Google Earth).

These moraine dammed lakes probably could define the LGM ice extent within these particular fjords and can be tentatively used as analogues for ice extent in other fjords. It should be noted that with the last glacial period ice advanced, retreated and resurged at various times through the past 65 ka at the Auckland Islands, using New Zealand evidence as an analogue (Barrell 2013).

In comparison to mainland New Zealand, where LGM ice cover was extensive over much of the mountainous areas of the South Island (46-42° S) and particular localities in the North Island (38-40° S) (Barrell 2013), the Auckland Islands had limited ice advances during the LGM despite its higher latitudes (~51° S). These differences and other differences between glacial histories within the sub-Antarctic region is in part a result of both latitudinal changes in climate and the topographical control of the glacial equilibrium line altitude required to grow and maintain glacial ice (Port 1975; Hodgson et al. 2014; Hoffman et al. 2016).

Islands such as South Georgia Island (54° S) and Kerguelen Islands (49° S) share similarities to the Auckland Islands through limited ice expansion at the LGM in comparison to earlier Pleistocene glaciations. Hodgson et al. (2014) provides potential insights to why LGM ice expansion was limited at this locality. The impacts of earlier glacially modified landscapes detrimentally affected the development of LGM ice development and was combined with moisture deprivation resulting from advancing, proximal sea ice at the LGM (Fraser et al. 2009). Bently et al. (2007) interpreted the extent of sea ice in the northern Weddell Sea and Scotia Sea as significant in determining the moisture content of depressions approaching South Georgia Island. Further, reduced moisture distribution is an outcome of a northward shift of the Southern Hemisphere Westerly Winds (SHWW) during the last glacial period and decreases the moisture supply from subtropical air masses. This subsequently intensified evaporation and sublimation rates at maritime and sub-Antarctic localities. As outlined by Hodgson et al. (2014) using sub-Antarctic case studies, changing moisture supply is important in assessing the mass balance of glaciers in the maritime and sub Antarctic regions, with altitude, temperature, insolation and terrestrial morphology being supporting factors. These case studies from similar latitude islands explain limited LGM ice relative to Pleistocene glaciations. They can be applied to the Auckland Islands setting to explain limited LGM expansion, while supporting the extensive terrestrial and submerged glacial evidence found in this region.

7.5 Exposed Landmass •

During the LGM, glacioeustatic sea level response resulted in a roughly 120 m lower sea level than is observed today (Yokoyama et al. 2000). This would have had extensive implications for the emergent landmass at the Auckland Islands during these periods. The modern combined Auckland Islands exposed landmass is ~625km ^{2} (~240 mi ^{2}); however during glacial periods of at least 120 m lower sea level, the exposed landmass is calculated to be at least three times (~2000 km ^{2}) the current Auckland Islands landmass (*Figure 7.21)*.

The exposed landmass to the east would have gone through phases of different environments as cyclic glacial and interglacial periods eroded the Cenozoic

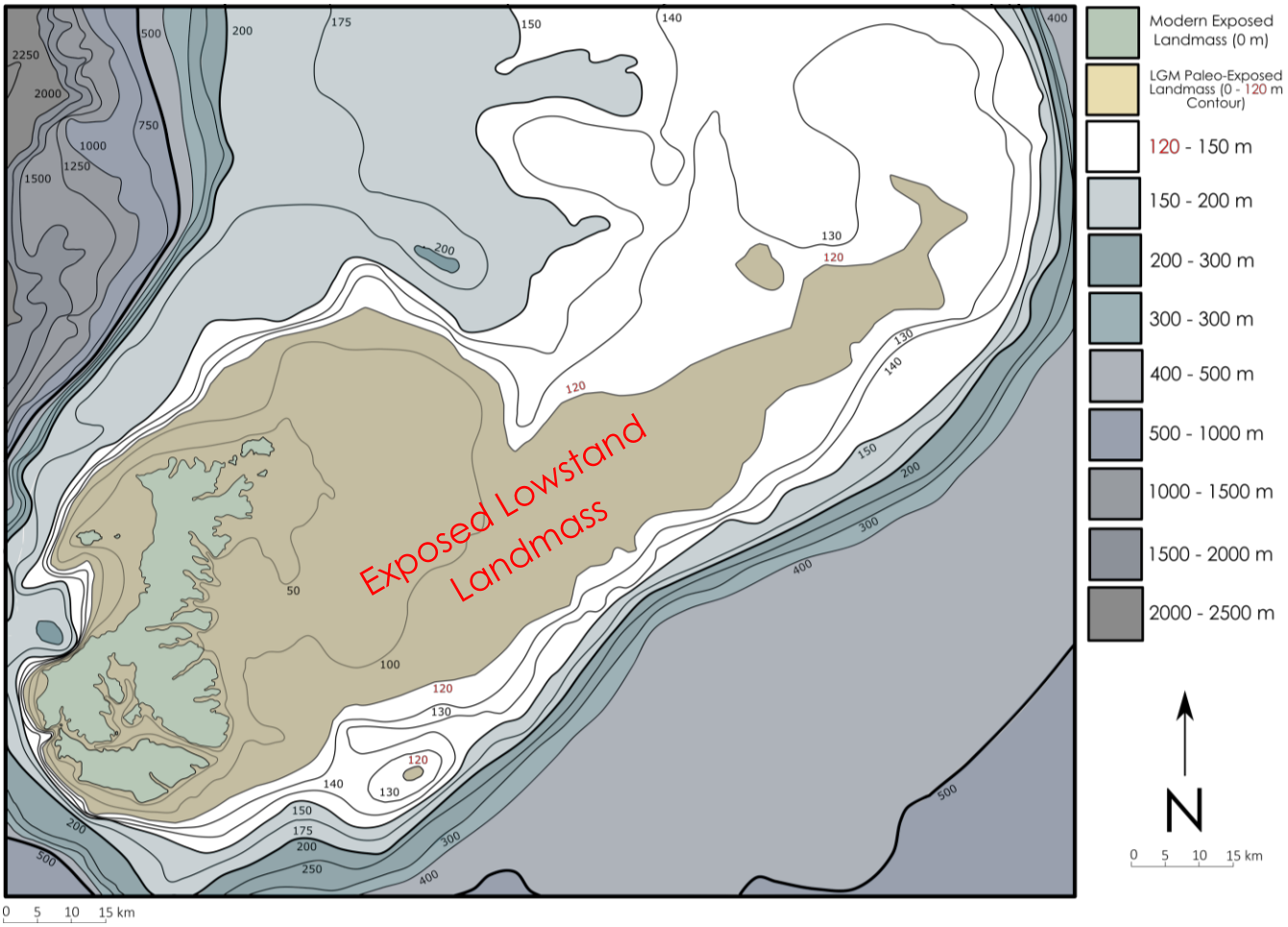

Figure 7.20 • Paleogeographical map of the exposed Auckland Islands land extent during the glacio-eustatic lowstand, reflecting global sea level at the LGM. Schematic generated by bathymetry contour maps from Land Information New Zealand (LINZ) marine charts.

volcanics and deposited sediments on the eastern shelf. At the LGM, the majority of the eastern shelf would have been an expansive, low-lying coastal plain, likely with braided river systems flowing from topographic highs in the west in an east/southeast direction. These river systems probably drained into the Carnley Sea Valley in the south and the Enderby Channel to the north. These findings have widespread implications for biogeographic distributions of the endemic flora and fauna assemblages present at Auckland Islands as well as the wider Antipodes Subantarctic Islands tundra ecoregion. The rapid marine transgression occurring in late glacial times would have caused sudden changes of the flora and fauna assemblages living on these eastern, lowland plains. This extended understanding of available biological refugia during glacioeustatic lowstands helps explain evolutionary patterns in biodiversity and biogeography of the unique endemic assemblages at this isolated location.

7.6 Lacustrine Deposits •

Due to the highly incised nature of the Auckland Island fjords and eastern shelf, there are numerous morphological controls that would allow for the development of paleo-lakes and depositional of associated lacustrine sediments. All fjords that exhibit over-deepened basins and entrance sills (buried or exposed) (e.g. Fly, Hanfield, McLennan, Norman, Port Ross and Carnley Harbour) would have supported paleo-lake environments at eustatic sea level lowstands. Terrestrial inputs within these lacustrine deposits provide high-resolution paleo-climate proxies, and are a wider research objective beyond the scope of this project. This proxy analysis would advance the current understanding of Quaternary climate parameters and de-glaciation rates at mid-high southern latitudes where geologic archives are sparse. However in comparison to North Sea studies where drowned and buried valleys have been investigated with the assistance of well control via

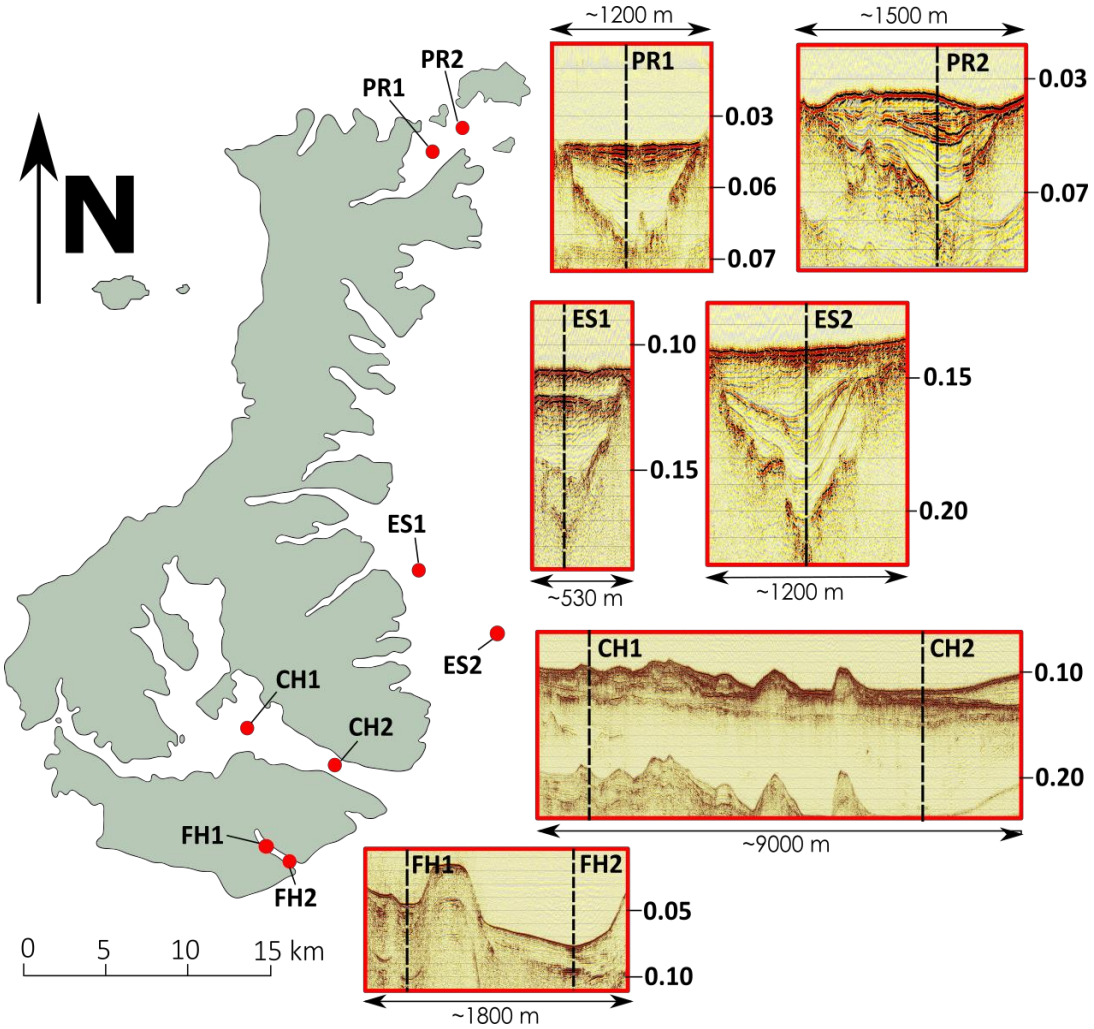

Figure 7.21 • Future coring targets at the Auckland Islands, with accompanying seismic line excerpts exhibiting specific sedimentary sequences. (PR - Port Ross, ES – Eastern Shelf, CH – Carnley Harbour, FH – Fly Harbour. Depth axis is measured in time (seconds).

drill cores, this method at this location is unlikely due to the ecological status of the sub-Antarctic islands. Core collection is likely confined to gravity and piston systems.

Locations presented here have been selected using seismic data, aiming to capture complete sequences and provide well control to seismic data sets (*Figure 7.21*). The two Port Ross localities (PR1 – 1115735.43, 4337992.94, PR2 – 1114772.36, 4338654.34) would aim to capture the unique stratigraphic infill of this Inlet, focusing on the main paleo-valley fill where previous authors (e.g. Fleming et al. 1976; McGlone 2002) concluded the presence of an extensive paleo-glacier during the last glacial period. Fly Harbour exhibits two basins separated by a large upstanding sill. Cores recovered from both sedimentary basins may provide insights into recent ice advances due to potential sedimentological differences between the basins (FH1 – 1115735.43, 4337992.94, FH2 – 1114772.36, 4338654.34). Although the thickness of the sedimentary package within the Main Arm of Carnley Harbour is out or reach of conventional coring systems, a drill core of this multi-facies sequence would provide extensive control to an area that has been over-run by an extensive paleo-glacier originating on an ice field centred on Carnley Harbour itself (CH1 – 1113192.47, 4345554.27, CH2 – 1119026.52, 4343439.88). This could provide a relatively complete sequence, since glacial ice was last present in Carnley Harbour, and the subsequent de-glaciation phases. Similar to Carnley Harbour, cores of the offshore infilled incised valley systems would provide valuable information for providing control on interpretations of multiple transgression and regression sequences throughout the Quaternary (ES1 – 1123114.09, 4355583.89, ES2 – 1126501.60, 4352443.82).

Chapter 8 •

Conclusions

8 Conclusions •

The leeward side of the sub-Antarctic Auckland Islands (51° 44'S, 166° 06'E) is dominated by Quaternary glacial landforms that extend offshore. Prior to this study, no submarine constraints of Quaternary glaciation extents (Hodgson et al. 2014) were present and LGM ice extent was unresolved (McGlone et al. 2000; McGlone et al. 2002; Quilty 2007). 1200 km of seismic data and an accompanying bathymetry survey concentrated on coastal fjords and inlets but also included an extensive section of the eastern shelf. These data sets presented here have provided new insights into the Quaternary glacial extent on both the emergent and submerged Auckland Island landmasses.

8.1 Incised Valley System • Eastern Shelf

Seismic reflection imaging reveals an extensive incised valley system to the east of the emergent Auckland Islands landmass with incisions observed up to ~185 m below contemporary sea level. These incised valleys originated during high-amplitude Pleistocene glacial cycles where glacial ice accumulated on two ice fields centred on the late Cenozoic Carnley and Ross volcanoes, respectively (Gamble & Adams 1985; Quilty 2007). Glacial ice flowed down in a radial arrangement from these former ice domes forming deeply cut glacial valleys extending at least 10 km to the now drowned eastern shelf during glacioeustatic lowstands. Glacial retreat during de-glaciation phases of these high-amplitude cycles resulted in these incised valleys becoming glacial sluiceways, draining the retreating ice masses. These valleys likely progressed into enclosed paleo-lake/fjord systems due to their highly irregular, incised nature as sea level transgressed the exposed landmass from the east. These post-glacial paleo-depositional environments are consistent with the draped sedimentary architecture observed within the incised valley stratigraphic infill sequence which is bound at the base by eroded bedrock and chaotic basal facies within the seismic data. The incised valley infill sequences likely preserve multiple Quaternary transgression/regression cycles. During lower- amplitude cycles, ice did not progress into the shelf but rather was characterised by alluvial systems within these infilled valleys, reworking the deposited sediment during sea level lowstands and shelf exposure. These valleys

flowed in an east/southeast direction, increasing in width and depth down valley. The valleys subsequently drain into the Carnley Sea Valley with flow direction being a function of bedrock topography. The more northern inlets (e.g. Haskell Bay and Port Ross) likely drained to the north into the Enderby Channel.

8.2 LGM Ice Extent •

Glacial ice during the Last Glacial Maximum (LGM) at the Auckland Islands was restricted to the impressions of previous Quaternary glaciations and was far less widespread. This is due to the lack of sedimentation observed within the fjord seismic data that would have been infilled if glacial ice did not advance during the LGM. Terrestrial evidence of moraine-dammed lakes at the heads of Musgrave and Granger Inlet provide a potential analogue for LGM ice extent. These lakes are dwarfed by the deeply cut glacial valleys in which they are situated. However specific glacial features associated with glacial extent such as terminal moraines are not immediately observed within the data and may be obscured due to overlying sediments. More expansive inlets such as Carnley Harbour had further limited ice extent, restricted to upper cirque basins due to the lack of topographical confinement. Carnley Harbour during the LGM was dominated by fluvial processes, with paleo-rivers flowing down from cirques within the Harbour catchment area. These rivers confluence to an area south of Musgrave Peninsula, flowing in a braided river system east down the Main Arm. This limited LGM ice extent, contrary to previously interpretation by Fleming et al. (1973), McGlone (2002), and Quilty (2007), is thought to be a result of an assortment of factors. The influence of profoundly eroded landforms of glacial origin, integrated with moisture depravation from proximal advancing Antarctic sea ice systems, and a different Southern Hemisphere Westerly Wind regime, is responsible for intensifying evaporation and sublimation rates, thus limiting extensive expansion of LGM ice at the Auckland Islands.

8.3 Exposed Auckland Islands Landmass during the LGM •

The LGM glacioeustatic lowstand (~120 m below current sea level) had a significant effect on the emergent Auckland Islands landmass observed today. An exposed land surface extending at least 100 km to the east was present during the

LGM, creating an exposed land surface at least three times the contemporary exposed landmass (~2000 km ^{2}). This exposed landmass would have been subject to dramatic change throughout the Quaternary, as glacial and fluvial erosional forces carved across the landscape. Due to the expansive eastern shelf and lack of significant topographical highs to the east of the modern landmass, glacial ice is unlikely to have entirely covered the exposed Auckland Islands landmass during the LGM, nor during higher-amplitude glacial cycles. During the LGM, the shelf was most likely an extensive, low-lying alluvial plain within the surveyed shelf area, draining into the Carnley Sea Valley to the south and Enderby Channel to the north. These insights into an exposed landmass during glacioeustatic lowstands have implications for other scientific disciplines relating to biogeographical distributions of highly endemic species present at the Auckland Islands.

8.4 Future Coring Targets •

Potential coring targets have been identified as targets for Southern Hemisphere Quaternary climate studies at the Auckland Islands. Many are beyond the breadth of this study. Numerous localities have been identified at Port Ross, Carnley Harbour, Fly Harbour and the Eastern Shelf which target areas where lacustrine and/or fluvial deposits are likely to be present. These localities are sediment traps that capture terrestrial inputs containing paleo-climate proxies. Such sediments act as coupled, dynamic response systems to the Southern Ocean and the Southern Hemisphere westerly wind belt (Gierlowski-Kordesch & Belts. 2006). The localities were selected due to their relative substantial post-glacial sedimentation which allows for an increased, higher-resolution record. These targets should play an internationally important role due to their location; occupying the mid-high southern latitudes in the Pacific sector where geologic archives are scarce.

8.5 Research Relevance to Previous Work•

Hodgson et al. (2014) classified sub-Antarctic and maritime Antarctic islands in relation to maximum ice volumes at the LGM. The Auckland Islands were originally classified as 'Type V: islands north of the Antarctic Polar Front with terrestrial evidence of LGM ice expansion'. However these new data sets and ice extent interpretations justifies the need for the Auckland Islands to be re-classified under

'Type II: Islands with a limited LGM extent but evidence of extensive earlier continental shelf glaciations'. This is due to the evidence for limited ice expansion during the LGM within fjord seismic profiles, combined with the extensive presence of deeply incised valleys on the eastern shelf formed by prior Pleistocene glaciations. This study addresses the appeal by Hodgson et al. (2014) for research focused towards the understudied sub-Antarctic glaciation history. This was achieved through (1) identifying onshore and offshore limits of past glaciation through geophysical methods, (2) sedimentary investigations and (3) identifying postglacial sequences as future coring targets. Beyond the scope of this research, further understanding of the timing and pattern of post-LGM glaciation can be achieved through dating methods. These new datasets and findings will contribute to future key paleo-climate work undertaken at the New Zealand sub-Antarctic Islands due to their unique location (mid-high southern latitudes) and relatively natural conditions. Key research themes outlined by the Department of Conservation's *New Zealand Sub-Antarctic Islands Research Strategy* (2006) have also been addressed in relation to defining an enlarged exposed landmass during sea level lowstands and LGM glacial extent with respect to ecosystem responses. These outcomes will progress research on the highly endemic ecosystems established on these Island and provide groundwork for further paleo-climate and atmospheric research in the Southern Ocean.

8.6 Future Work •

The results and interpretations from this study lay a significant framework for future multi-disciplinary research of the under-studied, wider sub-Antarctic region in the Southern Ocean. Using these data sets, the previously mentioned coring targets in post-glacial lacustrine deposits and other postglacial sequences can be used to understand the timing and pattern of deglaciation after the LGM at these localities.

Terrestrial cosmogenic nuclide dating (TCN) is fast becoming a baseline method for surface exposure dating, where geochronological techniques are used to estimate the length of time a rock surface has been exposed at the Earth's surface. This technique has been extensively used in Antarctica to estimate the retreat

history of glacial ice (e.g. Johnson et al. 2009; Mackintosh et al. 2014). This method could be applied at the Auckland Islands to provide exposure dates, where exact terrestrial and definitive submarine LGM extents are not accurately resolved. Accurate dating of exposure could further define glacial extent and timing of Auckland Island glaciation. These investigations of the dynamics of sub-Antarctic paleo-ice masses could provide vital indications of the link between Southern Hemisphere climate and ice sheet stability (Hodgson et al. 2014).

The large quantity of data (1200 km of seismic transects) collected in this highly dynamic, diverse locality provides the opportunity for more high-resolution studies on particular inlets or localities of interest. The scope of such studies could vary in relation to modern sediment transport, Quaternary sedimentary successions, water mass mixing or further seismic acquisition. Modern sediment transport processes and deposition occurring offshore within the seismic and bathymetric data have produced numerous seafloor current depositional features. These features are related to longshore currents that originate from the incessant westerly flows that the Auckland Islands is subjected to. These types of high-resolution sedimentary investigations combining seismic data sets with sedimentary core control within particular fjord and inlet localities will provide further insight into erosional and depositional regimes at these unique mid-high southern latitude localities.

Further seismic acquisition at the Auckland Islands at new localities could, for example, provide a more holistic understanding of the western shelf where Quaternary glaciers would have flowed. West facing cirque basins are still present that rest ~500 m above the heavily eroded coastline (*Figure 8.1*). Although terrestrial evidence for west flowing glacial valleys originating from these cirque basins have since been eroded, submarine evidence could still be preserved due to the substantial Quaternary Auckland Islands glaciations. Further seismic

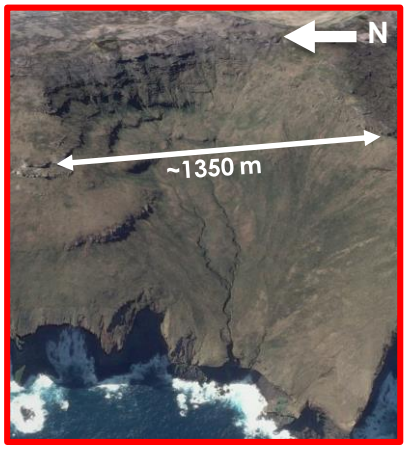

Figure 8.1 • West facing cirque basin on the heavily eroded western coastline. Locality is shown in *Figure 7.19*.

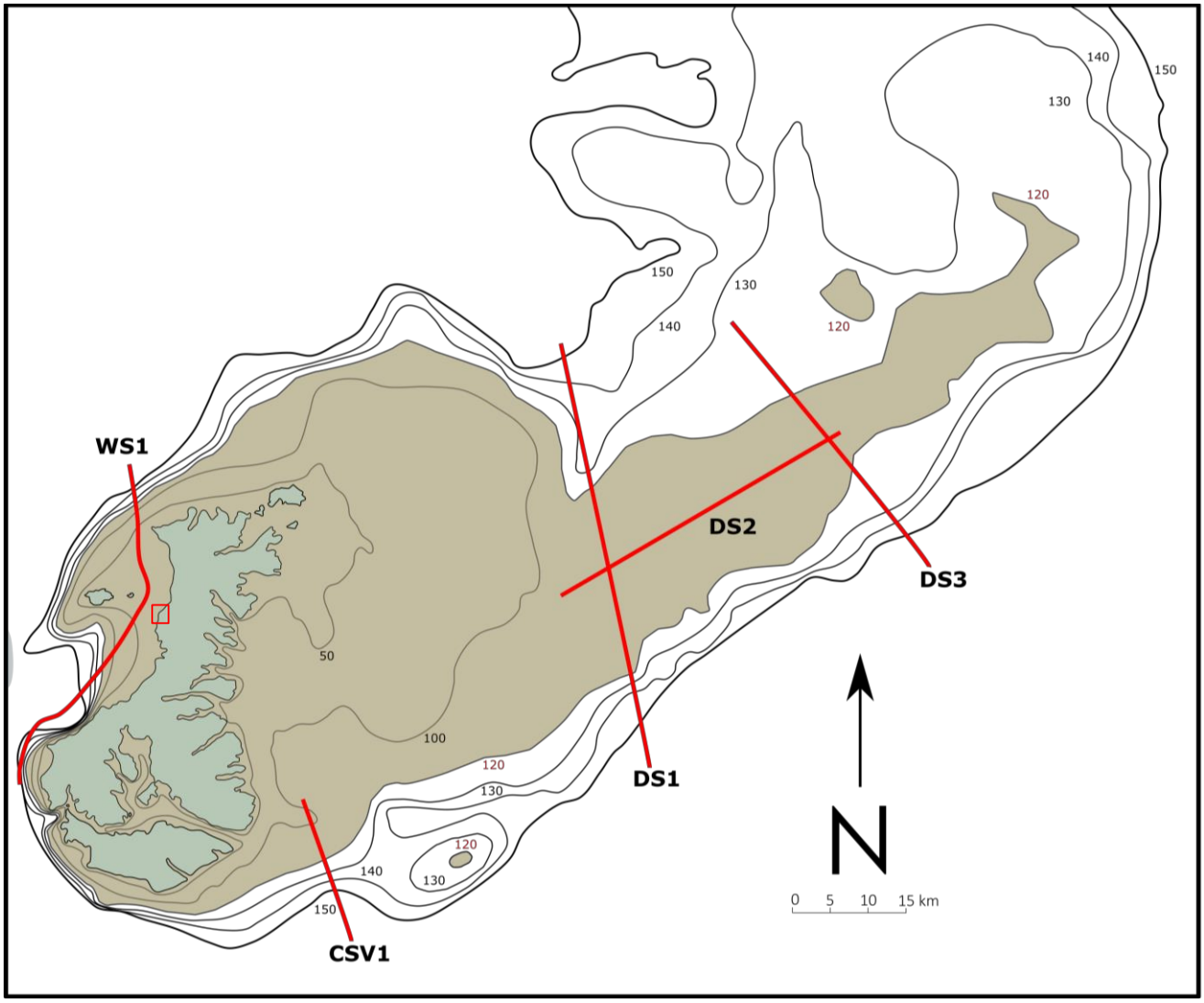

Figure 8.2 • Future seismic transects targeting new Auckland Island localities and the submerged, paleo-exposed landmass. (WS – Western Shelf, CSV – Carnley Sea Valley, DS – Distal Shelf)

transects focusing on the more distal eastern shelf, where land was exposed during glacioeustatic lowstands would more accurately define the exposed paleo-environment during these periods (*Figure 8.2)*. Such transects could answer questions regarding what kind of topography was observed further east on this low relief section of the exposed Auckland Islands in relation to potential complete ice cover in earlier Quaternary times.

9 References •

Adams RD 1962. Thickness of the Earth's Crust Beneath the Campbell Plateau. New Zealand Journal of Geology and Geophysics, 5 (1), 74-85.

Adams CJ 1981. Migration of Late Cenozoic Volcanism in the South Island of New Zealand and the Campbell Plateau.

Adams CJ 1983. Age of the Volcanoes and Granite Basement of the Auckland Islands, Southwest Pacific. New Zealand Journal of Geology and Geophysics, 26 (3), 227-237.

Ahmad J, Schmitt DR, Rokosh CD, Pawlowicz JG 2009. High-resolution seismic and resistivity profiling of a buried Quaternary subglacial valley: Northern Alberta, Canada. Geological Society of America Bulletin, 121(11-12), 1570-1583.

Aronson JL 1968. Regional Geochronology of New Zealand. Geochimica et cosmochimica acta, 32 (7), 669-697.

Barnard PL, Hanes DM, Rubin DM, Kvitek RG 2006. Giant sand waves at the mouth of San Francisco Bay. Eos, 87 (29), 285-286.

Barrie JV, Conway KW, Picard K, Greene HG 2009. Large-scale Sedimentary Bedforms and Sediment Dynamics on a Glaciated Tectonic Continental Shelf: Examples from the Pacific Margin of Canada. Continental Shelf Research, 29 (5), 796-806.

Barry K, Cavers D, Kneale C 1975. Recommended standards for digital tape formats. Geophysics, 40(2), 344–352.

Beggs JM 1978. Geology of the Metamorphic Basement and Late Cretaceous Oligocene Sedimentary Sequence of Campbell Island, Southwest Pacific Ocean. Journal of the Royal Society of New Zealand, 8 (2), 161-177.

Beggs JM, Challis GA, Cook RA 1990. Basement Geology of the Campbell Plateau: implications for Correlation of the Campbell Magnetic Anomaly System. New Zealand Journal of Geology and Geophysics, 33 (3), 401-404.

Bennett KD 1990. Milankovitch Cycles and their Effects on Species in Ecological and Evolutionary time. Paleobiology, 11-21.

Bergstrom DM and Chown SL 1999. Life at the Front: History, Ecology and Change on Southern Ocean islands. Trends in Ecology & Evolution 14.12: 472-477.

Brown AV, Cooper RA, Grindley GW 1982. Late Proterozoic to Devonian Sequences of Southeastern Australia, Antarctica and New Zealand and their Correlation (No. 9). Geological Society of Australia.

Brown MI 2015. A Holocene Paleoclimatic Record of Westerly Wind Variability from the Subantarctic Auckland Islands, New Zealand. Unpublished. Masters. Thesis, Otago University.

Campbell RJ 2015. Hydrographic surveying for ports and approaches. The International Hydrographic Review, 57(2).

Clark PU, Dyke AS, Shakun JD, Carlson AE, Clark J, Wohlfarth B, Mitrovica JX, Hostetler SW, McCabe Am 2009. The Last Glacial Maximum. Science 325(5941), 710-714.

Cook RA 1981. Geology and Bibliography of the Campbell Plateau, New Zealand. New Zealand Geological Survey Report, 97, 1-48.

Cook A, Poncet S, Cooper A, Herbert D, Christie D 2010. Glacier Retreat on South Georgia and Implications for the Spread of Rats. Antarctic Science, 22 (03), 255–263.

Cooper RA 1974. Age of the Greenland and Waiuta Groups, South Island, New Zealand. New Zealand Journal of Geology and Geophysics, 17 (4), 955-962.

Cullen DJ 1975. Autochthonous Rocks of the Bounty Island Region, Southwest Pacific Ocean. New Zealand Journal of Geology and Geophysics 18: 767-785.

Dalrymple RW 1994. History of research, types and internal organisation of incised-valley systems: introduction to the volume. Incised-valley systems: origin and sedimentary sequences. SEPM (Society for Sedimentary Geology), 3-10.

De Lisle JF 1964. The Climate of the Auckland Islands, Campbell Islands and Macquarie Island Included in a Symposium on 'The ecology of the Subantarctic Islands of New Zealand' at the 1964 Conference, 37 – 44

Denison RE, Coombs DS 1977. Radiometric Ages for Some Rocks from Snares and Auckland Islands, Campbell Plateau. Earth and Planetary Science Letters, 34(1), 23-29.

Ehlers J 1990. Reconstructing the Dynamics of the North-west European Pleistocene Ice Sheets. Quaternary Science Reviews 9, 71-83.

Ehlers J, Linke G 1989. The origin of deep buried channels of Elsterian age in north-west Germany. Journal of Quaternary Science 4 (3), 255-265

Ehlers J, Meyer KD, Stephan HJ 1984. Pre-Weichselian glaciations of north-west Europe. Quaternary Science Reviews 3, 1-40

Einvik-Heitmann V 2014. Unravelling the Secrets of the Subantarctic Auckland Island Inlets: An Environmental Magnetic Study of a Holocene Sediment Core. Unpublished. PGDip. Thesis, Otago University.

Fairbanks, RG, Matthews RK, 1978. The Marine Oxygen Isotope Record in Pleistocene Coral, Barbados, West Indies. Quaternary Research 10, 181-196.

Farmer DM, Freeland HJ 1983. The Physical Oceanography of Fjords. Progress in Oceanography, 12(2), 147-219.

Fenner JL, Carter L, Stewart R 1992. Late Quaternary Paleoclimatic and Paleoceanographic Change over Northern Chatham Rise, New Zealand. Marine Geology 108, 383–404.

Fenster MS, FitzGerald DM, Moore MS 2006. Assessing Decadal-Scale Changes to a Giant Sand Wave Field in Eastern Long Island Sound. Geology, 34 (2), 89-92.

Fleming CA, Mildenhall DC, Moar NT 1976. Quaternary sediments and plant microfossils from Enderby Island, Auckland Islands. Journal of the royal Society of New Zealand, 6(4), 433-458.

Fraser GS 1994. Sequences and sequence boundaries in glacial sluiceways beyond glacial margins. Incised-valley systems: origin and sedimentary sequences. SEPM (Society for Sedimentary Geology), 337-352.

Fraser CL, Nikula R, Spencer HG, Waters JM 2009. Kelp genes reveal effects of subantarctic sea ice during the Last Glacial Maximum. Proceedings of the National Academy of Sciences, 106(9), 3249-3253.

Gamble JA, Adams CJ 1985. Volcanic Geology of Carnley Volcano, Auckland Islands. New Zealand Journal of Geology and Geophysics, 28 (1), 43-54.

Gierlowski-Kordesch E, Kelts K 2006. Global Geological Record of Lake Basins (Vol. 1). Cambridge University Press.

Gordon JE, Haynes VM, Hubbard A 2008. Recent Glacier Changes and Climate Trends on South Georgia. Global and Planetary Change, 60 (1-2), 72–84.

Gorman AR, Bruce C, Preskett SA, Norris R, Choveaux R, Flemish H, Green C 2011. High-resolution Seismic and Side Scan Sonar Imaging of Active Structures and Quaternary Channels on the Shallow Shelf of Otago, Southeastern New Zealand. In AGU Fall Meeting Abstracts (Vol. 1, p. 1524)

Graham AG, Fretwell PT, Larter RD, Hodgson DA, Wilson CK, Tate AJ, Morris, P 2008. A New Bathymetric Compilation Highlighting Extensive Paleo–Cce Sheet Drainage on the Continental Shelf, South Georgia, sub-Antarctica. Geochemistry, Geophysics, Geosystems, 9 (7).

Heusser CJ 1989. Late Quaternary Vegetation and Climate of Southern Tierra del Fuego. Quaternary Research 31, 396 – 406.

Heusser CJ 1990. Late-Glacial and Holocene Vegetation and Climate of subantarctic South America. Review of Palaeobotany and Palynology 65, 9 – 15.

Hjelstuen BO, Haflidason H, Sejrup HP, Lysså A 2009. Sedimentary processes and depositional environments in glaciated fjord systems—Evidence from Nordfjord, Norway. Marine Geology, 258(1), 88-99.

Hodgson DA, Graham AGC, Roberts SJ, Bentley MJ, Cofaigh C, Verleyen E, Vyverman W, Jomelli V, Favier V, Brunstein D, Verfaillie D, Colhoun EA, Saunders KM, Selkirk PM, Mackintosh A, Hedding DW, Nel W, Kevin H, McGlone M, Van der Putten N, Dickens WA, Smith JA 2014. Terrestrial and Submarine Evidence for the Extent and Eiming of the Last Glacial Maximum and the Onset of Deglaciation on the Maritime-Antarctic and sub-Antarctic Islands. Quaternary Science Reviews 100:137-158.

Hodgson DA, Graham AG, Griffiths HJ, Roberts SJ, Cofaigh CÓ, Bentley, MJ, Evans DJ 2014. Glacial history of sub-Antarctic South Georgia based on the submarine geomorphology of its fjords. Quaternary Science Reviews, 89, 129-147.

Hoernle K, White JDL, van den Bogaard P, Hauff F, Coombs DS, Werner R, Timm C, Garbe-Schonberg D, Reay A, Cooper AF 2006. Cenozoic Intraplate Volcanism on New Zealand: Upwelling Induced by Lithospheric Removal. Earth and Planetary Science Letters, 248 (1), 350-367.

Hoffman MJ, Fountain AG, Liston GE 2016. Distributed modelling of ablation (1996–2011) and climate sensitivity on the glaciers of Taylor Valley, Antarctica. Journal of Glaciology, 62(232), 215-229.

Huuse M, & Lykke-Andersen H 2000. Overdeepened Quaternary valleys in the eastern Danish North Sea: morphology and origin. Quaternary Science Reviews, 19(12), 1233-1253.

Jansson P, Näslund JO 2009. Spatial and temporal variations in glacier hydrology on Storglaciären, Sweden.

Johnson JS, Smellie JL, Nelson AE, Stuart FM 2009. History of the Antarctic Peninsula Ice Sheet since the early Pliocene—evidence from cosmogenic dating of Pliocene lavas on James Ross Island, Antarctica. Global and Planetary Change, 69(4), 205-213.

Jordan P 2010. Analysis of overdeepened valleys using the digital elevation model of the bedrock surface of Northern Switzerland. Swiss Journal of Geosciences, 103(3), 375-384.

Kluiving SJ, Bosch JA, Ebbing JH, Mesdag CS, Westerhoff RS 2003. Onshore and offshore seismic and lithostratigraphic analysis of a deeply incised Quaternary buried valley system in the Northern Netherlands. Journal of Applied Geophysics, 53(4), 249-271.

Kubicki A 2008. Large and Very Large Subaqueous Dunes on the Continental Shelf off Southern Vietnam, South China Sea. Geo-Marine Letters, 28(4), 229-238.

Lamy F, Hebbeln D, Röhl U, Wefer G 2001. Holocene Rainfall Variability in Southern Chile: a Marine Record of Latitudinal Shifts of the Southern Westerlies. Earth and Planetary Science Letters, 185 (3), 369-382.

Lamy F, Kilian R, Arz AW, Francois JP, Kaiser J, Prange M, Steinke T 2010. Holocene Changes in the Position and Intensity of the Southern Westerly Wind Belt. Nature Geoscience 3, 695 – 699.

Mackintosh AN, Verleyen E, O'Brien PE, White DA, Jones RS, McKay R, Dunbar R, Gore DB, Fink D, Post AL, Miura H 2014. Retreat history of the East Antarctic Ice Sheet since the last glacial maximum. Quaternary Science Reviews, 100, pp.10-30.

Marshall SJ 2005. Recent advances in understanding ice sheet dynamics. Earth and Planetary Science Letters, 24 0(2), 191-204.

Markgraf V, Dodson JR, Kershaw AP, McGlone MS, Nicholls N 1992. Evolution of Late Pleistocene and Holocene Climates in the Circum-South Pacific Land Areas. Climate Dynamics, 6 (3-4), 193-211.

Meyers PA, Lallier-Vergès E 1999. Lacustrine sedimentary organic matter records of Late Quaternary paleoclimates. Journal of Paleolimnology, 21(3), 345-372.

McGlone MS 2002. The Late Quaternary Peat, Vegetation and Climate History of the Southern Oceanic Islands of New Zealand. Quaternary Science Reviews. 21.4: 683-707.

McGlone MS, Wilmshurst JM, Wiser SK 2000. Lateglacial and Holocene Vegetation and Climatic Change on Auckland Island, subantarctic New Zealand. The Holocene, 10 (6), 719-728.

Miall AD 1977. A review of the braided-river depositional environment. Earth-Science Reviews, 13, 1-62.

Miall AD 1985. Architectural-element analysis: a new method of facies analysis applied to fluvial deposits. Earth Science Reviews, 22, 261 – 308.

Miall AD 1996. The geology of fluvial deposits. Sedimentary facies, basin analysis, and petroleum geology.

Milankovitch M 1941. Kanon der Erdebestrahlung und seine Anwendung auf das Eiszeitenproblem. Königlich Serbische Akademie.

Morley JJ, Dworetzky BA 1993. Holocene Temperature Patterns in the South Atlantic, Southern and Pacific Oceans. (pp. 125-135). University of Minnesota Press).

Mussett AE, Khan MA 2000. Looking Into the Earth: An Introduction to Geological Geophysics. Cambridge University Press.

Nelson CS, Cooke PJ, Hendy CH, Cuthbertson AM 1993. Oceanographic and Climatic Changes over the Past 160,000 years at Deep Sea Drilling Project Site 594 off Southeastern New Zealand, Southwest Pacific Ocean. Paleoceanography, 8 (4), 435-458.

Nelson CS, Hendy IL, Neil HL, Hendy CH, Weaver PE 2000. Last Glacial Jetting of Cold Waters through the Subtropical Convergence Zone in the Southwest Pacific off Eastern New Zealand, and some Geological Implications. Palaeogeography, Palaeoclimatology, Palaeoecology, 156 (1), 103-121.

New Zealand Meteorological Service 1973. Summaries of Climatological Observations to 1970. New Zealand Meteorological Service Miscellaneous Publications 143.

Pickrill RA, Fenner JM, McGlone MS 1992. Late Quaternary evolution of a fjord environment in Preservation Inlet, New Zealand. Quaternary Research, 38(3), 331-346.

Pinter N, Gardner TW 1989. Construction of a Polynomial Model of Glacio-Eustatic Fluctuation: Estimating Paleo-Sea Levels Continuously Through Time. Geology 17, 295-298.

Piper DJW, Letson JRJ, De Iure AM, & Barrie CQ 1983. Sediment accumulation in low-sedimentation, wave-dominated, glaciated inlets. Sedimentary Geology, 36(2), 195-215.

Porter SC 1975. Equilibrium-line altitudes of late Quaternary glaciers in the Southern Alps, New Zealand. Quaternary research, 5(1), 27-47.

Powell RD, Molnia BF 1989. Glacimarine Sedimentary Processes, Facies and Morphology of the south-southeast Alaska Shelf and Fjords. Marine Geology, 85(2), 359-390.

Praeg D 2003. Seismic imaging of mid-Pleistocene tunnel-valleys in the North Sea Basin—high resolution from low frequencies. Journal of Applied Geophysics, 53(4), 273-298.

Quilty PG 2007. Origin and Evolution of the sub-Antarctic Islands: The Foundation. In Papers and Proceedings of the royal Society of Tasmania (Vol. 141, No. 1, pp. 35-58).

Rahmstorf S, England MH 1997. Influence of Southern Hemisphere Winds on North Atlantic Deep Water Flow. Journal of Physical Oceanography, 27 (9), 2040-2054.

Ravens J 1999. Globe claritas, seismic processing directory. Institute of Geological and Nuclear Sciences Technical Report 99/12. 307 p.

Renssen H, Seppä H, Crosta X, Goosse H, Roche DM 2012. Global Characterization of the Holocene Thermal Maximum. Quaternary Science Reviews, 48, 7-19.

Ritchie DD, Turnbull IM 1985. Cenozoic Sedimentary Rocks at Carnley Harbour, Auckland Islands, Campbell plateau. New Zealand Journal of Geology and Geophysics, 28(1), 23-41.

Sangree JB, Widmier JM 1979. Interpretation of Depositional Facies from Seismic Data. Geophysics, 44(2), 131-160.

Schumm SA 1994. Origin, evolution and morphology of fluvial valleys. Incised-valley systems: origin and sedimentary sequences. SEPM (Society for Sedimentary Geology), 11-28.

Scott JM, Turnbull IM, Auer A, Palin JM 2013. The sub-Antarctic Antipodes Volcano: a < 0.5 Ma HIMU-like Surtseyan volcanic outpost on the edge of the Campbell Plateau, New Zealand. New Zealand Journal of Geology and Geophysics, 56 (3), 134-153.

Scott JM, Turnbull IM, Sagar MW, Tulloch AJ, Waight TE, Palin JM 2015. Geology and Geochronology of the Sub-Antarctic Snares Islands/Tini Heke, New Zealand. New Zealand Journal of Geology and Geophysics, (ahead-of-print), 1-11.

Shackleton NJ 1987. Oxygen Isotopes, Ice Volume and Sea Level. Quaternary Science Reviews 6, 183}190.

Simpkin PG 2005. The Boomer Sound Source as a Tool for Shallow Water Geophysical Exploration. Marine Geophysical Researches, 26(2-4), 171-181.

Sly PG 1978. Sedimentary Processes In Lakes. In Lakes (pp. 65-89). Springer New York.

Speight R, Finlayson AM 1909. Physiography and Geology of the Auckland, Bounty and Antipodes Islands. Pp. 705-744 in: Chilton, C. ed. The subantarctic islands of New Zealand. Vol. 2.

Suggate RP 1990. Late Pliocene and Quaternary Glaciations of New Zealand. Quaternary Science Reviews 9, 175 – 195.

Stewart MA, Lonergan L, Hampson G 2013. 3D seismic analysis of buried tunnel valleys in the central North Sea: morphology, cross-cutting generations and glacial history. Quaternary Science Reviews, 72, 1-17.

Streten NA 1988. The Climate of Macquarie Island and its Role in Atmospheric Monitoring. Papers and Proceedings of the Royal Society of Tasmania 122, 91–106.

Syvitski JP, Burrell DC, Skei JM 2012. Fjords: Processes and Products. Springer Science & Business Media.

Toggweiler JR, Samuels B 1995. Effect of Drake Passage on the Global Thermohaline Circulation. Deep Sea Research Part I: Oceanographic Research Papers, 42 (4), 477-500.

Weaver PP, Carter L, Neil HL 1998. Response of Surface Water Masses and Circulation to Late Quaternary Climate Change East of New Zealand. Paleoceanography, 13 (1), 70-83.

Wellman P 1983. Hotspot Volcanism in Australia and New Zealand: Cainozoic and mid-Mesozoic. Tectonophysics, 96(3), 225-243.

West CJ 2005. New Zealand subantarctic islands research strategy. Department of Conservation.

Wright JB 1966. Contributions to Volcanic Succession and Petrology of the Auckland Islands, New Zealand. I. West Coast Section Through Ross Volcano. Transactions of the Royal Society of New Zealand. Geology, 3(16), 215.

Wright JB 1967. Contributions to Volcanic Succession and Petrology of the Auckland Islands. II. Upper parts of Ross Volcano. Transactions of the Royal Society of New Zealand. Geology, 5(2), 71.

Wright JB 1968. Contributions to Volcanic Succession and Petrology of the Auckland Islands, New Zealand. III. Minor Intrusives on Ross Volcano. Transactions of the Royal Society of New Zealand. Geology, 6(1), 1.

Wright JB 1970. Contributions to the Volcanic Succession and Petrology of the Auckland Islands, New Zealand. IV. Chemical Analyses from the Lower Half of the Ross Volcano. Transactions of the Royal Society of New Zealand. Earth Sciences, 8, 109-115.

Wright JB 1971. Contributions to the Volcanic Succession and Petrology of the Auckland Islands, New Zealand. V. Chemical Analyses from Upper Parts of the Ross Volcano, Including the Minor Intrusions. Journal of the Royal Society of New Zealand, 1(2), 175-183.

Van der Vegt P, Janszen A, Moscariello A 2012. Tunnel valleys: current knowledge and future perspectives. Geological Society, London, Special Publications, 368(1), 75-97.

Varma V, Prange M, Merkel U, Kleinen T, Lohnmann G, Pfeiffer M, Renssen H, Wagner A, Wagner S, and Schulz M 2012. Holocene evolution of the Southern Hemisphere westerly winds in transient simulations with global climate models. Climate of the Past, (8): 391-402.

Yilmaz Ö 2001. Seismic Data Analysis. Vol. 1. Tulsa: Society of Exploration Geophysicists.
Yokoyama Y, Lambeck K, De Deckker P, Johnston P, Fifield LK 2000. Timing of the Last Glacial Maximum from observed sea-level minima. Nature, 406 (6797), 713-716.

Zaitlin BA 1994. The stratigraphic organization of incised-valley systems associated with relative sea-level change. Incised-valley systems: origin and sedimentary sequences. SEPM (Society for Sedimentary Geology), 45-62.

Appendix

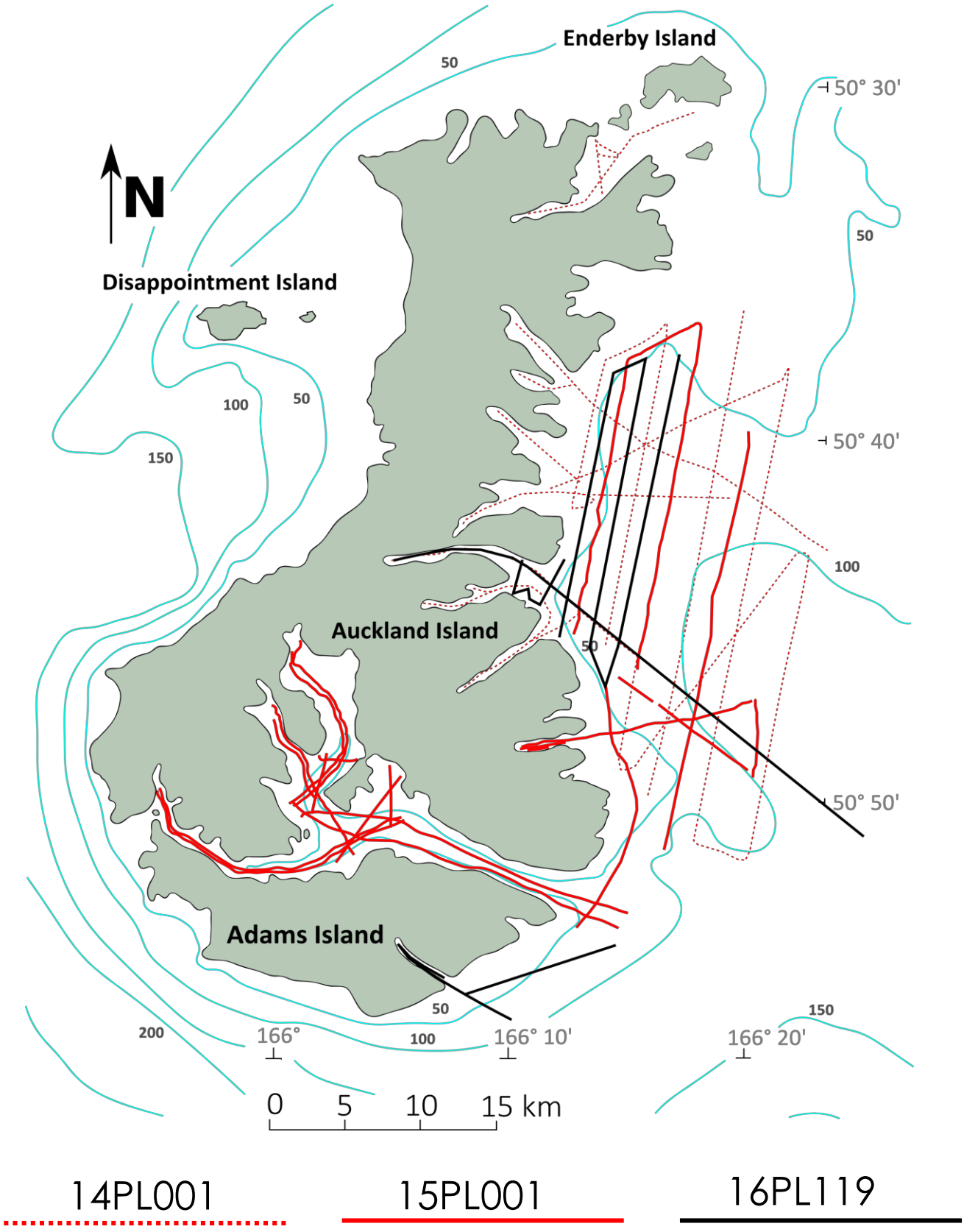

Appendix 1.1 • Seismic survey transects of 14PL001, 15PL001 and 16PL119 at the Auckland Islands presented against bathymetry contours.

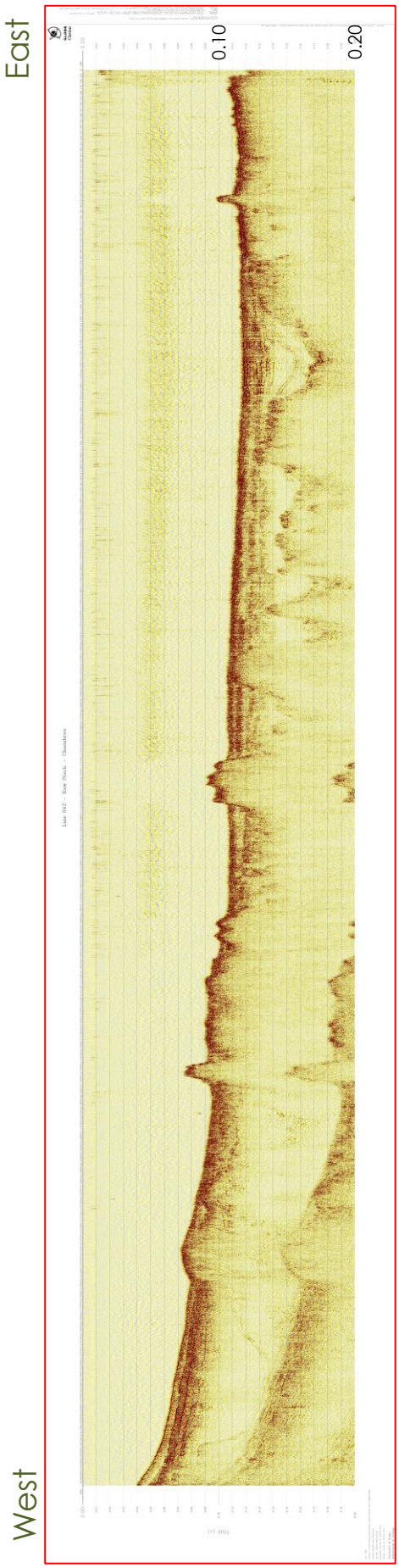

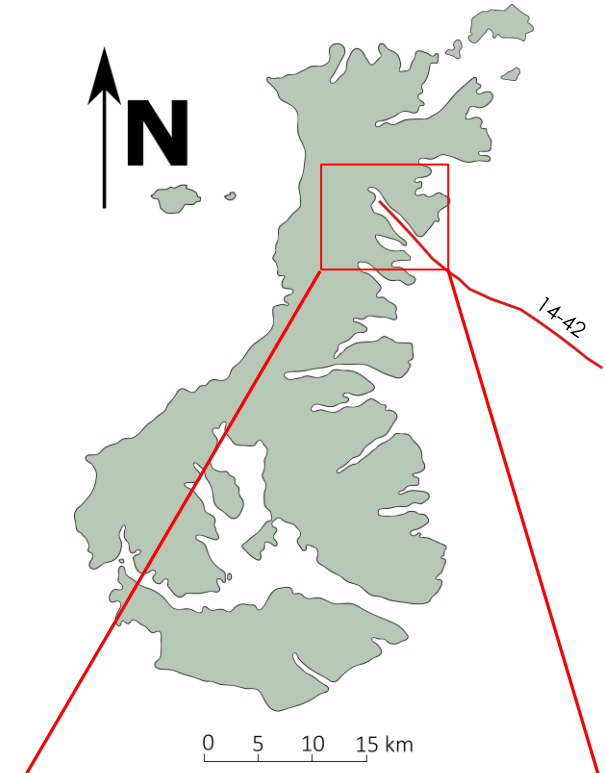

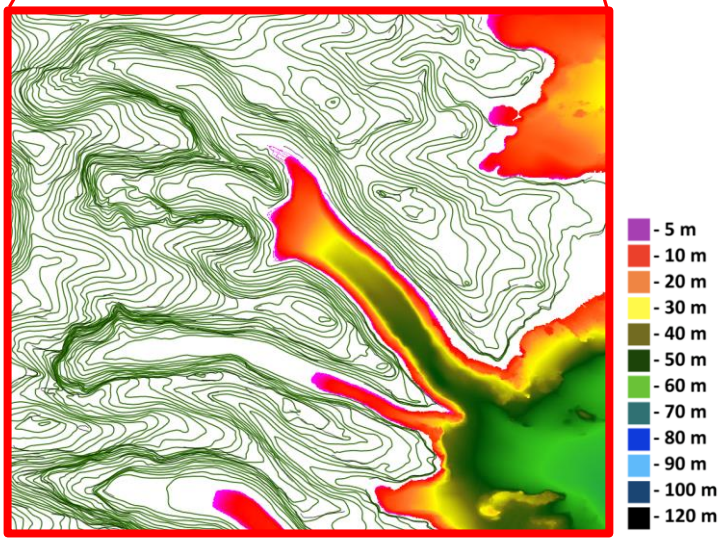

Appendix 1.2 • Line 14-42 acquired within Chambres Inlet. Line Length ~19.5 km with accompanying bathymetry and satellite image.

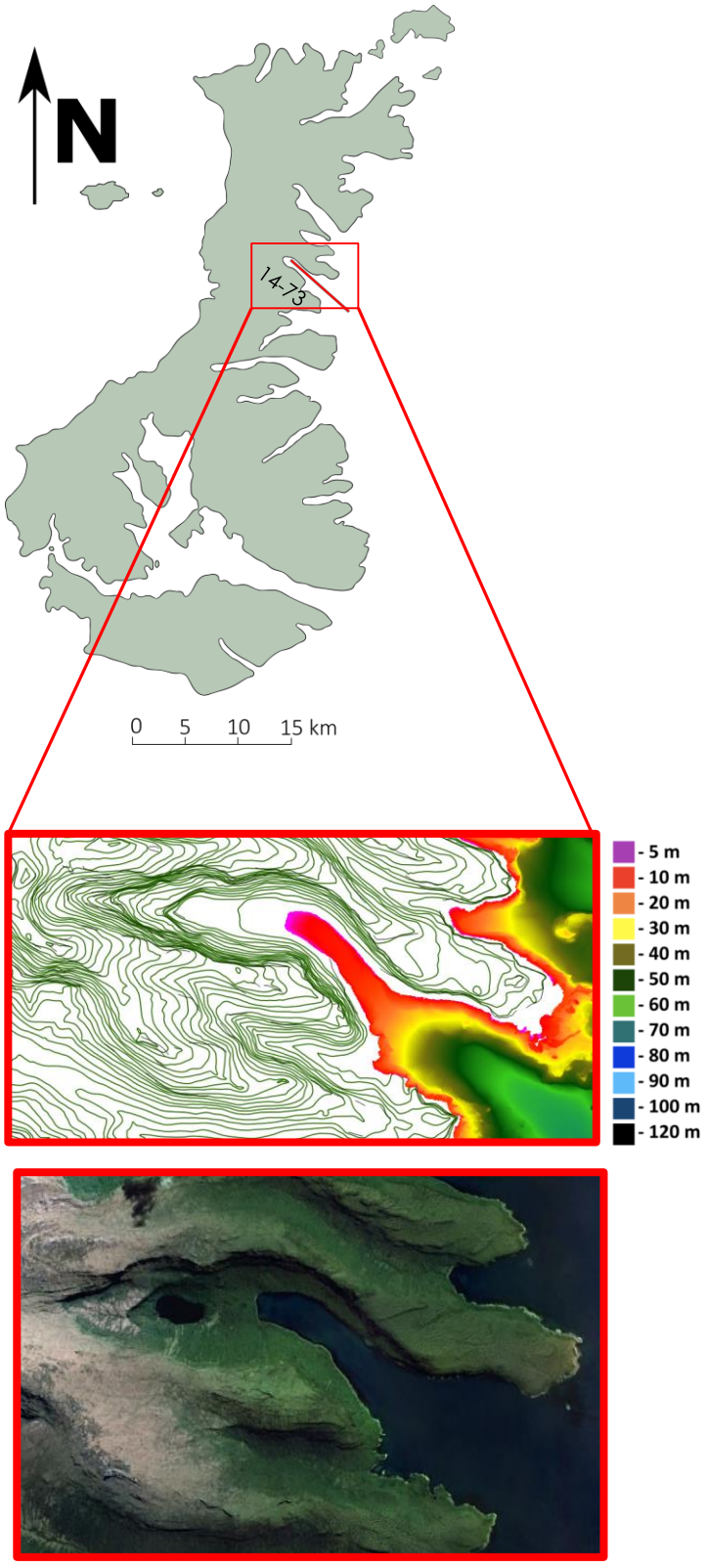

Appendix 1.3 • Line 14-73 acquired within Musgrave Inlet. Line Length ~5.4 km with accompanying bathymetry and satellite image.

A 1.3 North Arm, Hanfield Inlet • Line 14-29

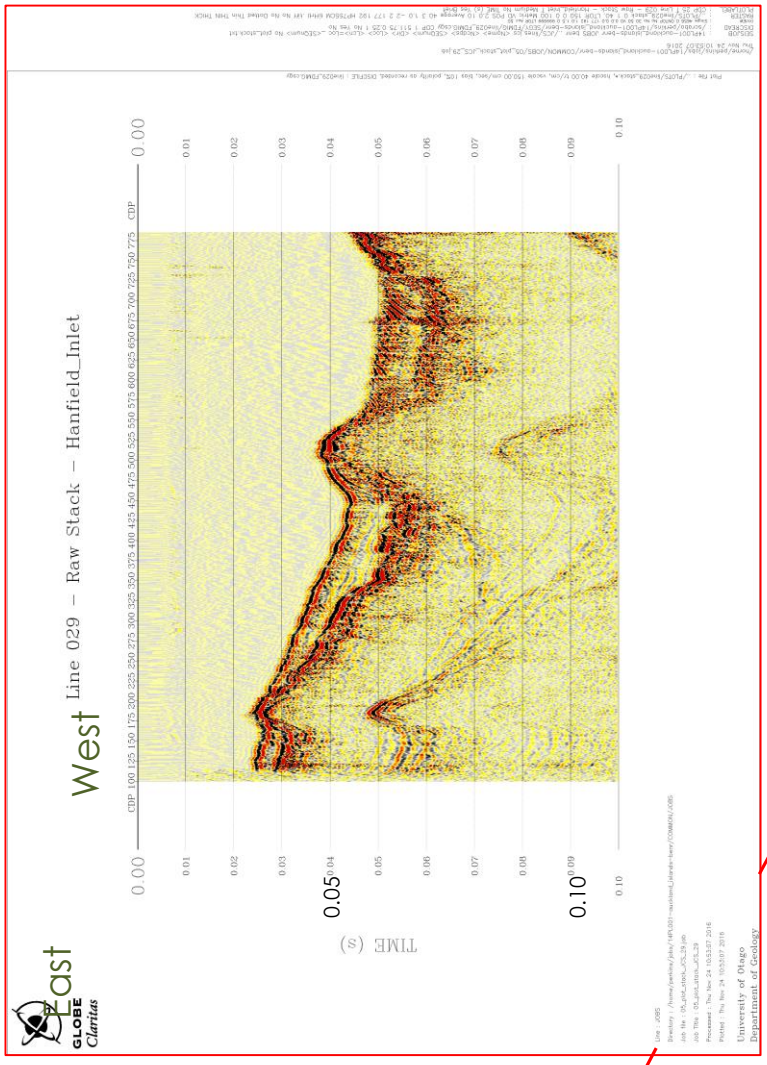

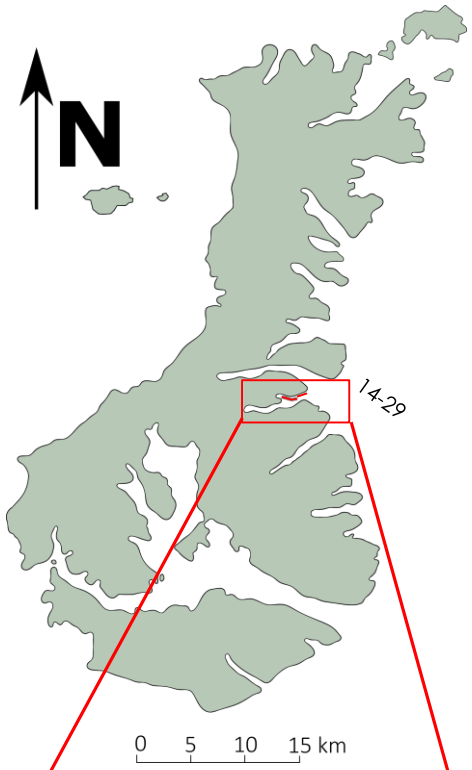

Appendix 1.4 • Line 14-29 acquired with the North Arm, Hanfield Inlet. Line Length ~2.1 km with accompanying bathymetry and satellite image.

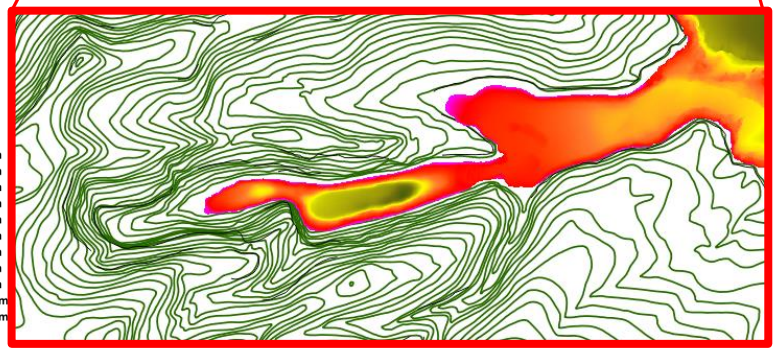

A 1.4 Deep Inlet • Line 14-17

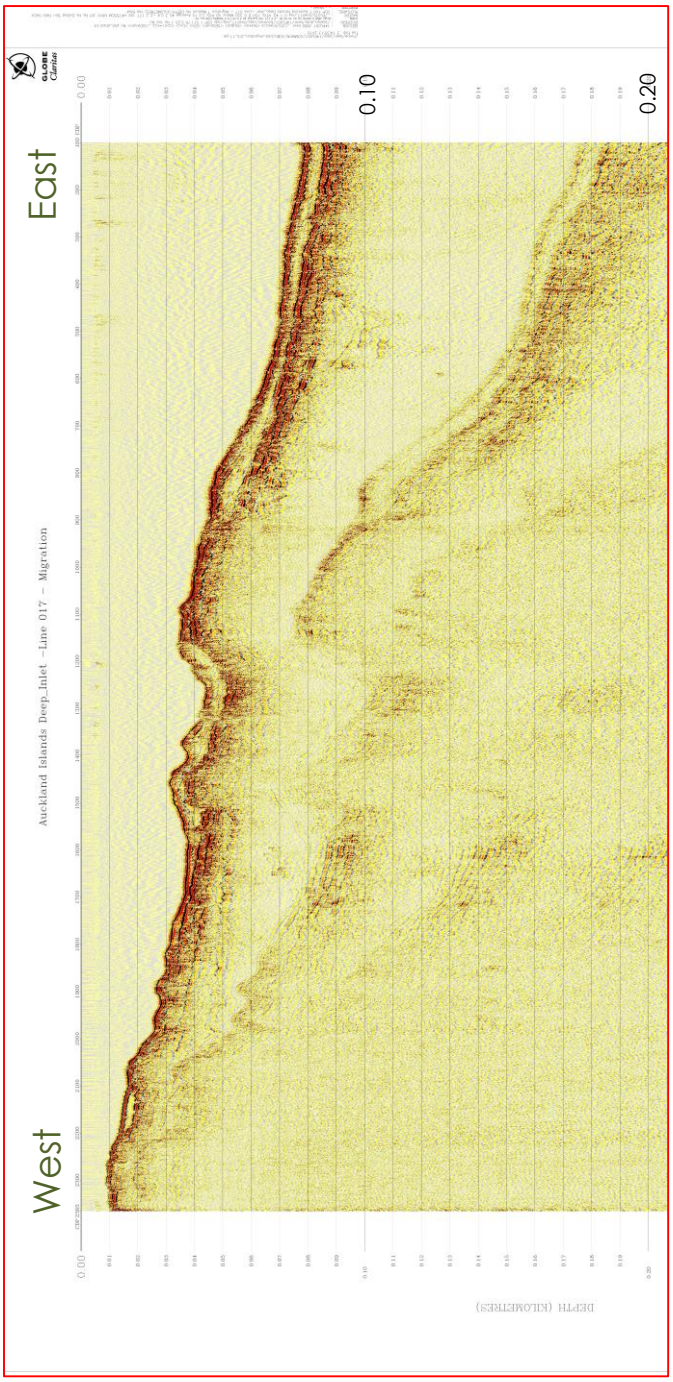

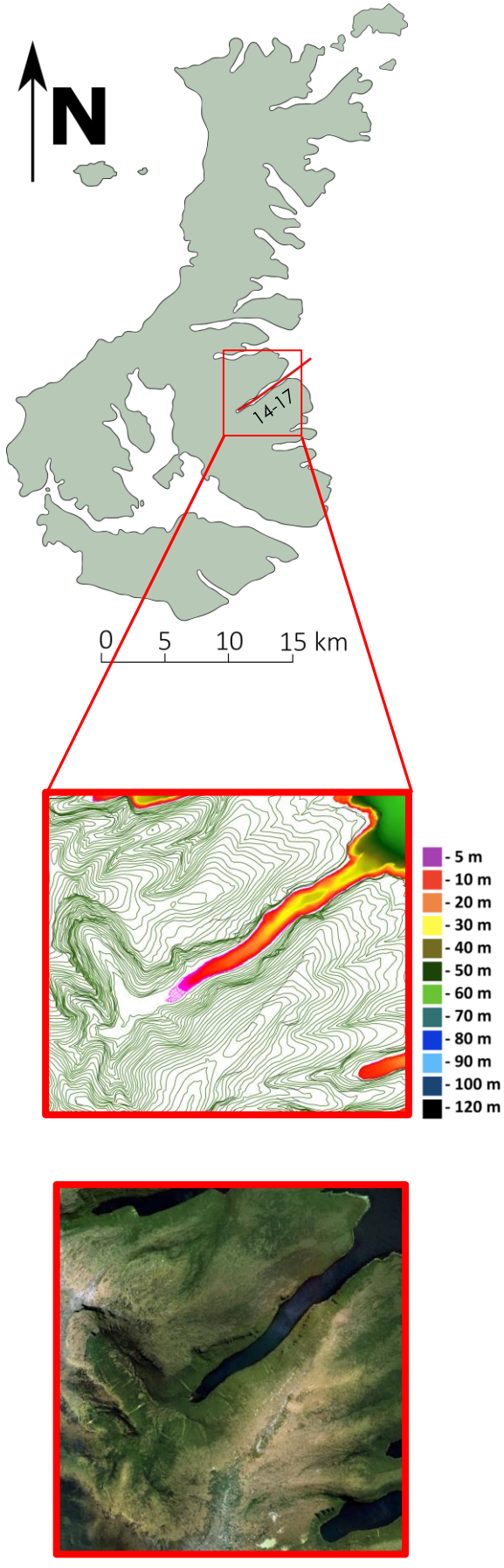

Appendix 1.5 • Line 14-17 acquired within Deep Inlet. Line Length ~7.9 km with accompanying bathymetry and satellite image. Vertical axis is in time – seconds).

A 1.5 Musgrave Harbour, Carnley Harbour • Line 15-05

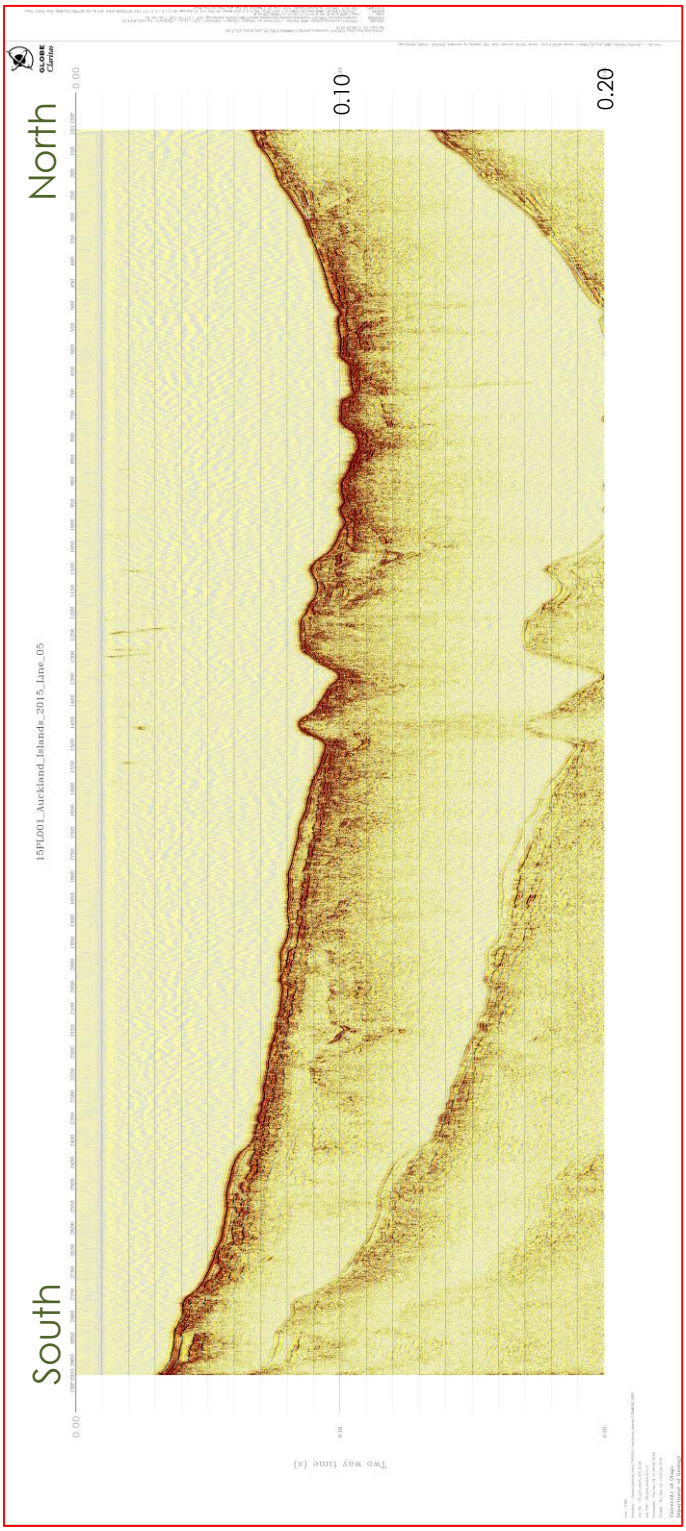

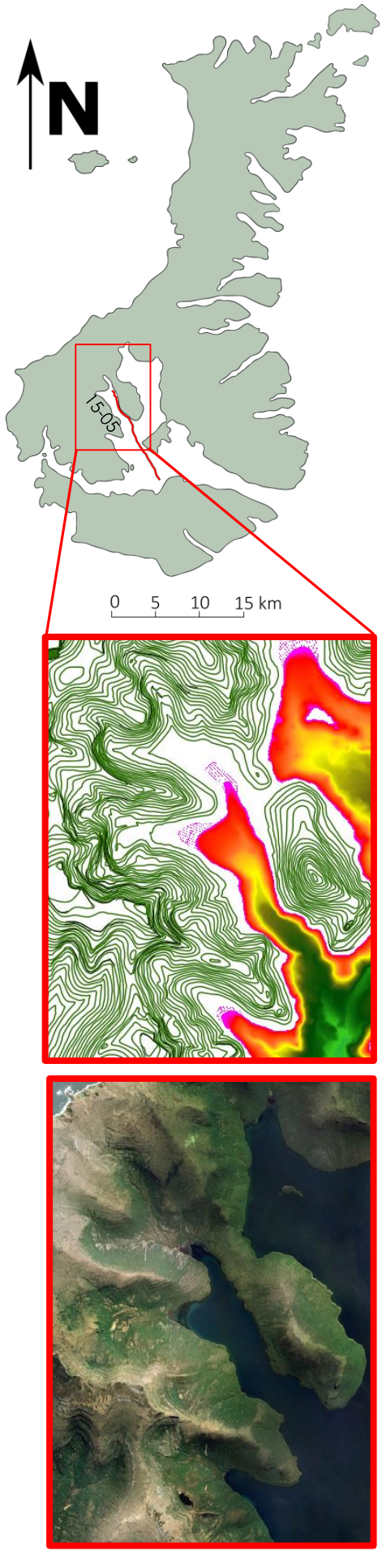

Appendix 1.6 • Line 15-05 taken acquired Musgrave Harbour, Carnley Harbour. Line Length ~8.8 km with accompanying bathymetry and satellite image.

A 1.6 Northern Arm, Carnley Harbour • Line 15-09

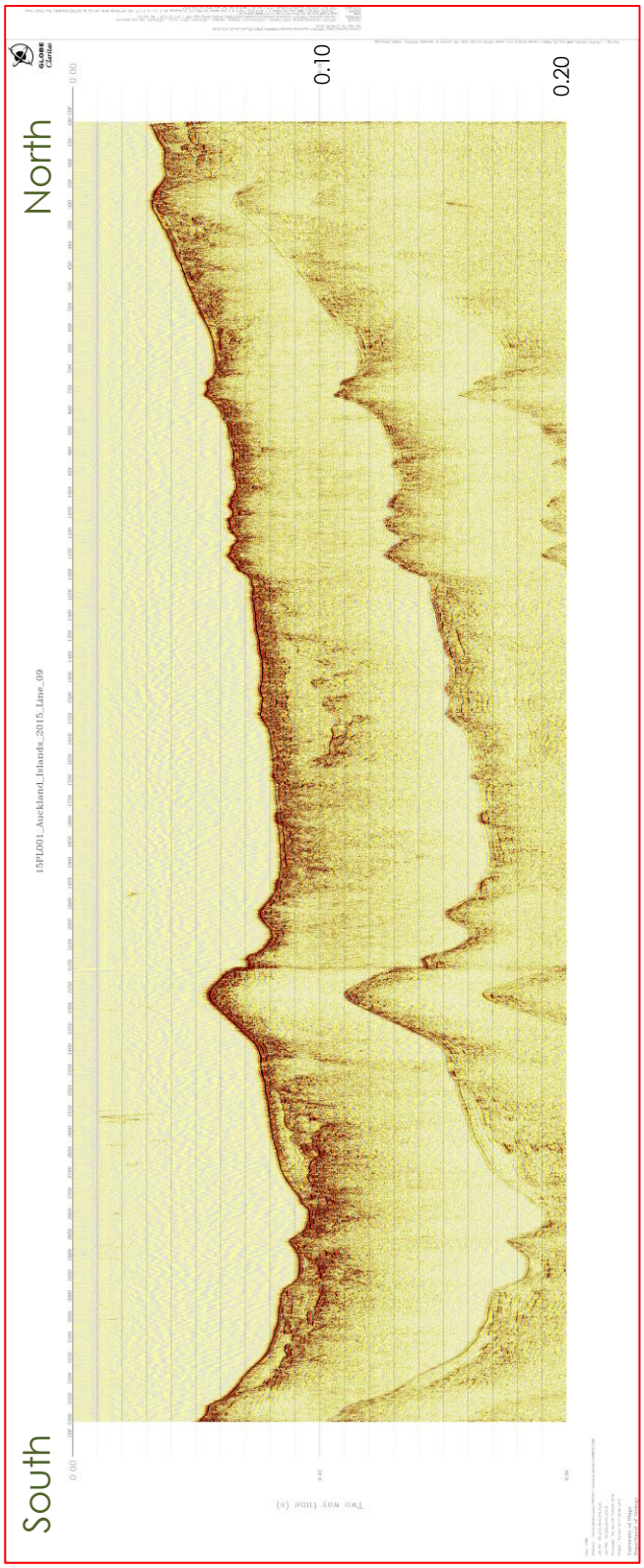

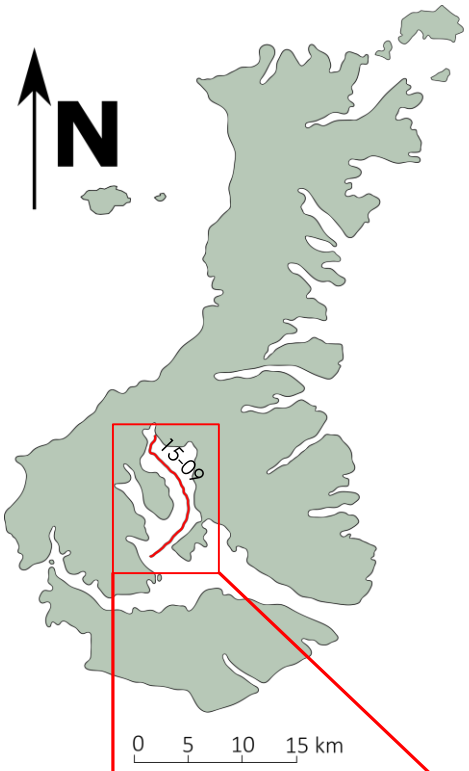

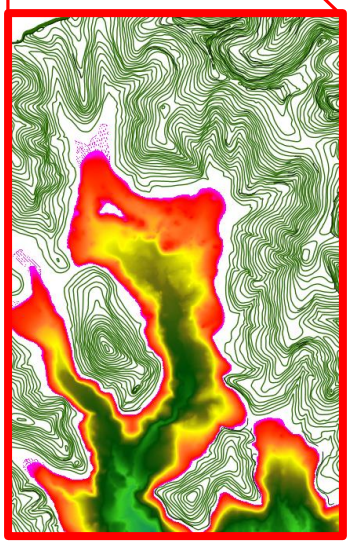

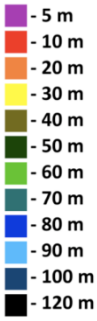

Appendix 1.7 • Line 15-09 acquired within the Northern Arm, Carnley Harbour. Line Length ~10.7 km with accompanying bathymetry and satellite image.

A 1.7 North Harbour and Haskell Bay • No seismic data

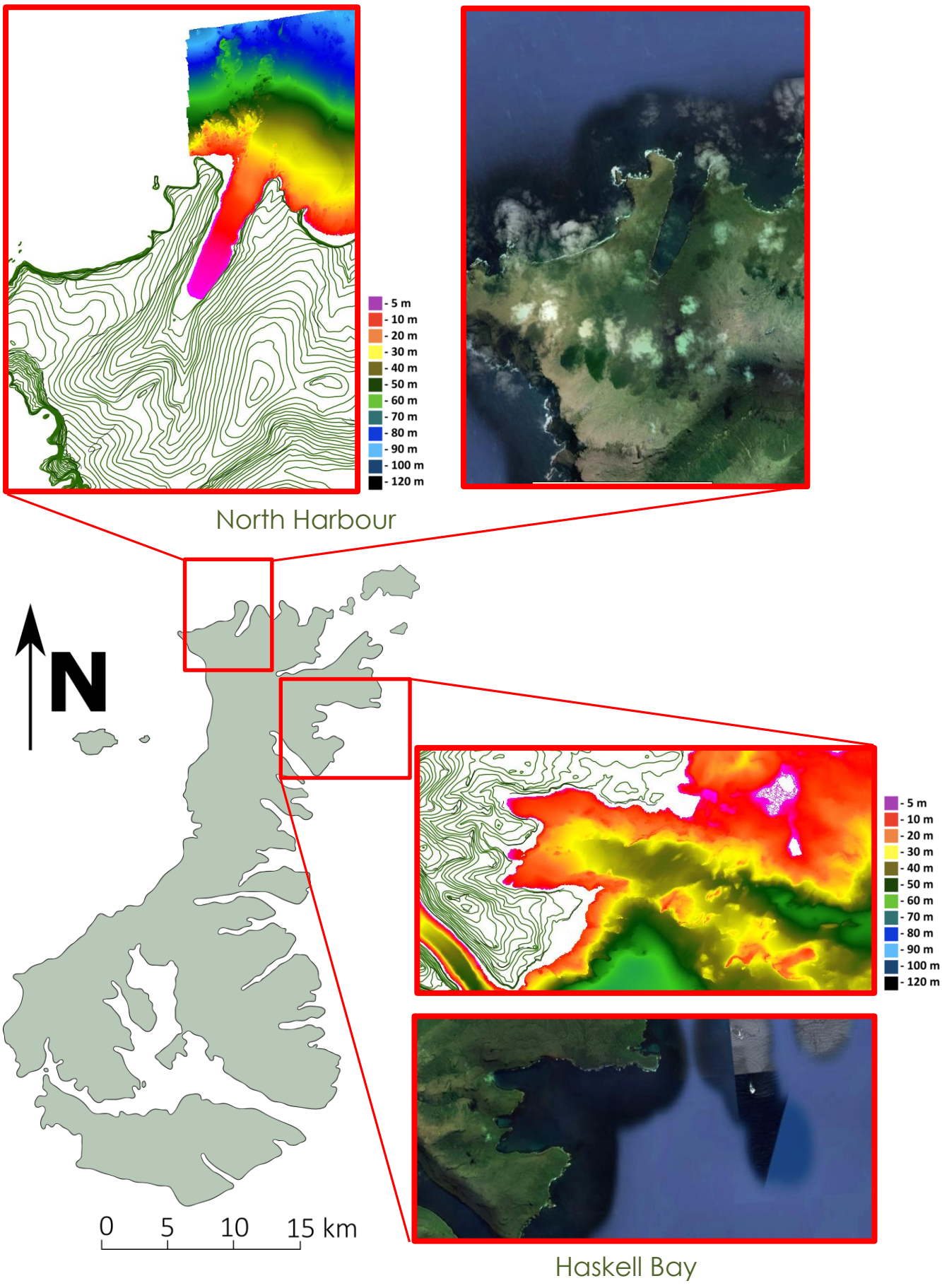

Appendix 1.8 • North Harbour (**top**) and Haskell Bay (**bottom**) localities, contours (20 m) and bathymetry. No seismic transects were acquired at these localities.